JUSTUS-LIEBIG-
UNIVERSITÄT
GIESSEN

P2X4 AND P2X7 RECEPTORS IN THE EXPRESSION AND RELEASE OF INTERLEUKIN-1β

P2X4- und P2X7- Rezeptoren bei der Expression und Sekretion von Interleukin-1β

INAUGURALDISSERTATION

Zur Erlangung des Doktorgrades der Naturwissenschaften
Dr. rer. nat.

Im Fachbereich 08
Biologie und Chemie
der Justus-Liebig-Universität Gießen

Vorgelegt von
Marie Suzanne Dippel
aus Gießen

Gießen, September 2024

Dekan	Prof. Dr. Holger Zorn
Erstgutachter	Prof. Dr. Ivan Manzini Tierphysiologie und Molekulare Biomedizin Justus-Liebig-Universität Gießen Heinrich-Buff-Ring 38, 35392 Gießen
Zweitgutachterin	Prof. Dr. Veronika Grau Klinik für Allgemein- und Thoraxchirurgie Sektion Experimentelle Chirurgie Feulgenstraße 10 – 12, 35392 Gießen

„Der am hoffnungslosesten dumme Mensch ist der, der sich nicht bewusst ist, klug zu sein.“

– Issac Asimov

Die vorliegende Arbeit wurde vom Deutschen Zentrum für Lungenforschung (DZL) gefördert. Sie wurde in der Klinik für Allgemein-, Viszeral- und Thoraxchirurgie der Uniklinik Gießen (Prof. Dr. med. Martin Schneider) in der Sektion Experimentelle Chirurgie unter der Leitung von Prof. Dr. rer. nat. Veronika Grau angefertigt. Die Betreuung der Arbeit im naturwissenschaftlichen Fachbereich wurde von Prof. Dr. Ivan Manzini übernommen. Das Thema wurde von Prof. Dr. Veronika Grau gestellt, unter deren Betreuung und in deren Labor diese Arbeit entstand. Die Sektion Experimentelle Chirurgie ist Teil des UGMLC (*Universities of Giessen and Marburg Lung Centre*), CPI (*Cardio Pulmonary Institute*, Deutschland) und des DZL (Deutsches Zentrum für Lungenforschung).

SELBSTSTÄNDIGKEITSERKLÄRUNG

Ich erkläre: Ich habe die vorgelegte Dissertation selbstständig und ohne unerlaubte fremde Hilfe und nur mit den Hilfen angefertigt, die ich in der Dissertation angegeben habe. Alle Textstellen, die wörtlich oder sinngemäß aus veröffentlichten Schriften entnommen sind, und alle Angaben, die auf mündlichen Auskünften beruhen, sind als solche kenntlich gemacht. Ich stimme einer evtl. Überprüfung meiner Dissertation durch eine Antiplagiat-Software zu. Bei den von mir durchgeführten und in der Dissertation erwähnten Untersuchungen habe ich die Grundsätze guter wissenschaftlicher Praxis, wie sie in der „Satzung der Justus-Liebig-Universität Gießen zur Sicherung guter wissenschaftlicher Praxis“ niedergelegt sind, eingehalten.

Ort, Datum

Unterschrift

ABSTRACT

Pro-inflammatory cytokines of innate immunity play a pivotal role in host defence against infection by modulating the gene expression of numerous target genes, including cytokines, cell surface receptors, and their own expression in neighbouring cells. Their expression can be induced by pathogen-associated molecular patterns (PAMPs) and damage-associated molecular patterns (DAMPs), such as lipopolysaccharide (LPS) and extracellular adenosine triphosphate (ATP). ATP can be released in large quantities by damaged cells, activating the P2RX7 in innate immune cells. The pro-inflammatory cytokine IL-1β is produced in its inactive form by mononuclear phagocytes upon 'priming' with LPS, while subsequent ATP-mediated P2RX7 activation leads to the maturation and release of the bioactive cytokine.

The present study aimed to investigate the role of the P2RX4, another ATP-sensitive receptor, in the secretion of IL-1β by human mononuclear phagocytes. Moreover, the function of the P2RX4 and the P2RX7 in the priming of mononuclear phagocytes was examined. The human monocytic THP-1 cell line, THP-1 cell-derived M1-like macrophages as well as primary human peripheral blood mononuclear cells and human peritoneal macrophages were primed with LPS and stimulated with the P2RX agonists BzATP or ATP or with nigericin in the absence or presence of different P2RX4 and P2RX7 antagonists, and the release of IL-1β was quantified.

The results demonstrated that the P2RX4 is also involved in the ATP-dependent secretion of IL-1β by mononuclear phagocytes. Furthermore, cells were primed with LPS in the presence of the antagonists, and the release of IL-1β and the pro-inflammatory IL-6, as well as the mRNA levels of *IL1B*, *IL6*, *IL10* and other cytokines, were analysed by ELISA or by real-time RT-PCR, respectively. In monocytic cells, treatment with the P2RX4 antagonist 5-B before priming resulted in increased *IL1B* mRNA expression and in increased ATP-independent IL-1β release. Additionally, there was a slight increase in *IL6* mRNA and IL-6 secretion, as wells as a clear-cut increase in *IL10* mRNA. Treatment with 5-B also resulted in the activation of caspase-3/-7 in monocytic THP-1 cells, which suggests that 5-B may induce apoptosis.

During major surgery or accidental trauma, the extensive release of ATP leads to massive cytokine release, which can cause life-threatening systemic hyperinflammation. While 5-B enhances the LPS-induced inflammation, which essentially contributes to host defence against infection, 5-B dampens IL-1β maturation and release in response to extracellular ATP, a potent trauma-associated DAMP. Presumably, the effects of 5-B are mediated via P2RX4. These findings may pave the way towards novel therapeutic strategies that protect surgical and traumatized patients against infection, while efficiently preventing sterile hyperinflammation.

ZUSAMMENFASSUNG

Pro-inflammatorische Zytokine der angeborenen Immunität spielen eine zentrale Rolle bei der Abwehr von Infektionen durch die Modulation der Genexpression zahlreicher Zielgene, darunter Zytokine, Zelloberflächenrezeptoren und ihre eigene Expression in Nachbarzellen. Ihre Expression kann durch pathogen-assoziierte molekulare Muster (PAMPs) und schadensassoziierte molekulare Muster (DAMPs) wie Lipopolysaccharid (LPS) und extrazelluläres Adenosintriphosphat (ATP) induziert werden. ATP kann von geschädigten Zellen in großen Mengen freigesetzt werden und den P2RX7 in angeborenen Immunzellen aktivieren. Das pro-inflammatorische Zytokin IL-1β wird in seiner inaktiven Form von mononukleären Phagozyten nach dem „*priming*“ mit LPS produziert, während die anschließende ATP-vermittelte P2RX7-Aktivierung zur Reifung und Aktivierung des reifen Zytokins.

In der vorliegenden Studie sollte die Rolle des P2RX4, eines weiteren ATP-sensitiven Rezeptors, bei der Sekretion von IL-1β durch mononukleäre Phagozyten untersucht werden. Außerdem wurde die Funktion von P2RX4 und P2RX7 beim „*priming*“ von menschlichen mononukleären Phagozyten untersucht. Die humane monozytäre THP-1 Zelllinie, aus THP-1-Zellen differenzierte M1-ähnliche Makrophagen und primäre humane periphere mononukleäre Blutzellen sowie humane Peritonealmakrophagen wurden mit LPS aktiviert und mit dem P2RX-Agonisten BzATP, ATP oder Nigericin in Abwesenheit oder Anwesenheit verschiedener P2RX4- und P2RX7-Antagonisten stimuliert. Anschließend wurde die Freisetzung von IL-1β quantifiziert.

Die Ergebnisse zeigten, dass P2RX4 auch an der ATP-abhängigen Sekretion von IL-1β durch mononukleäre Phagozyten beteiligt ist. Darüber hinaus wurden die Zellen in Gegenwart der Antagonisten mit LPS stimuliert, und die Freisetzung von IL-1β und des pro-inflammatorischen IL-6 sowie die mRNA-Spiegel von *IL1B*, *IL6*, *IL10* und anderen Zytokinen wurden mittels ELISA bzw. Echtzeit-RT-PCR analysiert. In monozytären Zellen führte die Behandlung mit dem P2RX4-Antagonisten 5-B vor dem „*priming*“ zu einer erhöhten *IL1B*-mRNA-Expression und zu einer erhöhten ATP-unabhängigen IL-1β-Freisetzung. Außerdem kam es zu einem leichten Anstieg der *IL6*-mRNA und der IL-6-Sekretion sowie zu einem deutlichen Anstieg der *IL10*-mRNA. Die Behandlung mit 5-B führte auch zur Aktivierung von Caspase-3/-7 in monozytären THP-1-Zellen, was vermuten lässt, dass 5-B die Apoptose auslösen kann.

Bei gravierenden chirurgischen Eingriffen oder Unfalltraumata führt die umfangreiche Freisetzung von ATP zu einer massiven Zytokinfreisetzung, die eine lebensbedrohliche systemische Hyperinflammation verursachen kann. Während 5-B die LPS-induzierte Entzündung verstärkt, die wesentlich zur Abwehr von Infektionen durch den Wirt beiträgt, dämpft 5-B die Reifung und Freisetzung von IL-1β als Reaktion auf extrazelluläres ATP, einem wichtigen Trauma-assoziierten DAMP. Vermutlich werden die Wirkungen von 5-B über P2RX4 vermittelt. Diese Erkenntnisse könnten den Weg zu neuen therapeutischen Strategien ebnen, die chirurgische und traumatisierte Patienten vor Infektionen schützen und gleichzeitig eine sterile Hyperinflammation wirksam verhindern.

CONTENTS

LIST OF ABBREVIATIONS

5-B	5-(3-Bromophenyl)-1,3-dihydro-2H-benzofuro[3,2-e]-1,4-diazepine-2-one
A43	3-[[5-(2,3-Dichlorophenyl)-1H-tetrazol-1-yl]methyl]pyridine hydrochloride
ASC	Apoptosis-associated speck-like protein containing a caspase-recruitment domain
ATP	Adenosine triphosphate
BCA	Bicinchoninic acid
BMDM	Bone marrow-derived macrophages
BSA	Bovine serum albumin
BzATP	2'(3')-O-(4-Benzoylbenzoyl)adenosine-5'-triphosphate
C-terminus	Carboxy-terminus
CD	Cluster of differentiation
CNS	Central nervous system
DAMP	Danger associated molecular pattern
DC	Dendritic cell
ddH_2O	Double distilled water
DMSO	Dimethyl sulfoxide
DNA	Deoxyribonucleic acid
EDTA	Ethylenediaminetetraacetic acid
ELISA	Enzyme-linked immunosorbent assay
FCS	Foetal calf serum
GSDMD	Gasdermin D
h	Hour(s)
hPBMCs	Human peripheral blood mononuclear cells
hPMs	Human peritoneal macrophages
HRP	Horseradish-peroxidase
IC50	Half maximal inhibitory concentration
ICC	Immunocytochemistry
IFN	Interferon
IFN-γ	Interferon gamma
IgG	Immunoglobulin
IL	Interleukin
IL-1β	Interleukin-1 beta
IL-1R1	Interleukin-1 receptor type 1
IL-10Rα/β	Interleukin-10 receptor subunit alpha/beta
IL-18Rα/β	Interleukin-18 receptor-related protein alpha/beta
IL-6Rα/β	Interleukin-6 receptor subunit alpha/beta
IRAK	Interleukin-1 receptor-associated kinase
JNJ	2-(Phenylthio)-N-[[tetrahydro-4-(4-phenyl-1-piperazinyl)-2H-pyran-4-yl]methyl-3-pyridinecarboxamide
LBP	LPS-binding protein
LDH	Lactate dehydrogenase
LPS	Lipopolysaccharide
LRRs	Leucine-rich repeats
Min	Minute(s)
MM	Molecular mass marker
MyD88	Myeloid differentiation primary response protein MyD88
n	Number of individual experiments
N-terminus	Amino-terminus
NEK7	Never in mitosis-A-related kinase 7
NF-κB	Nuclear factor ‘kappa-light-chain-enhancer’ of activated B-cells
NLR	Nucleotide-binding oligomerization domain-like receptor
NLRP3	NLR family pyrin domain-containing protein 3
NTC	No template control
P2RX4/7	P2X purinoceptor 4/7
PAMP	Pathogen associated molecular pattern

PBS	Dulbecco's phosphate buffered saline
PenStrep	Penicillin streptomycin
PMA	Phorbol 12-myristate 13-acetate
PPIA	Peptidylprolyl isomerase A
PRRs	Pattern recognition receptors
PSB	PSB-15417
PZB13	PZB13420052A
PZB15	PZB15517166A
RNA	Ribonucleic acid
ROS	Reactive oxygen species
RPMI	Roswell-Park-Memorial-Institute (RPMI) 1640 advanced
RT	Room temperature
RT-PCR	Reverse transcription polymerase chain reaction
SDS	Sodium dodecyl sulphate
SDS-PAGE	Sodium dodecyl sulphate-polyacrylamide gel electrophoresis
STAT3	Signal transducer and activator of transcription proteins 3
TFs	Transcription factors
TIR	Toll-interleukin 1 receptor
TLR	Toll-like receptor
TNF	Tumour necrosis factor
TNFR	Tumour necrosis factor receptor
TRAF	TNF receptor-associated factor
TRIS	Tris(hydroxymethyl)aminomethane

LIST OF TABLES

LIST OF FIGURES

INTRODUCTION

1 THE IMMUNE SYSTEM

1.1 OVERVIEW OF THE TWO BRANCHES OF THE VERTEBRATE IMMUNE SYSTEM

The immune system is a complex network of molecules, biological processes, and immune cells known as leukocytes. Its primary function is to protect the body from pathogens, pathogen-caused damage, cancer cells, and foreign bodies.

Innate immunity is a branch of the vertebrate immune system that provides the first line of defence by mediating responses in the initial critical period of exposure to a new pathogen. The innate immune system responds to a wide range of stimuli and is not specific to any particular pathogen. It serves as physical and chemical barriers throughout the body. When pathogens breach the physical barrier, innate immunity relies on a group of proteins and leukocytes to eliminate invasive pathogens. Innate leukocytes include basophils, eosinophils, and natural killer cells as well as phagocytic cells, namely neutrophils, dendritic cells (DCs), monocytes, and macrophages (Vijay 2018). These cell types are found in various tissues and are capable of quickly identifying the conserved features of pathogens. They become activated and respond in distinct cellular mechanisms to eliminate foreign particles, including bacteria, viruses, fungi, dead or dying cells, and cellular debris (Iwasaki et al. 2015). For instance, phagocytic cells take up foreign particles via phagocytosis and digest them within a specialized cellular compartment. The innate immune system can distinguish between self and non-self or damaged-self that poses a threat and react accordingly without causing harm to the host beyond what is necessary. Activated cells also attract other leukocytes to sites of inflammation by releasing signalling molecules known as chemokines, which are a type of cytokine. Cytokines are soluble, small non-structural proteins with pro-inflammatory or anti-inflammatory properties by inducing distinct cellular responses in their target cells. Cytokines also mediate the balance between humoral and cell-based immune responses. Cell-based immune responses include, in addition to phagocytes, cells of the adaptive branch of the vertebrate immune system (Iwasaki et al. 2015).

Adaptive immune responses can develop slowly after initial exposure to a new pathogen compared to innate immunity. This is because the selection of specific lymphocytes, followed by their activation and expansion, takes a long time to complete. However, the adaptive immune response is highly specific and lasts longer. Its main function is to remember encounters with specific pathogens and provide a rapid and specific response

when they attack again (Iwasaki et al. 2015). The lymphocytes that carry out the adaptive immune response are T and B cells. B cells produce antigen-specific antibodies that inactivate and mark their target for rapid elimination, while also memorizing characteristics of the antigen to provide immunological memory. T cells are classified into many subtypes with different functions, such as activation of B and T cells, immune-mediated cell death, or maintenance of tolerance to self-antigens (Iwasaki et al. 2015).

1.2 MONONUCLEAR PHAGOCYTES

1.2.1 MONOCYTES

Monocytes and macrophages have one-lobed nuclei and are collectively referred to as mononuclear phagocytes. It was originally thought that monocytes continuously leave the bloodstream and their only function is to differentiate into macrophages and DCs (van Furth et al. 1972). However, it is now known that tissue macrophages and DCs with the capacity of self-renewal can populate tissues already during embryogenesis and that monocytes play a variety of roles in inflammatory responses (Shapouri-Moghaddam et al. 2018).

Monocytes are derived from hematopoietic stem cells in the bone marrow, circulate in the blood, and can be divided into two subsets: classical and non-classical monocytes in humans (Ziegler-Heitbrock et al. 2010). Classical monocytes have migrating properties crossing the endothelium and invade peripheral tissues, whereas non-classical monocytes are patrolling cells with endothelial cell-supporting functions (Jakubzick et al. 2017). These subsets are distinguished based on the cell-specific expression of surface molecules classified using the cluster of differentiation (CD) nomenclature (Chan et al. 1988). CD proteins can act as receptors, ligands, or adhesion molecules. Chemokine receptors are a prominent example that bind signalling proteins, guiding recruitment and directional movements of cells (Palframan et al. 2001, Geissmann et al. 2003).

Non-classical monocytes express CD14 and CD16 (Passlick et al. 1989, Ziegler-Heitbrock et al. 2010). Classical monocytes are defined by the lack of CD16 but high levels of CD14, which is the most prevalent monocyte population in human blood. These cells have a half-life of approximately one day in circulation. Therefore, they either rapidly migrate, convert into the patrolling type in the bone marrow, or undergo programmed cell death (Jakubzick et al. 2017). In the steady-state, extravasation occurs constitutively into non-inflamed or lymphatic tissue. Here, the cells may survey the environment for antigens and exit the tissue via the lymphatics or undergo local apoptosis. However, monocytes are highly dynamic and versatile. They have the ability to replenish distinct tissue macrophages or DCs in the steady-state (Jakubzick et al. 2017). These short-lived effector cells, derived from

monocytes, contribute to various physiological activities such as arteriogenesis and angiogenesis (Shapouri-Moghaddam et al. 2018).

During infection, monocytes are recruited by chemokines or bacterial chemotactic factors and gain the ability to produce and release inflammatory mediators, which restrict microbial growth and invasion. Monocytes differentiate into macrophages, mediated by local growth factors, pro-inflammatory mediators, and pathogenic products. Furthermore, monocytes can transform into an antigen-presenting cell, enabling them to transport antigens to a draining lymph node and present them to lymphocytes (Hohl et al. 2009, Kim et al. 2009, Jakubzick et al. 2013). Several murine models of infectious diseases have demonstrated that migrating monocytes lead to the development of specialized tumour necrosis factor (TNF)-α- and inducible nitric oxide synthase-producing DCs in an inflammatory environment. This process directly contributes to the clearance of pathogens while the cells maintain monocyte size and characteristics (Serbina et al. 2003). However, it is important to note that excessive recruitment of monocytes can be detrimental and cause immunopathology during certain infections (Antonelli et al. 2010).

Additionally, monocyte recruitment is associated with the pathogenesis of various inflammatory diseases that are not caused by infection. For instance, in murine atherosclerosis models, monocytes infiltrate atherosclerotic lesions early on, influenced by chemokines (Tacke et al. 2007). The identified monocytes with migrating properties are considered part of the inflammatory response in experimental atherosclerosis. It is believed that these monocytes give rise to macrophages in lesions (Swirski et al. 2007). Another study suggests that monocytes accumulate continuously in atherosclerotic lesions in proportion to lesion size. Therefore, infiltration rates of monocytes could be used to estimate the severity of atherosclerosis (Swirski et al. 2006). Myocardial infarction triggers an acute inflammatory response in patients. At an early stage of the disease, migrating monocytes are recruited, followed by an increase in patrolling monocytes within the damaged tissue later on (Nahrendorf et al. 2007, Tsujioka et al. 2009). These studies demonstrate a biphasic monocyte recruitment to the heart in patients and mice, where the recruited cells differentiate into macrophages. The initial wave of recruitment may aid in the elimination of deceased cardiac cells, whereas macrophages in the later phase promote resolution of inflammation and tissue repair (Nahrendorf et al. 2007). However, inflammation can be detrimental to infarct tissue, as immune cells release pro-inflammatory cytokines, exacerbating the injury and causing further harm to the remaining intact cells.

1.2.2 MACROPHAGES

Classical monocytes can migrate into different tissues and differentiate into macrophages after exposure to specific stimuli. However, recent research has shown that most adult tissue-resident macrophages originate from the yolk sac during embryonic development, indicating their ability to self-renew and maintain themselves independently of monocytes in a steady state (Hashimoto et al. 2013, Yona et al. 2013, Epelman et al. 2014). Monocytes complement the tissue-resident macrophage compartment as required. Studies suggest that monocyte-derived macrophages primarily assist in host defence, while embryonic macrophages are involved in tissue remodelling, and both subtypes coexist in many organs (Shapouri-Moghaddam et al. 2018). The macrophage system is highly adaptable, exhibiting a variety of phenotypes in different tissues, each with its unique combination of embryonic and adult-derived macrophages (Epelman et al. 2014, Sheng et al. 2015, Ensan et al. 2016). These phenotypes occur through polarization, whereby the cells exhibit a phenotypical functional response to micro-environmental stimuli and signals. In a simplified classification, macrophages can be polarized into either a pro-inflammatory (M1) or anti-inflammatory (M2) phenotype (Stein et al. 1992, Mantovani et al. 2002, Mantovani et al. 2004, Verreck et al. 2004).

In inflamed tissues, macrophages are activated by recognition of pathogen associated molecular pattern (PAMPs) or damage-associated molecular patterns (DAMPs), for instance lipopolysaccharide (LPS), resulting in the production of pro-inflammatory cytokines. For instance, interleukin (IL)-12 is produced and drives the polarization of naïve T cells towards a helper cell subtype, which in turn induces the secretion of interferon gamma (IFN-γ). Activation of macrophages towards a M1 polarization by IFN-γ, TNF-α, or the granulocyte monocyte colony-stimulating factor (Hsieh et al. 1993, Verreck et al. 2004) leads to the production and secretion of higher amounts of pro-inflammatory cytokines, including TNF-α, interleukin-1 beta (IL-1β), IL-6, and IL-12, and generates high amounts of reactive oxygen species (ROS) (Shapouri-Moghaddam et al. 2018). Although these features contribute to pathogen removal, they can also cause ROS-induced tissue damage, impair tissue regeneration, and wound healing. Therefore, regulatory mechanisms driven by the anti-inflammatory functions of M2 macrophages are necessary to counterbalance the tissue damage driven by M1 macrophages. Polarization towards M2 macrophages occurs upon stimulation with IL-4 and IL-13, IL-10, or IL-33 (O'Farrell et al. 1998, Nelms et al. 1999, Lang et al. 2002). M2 Macrophages are further classified into four different types based on the activating stimulus they receive. They have an overall anti-inflammatory cytokine profile, characterized by low production of IL-12 and high production of IL-10 and tumour growth factor-β. M2 macrophages have a potent phagocytic capacity, enabling them to scavenge cell debris and apoptotic cells. They also possess pro-angiogenic and pro-fibrotic

properties, promoting tissue repair and wound healing (Kurowska-Stolarska et al. 2009, Jetten et al. 2014). It has been observed that when M2 macrophages are exposed to M1 signals, or vice versa, re-polarization occurs, indicating the high functional plasticity of macrophages (Shapouri-Moghaddam et al. 2018). In addition to their crucial role in host defence against pathogens, macrophages also play important roles in chronic diseases. In allergic asthma, macrophage-like cell populations in the airway lumen are attributed to type 2 cytokine-mediated airway inflammation (Julia et al. 2002). In Crohn's disease, intestinal macrophages produce larger amounts of pro-inflammatory cytokines than typical intestinal macrophages, contributing to the pathogenesis of the disease (Kamada et al. 2008). In chronic fibrotic diseases, the pro-inflammatory response of M1 macrophages may not be adequately controlled, leading to exacerbated tissue injury and subsequent aberrant wound healing (Duffield et al. 2005). As previously stated, monocytes are believed to give rise to macrophages in atherosclerosis, in which macrophages exhibit M1 characteristics and contribute to inflammation (Swirski et al. 2007). In a murine experimental autoimmune encephalomyelitis model of multiple sclerosis, inflammatory peripheral macrophages that have been activated migrate into inflamed tissue (Gordon et al. 1995, Heppner et al. 2005).

1.3 SIGNAL TRANSDUCTION VIA PATTERN RECOGNITION RECEPTORS

1.3.1 OVERVIEW OF PATTERN RECOGNITION RECEPTORS

Activation of innate immune cells is a crucial step in host defence. This process enables the previously described mechanisms of monocytes and macrophages to become effective. The activation occurs when specific chemical structures are recognized by a limited number of germline-encoded pattern recognition receptors (PRRs) (Janeway 1989, Li et al. 2021). PRRs are composed of ligand recognition domains that bind regular patterns of chemical structures, intermediate domains, and effector domains. The latter domains transmit signals by activating downstream pathways (Li et al. 2021). PRRs are classified into five families based on the homology of their respective protein domains: toll-like receptors (TLRs), nucleotide-binding oligomerization domain-like receptor (NLRs), retinoic acid-inducible gene-I-like receptors, C-type lectin receptors, and absent in melanoma-2-like receptors. These receptors are distributed across intracellular compartment membranes, the cytoplasm, and the cell membrane. They recognize two types of regular patterns of molecular structures (Li et al. 2021). The first type comprises PAMPs, which are highly conserved essential structures associated with different classes of pathogens (Janeway 1989). PAMPs are crucial for pathogen survival and enable the innate immune system to distinguish self from non-self. The second type of molecules that activate PRRs are DAMPs, which are endogenous components of the cytoplasm and nucleus that are released only from damaged cells, such as adenosine triphosphate (ATP) or high mobility group box

protein 1 (Seong et al. 2004). The binding of these molecular structures triggers signalling cascades via the effector domains of the PRRs, leading to the induction of several genes involved in immune host defence. The distinct ligands and different subcellular locations of PRRs translate into several common signalling pathways. First, this involves the similar structures and functions of the protein kinases, adaptor proteins, and transcription factors (TFs) involved in signal transduction. Second, these pathways can converge into common outcomes due to cross-talk (Li et al. 2021).

TLRs are the most prominent family of PRRs. They are integral membrane glycoproteins expressed either extracellularly or intracellularly (Fitzgerald et al. 2020). TLRs 1, 2, 4, 5, and 6 are expressed on the cell surface, while TLRs 3, 7, 8, and 9 are found in endolysosomal compartments and recognize microbial deoxyribonucleic acid (DNA) or ribonucleic acid (RNA). TLRs on the cell surface detect various ligands, such as peptides derived from flagellin, lipoproteins, and LPS with LPS being a common example (Fitzgerald et al. 2020). The N-terminal ectodomains, which are horseshoe-like shaped and consist of leucine-rich repeats (LRRs), bind these various ligands through homogenic or heterogenic receptor dimerization (Kim et al. 2007, Park et al. 2009). All TLRs have a similar domain organization, with an ectodomain followed by a single transmembrane domain and an intracellular toll-interleukin 1 receptor (TIR) domain. TIR domain-containing adaptor molecules can bind to the intracellular TIR domain after dimerization-induced conformational changes (Fitzgerald et al. 2020). Chapter 1.3.2 explains the activation and signalling of TLR4.

The cytoplasm is monitored by the largest family of PRRs, the NLRs. Viral replication often occurs in the cytoplasm. Some bacteria and eukaryotic parasites have mechanisms to escape phagosomes, and components produced upon infection can also appear in the cytoplasm (Li et al. 2021). The NLR family shares the nucleotide-binding domain, which is important for nucleic acid binding and the oligomerization step upon activation, and the C-terminal LRRs identify ligands (Ting et al. 2008). The NLR family can be divided into five subfamilies based on the effector domains at the Amino (N)-terminus (Ting et al. 2008). More information about the NLRP subfamily based on the NLR family pyrin domain-containing protein 3 (NLRP3) protein complex can be found in chapter 1.4.

1.3.2 TOLL-LIKE RECEPTOR 4 ACTIVATION AND SIGNALLING

TLR4 was the first PRR to be discovered in humans by Medzhitov et al. (1997). Shortly thereafter, LPS was identified as a microbial stimulus that activates TLR4 (Poltorak et al. 1998, Hoshino et al. 1999, Qureshi et al. 1999). LPS is a glycolipid composed of hydrophilic polysaccharides and an amphiphilic lipid A component. It is a constituent of the outer membrane of Gram-negative bacterial cell walls. The lipid A component is the conserved

molecular pattern of LPS that plays a crucial role in the immune response (Rietschel et al. 1994). To achieve high-sensitivity interactions, additional LPS-binding proteins are required upstream of TLR4, as TLR4 only forms weak contact with LPS (Fitzgerald et al. 2020). The soluble LPS-binding protein (LBP) binds LPS into a complex that is recognized by the LRR-containing CD14 (Gioannini et al. 2004). CD14 can exist as either a soluble or a membrane-bound protein (Wright et al. 1990, Frey et al. 1992). Regardless of its location, CD14 transfers LPS into a large hydrophobic pocket of the small, secreted protein lymphocyte antigen 96 after LBP dissociation (Visintin et al. 2001, Kim et al. 2007). TLR4-lymphocyte antigen 96 heterodimers make up the functional LPS receptor. To form these heterodimers, lymphocyte antigen 96 interacts steadily with the ectodomain of TLR4 (Shimazu et al. 1999, Park et al. 2009). This process enables TLR4 dimerization at picomolar levels of LPS, triggering a signal transduction cascade (Fitzgerald et al. 2020). A single bacterium can contain thousands of LPS molecules, which can form numerous LPS-CD14 complexes. These complexes can be present on thousands of macrophages, leading to a massive amplification of the inflammatory response. Additionally, soluble CD14 in the bloodstream may deliver LPS to cells that express TLR4 and MD2 but lack CD14. This process results in an enhanced immune response (Fitzgerald et al. 2020).

Upon activation of the LPS signalling cascade, TLR4 dimers can bind to cytosolic TIR-binding adaptor molecules. The TIR domain-containing adapter protein and TIR domain-containing adapter molecule 2 are known adaptor molecules that stimulate the assembly of respective cytosolic proteins and are utilized by distinct TLRs (Fitzgerald et al. 2020). It is noteworthy, TLR4 can engage both molecules, thereby activating distinct subsequent signalling pathways. The localization of TLR4 is thought to be a determining factor in the signalling process. TLR4-lymphocyte antigen 96 complexes translocate to lipid rafts in a CD14-dependent manner. Here, they can form high-affinity interactions with the TIR domain-containing adapter protein (Triantafilou et al. 2002, Kagan et al. 2006). The TIR domain-containing adapter protein recruits multiple copies of myeloid differentiation primary response protein MyD88 (MyD88), which forms a complex with members of the IL-1 receptor-associated kinase (IRAK) family of serine-threonine kinases via the N-terminal domain (Lin et al. 2010). The tight packing of IRAK drives autophosphorylation and subsequent recruitment of tumour necrosis factor receptor-associated factor (TRAF6) (Cao et al. 1996, Ferrao et al. 2014). TRAF6 activates the TAK1 protein kinase complex, leading to the activation of nuclear factor ‘kappa-light-chain-enhancer’ of activated B-cells (NF-κB) and MAPKs, which are key TFs associated with inflammatory responses. This activation induces the expression of pro-inflammatory genes such as those for TNF-α, IL-6, and the immature form of IL-1β (Wang et al. 2001). Additionally, TRAF6 mediates the induction of glycolysis via specific kinases. However, the consequences of this early shift in glycolysis

remain unclear. It may be the first step towards a long-term alteration of the metabolism of the cells (Fitzgerald et al. 2020). Following MyD88-dependent signalling at the plasma membrane, TLR4 may be internalized and interact with the TIR domain-containing adapter molecule 2 in endosomes (Kagan et al. 2008). CD14 mediates endocytosis, as its constitutive internalization is greatly accelerated upon LPS binding, leading to co-incident endocytosis of TLR4 (Tan et al. 2015). Subsequently, TIR domain-containing adapter molecule 2 and members of the TRAF family are recruited to form a protein complex. This delayed signalling results in the expression of type I IFNs (Fitzgerald et al. 2020). Overall, TLR4 stimulation by LPS, as well as by other PAMPs and DAMPs, induces an inflammatory cell response via MyD88- and TIR domain-containing adapter molecule 2-dependent pathways.

1.4 SIGNAL TRANSDUCTION VIA THE NLRP3 INFLAMMASOME

1.4.1 CONSTITUENTS OF THE NLRP3 INFLAMMASOME

Upon activation, TLRs induce the expression of pro-inflammatory cytokines, which are regulated at both the transcriptional and post-transcriptional levels to prevent an excessive inflammatory response. TLR4 activation by LPS leads to the production of an immature form of IL-1β called pro-IL-1β. The maturation and release of IL-1β and the related cytokine IL-18 depend on the activation of the NLRP3 inflammasome, an intracellular protein complex. The inflammasome is named after its NLR family members, which oligomerize to form an activating platform for a cysteine protease in response to PAMPs and DAMPs (Martinon et al. 2002). The NLRP3 protein comprises three domains: a pyrin domain at the N-terminus, a nucleotide-binding oligomerization domain in the middle, and LRR at the Carboxy-terminus (C-terminus). The nucleotide-binding oligomerization domain has ATPase activity, which enables oligomerization of several NLRP3 proteins upon activation (Duncan et al. 2007). The adaptor protein apoptosis-associated speck-like protein containing a caspase-recruitment domain (ASC) interacts with NLRP3 proteins through the pyrin domain and facilitates the recruitment and proteolytic activation of the protease caspase-1 to the inflammasome protein complex via their caspase-recruitment domain (Srinivasula et al. 2002, Vajjhala et al. 2012).

Caspase-1 is initially synthesized in an inactive form. It then oligomerizes and undergoes autoactivation within the inflammasome. Once activated, it cleaves the immature forms of cytokines IL-1β and IL-18, resulting in the production of biologically active forms of these cytokines (Manji et al. 2002, Martinon et al. 2002). Furthermore, gasdermin D (GSDMD) is cleaved by caspase-1, leading to the formation of pores in the plasma membrane via the N-terminal domain of GSDMD. This process results in pyroptosis, a type of cell death that is both lytic and pro-inflammatory (Fink et al. 2006, He et al. 2015). Pyroptosis leads to the

expulsion of intracellular pathogens from their replication environment, resulting in the release of cytokines and the creation of DAMPs (He et al. 2015). However, the formation of NLRP3 inflammasomes and activation of caspase-1 do not occur subsequently in response to TLR4 activation. Several substances that induce NLRP3 expression have been discovered, but they are mostly insufficient for inflammasome assembly (Bauernfeind et al. 2009). Therefore, a two-signal model has been proposed. The first signal, provided by microbial components or endogenous cytokines, primes the NLRP3 inflammasome. The second signal from the NLRP3 activators triggers the assembly.

1.4.2 PRIMING THE NLRP3 INFLAMMASOME: SIGNAL 1

In macrophages, priming stimuli such as ligands for TLRs, NLRs, or cytokine receptors, increase the expression of NLRP3 protein via NF-κB. This upregulation occurs under conditions in which the levels of NLRP3 are considered inadequate for activation (Bauernfeind et al. 2009, Franchi et al. 2009). However, it is important to note that priming signals do not affect the levels of ASC, pro-caspase-1, and pro-IL-18 (Bauernfeind et al. 2009). Although some studies have shown immediate activation of NLRP3 inflammasome upon priming with LPS without a second signal, which may be mediated by IRAK-1, a molecule downstream of MyD88, priming still plays a significant role in NLRP3 inflammasome activation through transcriptional regulation (Juliana et al. 2012, Lin et al. 2014). This is because the upregulation of NLRP3 protein leads to a more potent inflammatory response. Furthermore, priming affects NLRP3 activation at the post-transcriptional level via deubiquitination of its LRR domain (Juliana et al. 2012, Lopez-Castejon et al. 2013, Py et al. 2013). Priming also triggers NLRP3 phosphorylation, which is essential for NLRP3 oligomerization (Song et al. 2017). Overall, priming signals regulate NLRP3 inflammasome activation through both transcription-dependent and -independent pathways.

1.4.3 ACTIVATING THE NLRP3 INFLAMMASOME: SIGNAL 2

The second activating signal is triggered by various chemical stimuli, such as particulate matter, extracellular ATP, K^+ ionophores, pathogen-associated RNA, and pore-forming toxins from bacteria and fungi (Kelley et al. 2019). These stimuli are biochemically dissimilar, and there is no evidence that NLRP3 directly interacts with any of them. Therefore, it is assumed that they induce a common cellular signal detected by NLRP3. NLRP3 stimuli induce ionic flux, mitochondrial dysfunction, ROS production, and lysosomal damage, which act as second messengers that induce assembly of the NLRP3 inflammasome (Kelley et al. 2019). K^+ efflux is a common event in cells treated with most NLRP3 stimuli triggering NLRP3 inflammasome assembly and activation. For instance, cytosolic reduction of K^+ concentrations mediates IL-1β release from macrophages and

monocytes in response to ATP or nigericin (Perregaux et al. 1994, Mariathasan et al. 2006). Assembly might be caused either by a mechanism downstream of K^+ efflux or by K^+ efflux-independent pathways (Groß et al. 2016, Sanman et al. 2016). Other findings indicate that NLRP3 proteins undergo conformational changes upon K^+ efflux (Meng et al. 2009, Muñoz-Planillo et al. 2013). In conclusion, it is suggested that K^+ efflux may be sufficient, but not necessary, for NLRP3 inflammasome activation. The mechanism by which the NLRP3 inflammasome senses changes in intracellular K^+ levels, or whether other proteins regulate its activation, is yet to be determined. Additionally, Ca^{2+} mobilization also plays a role in NLRP3 inflammasome activation (Kelley et al. 2019). Some NLRP3 stimuli induce changes in intracellular Ca^{2+} levels, and Ca^{2+} depletion inhibits IL-1β secretion (Brough et al. 2003, Feldmeyer et al. 2007, Chu et al. 2009). Multiple sources of Ca^{2+} have been reported to contribute to the increase in intracellular Ca^{2+} levels during NLRP3 activation. However, Ca^{2+} mobilization is probably not essential for assembly and subsequent activation. In addition to Ca^{2+}, the role of a second messenger is also linked to Na^+ and Cl^- (Kelley et al. 2019). As Na^+ influx and Cl^- efflux alone seem insufficient, a regulatory role via the modulation of K^+ efflux has been proposed for both ionic events. Additionally, ROS have been proposed as a common signal for NLRP3 inflammasome activation, since most stimuli can induce ROS in treated cells. However, the data situation remains ambiguous. In the case of particulate matter as an activating signal, lysosomal damage, which occurs after phagocytosis of particulate matter, appears to function as a cellular signal. The mechanism underlying the release of active lysosomal enzymes into the cytosol and their potential to trigger NLRP3 inflammasome activation remains unclear (Kelley et al. 2019).

1.5 CYTOKINES

1.5.1 INFLAMMASOME-DEPENDENT CYTOKINES

Cytokines are small signalling proteins that are produced and released by various cell types for instance upon activation via PRRs. They facilitate systemic effects and immune responses in nearby cells that express the corresponding cytokine receptors by altering the gene expression of several target genes and their TFs, including other cytokines, surface receptors, and their own expression (Mantovani et al. 2019, Hirano 2021). The activity of the target cell is influenced towards either a pro- or anti-inflammatory immune response by this process. The effects particularly depend on the extracellular abundance of the respective cytokine, the presence of the complementary receptor, and downstream signals, which vary by cell type. Cytokines typically contain a signal peptide that is necessary for their extracellular release. However, IL-1β and IL-18 do not contain this peptide (Mantovani et al. 2019). Only post-transcriptional processing via the NLRP3 inflammasome leads to a mature and biologically active form, which can exit the cytoplasm.

The expression of immature IL-1β is induced by LPS binding to TLR4, TNF-α binding to its respective receptor, or IL-1 binding to interleukin-1 receptor type 1 (IL-1R1). Pro-IL-1β mRNA levels rise rapidly within minutes (min) and persist over different periods of time depending on the stimuli. Subsequently, the IL-1β precursor accumulates in the cytosol (Schindler et al. 1990). The 31 kDa-sized precursor cannot bind to IL-1R1 and is therefore biologically inactive (Mosley et al. 1987). Extracellular ATP has been primarily associated with IL-1β maturation among the various signals that activate NLRP3 inflammasomes (Perregaux et al. 2000, Qu et al. 2007). When assembly of NLRP3 inflammasomes is induced, active caspase-1 processes the pro-form at two distinct sites, producing the mature 17 kDa-sized form and another product with an unknown function (Howard et al. 1991). The N-terminal region is believed to function as a regulatory switch, concealing the receptor binding site. Proteolytic processing occurs within a limited region in this area (Hazuda et al. 1991). This post-translational maturation step is the rate-limiting step in IL-1β processing.

IL-1β is a cytokine that mediates important inter-cellular communication, has a broad spectrum of biological functions, and targets a diverse range of cells (Mantovani et al. 2019). Mature IL-1β is released from the cell through exocytosis of the secretory lysosome (Andrei et al. 1999), direct transporters, shedding of plasma membrane microvesicles, or GSDMD-dependent pores (Qu et al. 2007). Its regulator, IL-1RA, is also released and competes for binding to IL-1R1. The receptor antagonist, which is structurally similar to IL-1β, can block access to the receptor without evoking signalling (Hannum et al. 1990). Additionally, decoy receptors and intracellular inhibitors are employed. Therefore, the potential of IL-1β signalling is affected by the relative amounts of IL-1β and its respective antagonists. ILRs share the TIR domain with TLRs and dimerize upon ligand binding, which induces the recruitment of MyD88 (Gay et al. 1991, Cao et al. 1996). As with TLR4, MyD88 forms a complex with IRAK, which recruits TRAF6. This leads to the activation of NF-κB, MAPK proteins, and other important TFs in the target cell. The production of various molecules, such as the enzymes cyclooxygenase type 2, phospholipase A2, or the mediators inducible nitric oxide synthase-mediated prostaglandin-E2, platelet activating factor, nitric oxide, chemokines, IL-1β itself, IL-6, TNF-α and IL-1R, alter the immunologic response locally (Mantovani et al. 2019). Additionally, IL-1β signalling causes metabolic, physiological, haematological, and immunological alterations on a systemic level. This leads to a lowered pain threshold, fever, vasodilatation, and hypotension. Dysregulation of IL-1β signalling poses a risk of contributing to the pathogenesis of several diseases.

Macrophages, as well as other cell types including non-haematopoietic cells, produce the pro-inflammatory cytokine IL-18. It is believed to be constitutively expressed in an inactive form. Upon NLRP3 activation, which depends on pro-inflammatory stimuli, caspase-1

processes pro-IL-18 into its biologically active form (Gu et al. 1997). Once released, IL-18 exerts its effects on target cells by binding to IL-1 receptor-related protein interleukin-18 receptor-related protein alpha (IL-18Rα), followed by the binding of interleukin-18 receptor-related protein beta (IL-18Rβ) to form a trimer (Yasuda et al. 2019). IL-18Rα expression is induced, and IL-18Rβ is constitutively expressed on the cell surface of T cells, Natural killer cells, and non-haematological cells such as epithelial cells and nerve cells. Both receptor chains contain intracellular TIR domains, like TLR4 and IL-1R1. Consequently, intracellular IL-18R signalling is similar to that of IL-1R and TLR4. IL-18 binding activates NF-κB and MAPKs via the MyD88 pathway, inducing mostly the production of IFN-γ in the target cell. IFN-γ is necessary for macrophage polarization and for activation into an antigen-presenting cell. However, co-stimulation with IL-12 essentially enhances IL-18-mediated IFN-γ production. IL-18 regulates the production of several pro-inflammatory cytokines in distinct cell types, depending on the co-stimulating cytokines (Yasuda et al. 2019). This results in the pleiotropic properties of IL-18.

1.5.2 INFLAMMASOME-INDEPENDENT CYTOKINES

IL-6 is a pro-inflammatory cytokine that plays important roles in immune responses, haematopoiesis, bone metabolism, and embryonic development. Its gene expression can be triggered by various TLR ligands, IL-1β, TNF-α, ROS, and Zinc, and is mediated by NF-κB, signal transducer and activator of transcription proteins 3 (STAT3), and other key TFs (Hirano 2021). Epigenetic regulation also affects gene expression (Hu et al. 2016). Several post-transcriptional mechanisms regulate the stability of *IL6* mRNA. In response to LPS, IL-1β, and IL-6, a unique RNA-binding protein controls *IL6* mRNA stability by inhibiting ribonuclease-mediated degradation (Masuda et al. 2013). Positive feedback loops involving microRNAs that enhance NF-κB activity and proteins that block microRNAs, which induce IL-6 mRNA degradation, are activated via NF-κB (Iliopoulos et al. 2009, Iliopoulos et al. 2010). The synthesized IL-6 protein is biologically active and contains the signal peptide necessary for its extracellular release. Upon release, IL-6 can bind to target cells through the IL-6 receptor, which consists of membranous interleukin-6 receptor subunit alpha (IL-6Rα) and the signal transducer interleukin-6 receptor subunit beta (IL-6Rβ) containing an intracellular signalling domain (Hirano 2021). This binding model is limited to immune cells and hepatocytes that express both molecules. However, IL-6 has diverse functions that are divided by 'trans-signalling' and 'trans-presentation'. The latter occurs when IL-6, bound to IL-6Rα on one cell, acts on another cell expressing IL-6Rβ (Heink et al. 2017). During infection, sIL-6Rα enables ‘trans-signalling’ in cells that only express IL-6Rβ, such as endothelial cells, fibroblasts, and heart muscle cells (Lust et al. 1992). When a signal is initiated, the complex recruits the Janus kinase to IL-6Rβ, resulting in the phosphorylation of IL-6Rβ residues. This phosphorylation activates either STAT3 or the Notch- or

MAPK/NF-κB pathways depending on adaptor molecules (Hirano 2021). These pathways have an impact on each other and are negatively regulated by several molecules. STAT3 functions as a TF upon autophosphorylation, and together with the MAPK pathway, it mediates cell survival, proliferation, metastasis, and angiogenesis. The Notch pathway is important in cell differentiation. This results in the production of neutrophils in the bone marrow, growth of B cells, and suppression of regulatory T cells (Hirano 2021). IL-6 plays a crucial role in inducing fever and synthesising acute phase proteins. These proteins rapidly increase or decrease in blood plasma in response to inflammation evoking systemic immune reactions, such as fever, increased neutrophils circulation and accelerated peripheral leukocytes (Mantovani et al. 2023).

The pro-inflammatory cytokine TNF-α is released in response to infection or trauma via TLR-induced production. Activated monocytes, macrophages, lymphocytes, and other cell types generate the protein as a homotrimeric membrane-bound TNF-α, which is then cleaved into a monomer called soluble TNF-α (Dostert et al. 2019). The residual cytoplasmic domain of membrane-bound TNF-α migrates into the nucleus after cleavage. tumour necrosis factor receptor 1 (TNFR1) and TNFR2 mediate soluble TNF-α signalling. TNFR1 is expressed ubiquitously, while TNFR2 is expressed only on endothelial, neuronal, and immune cells. Both receptors bind adaptor proteins via their intracellular domain and mediate cellular effects upon TNF-α binding (Dostert et al. 2019). TNFR1 binds to the adaptor protein TNFR type 1-associated death domain protein via its death domain (Hsu et al. 1995). The TNFR type 1-associated death domain protein is a central scaffolding protein in the signalling complexes subsequently formed by several proteins, directing downstream signalling events. Receptor-interacting serine/threonine-protein kinase 1 is a crucial protein in all complexes and its activity is highly regulated by its ubiquitination status (Dostert et al. 2019). Ubiquitinated receptor-interacting serine/threonine-protein kinase 1 leads to the activation of NF-κB and c-Jun N-terminal kinases, resulting in the production of pro-inflammatory molecules and activation of survival pathways. Non-ubiquitinated receptor-interacting serine/threonine-protein kinase 1 forms complexes with pro-caspase-8, which is activated and triggers apoptosis. TNFR2 lacks the death domain and, therefore, cannot bind the TNFR type 1-associated death domain protein. The receptor interacts directly with proteins that are also part of TNFR1 complexes but with weaker binding affinity (Grech et al. 2005). Although both receptors activate NF-κB, TNFR2 is a weaker activator. The pleiotropic properties of soluble TNF-α result in its ability to induce cell death and inflammation via TNFR1 or cellular survival and tissue regeneration by binding to TNFR2. membrane-bound TNF-α is believed to signal primarily through TNFR2, playing a role in anti-inflammatory responses and cell proliferation.

Some cytokines possess anti-inflammatory properties, protecting the host from exaggerated responses to pathogens. They play crucial roles in wound healing, homeostasis, autoimmunity, and cancer development. IL-10 is an important anti-inflammatory cytokine that is produced by a variety of immune cells, including monocytes and macrophages, as well as some non-haematopoietic cells (Saraiva et al. 2020). The expression of IL-10 is induced in immune cells upon stimulation of several PRRs, including TLR4, and is mainly mediated by the MAPK pathway, including the MAPK p38. The production of IL-10 is also mediated by NF-κB activation downstream of PRR. IL-10 can regulate its own expression through a negative feedback loop by inhibiting the p38 pathway. Additionally, some IFNs have been shown to enhance IL-10 production at the post-transcriptional level by regulating mechanisms that stabilize IL-10 mRNA. After release, IL-10 induces cellular responses by binding to a heterodimeric receptor composed of two interleukin-10 receptor subunit alpha (IL-10Rα) and two IL-10Rβ proteins. The high-affinity IL-10Rα is mainly expressed in leukocytes, particularly macrophages, and is responsible for binding IL-10. This engagement leads to oligomerization with the ubiquitously expressed IL-10Rβ, allowing phosphorylation of the cytoplasmic tail of IL-10Rα, which is necessary for the recruitment of STAT3. Upon phosphorylation, STAT3 translocates to the nucleus and initiates a specific transcriptional program. The involvement of STAT3 in anti-inflammatory IL-10 and pro-inflammatory IL-6 signalling might be possible due to its cooperation with selective cofactors, resulting in distinct functions as a TF. The IL-10-mediated anti-inflammatory response involves the modulation of the local cytokine microenvironment by inhibiting the transcription of genes for cytokines, chemokines, costimulatory molecules, and adhesion molecules. IL-10 also limits antigen presentation, thereby preventing efficient development of T cell responses. Furthermore, IL-10 signalling inhibits the production and release of ROS intermediates and nitric oxide by the target cell (Saraiva et al. 2020).

2 P2X RECEPTORS WITHIN THE INNATE IMMUNE SYSTEM

2.1 GENERAL INFORMATION ABOUT P2 RECEPTORS

As previously mentioned, extracellular ATP induces inter alia K^+ efflux, which serves as a stimulus for the assembly of the NLRP3 inflammasome. ATP, which functions as a universal energy currency, is generated through glycolysis and oxidative phosphorylation, and typically reaches very high concentrations intracellularly, while only trace amounts are present in the extracellular space (Di Virgilio et al. 2020). This creates a strong gradient, both electrical and chemical, that would theoretically drive ATP out of the cell. Therefore, any breach of the plasma membrane integrity immediately results in passive ATP efflux. During inflammation, ischemic, or hypoxic tissue conditions, ATP levels can rise to several

tens or hundreds of micromoles per litre. Additionally, inflammatory or apoptotic cells contribute to the accumulation of extracellular ATP by releasing it through active mechanisms involving various vesicle- and channel-mediated pathways (Di Virgilio et al. 2020). In the inflammatory microenvironment, ATP functions as a DAMP and has multiple effects, such as activating the NLRP3 inflammasome, promoting the release of cytokines, chemokines, and growth factors, potentiating intracellular pathogen killing, promoting the migration of inflammatory cells, redirecting T-helper cell differentiation, stimulating the growth of stromal cells, and causing direct cytotoxicity (Di Virgilio et al. 2020).

Extracellular ATP mediates its effects through the binding to purinergic P2 receptors, which are categorized into two subgroups, termed P2X and P2Y purinoceptors (Burnstock et al. 1985, Valera et al. 1994). The P2Y subgroup consists of eight receptors, whereas seven mammalian P2X subtypes (P2X purinoceptor 1 (P2RX1) – P2RX7) have been identified (Di Virgilio et al. 2020). Metabotropic P2Y receptors bind ATP, ADP, UTP, and UDP, but the ionotropic P2X receptors bind predominantly ATP. The receptors exhibit different agonist affinity, ranging from low micromolar (most P2Y receptors) to millimolar levels (P2RX7). Upon ligand binding, G protein-coupled P2Y receptors activate phospholipase C, which initiates the production of mediators that increase intracellular Ca^{2+} or cyclic adenosine monophosphate levels (Giuliani et al. 2019). This can impact cell metabolism, such as autophagy initiation or regulation, ATP production, and apoptosis. P2X receptors, on the other hand, undergo conformational changes upon ligand binding, leading to the opening of a channel pore that is selective for Na^+, K^+, and Ca^{2+}. Na^+ and Ca^{2+} influx as well as K^+ efflux result in plasma membrane depolarization (Kanellopoulos et al. 2021). The ion fluxes induce signal transduction, which mediate distinct cellular responses. However, ATP signalling must be regulated to prevent overstimulation. Therefore, all cells are equipped with potent ectonucleotidases, which work as a negative feedback by degrading ATP to adenosine, a potent immunosuppressant (Beukers et al. 1993). Additionally, desensitization occurs when the receptor exhibits a decreased responsiveness upon repeated or chronic exposure to agonists. In the case of P2X receptors, P2RX1 and P2RX3 fully desensitize rapidly, while P2RX2, P2RX4, and P2RX5 show intermediate desensitization rates (Kanellopoulos et al. 2021). The P2RX7 has not only the lowest agonist affinity (EC_{50} 0.5 – 4 mM) but is also unable to desensitize (Surprenant et al. 1996, Chessell et al. 1998, Young et al. 2006, Young et al. 2007). P2X receptors can occur in three different states: the resting, closed state in the absence of an agonist, the open ATP-bound state, and the desensitized state (Hausmann et al. 2015). The desensitization rate determines the period of P2X receptors signal transduction and is therefore of high physiological relevance.

P2 receptors are widely expressed in various tissues and play a significant role in many pathophysiological processes, such as tissue homeostasis, wound healing,

neurodegeneration, inflammation, and cancer (Giuliani et al. 2019). This variety of functions can be fulfilled by the P2 receptor family due to the range of diverse subtypes with distinct nucleotide selectivity and varying agonist affinity (Di Virgilio et al. 2020). For instance, in the context of inflammation, P2RY1, P2RY2, P2RY6, and P2RX4 and P2RX7 are the most prominent P2 receptors, whereas P2RX7 has been extensively linked to numerous inflammatory and immune responses, such as contributing to K^+ efflux and subsequent NLRP3 assembly (Di Virgilio et al. 2020). P2RX4 also plays a crucial role in the central nervous system, where it is involved in synaptic transmission and neuropathic and inflammatory pain (Montilla et al. 2020).

2.2 EXPRESSION AND IMMUNOLOGICAL FUNCTION OF P2RX4 AND P2RX7

2.2.1 P2RX4

P2RX4 is not only localized at the cell surface, but also in lysosomes. For instance, in cultured rat microglial, vascular endothelial cells, and freshly isolated peritoneal macrophages, endogenous P2RX4 is predominantly found in lysosomes (Qureshi et al. 2007). The relative amounts of a pH-sensitive tagged P2RX4 construct at the plasma membrane and in lysosomes depends on the cell type while lysosomes always contain a larger fraction of the P2RX4 construct when comparing the embryonic kidney cell line HEK293, a murine microglial cell line, primary murine hippocampal neurons, and primary rat alveolar cells (Xu et al. 2014). Under physiological conditions, the acidic pH inhibits the P2RX4. However, when ATP is transported across the lysosomal membrane to the luminal side via a vesicular nucleotide transporter, ATP molecules increases the luminal pH causing ATP and P2RX4 activation (Huang et al. 2014). P2RX4 localization to lysosomes and activation appears to play a role in endolysosomal membrane fusion, as P2RX4-mediated Ca^{2+} release activates calmodulin, a fusion-promoting protein (Cao et al. 2015).

P2RX4 is ubiquitously expressed across the body with diverse functions in various organs, including the liver, lungs, heart, kidneys, and central nervous system (CNS) (Kanellopoulos et al. 2021). In the liver, P2RX4 signalling might be involved in tissue recovery after partial hepatectomy but also has pro-fibrogenic effects in a model of chronic injury. It is involved in surfactant secretion and fluid resorption in the lungs, and in the heart, P2RX4 stimulation offers a cardioprotective effect. P2RX4 plays a role in inflammation in the kidneys, exacerbating NLRP3-associated kidney diseases (Kanellopoulos et al. 2021). The P2RX4 is abundantly expressed in neurons and glial cells, where it contributes to physiologic synaptic transmission and neuronal plasticity due to its high affinity for ATP (Montilla et al. 2020). However, P2RX4 upregulation in CNS cells is also associated with various disorders, such as neuropathic pain, epilepsy, ischemic injury, chronic pain, and anxiety. In addition, upregulation in microglial cells is common in most acute and chronic neurodegenerative

diseases associated with inflammation, including Parkinson's disease, Alzheimer's disease, and multiple sclerosis (Montilla et al. 2020). For instance, this upregulation was observed in multiple studies in rodent experimental autoimmune encephalomyelitis (Masuda et al. 2012, Masuda et al. 2014, Vázquez-Villoldo et al. 2014, Zabala et al. 2018). Upregulation of P2RX4 in microglial or infiltrating macrophages is also associated with inflammatory responses during ischemic brain injuries (Montilla et al. 2020). The role of the receptor is, however, not entirely clear. While P2RX4 signalling seems to have a protective effect in experimental autoimmune encephalomyelitis by decreasing the expression of pro-inflammatory mediators in microglial (Zabala et al. 2018), P2RX4 signalling in ischemic brain injuries possibly contributes to infarct volume (Xiao et al. 2016). In spinal cord injury, P2RX4 activation leads to IL-1β production and infiltration of neutrophils and monocyte-derived M1 macrophages (Rivero Vaccari et al. 2012).

More recently, a role for P2RX4 in inflammation has emerged beyond the CNS. For instance, P2RX4 stimulation by low doses of ATP potentiates degranulation of murine bone marrow-derived mast cells, which is a crucial function of mast cells during allergic inflammatory reactions (Yoshida et al. 2017, Yoshida et al. 2020). Additionally, P2RX4 expression in murine lungs is associated with allergen-induced airway inflammation (Zech et al. 2016). Silencing P2RX4 in murine experimental rheumatoid arthritis improves disease-associated symptoms by significantly inhibiting synovial inflammation and joint destruction (Li et al. 2014). The mice also seem to have reduced serum levels of IL-1β, TNF-α, and IL-6 (Li et al. 2014). On a cellular level, P2RX4-induced Ca^{2+} influx is required for effective production of IL-1β and IL-18 via activation of P2RX7 in bone marrow-derived dendritic cells (Sakaki et al. 2013, Zech et al. 2016). However, in the context of diabetic nephropathy or experimental renal ischemia/reperfusion injury, P2RX4 might directly induce NLRP3 assembly, caspase-1 activation and subsequent IL-1β and IL-18 release after stimulation with extracellular ATP (Chen et al. 2013, Han et al. 2020). However, the comparison of purinergic receptor expression levels and activation between primary rhesus macaque microglial and bone marrow-derived macrophages (BMDMs), indicates, that ATP-induced IL-1β release from microglial depends on both P2RX4 and P2RX7 signalling, whereas release from BMDMs is independent of P2RX4 (Burm et al. 2016). Taken together, P2RX4 presumably plays a significant role in the ATP-induced NLRP3 inflammasome assembly and activation. However, this function is not thoroughly investigated and seems to differ among different cell types and tissues and possibly depends on a functional P2RX7.

2.2.2 P2RX7

Although P2RX7 is expressed on the plasma membrane of most murine and human cells, expression levels are particularly high in immune cells, where P2RX7 signalling is important for modulating both the innate and adaptive immune responses (Pelegrin 2021). Early on, P2RX7 was identified as the receptor mediating the effect of extracellular ATP, which strongly stimulates the release of IL-1β from murine macrophages (Ferrari et al. 1996, Ferrari et al. 1997). The discovery of the NLRP3 inflammasome finally placed P2RX7 in the right place, and to date, P2RX7 has been described as one of the most potent activators of the NLRP3 inflammasome (Pelegrin 2021). Although the P2RX7 shows very limited basal activity and low affinity for ATP, ATP concentrations high enough to induce significant activation are not unusual at inflammatory sites where extensive immune cell activation and tissue damage occur (Pellegatti et al. 2008, Wilhelm et al. 2010). Several studies have shown that P2RX7 is involved in ATP-dependent IL-1β maturation and release from LPS-primed murine peritoneal macrophages, BMDMs, and microglial cells, human monocytes and macrophages (Ferrari et al. 1996, Ferrari et al. 1997, Perregaux et al. 2000, Solle et al. 2001, Qu et al. 2007, Adinolfi et al. 2015). The most important events leading to NLRP3 assembly and activation that are induced by P2RX7 are the production of ROS, the depolarization of mitochondria, the destabilization of lysosomes, the intracellular Ca^{2+} increase, and the decrease in intracellular K^+. K^+ efflux mediated by P2RX7 is one of the key fundamental steps in NLRP3 activation, although the exact underlying molecular mechanisms remain unclear (Pelegrin 2021). P2RX7 and NLRP3 possibly physically interact at discrete subplasmalemmal cytoplasmic sites (Franceschini et al. 2015). Otherwise P2RX7 channel opening might causes a localized modification of the intracellular ion microenvironment that drives the recruitment and subsequent assembly of inflammasome components, because K^+ efflux enhances the interaction of NLRP3 with the never in mitosis-A-related kinase 7 (NEK7) protein, a crucial NLRP3 inflammasome activator (He et al. 2016, Schmid-Burgk et al. 2016, Shi et al. 2016).

Furthermore, P2RX7 plays not only a role in the induction of IL-1β maturation but is also involved in the formation of multivesicular bodies containing mature IL-1β. Multiple studies demonstrated that various cell types shed microvesicles containing IL-1β from their plasma membrane upon P2RX7 activation (MacKenzie et al. 2001, Bianco et al. 2005, Pizzirani et al. 2007, Qu et al. 2007). Stimulation of P2RX7 also induces the release of chemokines and TNF-α, CD14, IL-6 amongst many other cytokines via microvesicles (Shieh et al. 2014, Torre-Minguela et al. 2016). Additionally, P2RX7 stimulation supports additional ATP release, which then activates P2RX7 again in an autocrine manner. This results in an increase in sensitivity to ATP of the P2RX7-associated pore and in an amplified production of pro-inflammatory substances downstream of P2RX7 signalling (Pellegatti et al. 2005,

Yang et al. 2015). Playing a role in NLRP3 assembly, release of IL-1β and other cytokines as well as chemokines shows that P2RX7 contributes to the recruitment and activation of immune cells thereby modulating immune responses. This clear association of P2RX7 with inflammatory processes also shows its profound role in pathophysiological conditions such as muscular dystrophy, allograft rejection, graft-versus-host disease, and sterile liver inflammation (Sinadinos et al. 2015, Di Virgilio et al. 2017).

2.3 MOLECULAR STRUCTURE OF P2X RECEPTORS

2.3.1 GENERAL MOLECULAR STRUCTURE OF P2X RECEPTORS

All subtypes of P2X receptors bind ATP and subsequently undergo conformational changes that result in pore opening. The receptors consist of a large disulfide-rich extracellular loop containing N-linked glycosylation moieties and a ATP binding pocket, as well as two transmembrane domains (TM1 and TM2) forming the ion channel, and an intracellular N and longer C terminus (Kawate et al. 2009, Hattori et al. 2012, Mansoor et al. 2016). To form a functional receptor, three P2X receptors proteins are arranged around a channel pore. All P2X receptor proteins form heterotrimers except P2RX7, for which only homotrimers have been described so far. P2RX4 forms heterotrimers predominantly with P2RX5 and/or P2RX6, but also heterotrimers with P2RX1 and P2RX3 have been described (Torres et al. 1999, Antonio et al. 2014). Analysis of the crystal structure of P2RX4 and mutagenesis studies have led to the assumption that specific information for homomeric subunit-subunit interactions must be located in the ectodomain (Kawate et al. 2009, Hattori et al. 2012, Hausmann et al. 2015).

The trimeric structure of P2X receptors indicates the presence of three ATP binding sites. However, it is essential to note that these binding sites are not independent, and only a fully agonist-ligated channel that has bound three ATP molecules is sufficiently activated (Hattori et al. 2012). The binding sites are located at the interface of each pair of subunits and consist of a set of conserved residues in all human and rodent P2X receptors subtypes (Dal Ben et al. 2015). Upon ligand binding, the inter-subunit cavities tighten, and the monomers undergo an outward flexing and rotation, which alters the reciprocal orientation without altering the conformation (Hattori et al. 2012, Hausmann et al. 2015). This movement results in the crucial expansion of the extracellular region outside the channel pore, which is connected to the motion of the three TM1 and three TM2 helices, thereby generating the ion channel pore (Kawate et al. 2009, Hausmann et al. 2015). The few intramembrane contacts between the TM2 helices stabilize the closed channel but break in response to ATP when the TM helices move away from the central axis. Following this movement, new intra-subunit contacts occur, which stabilize the open channel (Hattori et al. 2012, Hausmann et al. 2015). The role of the N- and C-terminal domains varies between the

subtypes and is not yet fully determined. However, it is worth noting that a protein kinase C phosphorylation consensus site is conserved in all P2X receptors at the N terminus (Boué-Grabot et al. 2000). Furthermore, studies investigating different desensitization rates of P2X receptors subtypes suggest that these rates are primarily determined by TM domains as well as the intracellular domains (Werner et al. 1996, Koshimizu et al. 1999, He et al. 2002, Allsopp et al. 2011b).

According to Dal Ben et al., human P2X receptors exhibit varying degrees of sequence homology among their subtypes. The average sequence identity value, excluding the N- and C-termini, is 49.5 %, while excluding the TM domains, it is 47.3 % (Dal Ben et al. 2015). Ten conserved cysteines within the extracellular loop are identified, forming five disulfide bonds that significantly contribute to the structure of the loop and ATP binding pocket (Clyne et al. 2002, Ennion et al. 2002, Rokic et al. 2010). Notably, there is greater sequence conservation in the depth of the ATP cavity than at its entrance, which exhibits more variability. The inner part of the pocket comprises polar and/or positively charged residues that interact with the polar groups of ATP (Dal Ben et al. 2015). One subunit possesses three conserved lysine residues directly interacting with the phosphate groups of ATP, a conserved threonine providing a double H-bond interaction with the adenine, and a conserved glycine. The adjacent subunit contributes a conserved glycine, lysine, asparagine, and an arginine to the ATP binding cavity. These conserved residues provide polar interactions with the phosphate groups of ATP and in-between the P2X subunits thereby establishing a solid H-bond network in the depth of the pocket (Jiang et al. 2000, Fischer et al. 2007, Roberts et al. 2008, Roberts et al. 2009, Allsopp et al. 2011a, Dal Ben et al. 2015).

2.3.2 CHARACTERISTIC FEATURES OF P2RX4

The molecular structure of P2RX4 has been thoroughly investigated using the crystal structure of zebrafish P2RX4 (Kawate et al. 2009, Hattori et al. 2012), and is partially confirmed for the rat P2RX4 by Igawa et al. (2015). These studies have provided a foundation for structural analyses of the whole P2X receptor family; however, certain details only pertain to P2RX4. Hattori and Gouaux revealed that the phosphate oxygens of ATP bind to K70 and K72 of one subunit and to N296, R298, and K316 of the adjacent subunit within the binding pocket. The adenine base interacts with L191 and I232 and forms hydrogen bonds with the side chain and backbone of T189 and the backbone of K70 (Hattori et al. 2012). The fact that the negatively charged phosphate groups of ATP interact with highly conserved basic and polar amino acids underlines the findings, which were discussed in 2.2.1, that lysosomal P2RX4 is inactive when ATP is not in its active, tetra-anionic form at a lysosomal pH between 3.5 and 5.0. P2RX4 opens a small cation-permeable channel pore in the presence of extracellular Ca^{2+} but forms a larger pore allowing larger molecules

like propidium iodide and ethidium bromide to pass in the absence of Ca^{2+} indicating that the extracellular domains are involved in the permeability dynamics of the P2RX4 (Shinozaki et al. 2009).

As previously mentioned, P2RX4 is preferentially localized in lysosomes, where it is shielded from proteolysis by approximately six N-linked complex oligosaccharides (Qureshi et al. 2007). A tyrosine-motif in the C-terminus and the residues L22 and I23 at the N-terminus are required for P2RX4 localization to lysosomes, as mutations in the tyrosine-motif and/or mutations of the respective residues at the N-terminus to alanine increase the amounts of P2RX4 at the plasma membrane (Qureshi et al. 2007). Another motif in the C-terminus is required for endocytosis via a clathrin-dependent pathway, as this motif binds to a subunit of the clathrin adaptor complex (Royle et al. 2002). Furthermore, the residues K373 and Y374 at the C-terminus between the motifs involved in trafficking contribute to desensitization properties (Fountain et al. 2006). Replacing the lysine with arginine or cysteine at position 373 and the tyrosine with phenylalanine at position 374 strongly advances desensitization kinetics, suggesting that P2RX4 desensitization properties require an amino group rather than a guanidine group at position 373 and an aromatic moiety at position 374 (Fountain et al. 2006). Nonetheless, characteristics of the N- and C-termini cannot be validated by crystal structure of the zebrafish P2RX4, as the crystal structure constructs are missing both termini (Kawate et al. 2009, Hattori et al. 2012).

2.3.3 CHARACTERISTIC FEATURES OF P2RX7

P2RX7 is distinguished from other P2X receptors not only by its low sensitivity to ATP and the lack of being able to desensitize, but also by the fact that only functional homomeric complexes have been described thus far (Di Virgilio et al. 2017). Nonetheless, P2RX7 oligomers may incorporate additional subunits to form hexamers, particularly in the presence of positive allosteric modulators (Kim et al. 2001, Ferrari et al. 2004). The entrance of the ATP binding pocket of P2RX7 lacks positively charged amino acids resulting in hindered access for hydrophilic molecules compared to other P2X receptors (Dal Ben et al. 2015). Additionally, P2RX1 to P2RX5 feature a serine near the alpha phosphate group of ATP and a conserved lysine that interact with each other, whereas in the human P2RX7, a tyrosine replaces the serine. The larger volume of tyrosine compared to serine may decrease the cavity volume (Dal Ben et al. 2015). This might explain why P2RX7 has a lower affinity for ATP compared to other P2X receptors.

The fact that P2RX7 is not able to desensitize correlates with the observations that P2RX7 activation leads not only to the common cationic transmission, but also to an uptake of large hydrophilic molecules with sizes up to approximately 900 Dalton upon prolonged stimulation, which is reversible upon removal of the ATP stimulus (Munerati et al. 1994,

Falzoni et al. 1995). It was proposed that pore-forming partners such as pannexin-1 are recruited for increased permeability. However, macrophages from pannexin-1-deficient mice exhibit permeability increases to a similar extent as macrophages from wild-type mice after stimulation with ATP (Qu et al. 2007, Alberto et al. 2013). Moreover, recent studies question the notion that dilation of the P2RX7 pore occurs only upon prolonged stimulation, but rather suggest that the P2RX7 pore is wide enough in general (Harkat et al. 2017, Pippel et al. 2017). Anyhow, the C-terminal tail of P2RX7 is longer than the C-termini of other P2X receptors and is absolutely required for the large pore function of the P2RX7 (Surprenant et al. 1996, Adinolfi et al. 2010).

ATP binding to P2RX7 may cause reorientation of the three monomers so that a 'cytoplasmic gap' is formed by the interaction between the N- and C-termini, which partially covers the cytoplasmic end of the pore and stabilizes the open state (Mansoor et al. 2016). Perhaps, the prolonged C-terminal tail is needed to support TM2 movement generating the large pore, to stabilize the 'cytoplasmic gap', or to allow maximal ion permeability (Mansoor et al. 2016). Furthermore, the C-terminus of P2RX7 contains several identified lipid and protein binding motifs, including a SRC homology 3 domain, a short homology to TNFR1 with a death domain, two small regions that are homologous to interaction sites with the cytoskeleton, and a region at the far C-terminal end that shows homology with the LPS-binding region of LBP (Denlinger et al. 2001). More than 50 proteins physically interacting with P2RX7 have been identified so far, however, their binding sites as well as roles in receptor signalling remain unknown (Kopp et al. 2019). Some identified interactions might also be indirect or due to the association of multiprotein complexes in domains of the membrane. Furthermore, targeted rather than unbiased screening approaches and heterologous expression systems with overexpressed interaction partners have been frequently used for interactions studies. Therefore, the resulting data must be interpreted with caution. Kopp and colleagues therefore conclude that the P2RX7 C-terminus might have a more structural role and/or serves as a scaffold for temporary interactions in which Ca^{2+} signalling and interactions with membrane components play the prominent role (Kopp et al. 2019).

Additionally, ten splice variants of the human P2RX7 have been identified, with four being C-terminally truncated (P2RX7B, P2RX7C, P2RX7E, P2RX7G) (Cheewatrakoolpong et al. 2005, Feng et al. 2006). P2RX7A represents the full-length receptor, while the variants P2RX7G and P2RX7H contain an additional insertion that results in the deletion of TM1. P2RX7C is missing exon 4, P2RX7D is missing exon 5, P2RX7E is missing exons 7 and 8, and P2RX7F is missing exons 4 and 8. P2RX7I arises from a point mutation that generates a null allele, and P2RX7J is truncated and non-functional (Di Virgilio et al. 2017). It is noteworthy that P2RX7B is the predominant transcript in many tissues. P2RX7B monomers

lack the large pore function but retain channel activity, while heteromerization with P2RX7A subunits produces an enhanced response compared to homomeric P2RX7A (Cheewatrakoolpong et al. 2005, Adinolfi et al. 2010).

2.4 INTERACTION BETWEEN P2RX4 AND P2RX7

P2RX4 forms heterotrimers, while P2RX7 forms solely homotrimers. Nonetheless, because P2RX4 and P2RX7 both seem to play a role in NLRP3-mediated immune responses, these conclusions are still on debate. Successful co-immunoprecipitation of P2RX7 with tagged rat P2RX4 from transfected HEK293 cells or with endogenous murine P2RX4 from BMDMs suggest the possibility of heteromerization (Guo et al. 2007). Contradictive is that co-immunoprecipitation of membranes from cells co-transfected with tagged P2RX4 and tagged P2RX7 does not reveal heterotrimers (Antonio et al. 2011). In addition, lysates from different tissues or primary cultures of rat microglial and macrophages reveal only homotrimers (Nicke 2008, Boumechache et al. 2009). Measuring electrophysiological properties of ATP-induced currents also results in conflicting observations (Casas-Pruneda et al. 2009, Schneider et al. 2017). While cells transfected with different ratios of P2RX4 and P2RX7 cDNA show novel electrophysiological properties (Casas-Pruneda et al. 2009), *Xenopus laevis* oocytes co-expressing human P2RX4 and P2RX7 exhibit no new electrophysiological phenotype different from that of one or another receptor alone (Schneider et al. 2017). Furthermore, P2RX4 and P2RX7 exhibit different current kinetics in murine microglial cells indicating that the receptors are activated independently (Trang et al. 2020). It is worth noting, however, that some observations suggesting heterotrimerization may be due to an association between P2RX4 and P2RX7 homotrimers rather than the production of heterotrimers (Antonio et al. 2011).

However, several studies have reported functional interactions between the P2RX4 and P2RX7. For instance, P2RX4 activation potentiates P2RX7-mediated IL-1β release by either inducing an early increase in Ca^{2+} influx enhancing the influx upon P2RX7 stimulation (Kawano et al. 2012, Sakaki et al. 2013) or by upregulating P2RX7 expression (Zech et al. 2016). P2RX7-dependent Ca^{2+} influx is also associated with non-selective pore formation and activation of signal transduction leading to cell death (Kawano et al. 2012). Therefore, P2RX4-mediated Ca^{2+} influx may also promote P2RX7-dependent cell death (Kawano et al. 2012). However, some studies described in chapter 2.2.1 suggest that P2RX4 could also mediate these inflammatory responses independent of P2RX7.

Taken together, without definitive evidence supporting physical or functional interactions between P2RX4 and P2RX7, it is not possible to say whether P2RX4-mediated signalling is a support for P2RX7-dependent inflammation, or whether it may elicit additional independent inflammatory responses in immune cells.

3 AIM OF THIS WORK

The role of the P2RX7 in the activation of the NLRP3 inflammasome and the subsequent release of mature IL-1β is well-described (chapter 2.2.2). More recently, the hypothesis that P2RX4 also plays a role in this mechanism emerged, as several studies have shown that knockdown or inhibiting the P2RX4 decreases the ATP-dependent IL-1β release. However, most of these studies focused on murine but not on human cells or tissues (chapter 2.2.1). Further, the role of P2RX4 and P2RX7 in the priming of mononuclear phagocytes, which is the major driver of IL-1β responses in any immunological setting, is largely unknown. This exploratory study is designed to give first answers to the following questions (**Figure 1**):

I. **Which role plays the P2RX4 in the ATP-dependent IL-1β maturation?**

II. **Which role play P2RX4 and P2RX7 in the priming of human mononuclear phagocytes?**

III. **Which effect has the P2RX4 antagonist 5-B on apoptosis?**

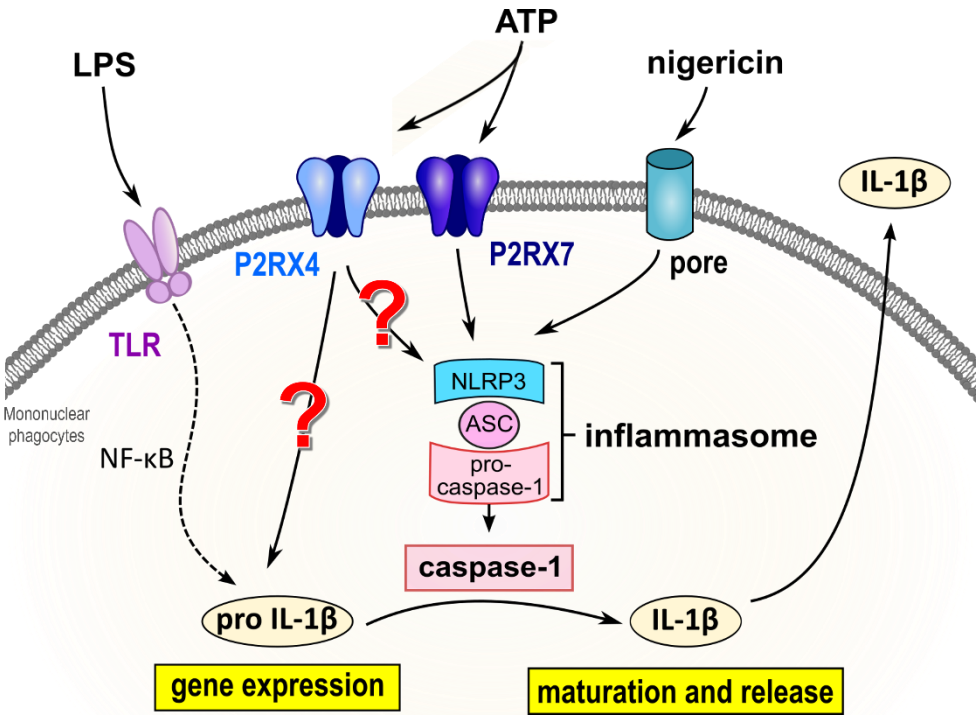

Figure 1: Schematic overview of IL-1β processing and maturation. LPS primes the cell by binding to TLR4 and inducing the gene expression of pro-IL-1β inter alia via NF-κB signalling. Extracellular ATP binds to the P2RX4 and P2RX7 and the bacterial toxin nigericin induces pore formation in the plasma membrane of the activated cell. Stimulation with ATP or nigericin both induce the assembly of NLRP3, ASC, and pro-caspase-1 to the NLRP3 inflammasome. As a result, pro-caspase-1 is cleaved into its active form and cleaves pro-IL-1β into the mature IL-1β, which is then released from the cell. LPS, lipopolysaccharide; TLR, toll-like receptor; NF-κB, nuclear factor 'kappa-light-chain-enhancer' of activated B-cells; IL-1β, interleukin-1β; ATP, adenosine triphosphate; P2RX4/7, P2X purinoceptor 4/7; NLRP3, NLR family pyrin domain-containing protein 3; ASC, Apoptosis-associated speck-like protein containing a caspase-recruitment domain.

These questions are tackled to gain more insight into the possible involvement of the P2RX4 in IL-1β expression and processing. For this purpose, the monocytic THP-1 cell line as well as THP-1 cell-derived macrophages are used. Additionally, primary human peripheral blood mononuclear cells (hPBMCs) and human peritoneal macrophages (hPMs) are used to validate the findings made with the cell line. Mononuclear phagocytes secrete IL-1β upon a first signal inducing pro-IL-1β expression and a second signal inducing the assembly of the NLRP3 inflammasome, IL-1β maturation and release (**Figure 1**).

To investigate the role of P2RX4 and P2RX7, the following antagonists of the receptors are utilized: 5-(3-Bromophenyl)-1,3-dihydro-2H-benzofuro[3,2-e]-1,4-diazepine-2-one (**5-B**), PSB-15417 (**PSB**), PZB15517166A (**PZB15**), and PZB13420052A (**PZB13**) are P2RX4 antagonists and 3-[[5-(2,3-Dichlorophenyl)-1H-tetrazol-1-yl]methyl]pyridine hydrochloride (**A43**) and 2-(Phenylthio)-N-[[tetrahydro-4-(4-phenyl-1-piperazinyl)-2H-pyran-4-yl]methyl-3-pyridinecarboxamide (**JNJ**) are P2RX7 antagonists. The influence of the P2RX4 and P2RX7 on the NLRP3 assembly and subsequent IL-1β release is investigated by priming human mononuclear phagocytes and adding the antagonists right before the second stimulus. 2'(3')-O-(4-Benzoylbenzoyl)adenosine-5'-triphosphate (BzATP)/ATP or nigericin are used as second stimuli to compare the ATP-dependent and ATP-independent NLRP3 inflammasome assembly and caspase-1 activation by measuring the IL-1β protein concentration within supernatants of the treated cells. P2RX7 antagonists are likely to inhibit the ATP-mediated inflammasome assembly and subsequent IL-1β release and are used as a comparison for the P2RX4 antagonists. Furthermore, the effects of the P2RX4 and P2RX7 antagonists on priming mononuclear phagocytes with LPS are investigated by adding the antagonists prior to the priming step. BzATP/ATP or nigericin are subsequently added and concentrations of released IL-1β are measured. Intracellular IL-1β protein levels in LPS-primed cells are analysed via Western blotting and *IL1B* mRNA levels via real-time reverse transcription polymerase chain reaction (RT-PCR).

Priming with LPS also induces the expression of other pro- and anti-inflammatory cytokines and of the ATP receptors. Therefore, the release of IL-6 of cells treated with P2X receptors antagonists prior to priming is analysed as well as the mRNA expression of *P2RX4*, *P2RX7*, *IL6*, *IL10*, *IL18*, and *TNF*. In an attempt to explain unexpected effects provoked by the P2RX4 antagonist 5-B, the possible induction of apoptosis is investigated by measuring caspase-3 and caspase-7 activity.

This study aims to elucidate a better understanding of the mechanisms controlling the IL-1β release by mononuclear phagocytes, with the objective of contributing to the development of novel therapeutic strategies for the treatment of systemic inflammatory diseases and extensive sterile inflammation, while maintaining the integrity of the host defence mechanism.

MATERIALS & METHODS

1 MATERIALS

1.1 REAGENTS

Table 1: List of reagents.

Name	Provider, order code
2-mercaptoethanol	Merck Sigma-Aldrich®, Darmstadt, #M6250
2-propanol	Merck Sigma-Aldrich®, #33539
6x DNA loading dye	Thermo Fisher Scientific, Waltham, MA USA, #R0611
Acetic acid, 100 %	Merck EMD Millipore, Darmstadt, #100063
Aluminium potassium sulphate dodecahydrate	Merck Sulpeco®, Darmstadt, #1.01047
APS, ammonium peroxydisulphate	Carl Roth, Karlsruhe, #9592
Apyrase from potatoes	Merck Sigma-Aldrich®, #A6410
ATP, adenosine triphosphate	Merck Sigma-Aldrich®, #A2383
BD Cytofix/Cytoperm™	BD, Franklin Lakes, NJ USA, #554722
BD Perm/Wash™	BD, #51-2091KZ
Bromophenol blue	Carl Roth, #A512
BSA, bovine serum albumin	Serva Electrophoresis, Heidelberg, #11930.03
BzATP, 2'(3')-O-(4-benzoylbenzoyl) adenosine-5'-triphosphate	Jena Bioscience, Jena, #NU-1620
DAB, 3,3'-diaminobenzidine tetrahydrochloride	Merck Sigma-Aldrich®, #D5905
ddH_2O, Aqua B. Braun	B. Braun, Melsungen, #0082479E
DMSO, dimethyl sulfoxide, anhydrous	Merck Sigma-Aldrich®, #276855
DNAse I, 2,500 U/ml	Thermo Fisher Scientific, #90083
Doxorubicin-hydrochloride	Merck Sigma-Aldrich®, #D1515
EDTA, ethylenediaminetetraacetic acid 0.5 M, pH 8.0	bioWORLD, Dublin, OH USA, #40120777
Ethanol	Merck Sigma-Aldrich®, #32205
FBS ultra-low endotoxin	Cell Concepts, Umkirch, #S-EUR30-I
FBS Xtra	Capricorn Scientific, Ebsdorfergrund, #FBS-16A
GelRed Nucleic Acid Stain, 10,000x	Biotrend *Chemikalien*, Köln, #41003
GeneRuler 100 bp Plus DNA Ladder	Thermo Fisher Scientific, #SM0323
Giemsa's azure eosin methylene blue solution	Merck Sigma-Aldrich®, #1.09204
Glycergel mounting medium	Agilent Dako, Santa Clara, CA USA, #C0563
Glycerol	Merck Sigma-Aldrich®, #G2025
Glycine, ≥ 99 %	Carl Roth, #3908
Haematoxylin monohydrate	Merck EMD Millipore, #1.15938
HCl, hydrochloric acid, 1 N	Merck EMD Millipore, #1.09057
HCl, 25 %	Carl Roth, #6331
Human monocyte colony-stimulating factor	Merck Sigma-Aldrich®, #SRP3110
Human serum	Merck Sigma-Aldrich®, #H6914
Hydrobin® 100 binder	Ambratec, Mainz
Hydrogen peroxide 30 %	Merck EMD Millipore, #1.07209
KCl, potassium chloride	Merck EMD Millipore, #1.04936
KH_2PO_4, potassium dihydrogen phosphate	Merck EMD Millipore, #1.04873
LPS from *E. coli* O26:B6	Merck Sigma-Aldrich®, #L2654
LPS from *E. coli* O111:B4	Merck Sigma-Aldrich®, #LPS25
Lumi-Light Western Blotting Substrate	Roche Diagnostics, Mannheim, #12015200001
May-Grünwald's eosin-methylene blue solution modified	Merck Sigma-Aldrich®, #1.01424

Methanol	Merck Sigma-Aldrich®, #32213
Monocyte attachment medium	PromoCell, Heidelberg, #C-28051
Murine serum	Merck Sigma-Aldrich®, #M5905
Mucocit® T disinfection	Schülke & Mayr, Norderstedt, #230120
NaCl, sodium chloride	Carl Roth, #3957
NaH_2PO_4, sodium dihydrogen phosphate dihydrate	Merck, Darmstadt, #1.06345
Nigericin sodium salt, ≥ 98 %	Merck Sigma-Aldrich®, #N7143
Neo-Mount®	Merck Sigma-Aldrich®, #1.09016
Nuclease-free water	Promega, Fitchburg, WI USA, #P1193
PBS, Dulbecco's phosphate buffered saline	Merck Sigma-Aldrich®, #D8537
PenStrep, penicillin streptomycin solution, 10,000 U/ml	Thermo Fisher Scientific, #15140-122
PMA, phorbol-12-myristate-13-acetate	Merck Sigma-Aldrich®, #P1585
Powdered milk	Carl Roth, #T145.3
Precision Plus Protein Dual Colour Standard	Bio-Rad Laboratories, Hercules, CA USA, #1610374
Protease inhibitor cocktail tablets	Roche Diagnostics, #11836153001
RBC lysis buffer 10x	BioLegend, San Diego CA USA, #420301
Recombinant human IFN-γ	R&D Systems, Minneapolis, MN USA, #285-IF
Recombinant murine IFN-γ	Merck Sigma-Aldrich®, #IF005
ROTI®-Block 10x	Carl Roth, #A151
Rotiphorese®Gel 30 (37.5:1)	Carl Roth, #3029
Rotiphorese® 50x TAE buffer	Carl Roth, #CL86
RPMI 1640 advanced	Capricorn Scientific, #RPMI-ADV
SDS, sodium dodecyl sulphate, ultra pure	Carl Roth, #2326
Sodium hydroxide, 1 N	Merck EMD Millipore, #1.09137
Sodium iodate	Merck Sulpeco®, #1.06525
SsoAdvanced Universal SYBR® Green Supermix	Bio-Rad Laboratories, #172527
SuperSignal™ West Dura Extended Duration Substrate	Thermo Fisher Scientific, #34076
TEMED, ≥98.5 %	Carl Roth, #2367
Tris(hydroxymethyl)aminomethane (TRIS), Trizma®, ≥ 99.9 %	Carl Roth, #4855
TRIS HCl	Merck Sigma-Aldrich®, #T3253
Trypan blue solution	Merck Sigma-Aldrich®, #T8154
Türk's solution	Merck EMD Millipore, #1.09277
Tween®-20	Merck Sigma-Aldrich®, #8.22184
UltraPure™ Agarose	Thermo Fisher Scientific, #16500
Z-VAD-FMK	Bachem, Bubendorf, CH #4026865

1.2 P2X RECEPTOR ANTAGONISTS

Table 2: List of P2RX4 antagonists.

	P2RX4 antagonists			
	5-BD	**PSB-15417**	**PZB15517166A**	**PZB13420052A**
IUPAC	5-(3-Bromophenyl)-1,3-dihydro-2H-benzofuro[3,2-e]-1,4-diazepin-2-one	-	-	-
Structural formula	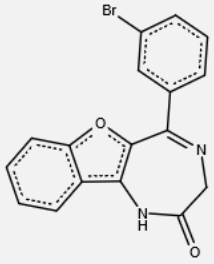	Structure undisclosed	Structure undisclosed	Structure undisclosed
References	(Casati et al. 2011, Balázs et al. 2013, Chen et al. 2013, Abdelrahman et al. 2017, Coddou et al. 2019, Han et al. 2020, Bidula et al. 2022)	(Schneider et al. 2017, Trang et al. 2020)	-	-
Provider	Tocris Bio-Techne® Bristol UK, #3579	Prof. Christa Müller, Pharmaceutical Institute, University of Bonn, Bonn	Prof. Christa Müller	Prof. Christa Müller

Table 3: List of P2RX7 antagonists.

	P2RX7 antagonists	
	A43	**JNJ**
IUPAC	3-{[5-(2,3-dichlorophenyl)-1H-1,2,3,4-tetrazol-1-yl]methyl}pyridine	N-[[4-(4-phenylpiperazin-1-yl)oxan-4-yl]methyl]-2-phenylsulfanylpyridine-3-carboxamide
Structural formula	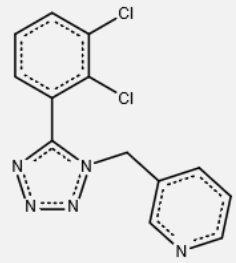	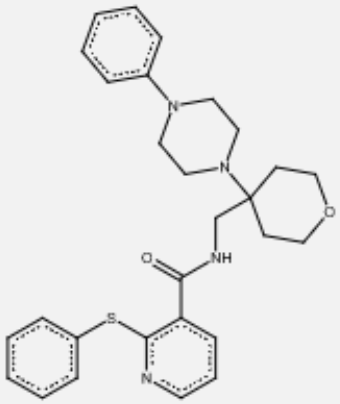
Provider References	(Nelson et al. 2006, Donnelly-Roberts et al. 2007, Clark et al. 2010, Ward et al. 2010, Kim et al. 2011, Draganov et al. 2015, Sathanoori et al. 2015)	(Chessell et al. 2005, Bhattacharya et al. 2013, Dos-Santos-Pereira et al. 2018, Uderhardt et al. 2019, Francistiová et al. 2021, McEwan et al. 2021)
	Tocris Bio-Techne®, #2972	Tocris Bio-Techne®, #5299

1.3 ANTIBODIES

Table 4: List of antibodies used for immunostaining. (1) 2.5 % powdered milk/PBS (w/v); (2) 1 % ROTI®-Block/PBS (v/v); (3) 1 % BSA/BD Perm/Wash™ (w/v) + 5 % human serum (v/v); (4) 5 % BSA/PBS-T (w/v); (5) 5 % human serum/BD Perm/Wash™. HRP, horseradish peroxidase; IgG, immunoglobulin G; ICC, immunocytochemistry; kDa, kilodalton; WB, Western blot.

	Antigen	Dilution, application	Host	Provider, order code
Primary antibodies	IL-1β, human (precursor: 31 kDa, mature form: 17 kDa)	1:5,000 in (1), WB	Mouse	National Cancer Institute, Frederick, MD USA
	β-actin, human (42 kDa)	1:500,000 in (2), WB	Mouse	Merck Sigma-Aldrich®, #A1978
	CD14, human	1:100 in (3), ICC	Mouse	BioLegend, #325602
	CD68, human	undiluted with 5 % human serum, ICC	Mouse	Agilent Dako, #GA613
Secondary HRP-linked antibodies	IgG, mouse	1:5,000 in (4), WB	Goat	Abcam, Cambridge UK, #ab6789
	IgG, mouse	1:50 in (5), ICC	Rabbit	Agilent Dako, #P0260
HRP-linked labelled polymer	"EnVision+" IgG, rabbit	undiluted with 5 % human serum, ICC	Mouse	Agilent Dako, #K400311-2

1.4 OLIGONUCLEOTIDES FOR REAL-TIME RT-PCR OF CDNA

Table 5: List of oligonucleotides, called primer pairs, used for real-time RT-PCR. All pairs were received from Thermo Fisher Scientific. *Product size according to NCBI Primer-Blast. F, forward; R, reverse; Eff, efficiency; bp, base pairs.

Target genes	Sequence in 5' to 3'	Eff. [%]	Product size*	Source DOI
PPIA	**F:** TCCTGGCATCTTGTCCAT **R:** TGCTGGTCTTGCCATTCCT	100	179 bp	10.1371/journal.pone.0048367
IL1B	**F:** TTACAGTGGCAATGAGGATGAC **R:** GTCGGAGATTCGTAGCTGGAT	94	121 bp	10.1371/journal.pone.0011765
IL6	**F:** AGACAGCCACTCACCTCTTCAG **R:** TTCTGCCAGTGCCTCTTTGCTG	100	132 bp	10.3390/ph14100987
IL10	**F:** GCCTAACATGCTTCGAGATC **R:** TGATGTCTGGGTCTTGGTTC	100	206 bp	10.4049/jimmunol.178.8.4779
IL18	**F:** GCTGAAGATGATGAAAACCTGGAA **R:** AAATATGGTCCGGGGTGCATT	100	171 bp	Generated with primer3.org
TNF	**F:** CCCAGGGACCTCTCTCTAATCA **R:** AGCTGCCCCTCAGCTTGAG	100	116 bp	10.3390/ph14100987
P2RX4	**F:** GGAGAACGCAGGACACAG **R:** CCTTCCCAAACACAATGATG	100	272 bp	10.4049/jimmunol.1501585
P2RX7	**F:** ATACAGTTTCCGTCGCCTTG **R:** AACGGATCCCGAAGACTTTT	98	134 bp	10.3389/fimmu.2017.01529

1.5 CELL LINES

Table 6: List of cell lines

Cell line	Cell origin	Provider
THP-1	Peripheral blood of a 1-year-old male patient with acute monocytic leukaemia	Leibniz Institute, DSMZ-German Collection of Microorganisms and Cell Cultures, Braunschweig

1.6 ASSAY KITS

Table 7: List of assay kits.

Name	Provider, order code
Apo-ONE® Homogeneous Caspase-3/7 Assay	Promega, #G7792
CytoTox96® Non-Radioactive Cytotoxicity Assay	Promega, #G1780
DuoSet ELISA Ancillary Reagent Kit 2	R&D Systems, #DY008
Human IL-1β/IL-1F2 DuoSet ELISA	R&D Systems, #DY201
Human IL-6 DuoSet ELISA	R&D Systems, #DY206
Micro BCA™ Protein-Assay-Kit	Thermo Scientific, #23235
QuantiTect® Reverse Transcription Kit	Qiagen, Venlo Netherlands, #205311
RNase-Free DNase Set	Qiagen, #79254
RNeasy® Plus mini Kit	Qiagen, #74134

1.7 CONSUMABLE SUPPLIES

Table 8: List of consumable supplies.

Name	Producer
8-well chamber-view slide	Sarstedt, Nümbrecht
10-well chamber-view slide	Greiner Bio-One, Kremsmünster
12-well cell culture plate	Greiner Bio-One, #665180
48-well cell culture plate	Greiner Bio-One, #677180
96-well black polystyrene microplate	R&D Systems
96-well microplate	Greiner Bio-One
CytoOne® cell scraper	Starlab International, Hamburg
Filter tips 10 µl, 200 µl, 1000 µl	Nerbe plus, Winsen
Leucosep™ tubes, 50 ml	Greiner Bio-One
MicroAmp® Fast Optical 96-well reaction plate	Thermo Fisher Scientific Applied Biosystems
Pipettes 5 ml, 10 ml, 25 ml	Greiner Bio-One
Pipette tips 10 µl, 200 µl, 1000 µl	Sarstedt
Polyvinylidene difluoride transfer membrane Immobilon®-P	Merck Millipore
Reaction tubes 0.5 ml, 1.5 ml	Sarstedt
Steel balls, stainless	Amelung, Lemgo
Syringe Omnifix® 5 ml, 10 ml, 20 ml	B. Braun
TC flasks T25	Sarstedt
Tubes 15 ml, 50 ml	Greiner Bio-One
Tubes 250 ml	Thermo Fisher Scientific
Optical Adhesive Covers	Thermo Fisher Scientific Applied Biosystems

1.8 EQUIPMENT & SOFTWARE

Table 9: List of equipment & Software.

Name	Provider
Biosafety cabinet MSC-Advantage™	Thermo Fisher Scientific
Blotting / electrophoresis tank + accessories	Von Keutz *Labortechnik*, Reiskirchen
Centrifuge Cellspin I	Tharmac, Limburg an der Lahn
Centrifuge Rotina 420R	Andreas Hettich, Tuttlingen
Centrifuge Mikro 220R	Andreas Hettich
CLARIOstar^{PLUS} plate reader	BMG Labtech, Offenburg
CO_2 incubator HERAcell 240i	Thermo Fisher Scientific
Counting chamber improved Neubauer	Laboroptik, Lancing, United Kingdom
Electrophoresis power supply EV231	Consort, Turnhout, Belgium
Epoch microplate spectrophotometer	Agilent Technologies, Santa Clara, CA USA
Fluorescence microscope Olympus BX51	Olympus, Tokio Japan
Fluostar Optima Photometer	BMG Labtech
iBright 1500	Thermo Fisher Scientific
iBright Analysis Software	Thermo Fisher Scientific
Inkscape vector graphics editor 1.3.2	Free software distributed under the GNU General Public License, version 3
Mastercycler gradient	Eppendorf, Hamburg
Micro Scale Mettler AE100	Mettler-Toledo, Gießen
Microscope camera Axiocam 305 color	Carl Zeiss Microscopy, Jena
Mixer Mill MM 301	Retsch, Haan
Nanodrop 1000 Spectrophotometer	VWR International, Darmstadt
pH / mv meter UltraBasic UB-10	Denver Instrument, Göttingen
Pipette pipetus®	Hirschmann *Laborgeräte*, Eberstadt
Pipettes 1 – 10 µl, 10 – 100 µl, 100 – 1000 µl	Eppendorf
Scale KERN$_{PU}$	KERN & SOHN, Balingen-Frommern
SPSS statistic software version 27.0.0.0	IBM Deutschland, Ehningen
StepOnePlus Real-Time PCR System	Thermo Fisher Scientific
Transilluminator	Biozym Scientific, Oldendorf
Transmitted-light microscope Leica DMLS	Leica Microsystems, Wetzlar
Ultrasonic cleaner	VWR International
Vortex LLG® uniTEXER	Lab Logistics Group, Meckenheim
Water bath	Köttermann, Uetze
ZEN (blue edition) Software	Carl Zeiss Microscopy, Jena

2 METHODS

2.1 CELL BIOLOGICAL METHODS

2.1.1 CULTURING AND PASSAGING OF THE HUMAN MONOCYTIC CELL LINE THP-1

The human cell line THP-1, originating from acute monocytic leukaemia, was used for preliminary studies. Monocytic THP-1 cells were cultured in Roswell-Park-Memorial-Institute 1640 advanced (RPMI) supplemented with 10 % FBS – further referred to 'RPMI complete' – under sterile conditions. FBS from two different providers was used. Cells were incubated at 37°C with 5 % CO_2 saturation in a humidified CO_2 incubator and routinely passaged two times a week to maintain 3 – 4 x 10^6 cells per TC flask T25. For passaging, cells were harvested by centrifugation at 500 x g for 8 min and resuspended in 5 ml fresh RPMI complete. The cell number was determined, and the required amount of the cell suspension was transferred to a new cell culture TC flask T25 and filled up with RPMI complete.

2.1.2 DIFFERENTIATION OF MONOCYTIC THP-1 CELLS TO THP-1 CELL-DERIVED MACROPHAGES

For differentiation of monocytic THP-1 cells into M1-like macrophages, cells were harvested by centrifugation at 500 x g for 8 min and resuspended in fresh RPMI with 10 % foetal calf serum (FCS) and 1 % penicillin streptomycin (PenStrep) solution – further referred to 'RPMI PenStrep'. The cell number was determined, adjusted to 1 x 10^6 cells per ml and 0.3 x 10^6 cells were transferred to wells of a 12-well plate. Wells were filled up to 1 ml with RPMI PenStrep supplemented with phorbol 12-myristate 13-acetate (PMA) to receive a final concentration of 50 nM PMA per well. After 24 hours (h) incubation at 37°C and 5 % CO_2 saturation in a humidified CO_2 incubator, cells were washed with warm RPMI complete before RPMI PenStrep was added for additional 24 h. The following day, cells received for differentiation into M1-like macrophages RPMI PenStrep supplemented with 10 ng/ml recombinant human IFN-γ and 10 ng/ml LPS, from *E. coli* O111:B4, for 48 h incubation. Cells that did not receive this treatment differentiated into M0-like macrophages. On the fifth day, THP-1 M1-like macrophages were washed, RPMI complete was added, and the cells were primed and stimulated as described in chapter 2.1.3. THP-1 macrophages were stained using May-Grünwald and Giemsa's dye described in chapter 2.1.6.

2.1.3 STIMULATION OF THP-1 CELLS

Monocytic THP-1 cells were harvested by centrifugation at 500 x g for 8 min and resuspended in fresh RPMI. The cell number was determined and RPMI was added, so that 0.5 x 10^6 cells per 500 µl could be transferred to the wells of a 48-well plate. THP-1 cell-derived macrophages were differentiated in 12-well plates as described before and stimulated in RPMI complete. An exception to this were macrophages stimulated for Western blot analysis, as these were maintained in RPMI. Monocytic THP-1 cells as well as THP-1 cell-derived M1-like macrophages were primed with 1 µg/ml LPS, from *E. coli* O26:B6, for 5 h. To induce IL-1β secretion, 100 µM BzATP, 1 or 2 mM ATP, or 50 µM nigericin were added to the cells for 40 min. P2X receptors antagonists were either added prior to priming with LPS (①), or right before the second signal (②) (**Figure 2**). In every set of experiments, control samples of untreated cells, cells primed with LPS, and cells primed with LPS and stimulated with BzATP, ATP, or nigericin alone, were included. Additionally, the vehicle dimethyl sulfoxide (DMSO) [0.1 %] was added to a second control sample. When nigericin was applied, apyrase [0.5 U] was added simultaneously. Cells were maintained at 37°C and 5 % CO_2 in a humidified CO_2 incubator during any incubation period. At the end, plates were centrifuged at 500 x g for 8 min at 4°C and supernatants were collected in reaction tubes and stored at -20°C until IL-1β or IL-6 enzyme-linked immunosorbent assay (ELISA) and measurements of lactate dehydrogenase (LDH) activity were conducted. The cells remained in the plate and were stored at -20°C for later real-time RT-PCR or Western blot analysis.

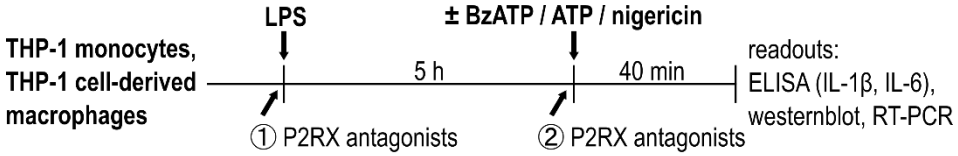

Figure 2: Schematic workflow of the stimulation of THP-1 cells. THP-1 cells – monocytes or macrophages – were incubated with LPS for 5 h. P2X receptors antagonists were either added prior to LPS application (①) or prior to BzATP, ATP or nigericin incubation (②). Afterwards, supernatants were collected for ELISA and cells for Western blot or real-time RT-PCR experiments. LPS, lipopolysaccharide. BzATP, 2'(3')-O-(4-Benzoylbenzoyl)adenosine-5'-triphosphate. ATP, adenosine triphosphate.

2.1.4 PURIFICATION AND STIMULATION OF HUMAN PERIPHERAL BLOOD MONONUCLEAR CELLS

For the isolation of hPBMCs, blood from healthy donors was obtained in the context of the clinical study AZ98/23, which was approved by the ethical review committee of the Justus-Liebig University. Non-smoking adults without pre-existing diseases, who were included in the study, were informed by the principal investigator (Prof. Dr. med. Andreas Hecker) and a written informed consent was given.

Whole blood supplemented with 1 mM ethylenediaminetetraacetic acid (EDTA) was diluted with Dulbecco's phosphate buffered saline (PBS)/0.1 % bovine serum albumin (BSA) in equal shares. Subsequently, hPBMCs were separated from whole blood by density gradient centrifugation. For that, the sample was carefully transferred to a Leucosep™ tube and centrifuged at 800 x g for 25 min. The upper phase was carefully removed, the interphase transferred to a new tube and filled up to 50 ml with PBS/0.1 % BSA. The diluted interphase was centrifuged at 500 x g for 8 min. The pellet was washed again and then resuspended in monocyte attachment medium. The cell number was determined, the volume adjusted to 1 x 10^6 cells per ml and 0.5 x 10^6 cells were transferred to wells of a 48-well plate. hPBMCs were primed with 5 ng/ml LPS, from *E. coli* O26:B6, for 3 h. Adherent cells were selected by exchanging the medium to RPMI and further incubation for 20 min. In IL-1β release experiments, hPBMCs were subsequently treated with 100 µM BzATP or 50 µM nigericin for 30 min. P2X receptors antagonists were either added prior to priming with LPS (①), or right before adding BzATP or nigericin (②) (**Figure 3**). In every set of experiments, control samples of untreated cells, cells primed with LPS, and cells primed with LPS and stimulated with BzATP or nigericin alone, were included. Additionally, the vehicle DMSO [0.1 %] was added to a second control sample. When nigericin was applied, apyrase [0.5 U] was added simultaneously. Cells were maintained at 37°C and 5 % CO_2 in a humidified CO_2 incubator during any incubation period. At the end, plates were centrifuged at 500 x g for 8 min at 4°C, supernatants were collected and stored at -20°C until ELISA and measurements of LDH activity were conducted. Cells remained in the plate and were stored at -20°C for real-time RT-PCR experiments.

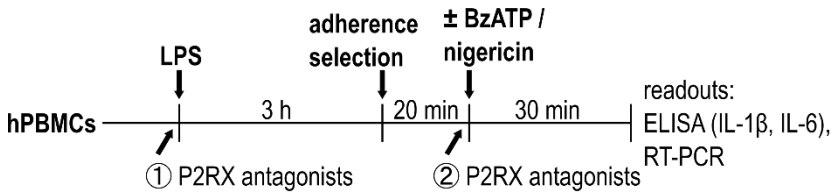

Figure 3: Schematic workflow of the stimulation of hPBMCs. Human PBMCs were incubated with LPS for 3 h and underwent adherence selection for 20 min. P2X receptors antagonists were either added prior to LPS application (①) or prior to BzATP or nigericin incubation (②). Afterwards, supernatants were collected for ELISA and cells for Western blot or real-time RT-PCR experiments. hPBMCs, human peripheral blood mononuclear cells. LPS, lipopolysaccharide. BzATP, 2'(3')-O-(4-Benzoylbenzoyl)adenosine-5'-triphosphate.

2.1.5 PURIFICATION AND STIMULATION OF HUMAN PERITONEAL MACROPHAGES

For the isolation of hPMs, peritoneal dialysate from donors was obtained in the context of the clinical study AZ251/20, which was approved by the ethical review committee of the Justus-Liebig University. Included were patients older than 18 years who were admitted to hospital for planned peritoneal dialysis training. This took place 14 days after the initial implantation of a peritoneal dialysis catheter either due to chronic renal insufficiency requiring dialysis or due to cardiorenal syndrome with refractory ascites. The patients included in the study were informed by the principal investigator (Dr. med. Anca-Laura Amati) and a written informed consent was signed by all patients. Exclusion criteria were chronic or acute infectious diseases, increased inflammatory parameters (leucocytosis, C-reactive protein above 10 mg/l, procalcitonin levels above 0.5 ng/ml, or fever), ongoing antibiotic therapy, immunosuppressive therapy, chemotherapy within the last 3 month, pregnancy, or lack of consent.

The ice-cold dialysate was transferred to pre-cooled tubes (250 ml) and centrifuged at 200 x g for 20 min at 4°C. After supernatants were discarded, the pellets were resuspended in 5 ml ice cold PBS/0.1 % BSA, combined in a tube (50 ml) and centrifuged at 500 x g for 8 min at 4 C. The supernatant was discarded, and the pellet resuspended in 5 ml 1 x RBC lysis buffer and incubated for 6 min at room temperature (RT). The reaction was stopped by adding PBS/0.1 % BSA and centrifugation at 500 x g for 8 min at 4°C. The pellet was resuspended in 5 – 20 ml RPMI PenStrep after discarding the supernatant. The cell number was determined, the volume adjusted to 1 x 10^6 cells per ml and 1 x 10^6 cells were transferred to wells of a 12-well plate. Cells were maintained at 37°C and 5 % CO_2 in a humidified CO_2 incubator overnight. The next morning, adherent cells were selected by exchanging RPMI PenStrep to fresh RPMI complete. hPMs were primed with 0.1 µg/ml LPS, from *E. coli* O26:B6, for 5 h. For IL-1β release experiments, hPMs were subsequently treated with 100 µM BzATP for 40 min. The P2X receptors antagonists were either added prior to LPS priming (①), or right before BzATP (②) (**Figure 4**). In every set of experiments, control samples of untreated cells, cells primed with LPS, and cells primed with LPS and stimulated with BzATP alone were included. Additionally, the vehicle DMSO [0.1 %] was added to a second control sample. Cells were maintained at 37°C and 5 % CO_2 in a humidified CO_2 incubator during any incubation period.

At the end, plates were centrifuged at 500 x g for 8 min at 4°C, supernatants were collected and stored at -20°C until ELISA and measurements of LDH activity were conducted.

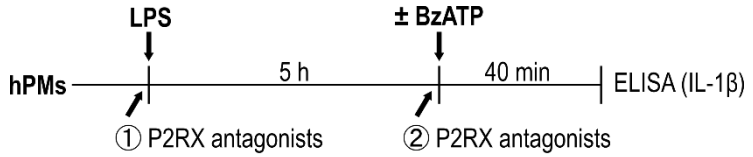

Figure 4: Schematic workflow of the stimulation of human peritoneal macrophages. hPMs were incubated with LPS for 5 h. P2X receptors antagonists were either added prior to LPS application (①) or prior to BzATP incubation (②). Afterwards, supernatants were collected for ELISA. hPMs, human peritoneal macrophages. LPS, lipopolysaccharide. BzATP, 2'(3')-O-(4-Benzoylbenzoyl)adenosine-5'-triphosphate.

2.1.6 STAINING OF THP-1 MACROPHAGES

The morphology of M0-like and M1-like macrophages were assessed via microscopy. First, THP-1 cells were harvested by centrifugation at 500 x g for 8 min and resuspended in RPMI PenStrep. The cell number was determined, adjusted to 1 x 10^6 cells per ml and 0.1 x 10^6 cells per well were transferred to two 8-well chamber-view slides. The cells were treated the following days as described in chapter 3.1.2, except some cells, which received RPMI PenStrep without recombinant human IFN-γ and LPS for differentiation into macrophage-like THP-1 cells – so called M0-like macrophages. On the fifth day, cells were washed with phosphate buffered saline (PBS), followed by fixation with BD Cytoperm™ for 20 min on ice. Thereafter, cells were washed again and air-dried. M0-like macrophages were stained with May-Grünwald's dye for 1 min, then incubated in double distilled water (ddH_2O) for 5 min, followed by Giemsa's staining for 4 min. M1-like macrophages were incubated with May-Grünwald's staining for 2 min, followed by 5 min ddH_2O and Giemsa's staining for 15 min. After staining, the wells were removed, slides cleaned thoroughly with ddH_2O, dried and sealed with Neo-Mount® before microscopy.

2.1.7 IMMUNOCYTOCHEMICAL STAINING OF HUMAN PERITONEAL MACROPHAGES

For cell counting via microscopy, cells were harvested as described in chapter 2.1.5 and 0.1 x 10^6 cells were transferred to 10-well chamber-view slides or cytospots were made. The cytospots were centrifuged at 28 x g for 4 min in a centrifuge cellspin I, fixated with BD Cytoperm™ for 20 min on ice. Thereafter, cytospots were washed with PBS/0.1 % BSA, dried and stored at 4°C. The chamber-view slides were maintained at 37°C and 5 % CO_2 in a humidified CO_2 incubator overnight. The following day, medium was discarded, and cells were fixated with BD Cytoperm™ for 20 min on ice and washed with ice-cold PBS/0.1 % BSA. The slides were dried at RT before storing them at 4°C until immunocytochemistry (ICC) was conducted. Prior to staining, cytospots and chamber-view slides were incubated with PBS/1 % hydrogen peroxide on ice for 30 min, washed three times with PBS, and incubated with BD Perm/Wash™/1 % BSA for 30 min at RT. Samples were incubated with primary antibodies against CD14 and CD68 (**Table 4**) for 1 h. After washing three times with BD

Perm/Wash™, secondary horseradish-peroxidase (HRP)-conjugated antibodies (**Table 4**) were added for 1 h at RT. Some samples were washed three times with BD Perm/Wash™ after incubation with the secondary antibody and before EnVision+ was applied for 30 min at RT. Thereafter, all samples were washed three times with 1 x TBS before they were incubated with DAB in PBS/0.015 % hydrogen peroxide [0.5 mg/ml] for 10 min at RT. At last, samples were stained with Mayer's Haematoxylin for 6 min and then sealed with Glycergel mounting medium before microscopy.

TBS 10x: 0.5 M TRIS, 1.54 mM NaCl, 5 % (v/v) HCl pH 7.6

Mayer's Haematoxylin: 0.1 M aluminium potassium sulphate dodecahydrate, 3.31 mM haematoxylin monohydrate, 1 mM sodium iodate

2.1.8 CLASSIFICATION OF CELL TYPES IN PERITONEAL DIALYSATE SAMPLES

The distribution of cell types in peritoneal dialysate samples before and after adherence selection was assessed via microscopy. Cells on cytospots, representing the original composition of cell populations in the peritoneal dialysate samples, and on chamber-view slides, showing adherent cells after the complete isolation protocol, were counted in 6 – 9 randomly selected areas via ZEN (blue edition) software. Cells are ICC stained and were categorized into $CD14^+$ or $CD14^-$ cells or into $CD68^+$ and $CD68^-$ cells. Granulocytes were identified by their dark-brown stained granules and multi-lobed nuclei. After counting, percentages of $CD14^+$ and $CD68^+$ macrophages before and after adherence selection were calculated and compared.

2.1.9 CELLS LYSIS

Immediately after stimulation of THP-1 cells, cells were lysed under denaturing conditions for sodium dodecyl sulphate-polyacrylamide gel electrophoresis (SDS-PAGE) and following Western blot analysis. Therefore, RPMI was completely discarded and 75 µl cold SB0 buffer added to each well. Cells were incubated for 15 min on ice before 75 µl SB1 buffer was added, and the cells in 12-well plates immediately stored at -20°C until further procedures were carried out. After thawing, cells were collected in tubes by scrapping them from the plate surface, and mechanically disrupted with a steel ball inside the tube by using the mixer mill for 10 min. At last, cell suspensions were incubated for 15 min in an ultrasonic cleaner, before a bicinchoninic acid (BCA) protein assay was carried out as described in chapter 2.2.4.

Sample buffer 0: 6.25 mM TRIS/HCl, 600 U DNase I, proteinase inhibitor cocktail 1 x pH 6.8

Sample buffer 1: 6.25 mM TRIS/HCl, 2 % (w/v) SDS, proteinase inhibitor cocktail 1 x pH 6.8

2.2 PROTEIN BIOCHEMICAL METHODS

2.2.1 ENZYME-LINKED IMMUNOSORBENT ASSAY (ELISA)

The concentration of IL-1β or IL-6 in cell culture supernatants was measured to validate the influence of P2X receptors treatment on cytokine secretion. Human IL-1β/IL-1F2 DuoSet ELISA kit or human IL-6 DuoSet ELISA kit were used. In general, these assays employ the quantitative sandwich enzyme immunoassay technique, by which an immobilized antibody specific for a target protein binds any target protein present in samples. A second antibody binding to the antibody-protein complex is linked to an enzyme, which converts its substrate resulting in a colour change. Because the intensity of colour change is in proportion to the amount of bound target protein, the concentration of the desired protein can be colorimetrically quantified.

The protocols were implemented as specified by the manufacturer. The DuoSet ELISA Ancillary Reagent Kit 2 was additionally used. The optical density of each sample and RPMI or RPMI complete was determined by using the Fluostar Optima photometer at 450 nm. The optical density of medium was subtracted from the results of the samples. The lower detection limit of the IL-1β ELISA kit is 3.9 pg/ml, while that of the IL-6 assay is 9.4 pg/ml. The IL-1β or IL-6 concentration of each sample was calculated using a linear equation of a serial dilution of recombinant human IL-1β standard or IL-6 standard with known concentration, respectively.

2.2.2 ESTIMATION OF CELL DEATH

LDH activity in cell culture supernatants was measured simultaneously with IL-1β ELISA to quantify the influence of treatment with P2X receptors antagonists on cell death. LDH activity was implemented using the CytoTox96® Non-Radioactive Cytotoxicity Assay, which is a colorimetric assay quantifying LDH activity, a stable cytosolic enzyme. Released LDH converts supplied lactate into pyruvate, a reaction that is linked to the conversion of a tetrazolium salt into a red formazan product. Colour intensity is proportional to the number of damaged cells and can be colorimetrically quantified.

The protocol was implemented as specified by the manufacturer. Optical density measurements were carried out at 490 nm using Epoch microplate spectrophotometer. In addition to the samples, the optical density of RPMI or RPMI complete was also measured and subtracted from all values. The percentage LDH activity of samples was calculated in proportion to the optical density of an identical number of lysed cells that was set to 100 % representing the total LDH release.

2.2.3 CASPASE ACTIVITY ASSAY

The activity of caspase-3 and caspase-7 was measured using the Apo-ONE® Homogeneous Caspase-3/7 Assay. Upon cleavage of the peptide substrate, which is a part of the assay kit, by caspase-3 and caspase-7, the conjugated dye becomes fluorescent when excited at a wavelength of 498 nm. The amount of fluorescent product is proportional to the amount of active caspase-3 and caspase-7 present in the sample.

Monocytic THP-1 cells were harvested by centrifugation at 500 x g for 8 min and resuspended in fresh RPMI. The cell number was determined and RPMI was added, so that 1 x 10^5 cells per 100 µl could be transferred to the wells of a 96-well black polystyrene microplate. Substances were added to the cells, thereafter the cells were primed with 1 µg/ml LPS from *E. coli* O26:B6 for 5 h. Cells were maintained at 37°C and 5 % CO_2 in a humidified CO_2 incubator for 30 min or 60 min. Then, fluorescence measurements were carried out at an excitation wavelength range of 488 nm and an emission wavelength range of 535 nm using the CLARIOstar^{PLUS} plate reader. Additional to the samples, the emission of RPMI was also measured and the corresponding values subtracted from all values.

2.2.4 QUANTITATION OF TOTAL PROTEIN BY BCA PROTEIN ASSAY

The protein concentration of lysed cells was determined using a Micro BCA™ Protein-Assay-Kit for following Western blot analysis. Proteins reduce Cu^{2+} to Cu^{+} in an alkaline environment. Cu^{+} reacts with two molecules BCA to form a purple-coloured reaction product. The absorption of this complex is linear with increasing protein concentrations and the amount of protein in the target sample can be calculated using a linear equation of a serial dilution of BSA with known concentrations.

The used protocol differs from the manufacturer's protocol. For the serial dilution, a BSA solution of 100 µg/ml was diluted several times to acquire a series of BSA standard solutions in the range of 50 µg/ml to 1.25 µg/ml. Then, 1 part standard was diluted with 49 parts NaCl-solution, and 1 part sample was mixed with 499 parts NaCl-solution. In a 96-well microplate, 150 µl diluted standards and samples were pipetted, followed by addition of 150 µl BCA working reagent, consisting of 25 parts reagent A, 24 parts reagent B plus 1 part reagent C. After incubation at 37°C for 2 h, the absorbance at 580 nm was measured using the Fluostar Optima photometer and the protein content in the samples was calculated.

2.2.5 SODIUM DODECYL SULPHATE POLYACRYLAMIDE GEL ELECTROPHORESIS (SDS-PAGE)

SDS-PAGE was performed to separate proteins according to their molecular mass. As SDS unfolds proteins and coats them with a negative charge, proteins can migrate within an acrylamide gel in an electric field towards the anode with different speed depending on their mass.

First, the separation gel was cast between two glass plates. A stacking gel was cast on top of the polymerized separation gel and a comb inserted. After complete polymerization, the gels were placed in an electrophoresis tank filled with SDS running buffer. Samples diluted in sample buffer 1 were mixed in equal shares with sample buffer 2 and incubated at 90°C for 5 min, followed by centrifugation at 7500 x g for 5 min. 10 µg protein of each sample was loaded alongside with 10 µl Precision Plus Protein Dual Colour Standard. The gel was run at a constant voltage of 80 V for 10 min to gather the proteins in the upper stacking gel and subsequently, at a constant voltage of 120 V for 80 min to accomplish the migration through the separation gel.

Stacking gel:	54.82 % (v/v) H_2O, 32.08 % (v/v) upper gel buffer, 12.69 % (v/v) Rotiphorese®Gel, 0.23 % (w/v) APS, 0.18 % (v/v) TEMED	
12 % separating gel:	41.77 % (v/v) H_2O, 24.65 % (v/v) lower gel buffer, 33.33 % (v/v) Rotiphorese®Gel, 0.18 % (w/v) APS, 0.07 % (v/v) TEMED	
Upper gel buffer:	0.5 M TRIS, 1.5 % (v/v) HCl, 0.4 % (w/v) SDS	pH 6.8
Lower gel buffer:	1.5 M TRIS, 0.83 % (v/v) HCl, 0.4 % (w/v) SDS	pH 8.8
SDS running buffer:	25 mM TRIS, 192 mM Glycine, 0.1 % (w/v) SDS	
Sample buffer 2:	62.5 mM TRIS/HCl, 20 % (v/v) Glycerol, 10 % (v/v) 2-mercapto-ethanol, 2 % (w/v) SDS, 0.002 % (w/v) bromophenol blue, proteinase inhibitor cocktail 1 x	pH 6.8

2.2.6 WESTERN BLOT

Western blot analysis was carried out to investigate changes in intracellular (pro-)IL-1β protein levels after treatment with P2X receptors antagonists. Therefore, proteins are immobilized on a membrane and antigens are detected by specific antibodies, enzyme-linked secondary antibodies and chemiluminescence.

In detail, a polyvinylidene difluoride transfer membrane was activated by incubation in methanol for at least one min and shortly washed with transfer buffer afterwards. Then, two sponges, filter paper, the separating gel, the membrane, filter paper, and a sponge were placed within a holder cassette, which was inserted into a blotting tank so that the membrane was facing the anode. The tank was filled with transfer buffer and proteins were transferred from the separating gel onto the membrane at a constant current of 90 mA for 90 min. Protein binding sites on the membrane were blocked with 5 % (w/v) milk powder in 1 x PBS for one h.

After overnight incubation with primary antibodies (**Table 4**) at 4°C and after four washing steps with 1 x PBS containing 0.1 % Tween®-20 for 8 min each, the membrane was incubated in diluted HRP-labelled secondary antibodies (**Table 4**) for 90 min. The membrane was washed three times with 1 x PBS/0.1 % Tween®-20 and once with 1 x PBS for 10 min. Bound HRP was detected by SuperSignal™ West Dura Extended Duration Substrate to detect (pro-)IL-1β or by Lumi-Light Western Blotting Substrate when detecting β-actin. Western blots were documented with the iBright 1500 system.

Transfer buffer:	24.76 mM TRIS, 190 mM glycine, 20 % (v/v) methanol, 0.1 % (w/v) SDS
PBS 10x:	1.37 M NaCl, 91.28 mM NaH_2PO_4, 26.83 mM KCl, 14.7 mM KH_2PO_4, 0.8 % (v/v) HCl pH 7.2

2.3 MOLECULAR BIOLOGY METHODS

2.3.1 RNA EXTRACTION AND CDNA SYNTHESIS

A RNeasy® Plus mini kit was used to isolate RNA from THP-1 cells or hPBMCs after treatment to generate cDNA for following real-time RT-PCR experiments. The protocol was mainly implemented as specified by the manufacturer and only changed minimally. Briefly, the RW1 washing step was divided into two steps with a DNase incubation for 25 min in between. Therefore, the RNase-Free DNase kit was used following the manufacturer's protocol. The RNA was eluted in 35 µl RNase-free water and the quantity measured using the Nanodrop 1000 by VWR. RNA samples were directly used for cDNA synthesis.

For cDNA synthesis, 100 ng of total RNA was reversely transcribed utilizing the QuantiTect® Reverse Transcription kit following the manufacturer's protocol. The incubation steps were conducted using the Eppendorf Mastercycler gradient. cDNA was stored at -20°C.

2.3.2 REAL-TIME POLYMERASE CHAIN REACTION

Real-time PCR was conducted to validate changes in gene expression upon treatment with P2X receptors antagonists. In real-time PCR, amplicons of cDNA templates are doubled each amplification cycle using sequence-specific oligonucleotides, heat-stable DNA polymerase, and thermal cycling. Amplicons are measured each cycle via fluorescent double-stranded DNA-binding dyes. Sequences of the used oligonucleotide pairs for genes of interest were established in previous studies (**Table 5**). Nonetheless, the efficiency was examined by preparing a standard curve of serially diluted cDNA of untreated cells. The ratio of the number of produced DNA fragments at the end of a cycle divided by the number at the start of the same cycle defines PCR efficiency (**Table 5**). A 100 % efficiency represents doubling of the target sequence each cycle.

For real-time PCR experiments, 5 ng cDNA was mixed in a MicroAmp® Fast Optical 96-well reaction plate with a master mix containing 10 µl SsoAdvanced Universal SYBR® Green Supermix (contains dNTPs, $MgCl_2$, SYBR® Green I, Sso7d fusion polymerase), 1.4 µl 5 µM primer forward, 1.4 µl 5 µM primer reverse (**Table 5**), and 6.2 µl nuclease-free water. A negative control without cDNA input gave information about master mix contaminations. Finally, the plate was sealed with optical adhesive covers, briefly centrifuged, and loaded into the StepOne Plus PCR system with the following PCR program:

Table 10: Real-time RT-PCR program.

Stage	Cycle count	Temperature	Duration [min]	Description
Initiation	1	50°C 95°C	02:00 05:00	Polymerase activation DNA denaturation
Cycling	40	95°C 61°C 72°C	00:05 00:07 00:30	DNA denaturation Annealing Extension + plate read
Melt curve	1 hold	62°C increase to95°C	01:00 + 0.5°C per 00:15	 plate read

The mean cycle threshold (Ct) value of duplicates was used to calculate the fold change gene expression level based on the 2-ΔΔCT method. The method compares the difference in expression between genes of interest and the reference gene peptidylprolyl isomerase A (*PPIA*) and between the control condition (cells treated with LPS) and samples treated with LPS and P2X receptors antagonists. Ct values for the target genes in both the test samples and control samples are normalized in relation to *PPIA*.

2.3.3 AGAROSE GEL ELECTROPHORESIS

An agarose gel electrophoresis was occasionally conducted after real-time RT-PCR to verify the size of the amplicons. To produce the gels, 1.8 % agarose in 100 ml 1 x Rotiphorese TAE buffer was boiled up and mixed with 5 µl GelRed nucleic acid stain 10,000 x. The liquid was cast into a cassette and a comb was inserted. The polymerized gel was inserted to an electrophoresis tank with 1 x Rotiphorese TAE buffer. Samples were diluted 1:10, mixed with DNA loading dye, and loaded next to 2 µl of the GeneRuler 100 bp Plus DNA ladder. After applying 100 V for 45 min, the gel was placed on a transilluminator for taking photos.

2.4 STATISTICS

Statistical analyses were performed using SPSS statistic software version 27. Paired data, obtained in cytokine release experiments, real-time RT-PCR, densitometric analysis, and caspase-assays were analysed by the Friedman test and, if statistically significant with a p value ≤ 0.05, followed by the Wilcoxon signed-rank test. Regarding the Wilcoxon signed-rank test, results with a p value ≤ 0.05 are considered statistically significant and marked accordingly in the figures. The number of individual experiments (n) is indicated in the figures. When primary cells were investigated, the n-number represents data obtained from the cells of

individual humans. In experiments with THP-1 cells, the n-number refers to independent experiments, which were performed on different days with different cell passages. Data were visualized using Inkscape vector graphics editor 1.3.2.

RESULTS

1 CHARACTERISTICS OF THE THP-1 CELL LINE

1.1 MORPHOLOGICAL CHARACTERISTICS OF THP-1 CELL-DERIVED MACROPHAGES

In the course of this study, the THP-1 cell line originating from peripheral blood of a 1-year-old boy with acute monocytic leukaemia was used. In some cases, cells were differentiated into macrophages. The morphology of stained macrophages was assessed to confirm successful differentiation of THP-1 cells (**Figure 5**).

THP-1 M0-like macrophages depicted a rounded or a spindle-shaped morphology (**Figure 5A**), while in M1-like macrophages a fibroblast-like, spindle-shaped morphology dominated (**Figure 5B**). M0-like macrophages were smaller compared to M1-like macrophages and THP-1 cell-derived M1-like macrophages possessed amoeboid protrusions.

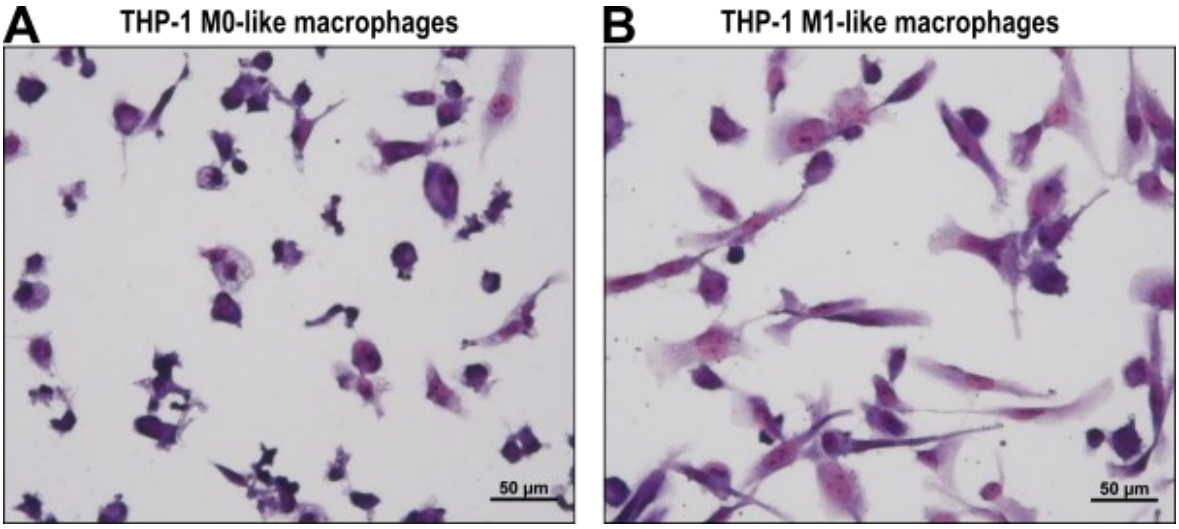

Figure 5: THP-1 cell-derived M0-like and M1-like macrophages. PMA-treated THP-1 cells were either left untreated for a M0-like phenotype **(A)** or treated with IFN-γ and LPS for 48 h for M1-like differentiation. Fixated cells were stained with May-Grünwald and Giemsa staining. All pictures were taken from one representative experiment out of 3. Scale bar: 50 µm.

1.2 IL-1β RELEASE BY MONOCYTIC THP-1 CELLS AND THP-1 CELL-DERIVED M1-LIKE MACROPHAGES

The IL-1β concentration was measured in cell culture supernatants of monocytic THP-1 cells and THP-1 cell-derived M1-like macrophages by ELISA. The cells were primed with 1 µg/ml LPS for 5 h followed by stimulation with BzATP (100 µM), ATP (1 or 2 mM), or nigericin (50 µM) for 40 min. Untreated cells and cells primed with LPS served as controls in every experimental setting.

Figure 6 shows a summary of IL-1β concentrations in cell culture supernatants of Monocytic THP-1 cells (A) and THP-1 cell-derived M1-like macrophages (B). In supernatants of untreated monocytic cells, IL-1β concentrations were below the detection limit of the assay (**Figure 6A**). In supernatants of cells primed with LPS, 9 pg/ml (median) IL-1β was detected ($p \leq 0.000$ versus untreated). Additional treatment with BzATP increased the concentration to 84 pg/ml ($p \leq 0.000$ versus LPS) and in presence of the vehicle DMSO [0.1 %] to 88 pg/ml ($p \leq 0.000$ versus LPS). While adding nigericin, IL-1β concentrations of 308 pg/ml ($p \leq 0.000$ versus LPS) were measured in cell culture supernatants, which is similar to the amounts in presence of DMSO: 299 pg/ml ($p \leq 0.000$ versus LPS) (**Figure 6A**). In case of THP-1 cell-derived M1-like macrophages, IL-1β concentrations of 44 pg/ml were measured in cell culture supernatants of untreated cells and upon treatment with LPS 153 pg/ml ($p \leq 0.000$ versus untreated) (**Figure 6B**). Later on, adding 1 mM ATP resulted in 515 pg/ml IL-1β concentrations compared to 516 pg/ml when DMSO was added (both: $p \leq 0.000$ versus LPS). The IL-1β concentration levels in cell culture supernatants increased up to 893 pg/ml upon stimulation with 2 mM ATP or 875 pg/ml in the presence of 2 mM ATP and DMSO (both: $p \leq 0.000$ versus LPS). Stimulation with nigericin resulted in 767 pg/ml IL-1β ($p \leq 0.000$ versus LPS). Similar amounts of IL-1β in cell culture supernatants were measured in the presence of DMSO: 723 pg/ml ($p \leq 0.000$ versus LPS) (**Figure 6B**).

Simultaneously to the IL-1β concentration, the LDH activity in cell culture supernatants was measured. Compared to the maximal LDH activity in a sample of lysed cells, which was set to 100 %, a median LDH activity of 4.6 % (median) in the supernatants of untreated monocytic THP-1 cells was measured (**Table S-1**). Supernatants of cells primed with LPS showed 5 % LDH activity. Subsequent treatment with BzATP resulted in 6.3 % LDH activity and additional DMSO application in 6.7 %. When nigericin was applied in the absence or presence of DMSO, 13.1 % LDH activity was measured. In supernatants of untreated THP-1 cell-derived M1-like macrophages 5 % LDH activity was measured (**Table S-2**). Treatment with LPS resulted in a median 8.7 % LDH activity. When 1 mM ATP was added, 19 % LDH activity was measured while adding DMSO together with 1 mM ATP resulted in 19.5 %. Supernatants of cells treated with 2 mM ATP showed a median LDH activity of 18.8 %, compared to 18.6 % when DMSO was added. Treatment with nigericin resulted in 23.6 % LDH activity, with or without DMSO, indicating that the vehicle DMSO did not alter the viability of THP-1 cells.

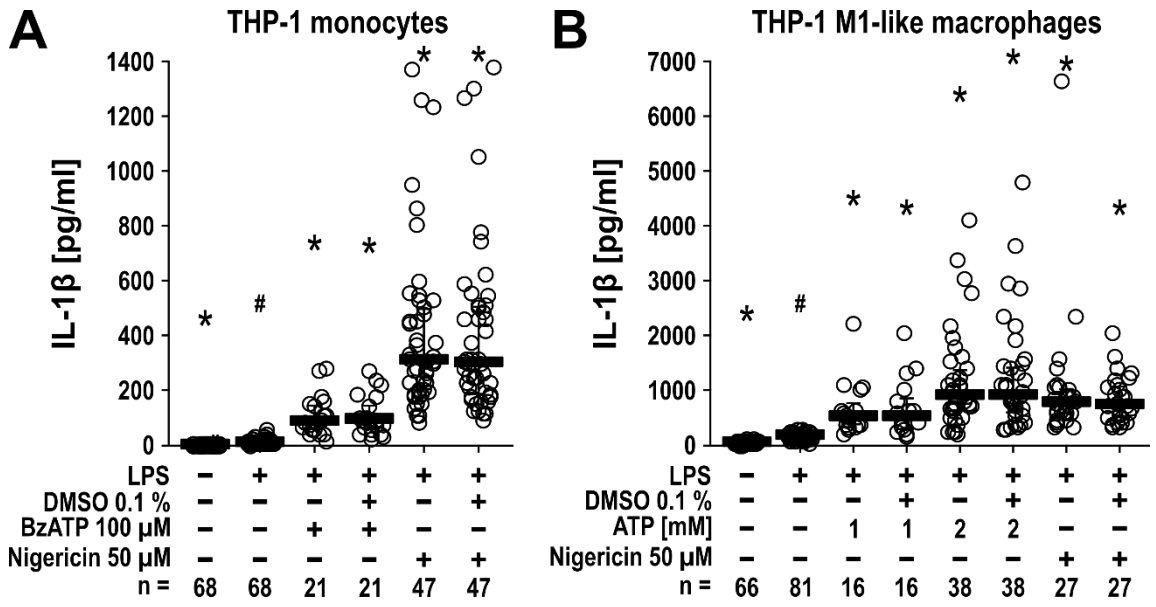

Figure 6: IL-1β release by (A) monocytic THP-1 cells and (B) THP-1 cell-derived M1-like macrophages. Cells were either left untreated or primed with LPS (1 µg/ml) in absence or presence of 0.1 % DMSO for 5 h. Thereafter, BzATP (100 µM), ATP (1 mM, 2 mM), or nigericin (50 µM) were added for 40 min to LPS-primed cells. IL-1β was measured in cell culture supernatants. Data are presented as individual data points, bars represent median, whiskers percentiles 25 and 75. Friedman-test followed by Wilcoxon signed-rank test. # $p \leq 0.05$ significantly different from untreated cells. * $p \leq 0.05$ significantly different from LPS-primed THP-1 cells. LPS, lipopolysaccharide; DMSO, dimethyl sulfoxide; BzATP, 2'(3')-O-(4-Benzoylbenzoyl)adenosine-5'-triphosphate; ATP, adenosine triphosphate.

Due to a high variability of the IL-1β release in THP-1 cells, results were normalized in the following analyses. Corresponding LDH activity are listed in supplementary tables S-1 and S-2.

2 CHARACTERISTICS OF PRIMARY CELLS

2.1 CLASSIFICATION OF CELL TYPES IN PERITONEAL DIALYSATE SAMPLES

For this study, primary hPMs from donors receiving peritoneal dialysis training were also used. Staining of cells before and after completion of the enrichment of macrophages were performed to evaluate the relative abundance of hPMs in the samples. The original cell population represents all cell types in the peritoneal dialysate samples. After completing the isolation protocol, the samples contained only adherent cells. Macrophages are presented by cells positive for CD14 or CD68. Staining of the original cell population revealed rounded cells with round nuclei or nuclei divided into several lobes (**Figure 7A, upper row**). The samples included $CD14^+$ and $CD14^-$ cells, whereas $CD14^+$ cells exhibited different staining intensities. The original cell population also included $CD68^-$ cells and cells positive for CD68, again with different staining intensities (**Figure 7A, upper row**). Staining of the adherent cell populations revealed cells with a fibroblast-like morphology, the shapes of the nuclei were unsegmented (**Figure 7A, bottom row**). Cells positive as well as negative for CD14 could be detected. The CD14-signal seemed to be more intense at the cell membranes. The adherent cell populations included $CD68^+$ and $CD68^-$ cells, whereas the $CD68^+$ cells can be divided into cells that exhibit

strong signals locally condensed within the cells and cells with a weaker signal across the whole cytoplasm (**Figure 7A, bottom row**). Figure 7B shows that the abundance of $CD14^+$ cells increased significantly after completion of the isolation protocol ($p = 0.043$). The percentage of $CD68^+$ cells was also significantly increased in the adherent cell population compared to the original peritoneal dialysate sample ($p = 0.043$) (**Figure 7C**).

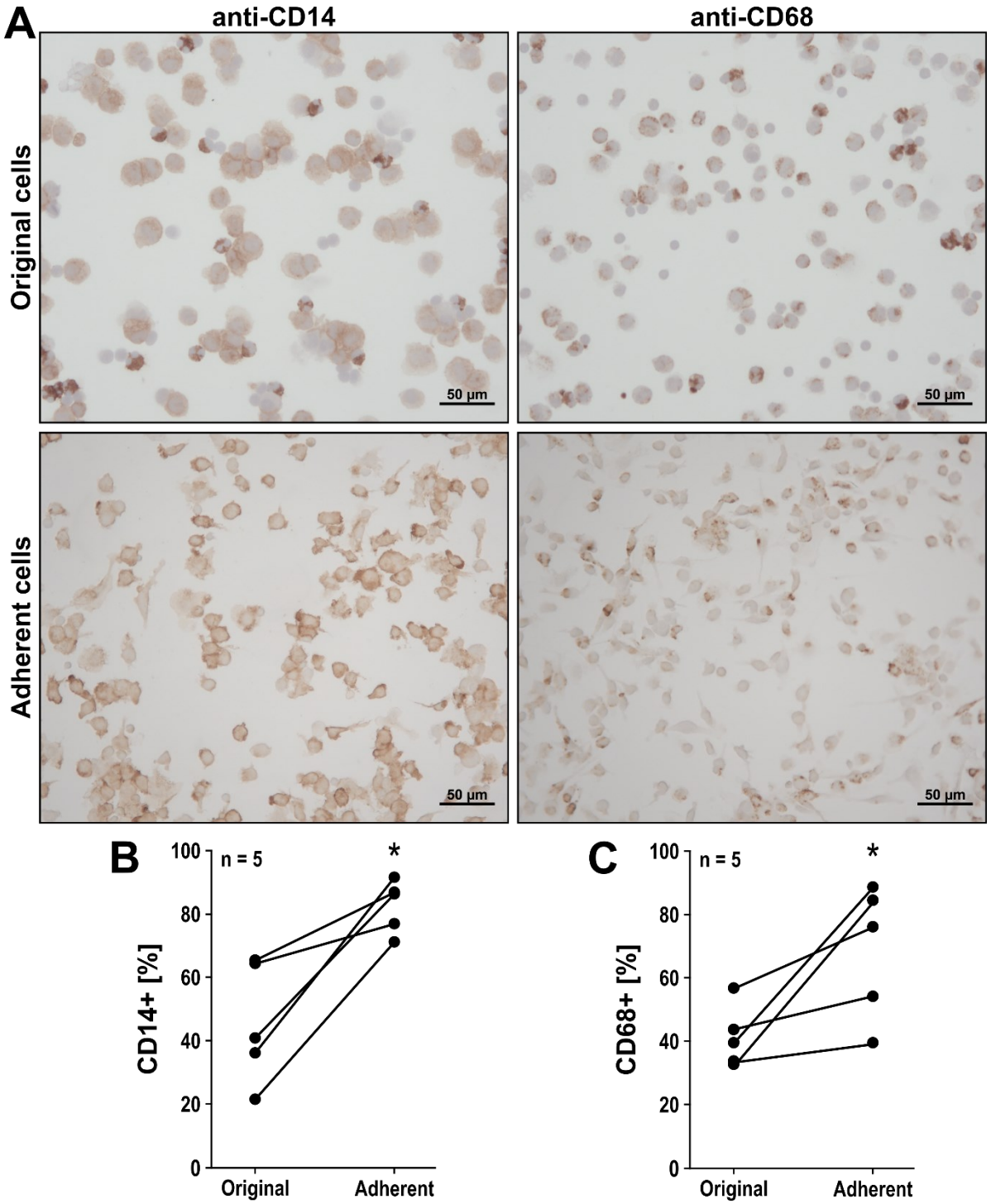

Figure 7: Immunocytochemical staining of human peritoneal cells. Immunocytochemical staining for macrophage markers CD14 and CD68 before and after isolation protocol. **(A)** Upper row: Original composition of cell types in the peritoneal dialysate samples. Bottom row: Composition of adherent cell types. Left panel: Staining with anti-CD14 antibody. Right panel: Staining with anti-CD68 antibody. Scale bar: 50 µm. All pictures were taken from one representative experiment out of 5. Percentages of $CD14^+$ **(B)** and $CD68^+$ **(C)** macrophages in the peritoneal dialysate and in the adherent cell populations. Data are presented as individual data points; data from the same patients are connected. Friedman-test followed by Wilcoxon signed-rank test. * $p \leq 0.05$ significantly different from original composition.

2.2 IL-1β RELEASE BY HPBMCS AND HPMS

In addition to the THP-1 cell line and hPMs, primary hPBMCs from healthy donors were used. hPBMCs were primed with 5 ng/ml LPS for 3 h followed by adherence selection of mononuclear cells. Thereafter, cells were stimulated with BzATP (100 µM) or nigericin (50 µM) for 30 min. The IL-1β concentration in cell culture supernatants was measured via ELISA. Untreated cells and cells primed with LPS served as controls in every experimental setting.

Figure 8 shows a summary of the IL-1β concentrations in pg/ml in cell culture supernatants of hPBMCs (A) and hPMs (B) of individual sets of experiments. In the untreated condition, IL-1β concentrations were below the lower detection limit of the assay, while adding LPS resulted in a median IL-1β concentration levels of 23 pg/ml ($p = 0.000$ versus untreated) (**Figure 8A**). Subsequent treatment with BzATP increased the concentration up to 238 pg/ml ($p = 0.018$ versus LPS) or to 250 pg/ml IL-1β when DMSO was also applied ($p = 0.018$ versus LPS). Nigericin application induced 834 pg/ml IL-1β ($p = 0.008$ versus LPS) and additional DMSO application 762 pg/ml IL-1β concentration ($p = 0.008$ versus LPS). DMSO did not severely change the IL-1β concentration in cell culture supernatants of hPBMCs (**Figure 8A**). In supernatants of untreated hPMs, no IL-1β above the lower detection limit was measurable (**Figure 8B**). Treatment with LPS resulted in a median 47 pg/ml IL-1β ($p = 0.043$ versus untreated), while additional BzATP application increased levels to 2495 pg/ml ($p = 0.043$ versus LPS) and when DMSO was also applied, IL-1β concentration in supernatants came to 3217 pg/ml ($p = 0.043$ versus LPS) (**Figure 8B**).

The LDH activity in cell culture supernatants of hPBMCs and hPMs was also measured. Compared to the maximal LDH activity in a sample of lysed cells, which was set to 100 % activity, LDH activity of 1 % (median) in the supernatants of untreated hPBMCs was measured (**Table S-3**). Priming with LPS resulted in 0.7 % LDH activity. Supernatants of cells additionally treated with BzATP showed 2.5 % LDH activity, while DMSO application resulted in 2.1 % LDH activity. Nigericin application resulted in 23.5 % and additional DMSO in 24 % LDH activity in cell culture supernatants (**Table S-3**). Samples of untreated hPMs showed 2 % LDH activity, while stimulation with LPS resulted in 3 % LDH activity (**Table S-4**). Supernatants of cells additionally treated with BzATP showed a median LDH activity of 15.2 %, while DMSO addition resulted in 19.1 % LDH activity (**Table S-4**). The application of DMSO did not change the viability of hPBMCs and hPMs.

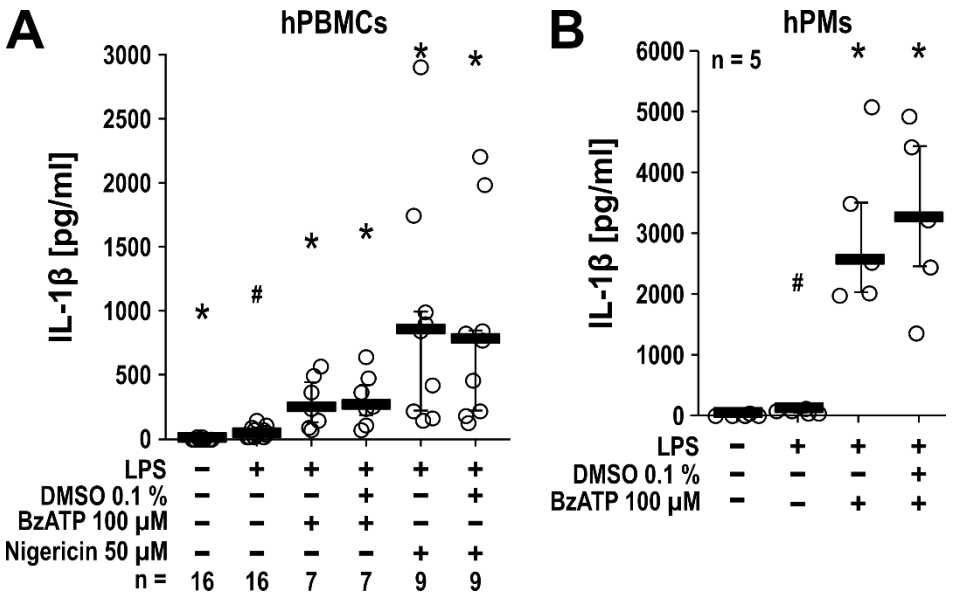

Figure 8: IL-1β release by hPBMCs and hPMs. (A) hPBMCs were either untreated or primed with LPS (5 ng/ml) in absence or presence of 0.1 % DMSO for 3 h. Thereafter, BzATP (100 µM) or nigericin (50 µM) were added for 30 min to LPS-primed cells. **(B)** hPMs were either untreated or primed with LPS (0.1 µg/ml) in absence or presence of 0.1 % DMSO for 5 h. Thereafter, BzATP (100 µM) was added for 40 min to LPS-primed cells. IL-1β was measured in cell culture supernatants. Data are presented as individual data points, bars represent median, whiskers percentiles 25 and 75. Friedman-test followed by Wilcoxon signed-rank test. # $p \leq 0.05$ significantly different from untreated cells. * $p \leq 0.05$ significantly different from LPS-primed cells. hPBMCs, human peripheral blood mononuclear cells; hPMs, human peritoneal macrophages; LPS, lipopolysaccharide; DMSO, dimethyl sulfoxide; BzATP, 2'(3')-O-(4-Benzoylbenzoyl)adenosine-5'-triphosphate.

Like in THP-1 cells, the IL-1β release by hPBMCs showed a high variability. Therefore, these results were also normalized in the following analyses. Corresponding LDH activity are listed in supplementary tables S-3 and S-4.

3 EFFECTS OF P2X RECEPTORS ANTAGONISTS ON IL-1β EXPRESSION AND SECRETION

3.1 EFFECTS OF P2X RECEPTORS ANTAGONISTS ON ATP-DEPENDENT IL-1β RELEASE

3.1.1 IL-1β RELEASE BY THP-1 CELLS

To explore the role of P2RX4 and P2RX7 in IL-1β secretion by THP-1 cells, various antagonists were given prior to signal 1 'priming' or prior to signal 2 'activation' and the IL-1β concentration in cell culture supernatants was measured. In previous studies of our lab, concentration response experiments of 5-B and A43 were conducted (Ettischer L. unpublished). The concentration response experiment for JNJ is shown in Figure S-1. Concentrations of the P2RX4 antagonists PSB, PZB15, and PZB13 were applied as suggested by the provider (Prof. Christa Müller, Bonn). The IL-1β concentration in supernatants of positive control samples in which cells were primed with LPS and stimulated with BzATP alone (monocytic THP-1 cells, **Figure 9**) or ATP (THP-1 cell-derived M1-like macrophages, **Figure 10**) was set to 100 %. In a set of experiments, the effects of the P2RX4 antagonists and A43 were investigated. Later

on, different sets of experiments were conducted, in which the P2RX7 antagonists A43 and JNJ were used. These sets of experiments were combined in Figure 9. This explains the high n numbers for the control samples (LPS combined with BzATP), which were included in all experiments. In Figure 10, a set of experiments including 5-B, PSB, A43, and respective controls, and a second set of experiments including all listed antagonists and respective controls were combined.

When monocytic THP-1 cells were treated with the P2RX4 antagonist 5-B (10 µM, p = 0.028; 20 µM, p = 0.046) prior to LPS application, stimulation with BzATP resulted in significantly increased IL-1β concentrations (**Figure 9**). Incubation with the other P2RX4 antagonists PSB (p = 0.028), PZB15 (p = 0.028), and PZB13 (p = 0.028) on the other hand significantly reduced the IL-1β concentrations. Treatment with both P2RX7 antagonists prior to stimulation with LPS resulted in very low concentrations of IL-1β in cell culture supernatants under the same conditions: A43 (p = 0.007) and JNJ (p = 0.024). When the antagonists were given just prior to stimulation with BzATP, 5-B slightly decreased IL-1β in supernatants at a concentration of 20 µM (p = 0.046). Again, PSB (p = 0.028), PZB15 (p = 0.027), and PZB13 (p = 0.024) significantly and efficiently reduced the IL-1β concentrations as well as the P2RX7 antagonists A43 (p = 0.007) and JNJ (p = 0.027) (**Figure 9**).

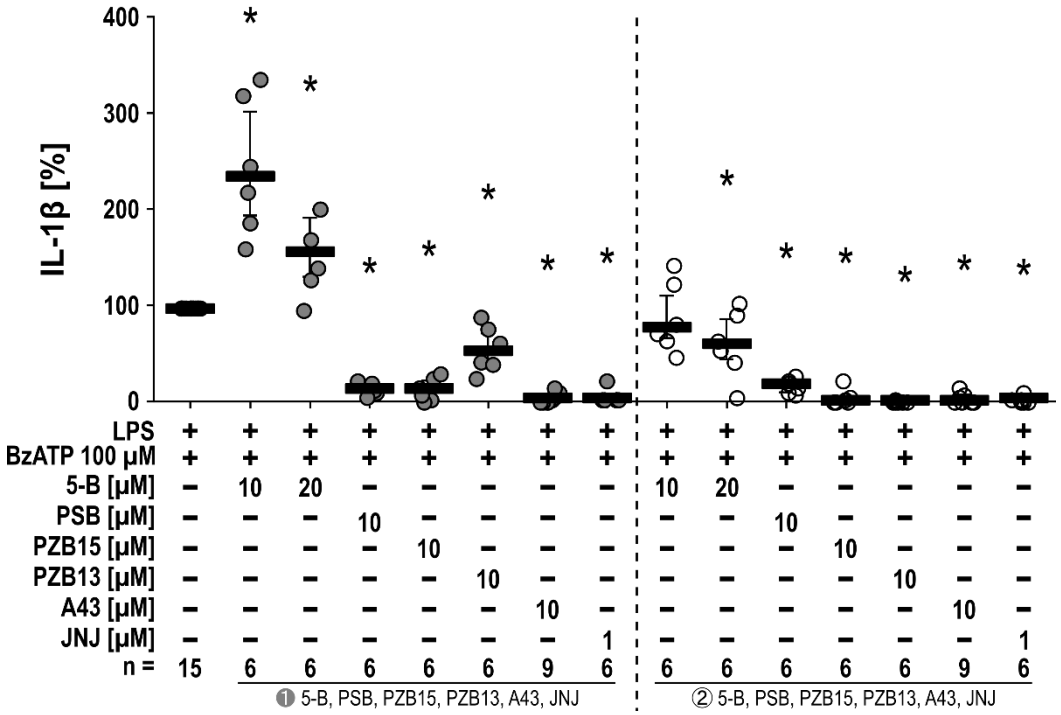

Figure 9: The impact of P2RX4 and P2RX7 antagonists on the BzATP-induced IL-1β release by monocytic THP-1 cells. Cells were primed with LPS (1 µg/ml) for 5 h in the absence or presence (❶) of the P2RX4 antagonists 5-B (10, 20 µM), PSB (10 µM), PZB15 (10 µM), PZB13 (10 µM), or the P2RX7 inhibitors A43 (10 µM) or JNJ (1 µM). Thereafter, BzATP (100 µM) was added for 40 min in the absence or presence (②) of the antagonists and IL-1β was measured in cell culture supernatants. The IL-1β concentration in experiments in which primed cells were stimulated with BzATP in the presence of the vehicle was set to 100 % and all other values were calculated accordingly. Data are presented as individual data points, bars represent median, whiskers percentiles 25 and 75. Friedman-test followed by Wilcoxon signed-rank test. ∗ $p \leq 0.05$ significantly different from samples in which only BzATP was given to LPS-primed monocytic THP-1 cells. LPS, lipopolysaccharide; BzATP, 2'(3')-O-(4-Benzoylbenzoyl)adenosine-5'-triphosphate; 5-B, 5-(3-Bromophenyl)-1,3-dihydro-2H-benzofuro[3,2-e]-1,4-diazepin-2-one; PSB, PSB-15417; PZB15, PZB15517166A; PZB13, PZB13420052A; A43, 3-{[5-(2,3-dichlorophenyl)-1H-1,2,3,4-tetrazol-1-yl]methyl}pyridine; JNJ, N-[[4-(4-phenylpiperazin-1-yl)oxan-4-yl]methyl]-2-phenylsulfanylpyridine-3-carboxamide.

THP-1 cell-derived M1-like macrophages were treated with two different concentrations of ATP for comparison (**Figure 10**). Figure 10A shows cells primed with LPS and stimulated with 1 mM ATP. Here, treatment with 5-B prior to priming decreased the IL-1β concentration in supernatants of cells primed with LPS and stimulated with ATP (10 µM; $p = 0.001$). The P2RX4 antagonists PSB ($p = 0.001$), PZB15 ($p = 0.018$), and PZB13 ($p = 0.018$) as wells as the P2RX7 antagonist A43 ($p = 0.004$) also significantly reduced the IL-1β levels. When given prior to ATP, all antagonists reduced IL-1β: 5-B (10 µM: $p = 0.002$), PSB ($p = 0.043$), PZB15 ($p = 0.018$), PZB13 ($p = 0.018$), and A43 ($p = 0.007$) (**Figure 10A**).

Similar results were obtained with 2 mM ATP application (**Figure 10B**). Treatment with 5-B before priming did not induce significant alterations in supernatants of cells primed with LPS and stimulated with ATP, while PSB ($p = 0.001$), PZB15 ($p = 0.018$), and PZB13 ($p = 0.017$) significantly reduced IL-1β concentrations. No IL-1β was measurable in cell culture supernatants of THP-1 cell-derived M1-like macrophages, when the cells were treated with A43 before priming with LPS ($p = 0.005$). Incubation with 2 mM ATP in the presence of 10 µM 5-B slightly decreased IL-1β concentration in supernatants of cells primed with LPS ($p = 0.002$). The other P2RX4 antagonists also significantly decreased the IL-1β concentration: PSB ($p = 0.018$), PZB15 ($p = 0.018$), and PZB13 ($p = 0.018$). Again, application of A43 shortly before ATP resulted in IL-1β in cell culture supernatants below the threshold of detection ($p = 0.007$) (**Figure 10B**).

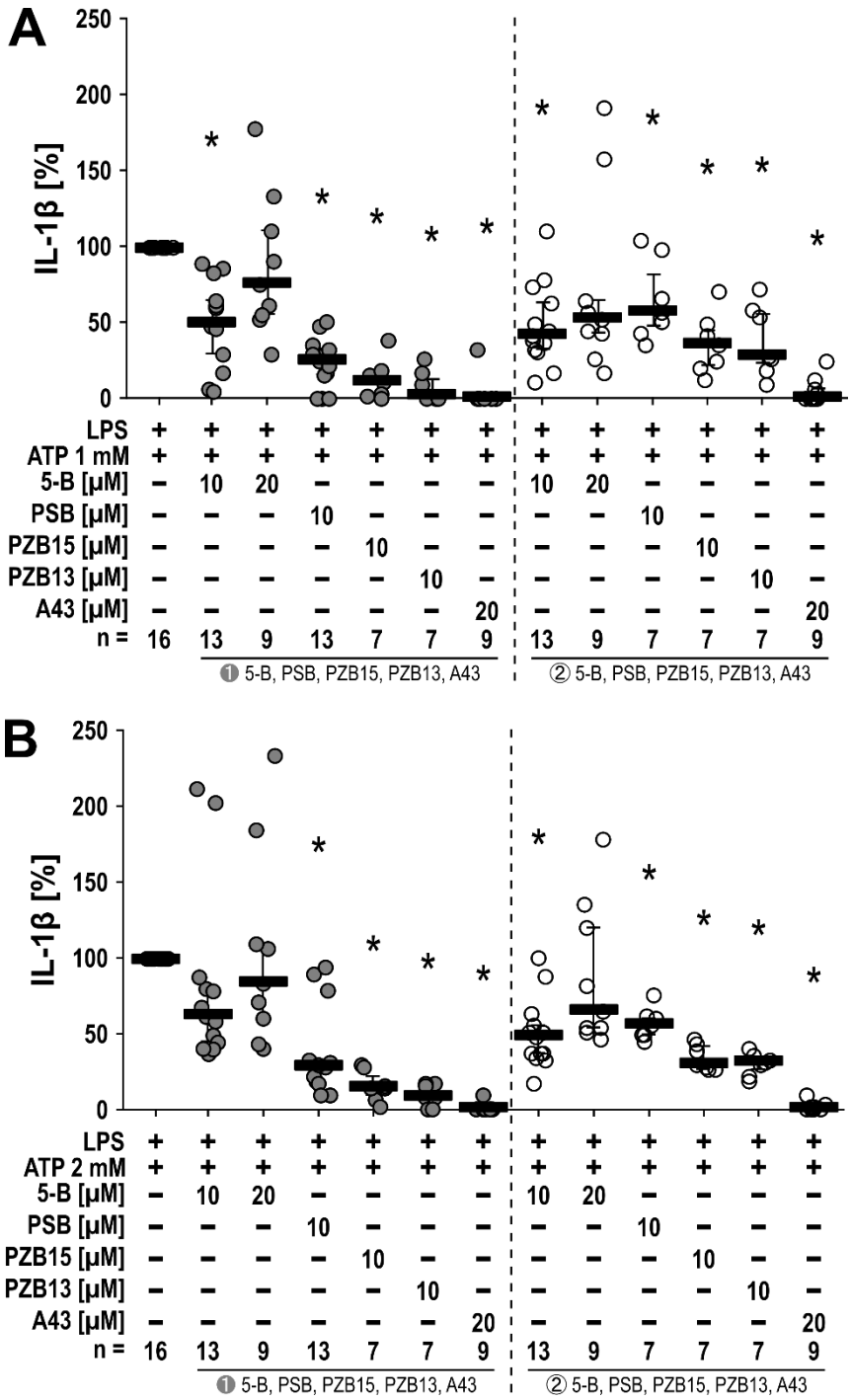

Figure 10: The impact of P2RX4 and P2RX7 antagonists on the ATP-induced IL-1β release by THP-1 cell-derived M1-like macrophages. THP-1 cells were differentiated into THP-1 M1-like macrophages. Cells were primed with LPS (1 µg/ml) for 5 h in the absence or presence (❶) of the P2RX4 antagonists 5-B (10, 20 µM), PSB (10 µM), PZB15 (10 µM), PZB13 (10 µM) or the P2RX7 inhibitor A43 (20 µM). Thereafter, **(A)** ATP (1 mM) or **(B)** ATP (2 mM) was added for 40 min the absence or presence (②) of the antagonists and IL-1β was measured in cell culture supernatants. The IL-1β concentration in experiments in which primed cells were stimulated with ATP in the presence of the vehicle was set to 100 % and all other values were calculated accordingly. Data are presented as individual data points, bars represent median, whiskers percentiles 25 and 75. Friedman-test followed by Wilcoxon signed-rank test. ∗ $p \leq 0.05$ significantly different from samples in which only ATP was given to LPS-primed THP-1 M1-like macrophages. LPS, lipopolysaccharide; ATP, adenosine triphosphate; 5-B, 5-(3-Bromophenyl)-1,3-dihydro-2H-benzofuro[3,2-e]-1,4-diazepin-2-one; PSB, PSB-15417; PZB15, PZB15517166A; PZB13, PZB13420052A; A43, 3-{[5-(2,3-dichlorophenyl)-1H-1,2,3,4-tetrazol-1-yl]methyl}pyridine.

3.1.2 IL-1β RELEASE BY HPBMCS AND HPMS

The effects of P2X receptors antagonists on hPBMCs and hPMs were investigated for verification of the data on the THP-1 cell line in primary cells. Various antagonists were given prior to signal 1 'priming' (LPS) or prior to signal 2 'activation' (BzATP) and IL-1β concentrations in cell culture supernatants were measured. The IL-1β concentration in supernatants of the positive control samples in which cells primed with LPS were stimulated with BzATP alone was set to 100 %. Of note, in contrast to experiments on monocytic THP-1 cells, the cell culture medium of hPBMCs is replaced 20 min before application of BzATP during selection of adherent cells (**Figure 3**).

Treatment with 5-B prior to priming significantly increased the IL-1β concentration in supernatants of hPBMCs that were primed with LPS and stimulated with BzATP (**Figure 11**). Unlike in THP-1 cells, the decreasing effect of the other P2RX4 antagonists PSB, PZB15, and PZB13 when applied prior to LPS could not be observed in hPBMCs. Incubation with the P2RX7 antagonist JNJ did not alter IL-1β under the same conditions. Application of 5-B ($p = 0.028$), PSB ($p = 0.028$), PZB15 ($p = 0.028$), and JNJ ($p = 0.046$) just before stimulation with BzATP significantly decreased IL-1β concentrations (**Figure 11**).

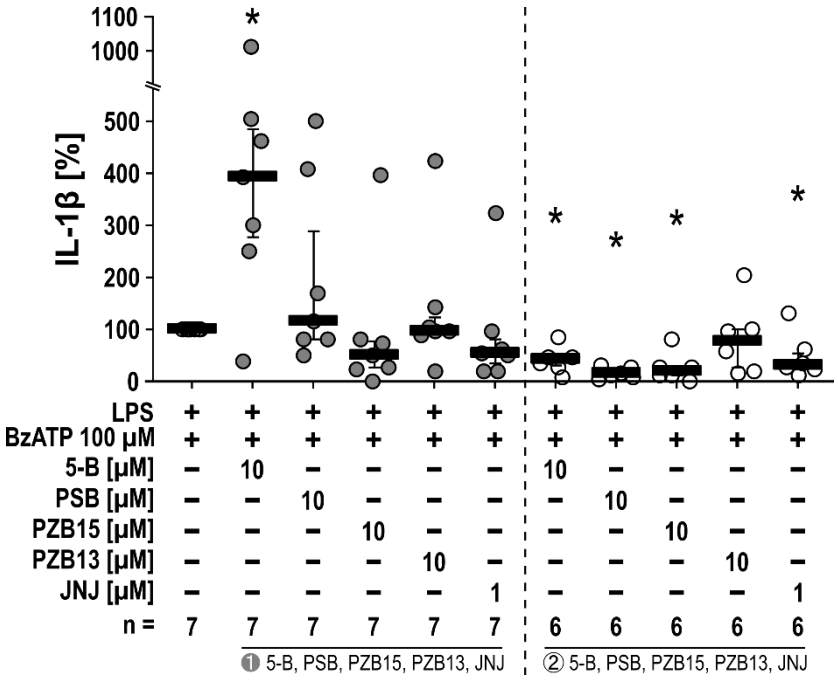

Figure 11: The impact of P2RX4 and P2RX7 antagonists on the BzATP-induced IL-1β release by hPBMCs. hPBMCs were primed with LPS (5 ng/ml) for 3 h in the absence or presence (❶) of the P2RX4 antagonists 5-B (10 µM), PSB (10 µM), PZB15 (10 µM), PZB13 (10 µM), or the P2RX7 inhibitor JNJ (1 µM). Thereafter, BzATP (100 µM) was added for 30 min the absence or presence (②) of the antagonists and IL-1β was measured in cell culture supernatants. The IL-1β concentration in experiments in which primed cells were stimulated with BzATP in the presence of the vehicle was set to 100 % and all other values were calculated accordingly. Data are presented as individual data points, bars represent median, whiskers percentiles 25 and 75. Friedman-test followed by Wilcoxon signed-rank test. ∗ $p \leq 0.05$ significantly different from samples in which only BzATP was given to LPS-primed hPBMCs. LPS, lipopolysaccharide; BzATP, 2'(3')-O-(4-Benzoylbenzoyl)adenosine-5'-triphosphate; 5-B, 5-(3-Bromophenyl)-1,3-dihydro-2H-benzofuro[3,2-e]-1,4-diazepin-2-one; PSB, PSB-15417; PZB15, PZB15517166A; PZB13, PZB13420052A; JNJ, N-[[4-(4-phenylpiperazin-1-yl)oxan-4-yl]methyl]-2-phenylsulfanylpyridine-3-carboxamide.

Figure 12 shows that treatment with 5-B prior to priming significantly decreased the IL-1β concentration in supernatants of hPMs primed with LPS and stimulated with BzATP by 33 % ($p = 0.042$), while stimulation with A43 prior to LPS treatment resulted in IL-1β concentrations below the limit of detection ($p = 0.042$). When the antagonists were added prior to BzATP, the results were similar: 5-B decreased the IL-1β concentration by 37 % compared to the positive control ($p = 0.043$) and after treatment with A43, the protein levels were again lower than the detection limit ($p = 0.039$) (**Figure 12**).

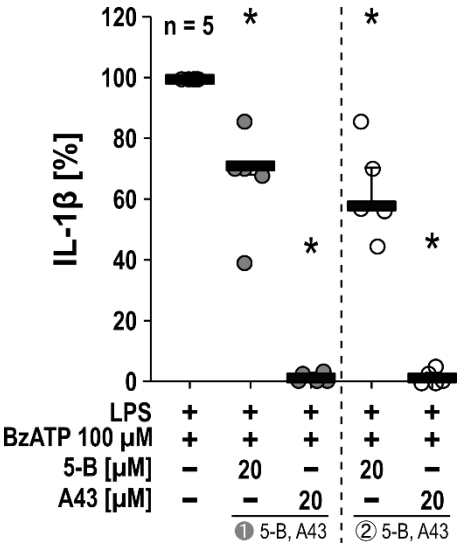

Figure 12: The impact of P2RX4 and P2RX7 antagonists on the BzATP-induced IL-1β release by hPMs. hPMs were primed with LPS (0.1 µg/ml) for 5 h in the absence or presence (❶) of the P2RX4 antagonist 5-B (20 µM) or the P2RX7 inhibitor A43 (20 µM). Thereafter, BzATP (100 µM) was added for 40 min the absence or presence (②) of the antagonists and IL-1β was measured in cell culture supernatants. The IL-1β concentration in experiments in which primed cells were stimulated with BzATP in the presence of the vehicle was set to 100 % and all other values were calculated accordingly. Data are presented as individual data points, bars represent median, whiskers percentiles 25 and 75. Friedman-test followed by Wilcoxon signed-rank test. ∗ $p \leq 0.05$ significantly different from samples in which only BzATP was given to LPS-primed hPMs. LPS, lipopolysaccharide; BzATP, 2'(3')-O-(4-Benzoylbenzoyl)adenosine-5'-triphosphate; 5-B, 5-(3-Bromophenyl)-1,3-dihydro-2H-benzofuro[3,2-e]-1,4-diazepin-2-one; A43, 3-{[5-(2,3-dichlorophenyl)-1H-1,2,3,4-tetrazol-1-yl]methyl}pyridine.

3.2 EFFECTS OF P2X RECEPTORS ANTAGONISTS ON ATP-INDEPENDENT IL-1β RELEASE

3.2.1 IL-1β RELEASE BY THP-1 CELLS

To investigate the effects of P2X receptors antagonists on cell priming with LPS and on the stimulation of IL-1β maturation by a stimulus independent of ATP, ATP-independent secretion of IL1-β from monocytic THP-1 cells and THP-1 cell-derived macrophages was induced by the pore-forming toxin nigericin. The IL-1β concentration in supernatants cells primed with LPS and stimulated with nigericin alone was set to 100 %. In a first set of experiments, the effects of P2RX4 antagonists and A43 were investigated. Later on, a second set of experiments was conducted, in which the P2RX7 antagonist JNJ was used along with the respective controls. These different sets of experiments were combined in Figure 13. In Figure 14, a set of experiments including the P2RX4 antagonists and A43 and a set of experiments including both

P2RX7 antagonists (A43 and JNJ) were combined. This explains the high n numbers for the control samples, which were included in all experiments.

In monocytic THP-1 cells, treatment with 5-B ($p = 0.002$) or with PZB13 ($p = 0.019$) prior to priming significantly increased the IL-1β concentration in supernatants of cells primed with LPS and stimulated with nigericin (**Figure 13**). PSB did not induce significant alterations and PZB15 significantly reduced the IL-1β concentration ($p = 0.002$). Treatment with the P2RX7 antagonist A43 did not result in altered IL-1β levels, but incubation with JNJ increased the IL-1β concentration under the same condition ($p = 0.028$). When given just prior to nigericin, the P2RX4 and P2RX7 antagonists did not induce changes in the IL-1β concentration in cell culture supernatants – except PSB by tendency ($p = 0.075$), PZB13 ($p = 0.028$) and JNJ ($p = 0.043$), that slightly decreased the concentration (**Figure 13**).

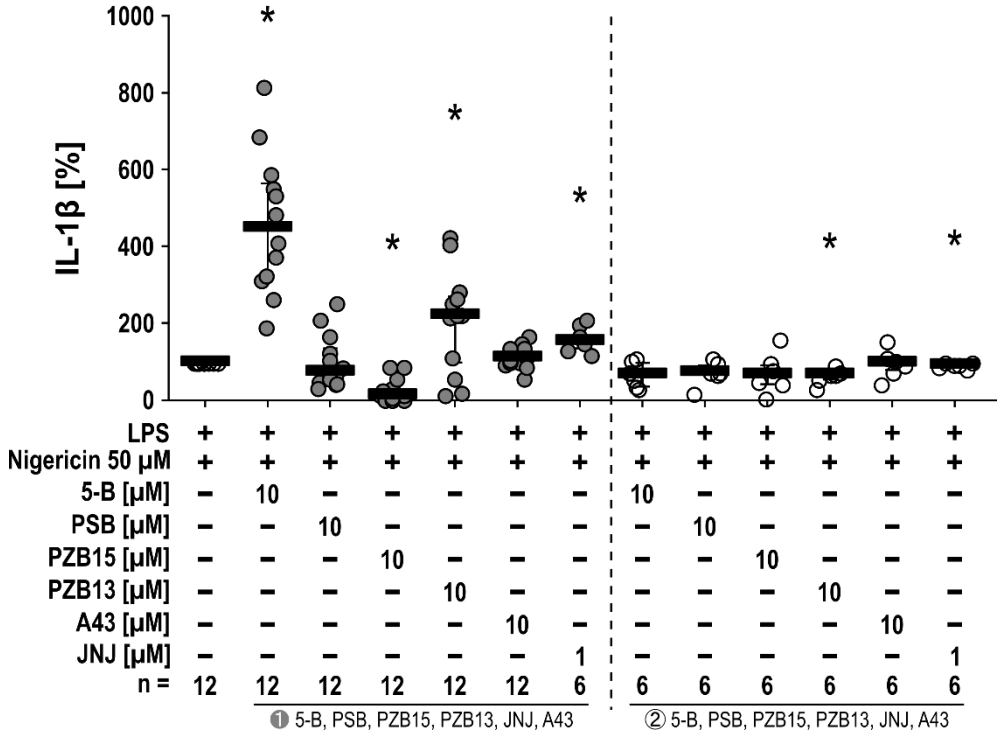

Figure 13: The impact of P2RX4 and P2RX7 antagonists on the nigericin-induced IL-1β release by monocytic THP-1 cells. Cells were primed for 5 h with LPS (1 µg/ml) in the absence or presence (❶) of the P2RX4 antagonists 5-B (10 µM), PSB (10 µM), PZB15 (10 µM), PZB13 (10 µM), or the P2RX7 inhibitors A43 (10 µM), JNJ (1 µM). Thereafter, nigericin (50 µM) was added for 40 min the absence or presence (②) of the antagonists. IL-1β was measured in cell culture supernatants. The IL-1β concentration in experiments in which primed cells were stimulated with nigericin in the presence of the vehicle was set to 100 % and all other values were calculated accordingly. Data are presented as individual data points, bars represent median, whiskers percentiles 25 and 75. Friedman-test followed by Wilcoxon signed-rank test. ∗ $p \leq 0.05$ significantly different from samples in which only nigericin was given to LPS-primed monocytic THP-1 cells. LPS, lipopolysaccharide; 5-B, 5-(3-Bromophenyl)-1,3-dihydro-2H-benzofuro[3,2-e]-1,4-diazepin-2-one; PSB, PSB-15417; PZB15, PZB15517166A; PZB13, PZB13420052A; A43, 3-{[5-(2,3-dichlorophenyl)-1H-1,2,3,4-tetrazol-1-yl]methyl}pyridine; JNJ, N-[[4-(4-phenylpiperazin-1-yl)oxan-4-yl]methyl]-2-phenylsulfanylpyridine-3-carboxamide.

Unlike in Monocytic THP-1 cells, stimulation with 5-B prior to priming with LPS did not alter the nigericin-mediated increase in the IL-1β concentration in cell culture supernatants of THP-1 cell-derived M1-like macrophages (**Figure 14**). The P2RX4 antagonists PSB ($p = 0.008$), PZB15 ($p = 0.007$), and PZB13 ($p = 0.008$) decreased the IL-1β concentration under the same

conditions. The P2RX7 antagonists A43 and JNJ did not induce significant alterations when given prior to LPS. When given prior to nigericin, only the P2RX4 antagonists 5-B (p = 0.028) and PZB15 (p = 0.028) induced a significant reduction and JNJ (p = 0.086) induced a tendentially reduction in the IL-1β concentration in supernatants of THP-1 cell-derived M1-like macrophages primed with LPS (**Figure 14**).

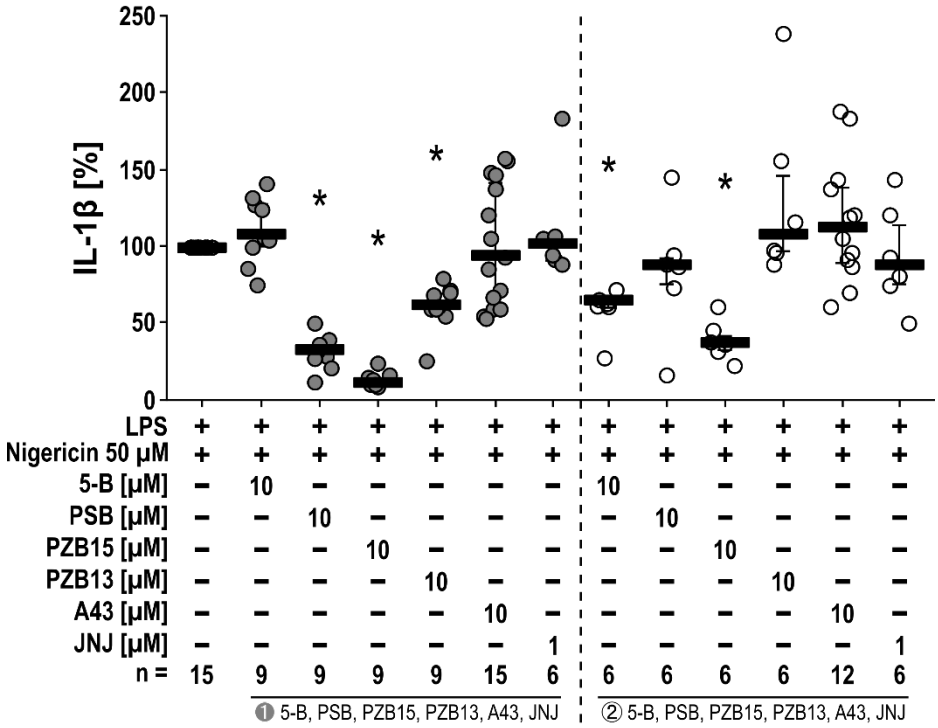

Figure 14: The impact of P2RX4 and P2RX7 antagonists on the nigericin-induced IL-1β release by THP-1 cell-derived M1-like macrophages. THP-1 cells were differentiated into THP-1 M1-like macrophages. Cells were primed with LPS (1 µg/ml) for 5 h in the absence or presence (❶) of the P2RX4 antagonists 5-B (10 µM), PSB (10 µM), PZB15 (10 µM), PZB13 (10 µM), or the P2RX7 antagonists A43 (10 µM) or JNJ (1 µM). Thereafter, nigericin (50 µM) was added for 40 min the absence or presence (②) of the antagonists and IL-1β was measured in cell culture supernatants. The IL-1β concentration in experiments in which primed cells were stimulated with nigericin in the presence of the vehicle was set to 100 % and all other values were calculated accordingly. Data are presented as individual data points, bars represent median, whiskers percentiles 25 and 75. Friedman-test followed by Wilcoxon signed-rank test. ∗ p ≤ 0.05 significantly different from samples in which only nigericin was given to LPS-primed THP-1 M1-like macrophages. LPS, lipopolysaccharide; 5-B, 5-(3-Bromophenyl)-1,3-dihydro-2H-benzofuro[3,2-e]-1,4-diazepin-2-one; PSB, PSB-15417; PZB15, PZB15517166A; PZB13, PZB13420052A; A43, 3-{[5-(2,3-dichlorophenyl)-1H-1,2,3,4-tetrazol-1-yl]methyl}pyridine; JNJ, N-[[4-(4-phenylpiperazin-1-yl)oxan-4-yl]methyl]-2-phenylsulfanylpyridine-3-carboxamide.

3.2.2 IL-1β RELEASE BY HPBMCS

For a comparison of the monocytic THP-1 cell line and primary monocytic cells, the ATP-independent IL-1β concentration in cell culture supernatant of hPBMCs primed with LPS and stimulated with nigericin was also investigated. Again, various antagonists were given prior to signal 1 'priming' (LPS). The IL-1β concentration in supernatants of samples in which LPS-primed cells were stimulated only with nigericin was set to 100 %.

The P2RX4 antagonist 5-B increased the IL-1β concentration significantly (p = 0.011), although the data were variable (**Figure 15**). This could also be observed with PZB13 (p = 0.012) and

A43 (p = 0.05), while treatment with JNJ tended to induce an increase in IL-1β levels in supernatants of cells primed with LPS and stimulated with nigericin (p = 0.091) (**Figure 15**).

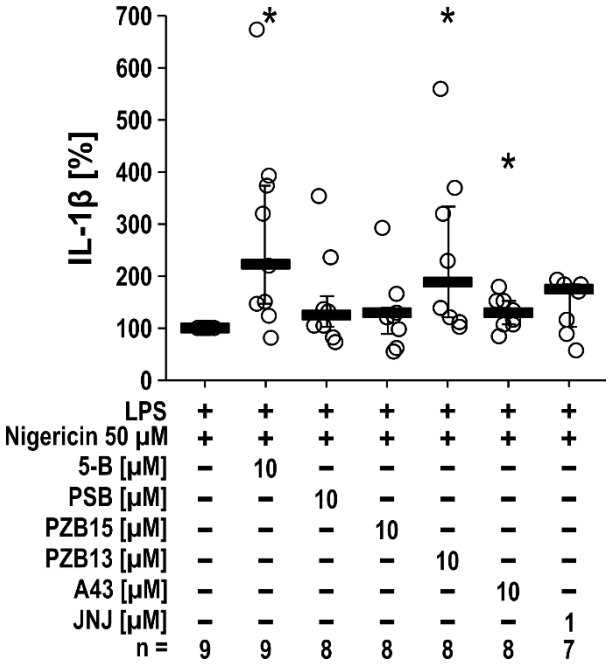

Figure 15: The impact of P2RX4 and P2RX7 antagonists on the nigericin-induced IL-1β release by hPBMCs. hPBMCs were primed with LPS (5 ng/ml) for 3 h in the absence or presence of the P2RX4 antagonists 5-B (10 µM), PSB (10 µM), PZB15 (10 µM), PZB13 (10 µM), or the P2RX7 inhibitors A43 (10 µM), JNJ (1 µM). Thereafter, nigericin (50 µM) was added for 30 min and IL-1β was measured in cell culture supernatants. The IL-1β concentration in experiments in which primed cells were stimulated with nigericin in the presence of the vehicle was set to 100 % and all other values were calculated accordingly. Data are presented as individual data points, bars represent median, whiskers percentiles 25 and 75. Friedman-test followed by Wilcoxon signed-rank test. ∗ p ≤ 0.05 significantly different from samples in which only nigericin was given to LPS-primed hPBMCs. LPS, lipopolysaccharide; 5-B, 5-(3-Bromophenyl)-1,3-dihydro-2H-benzofuro[3,2-e]-1,4-diazepin-2-one; PSB, PSB-15417; PZB15, PZB15517166A; PZB13, PZB13420052A; A43, 3-{[5-(2,3-dichlorophenyl)-1H-1,2,3,4-tetrazol-1-yl]methyl}pyridine; JNJ, N-[[4-(4-phenylpiperazin-1-yl)oxan-4-yl]methyl]-2-phenylsulfanylpyridine-3-carboxamide.

3.3 EFFECTS OF P2X RECEPTORS ANTAGONISTS ON THE 5-B-MEDIATED INCREASE IN IL-1β RELEASE

3.3.1 ATP-DEPENDENT IL-1β RELEASE

The following experiments were performed to answer the question, if the effects of 5-B on priming monocytic cells with LPS can be antagonized by other P2X receptors antagonists. Therefore, hPBMCs were stimulated with 5-B prior to priming with LPS, while other P2X receptors antagonists were added either simultaneously or prior to stimulation with BzATP. The IL-1β concentration in supernatants of the positive control samples in which cells were primed with LPS and stimulated with BzATP alone was set to 100 %. As already mentioned and depicted in Figure 3, the cell culture medium was exchanged 20 min before application of BzATP.

Again, 5-B induced a significant increase in IL-1β concentrations in supernatants of hPBMCs primed with LPS and stimulated with BzATP (p = 0.028 versus control). When given simultaneously, the P2RX4 antagonists PSB, PZB15, PZB13, and the P2RX7 antagonist JNJ

reversed the 5-B-mediated increase in IL-1β concentrations in supernatants of hPBMCs primed with LPS and stimulated with BzATP (**Figure 16A**). PSB not only reduced the IL-1β concentration compared to stimulation with 5-B (p = 0.018), but also reduced it compared to the positive control (reduction of 49.5 %). PZB15 (p = 0.018 versus 5-B), PZB13 (p = 0.028 versus 5-B), and JNJ (p = 0.043 versus 5-B) reduced IL-1β concentrations to the levels of the positive control (**Figure 16A**). Application of the antagonists shortly before treatment with BzATP reduced the 5-B-mediated increase in IL-1β concentrations only when PSB (p = 0.028 versus 5-B) and JNJ (p = 0.043 versus 5-B) were used, whereas treatment with PZB15 showed a similar tendency (p = 0.063 versus 5-B) (**Figure 16B**).

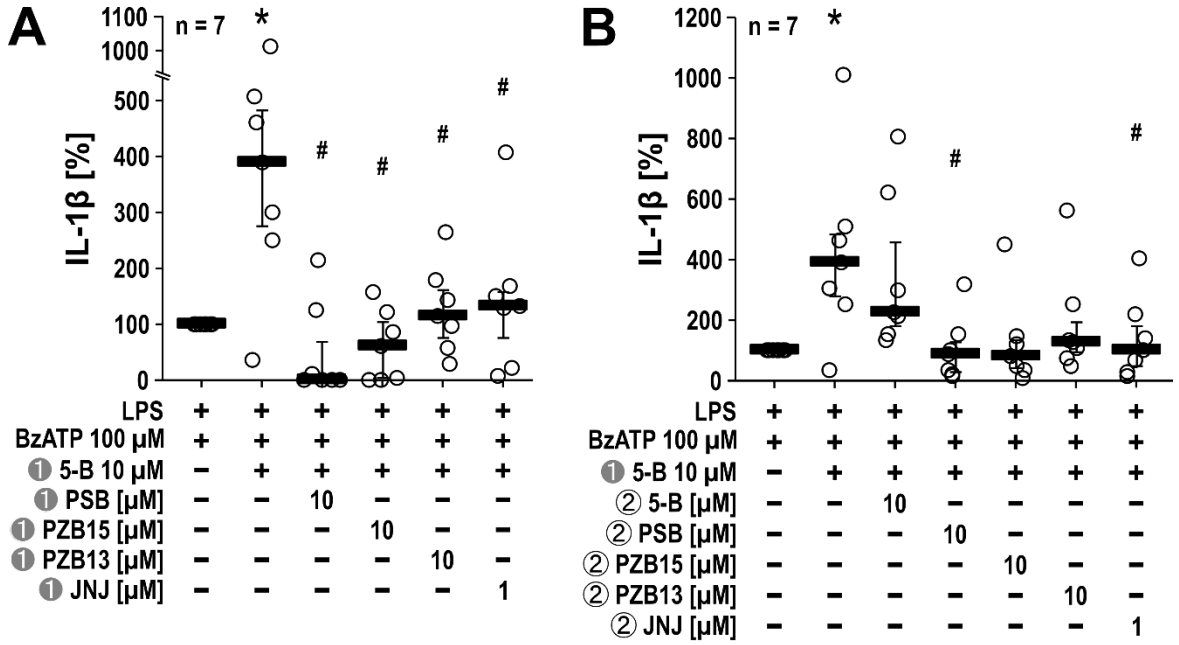

Figure 16: The impact of the P2RX4 antagonist 5-B combined with P2RX4 and P2RX7 antagonists on BzATP-induced IL-1β release by hPBMCs. Cells were primed for 3 h with LPS (5 ng/ml) in the absence or presence (①) of the P2RX4 antagonist 5-B (10 µM). **(A)** The P2RX4 antagonists PSB (10 µM), PZB15 (10 µM), or PZB13 (10 µM) or the P2RX7 inhibitor JNJ (1 µM) were added simultaneously (❶). Thereafter, BzATP (100 µM) was added for 30 min. **(B)** The antagonists were added prior to stimulation with BzATP (②). IL-1β was measured in cell culture supernatants. The IL-1β concentration in experiments in which primed cells were stimulated with BzATP in the presence of the vehicle was set to 100 % and all other values were calculated accordingly. Data are presented as individual data points, bars represent median, whiskers percentiles 25 and 75. Friedman-test followed by Wilcoxon signed-rank test. ∗ p ≤ 0.05 significantly different from samples in which only BzATP was given to LPS-primed hPBMCs. # p ≤ 0.05 significantly different from samples in which only 5-B was present in BzATP-stimulated and LPS-primed hPBMCs. hPBMCs, human peripheral blood mononuclear cells; LPS, lipopolysaccharide; BzATP, 2'(3')-O-(4-Benzoylbenzoyl)adenosine-5'-triphosphate; 5-B, 5-(3-Bromophenyl)-1,3-dihydro-2H-benzofuro[3,2-e]-1,4-diazepin-2-one; PSB, PSB-15417; PZB15, PZB15517166A; PZB13, PZB13420052A; JNJ, N-[[4-(4-phenylpiperazin-1-yl)oxan-4-yl]methyl]-2-phenylsulfanylpyridine-3-carboxamide.

3.3.2 ATP-INDEPENDENT IL-1β RELEASE

In the next sets of experiments, monocytic THP-1 cells were treated with 5-B or PZB13 prior to priming with LPS, while other P2X receptors antagonists were either added simultaneously or prior to stimulation with nigericin. Further, hPBMCs were stimulated with 5-B in combination with the other antagonists before priming with LPS and later stimulated with nigericin. The IL-1β concentration in supernatants of positive control samples in which cells were primed with LPS and stimulated with nigericin alone was set to 100 %. Again, the cell culture medium of hPBMCs was exchanged 20 min before application of nigericin (**Figure 3**).

Treatment with 5-B during priming with LPS followed by stimulation with nigericin showed again a robust increase of IL-1β concentration in cell culture supernatants of monocytic THP-1 cells ($p = 0.028$ versus control) (**Figure 17A, B**). Application of the other P2RX4 antagonists simultaneously with 5-B reversed the 5-B-induced increase of IL-1β as it resulted in concentrations similar to stimulation with nigericin alone: PSB ($p = 0.027$ versus 5-B), PZB15 ($p = 0.027$ versus 5-B), and PZB13 ($p = 0.028$ versus 5-B) (**Figure 17A**). The combination with the P2RX7 antagonists did not result in significant alterations compared to 5-B alone (**Figure 17A**). Application of the P2RX4 antagonist PSB prior to stimulation with nigericin resulted in a minor reduction of the 5-B-induced increase of IL-1β levels ($p = 0.028$ versus 5-B), while the other P2RX4 and P2RX7 antagonists did not provoke any significant changes (**Figure 17B**).

Treatment with PZB13 provoked an increase in IL-1β concentrations in cell culture supernatants of cells primed with LPS and stimulated with nigericin although with a high variability (**Figure 17C, D**). When the respective data in Figure 17C and D were evaluated together, a significant p-value was obtained ($p = 0.05$ versus control, $n = 12$). Application of 5-B simultaneously with PZB13 reversed the PZB13-induced increase as it resulted in IL-1β levels similar to stimulation with nigericin alone ($p = 0.046$ versus PZB13) (**Figure 17C**). PZB15 showed similar tendencies ($p = 0.075$ versus PZB13). PSB not only reduced the IL-1β concentration compared to stimulation with PZB13 ($p = 0.028$), but also reduced it compared to the positive control (reduction of 33.62 %). While the P2RX7 antagonist did not induce any changes, increased treatment with JNJ slightly the IL-1β concentration compared to stimulation with PZB13 alone prior to priming ($p = 0.027$) (**Figure 17D**). Application of the P2X receptors antagonists prior to nigericin stimulation resulted in a significant decrease of the PZB13-induced increase of IL-1β concentrations: 5-B ($p = 0.028$ versus PZB13), PSB ($p = 0.028$ versus PZB13), PZB13 ($p = 0.028$ versus PZB13), as well as the P2RX7 antagonists A43 ($p = 0.028$ versus PZB13) and JNJ ($p = 0.028$ versus PZB13) (**Figure 17D**). Again, the combination of PZB13 given prior to priming and PSB applied just before stimulation with nigericin resulted in a decrease of IL-1β concentration compared to the control (37.66 %) (**Figure 17D**). IL-1β IL-1β

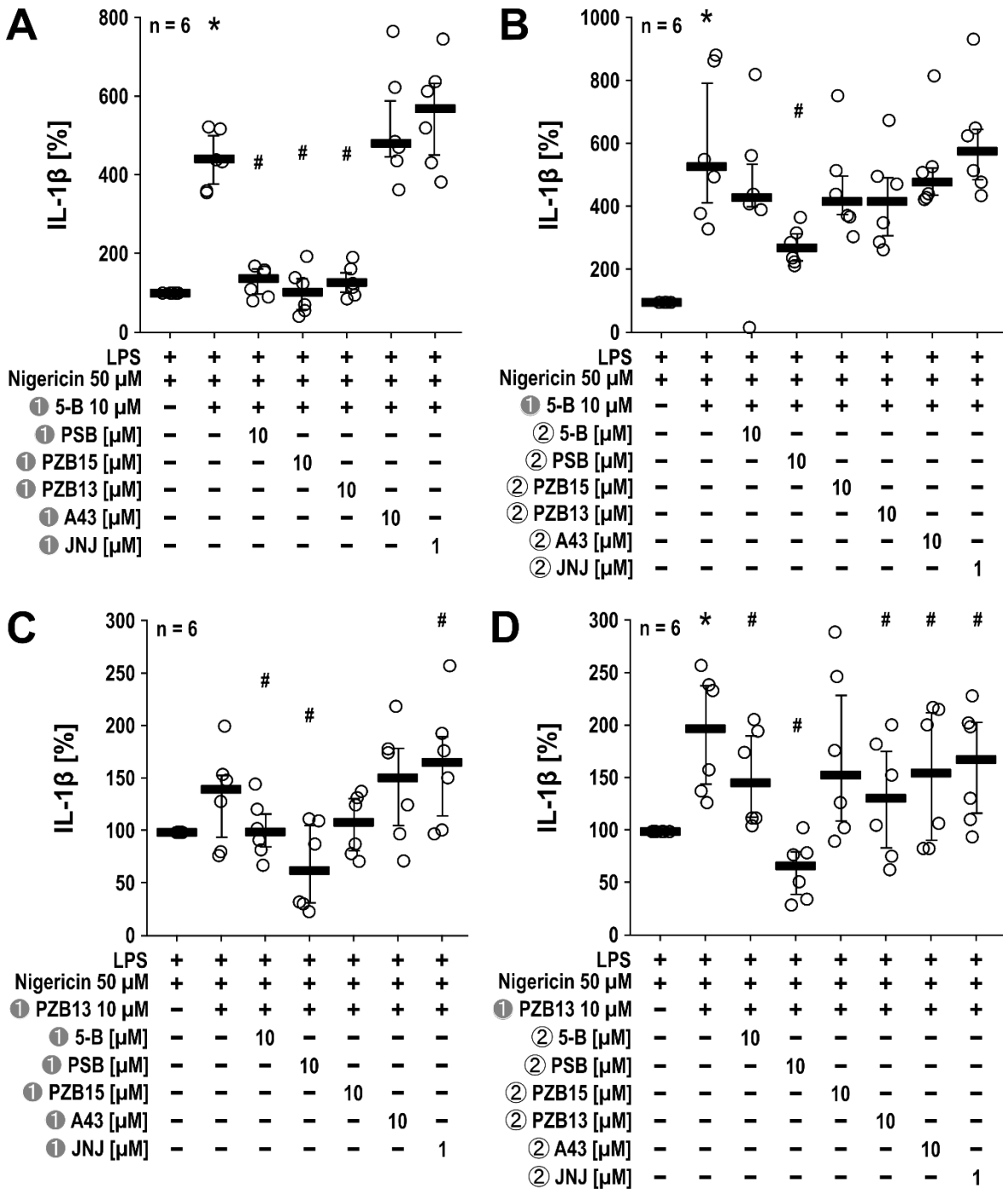

Figure 17: The impact of the P2RX4 antagonists 5-B and PZB13 combined with P2RX4 and P2RX7 antagonists on the nigericin-induced IL-1β release by monocytic THP-1 cells. Cells were primed for 5 h with LPS (1 µg/ml) in the absence or presence (❶) of the P2RX4 antagonist **(A, B)** 5-B (10 µM) or **(C, D)** PZB13 (10 µM). Additional P2RX4 antagonists PSB (10 µM), PZB15 (10 µM), or PZB13 (10 µM), or the P2RX7 inhibitors A43 (10 µM) or JNJ (1 µM) were **(A, B)** also added prior to LPS application. Thereafter, nigericin (50 µM) was added for 40 min in the absence or **(C, D)** presence (②) of the antagonists. IL-1β was measured in cell culture supernatants. The IL-1β concentration in experiments in which primed cells were stimulated with nigericin in the presence of the vehicle was set to 100 % and all other values were calculated accordingly. Data are presented as individual data points, bars represent median, whiskers percentiles 25 and 75. Friedman-test followed by Wilcoxon signed-rank test. * $p \leq 0.05$ significantly different from samples in which only nigericin was given to LPS-primed monocytic THP-1 cells. # $p \leq 0.05$ significantly different from samples in which only 5-B or PZB13 was present in THP-1 cells primed with LPS and stimulated with nigericin. LPS, lipopolysaccharide; 5-B, 5-(3-Bromophenyl)-1,3-dihydro-2H-benzofuro[3,2-e]-1,4-diazepin-2-one; PSB, PSB-15417; PZB15, PZB15517166A; PZB13, PZB13420052A; A43, 3-{[5-(2,3-dichlorophenyl)-1H-1,2,3,4-tetrazol-1-yl]methyl}pyridine; JNJ, N-[[4-(4-phenylpiperazin-1-yl)oxan-4-yl]methyl]-2-phenylsulfanylpyridine-3-carboxamide.

In hPBMCs, the 5-B-induced increase of IL-1β (p = 0.011 versus control) was not reversed by simultaneous application of other P2X receptors antagonists, although PZB15 tended to reduce it (p = 0.093 versus 5-B). Of note, the variability of the data was high (**Figure 18**).

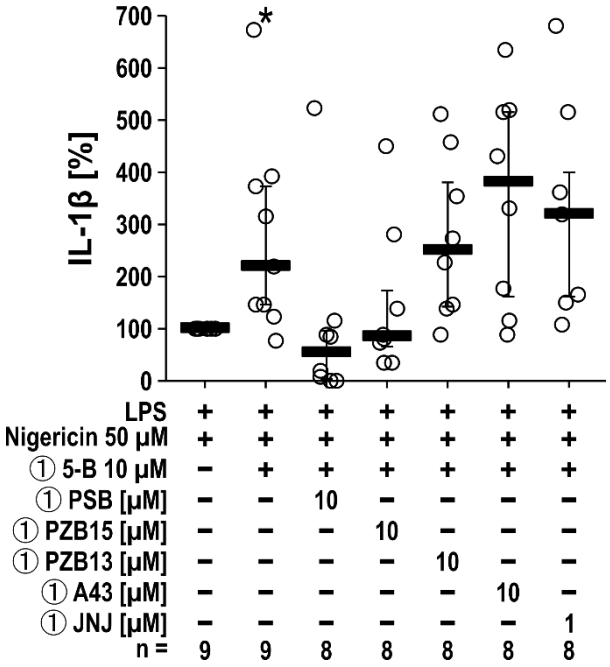

Figure 18: The impact of the P2RX4 antagonist 5-B combined with P2RX4 and P2RX7 antagonists on nigericin-induced IL-1β release by hPBMCs. Cells were primed for 3 h with LPS (5 ng/ml) in the absence or presence (①) of the P2RX4 antagonist 5-B (10 µM) together with the P2RX4 antagonists PSB (10 µM), PZB15 (10 µM), or PZB13 (10 µM) or the P2RX7 antagonists A43 (10 µM) or JNJ (1 µM). Thereafter, nigericin (50 µM) was added for 30 min and IL-1β was measured in cell culture supernatants. The IL-1β concentration in experiments in which primed cells were stimulated with nigericin in the presence of the vehicle was set to 100 % and all other values were calculated accordingly. Data are presented as individual data points, bars represent median, whiskers percentiles 25 and 75. Friedman-test followed by Wilcoxon signed-rank test. ∗ p ≤ 0.05 significantly different from samples in which only nigericin was given to LPS-primed hPBMCs. hPBMCs, human peripheral blood mononuclear cells. LPS, lipopolysaccharide; 5-B, 5-(3-Bromophenyl)-1,3-dihydro-2H-benzofuro[3,2-e]-1,4-diazepin-2-one; PSB, PSB-15417; PZB15, PZB15517166A; PZB13, PZB13420052A; A43, 3-{[5-(2,3-dichlorophenyl)-1H-1,2,3,4-tetrazol-1-yl]methyl}pyridine; JNJ, N-[[4-(4-phenylpiperazin-1-yl)oxan-4-yl]methyl]-2-phenylsulfanylpyridine-3-carboxamide.

3.4 EFFECTS OF P2X RECEPTORS ANTAGONISTS ON INTRACELLULAR IL-1β PROTEIN LEVELS

Western blot analysis was performed to investigate the effect of P2X receptors antagonists on the intracellular IL-1β protein levels of THP-1 cell-derived M1-like macrophages, which were primed with 1 µg/ml LPS for 5 h in presence of the antagonists. The amount of (pro-)IL-1β was estimated relative to the reference protein β-actin using densitometry. The respective protein levels of control cells stimulated with LPS was set to 1 AU.

A representative picture of a Western blot shows that no IL-1β could be detected in untreated cells (**Figure 19A**). Priming with LPS resulted in detectable amounts of pro-IL-1β (31 kDa), while the mature IL-1β (17 kDa) was not detectable. Addition of P2RX4 antagonists or the P2RX7 antagonist A43 also resulted in detectable pro-IL-1β protein amounts. Detection of β-actin showed almost similar protein amounts in every sample (**Figure 19B**). Treatment with LPS increased pro-IL-1β protein amounts compared to 0.05 IL-1β AU of untreated THP-1 cell-

derived M1-like macrophages (p = 0.028) (**Figure 19C**). Densitometric analysis revealed a slight but not significant increase after stimulation with 5-B (p = 0.075). The other P2RX4 antagonists PSB (p = 0.028), PZB15 (p = 0.028), and PZB13 (p = 0.046) significantly reduced intracellular pro-IL-1β levels. The P2RX7 antagonist A43 did not induce any alterations (**Figure 19C**).

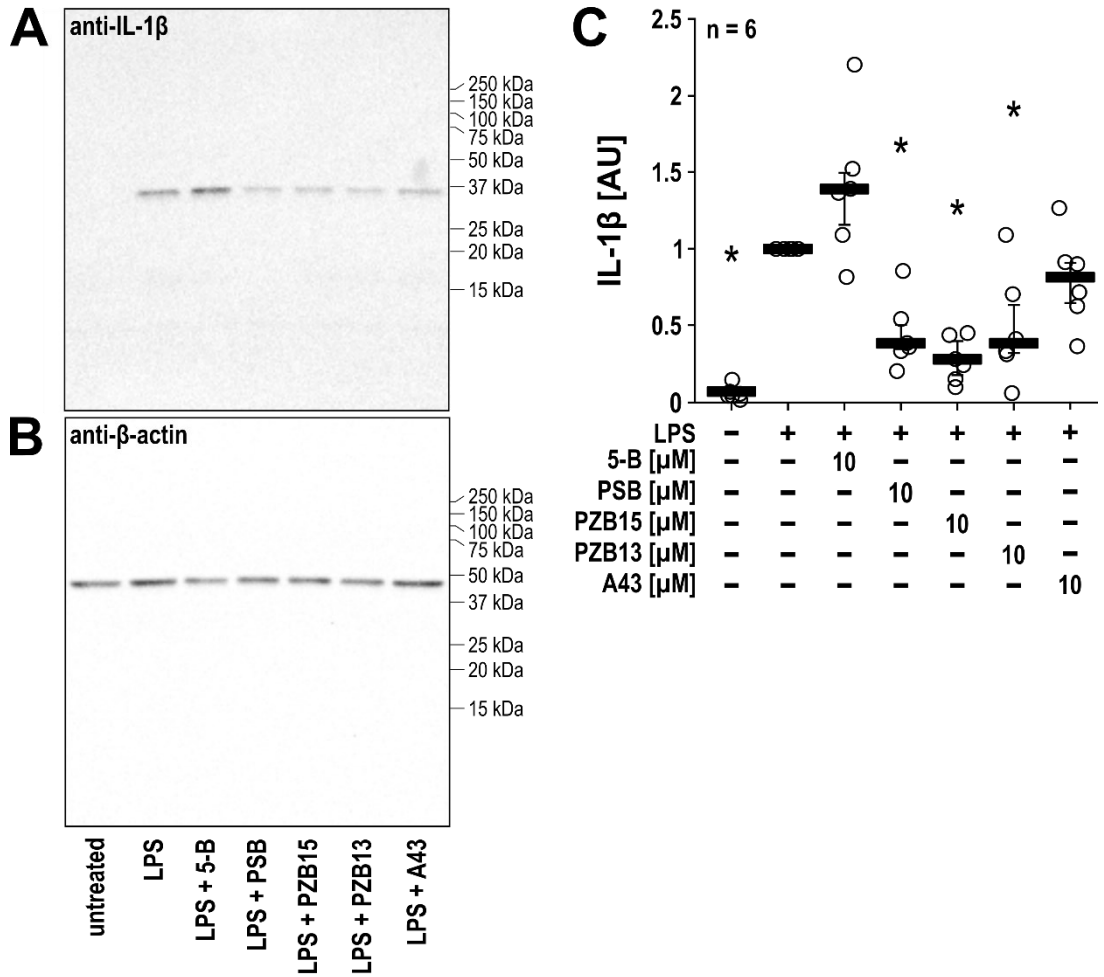

Figure 19: The impact of P2RX4 and P2RX7 antagonists on intracellular pro-IL-1β protein levels by THP-1 cell-derived M1-like macrophages. THP-1 cells were differentiated into THP-1 M1-like macrophages. Cells were primed with LPS (1 µg/ml) for 5 h in the presence of the P2RX4 antagonists 5-B (10 µM), PSB (10 µM), PZB15 (10 µM), or PZB13 (10 µM) or the P2RX7 antagonist A43 (10 µM). After cell lysis, gel electrophoresis and subsequent Western blotting were performed to estimate the protein amount of **(A)** IL-1β and **(B)** β-actin, which was selected as a reference protein. One representative experiment out of 6. **(C)** Changes in the protein levels of pro-IL-1β were estimated by densitometry. The protein levels in experiments in which cells were primed in the presence of the vehicle was set to 1 AU and all other values were calculated accordingly. Data are presented as individual data points, bars represent median, whiskers percentiles 25 and 75. Friedman-test followed by Wilcoxon signed-rank test. ∗ p ≤ 0.05 significantly different from samples of LPS-primed THP-1 M1-like macrophages. kDa, kilodalton; AU, arbitrary units; LPS, lipopolysaccharide; 5-B, 5-(3-Bromophenyl)-1,3-dihydro-2H-benzofuro[3,2-e]-1,4-diazepin-2-one; PSB, PSB-15417; PZB15, PZB15517166A; PZB13, PZB13420052A; A43, 3-{[5-(2,3-dichlorophenyl)-1H-1,2,3,4-tetrazol-1-yl]methyl}pyridine.

4 EFFECTS OF P2X RECEPTORS ANTAGONISTS ON IL-6 RELEASE

4.1 IL-6 RELEASE BY THP-1 CELLS

To explore the role of P2RX4 and P2RX7 in IL-6 secretion by THP-1 cells, the various P2RX4 and P2RX7 antagonists were given prior to stimulation with LPS and the IL-6 concentration in cell culture supernatants of monocytic THP-1 cells and THP-1 cell-derived M1-like macrophages was measured. The IL-6 concentration in supernatants of control cells stimulated with LPS was set to 100 %. First, 5-B, PSB, and A43 were investigated in a set of experiments including different concentrations of 5-B and A43 and later, a second set of experiments included all P2RX4 and P2RX7 antagonists. These sets of experiments were combined in Figure 20 explaining the high n numbers for the control samples, which were included in all experiments.

Figure 20 shows that IL-6 concentrations were significantly increased in supernatants of monocytic THP-1 cells after stimulation with LPS ($p = 0.001$). The P2RX4 antagonist 5-B at a concentration of 20 µM slightly decreased IL-6 concentrations ($p = 0.012$), while lower 5-B concentrations did not alter IL-6 levels. PZB15 also tended to decrease IL-6 concentrations ($p = 0.074$). Treatment with PSB or PZB13 did not induce any alterations. The P2RX7 antagonists A43 at 10 µM and JNJ did not influence IL-6, while the higher concentration of A43 slightly but significantly ($p = 0.05$) increased IL-6 concentrations in supernatants of monocytic THP-1 cells (**Figure 20**).

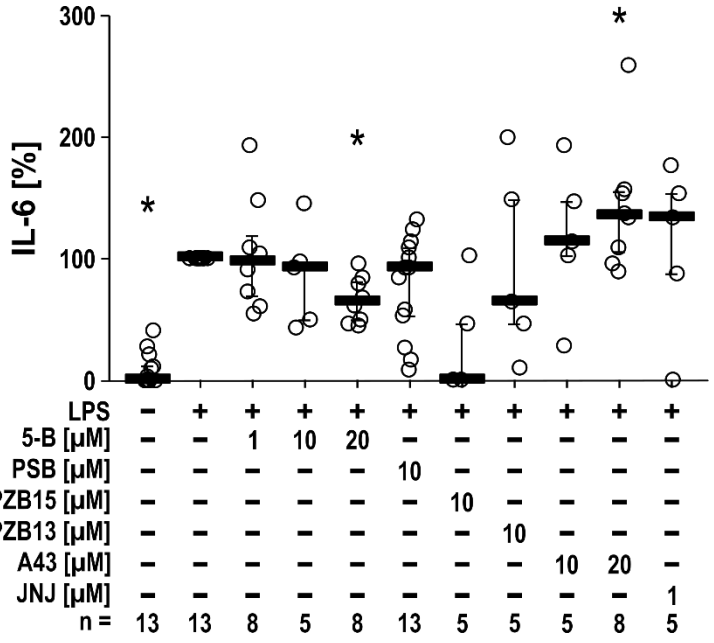

Figure 20: The impact of P2RX4 and P2RX7 antagonists on the IL-6 release by monocytic THP-1 cells. Cells were stimulated with LPS (1 µg/ml) for 5 h in the absence or presence of the P2RX4 antagonists 5-B (1, 10, 20 µM), PSB (10 µM), PZB15 (10 µM), or PZB13 (10 mM) or the P2RX7 inhibitors A43 (10, 20 µM) or JNJ (1 µM). Thereafter, IL-6 was measured in cell culture supernatants. The IL-6 concentration in samples in which cells were only stimulated with LPS in the presence of the vehicle was set to 100 % and all other values were calculated accordingly. Data are presented as individual data points, bars represent median, whiskers percentiles 25 and 75. Friedman-test followed by Wilcoxon signed-rank test. ∗ $p \leq 0.05$ significantly different from LPS-stimulated monocytic THP-1 cells. LPS, lipopolysaccharide; 5-B, 5-(3-Bromophenyl)-1,3-dihydro-2H-benzofuro[3,2-e]-1,4-diazepin-2-one; PSB, PSB-15417; PZB15, PZB15517166A; PZB13, PZB13420052A; A43, 3-{[5-(2,3-dichlorophenyl)-1H-1,2,3,4-tetrazol-1-yl]methyl}pyridine; JNJ, N-[[4-(4-phenylpiperazin-1-yl)oxan-4-yl]methyl]-2-phenylsulfanylpyridine-3-carboxamide.

Like monocytic cells, supernatants of THP-1 cell-derived M1-like macrophages showed increased IL-6 concentration after stimulation with LPS compared to untreated cells ($p = 0.005$) (**Figure 21**). The P2RX4 antagonist 5-B decreased IL-6 levels by about 40 % (10 µM: $p = 0.005$, 20 µM: $p = 0.0028$) when applied before priming with LPS. PSB alone did not induce alterations and it also did not reverse the effect of 5-B when given simultaneously prior to priming ($p = 0.007$ versus LPS). The P2RX7 antagonist A43 slightly decreased IL-6 under the same conditions ($p = 0.027$). Stimulation with 5-B in the absence of LPS resulted in IL-6 concentrations in supernatants of THP-1 cell-derived macrophages slightly above the limit of detection similar to untreated cells ($p = 0.027$) (**Figure 21**).

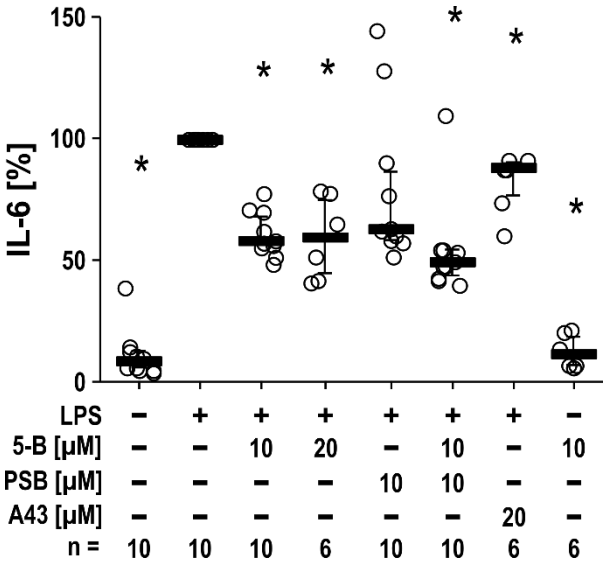

Figure 21: The impact of P2RX4 and P2RX7 antagonists on the IL-6 release by THP-1 cell-derived M1-like macrophages. THP-1 cells were differentiated into THP-1 M1-like macrophages. Cells were stimulated with LPS (1 µg/ml) for 5 h in the absence or presence of the P2RX4 antagonists 5-B (10, 20 µM) or PSB (10 µM), or the P2RX7 inhibitor A43 (20 µM). Thereafter, IL-6 was measured in cell culture supernatants by ELISA. The IL-6 concentration in samples in which cells were only stimulated with LPS in the presence of the vehicle was set to 100 % and all other values were calculated accordingly. Data are presented as individual data points, bars represent median, whiskers percentiles 25 and 75. Friedman-test followed by Wilcoxon signed-rank test. ∗ $p \leq 0.05$ significantly different from LPS-stimulated THP-1 M1-like macrophages. LPS, lipopolysaccharide; 5-B, 5-(3-Bromophenyl)-1,3-dihydro-2H-benzofuro[3,2-e]-1,4-diazepin-2-one; PSB, PSB-15417; PZB15, PZB15517166A; PZB13, PZB13420052A; A43, 3-{[5-(2,3-dichlorophenyl)-1H-1,2,3,4-tetrazol-1-yl]methyl}pyridine; JNJ, N-[[4-(4-phenylpiperazin-1-yl)oxan-4-yl]methyl]-2-phenylsulfanylpyridine-3-carboxamide.

4.2 IL-6 SECRETION BY HPBMCS

Next, the effects of P2RX4 and P2RX7 antagonists on the secretion of IL-6 by hPBMCs primed with LPS were investigated. Again, antagonists were given prior to stimulation with LPS and the IL-6 concentration in cell culture supernatants of hPBMCs was measured. The IL-6 concentration in supernatants of control cells stimulated with LPS was set to 100 %.

Like in THP-1 cells, IL-6 concentrations increased after stimulation with LPS compared to untreated cells ($p = 0.011$) (**Figure 22**). Stimulation with 5-B significantly increased ($p = 0.025$), while PZB13 tended to increase IL-6 concentrations ($p = 0.069$). Other P2RX4 antagonists did not induce any changes. The P2RX7 antagonist A43 significantly increased ($p = 0.025$) IL-6 concentration by 34.7 %, but stimulation with JNJ did not result in any alterations of the IL-6 concentration in supernatants of hPBMCs primed with LPS (**Figure 22**).

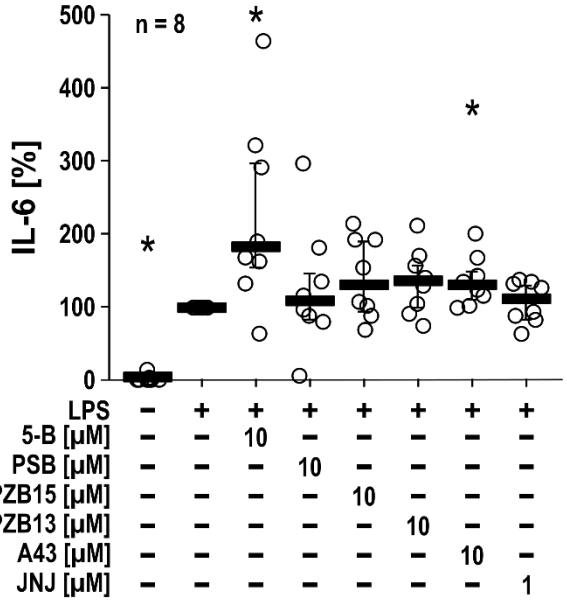

Figure 22: The impact of P2RX4 and P2RX7 antagonists on the IL-6 release by hPBMCs. Cells were primed with LPS (5 ng/ml) for 3 h in the absence or presence of the P2RX4 antagonists 5-BD (10 µM), PSB (10 µM), PZB15 (10 µM), or PZB13 (10 µM) or the P2RX7 inhibitors A43 (10 µM) or JNJ (1 µM). Thereafter, IL-6 was measured in cell culture supernatants by ELISA. The IL-6 concentration in experiments in which cells were primed in the presence of the vehicle was set to 100 % and all other values were calculated accordingly. Data are presented as individual data points, bars represent median, whiskers percentiles 25 and 75. Friedman-test followed by Wilcoxon signed-rank test. ∗ $p \leq 0.05$ significantly different from LPS-primed hPBMCs. LPS, lipopolysaccharide; 5-B, 5-(3-Bromophenyl)-1,3-dihydro-2H-benzofuro[3,2-e]-1,4-diazepin-2-one; PSB, PSB-15417; PZB15, PZB15517166A; PZB13, PZB13420052A; A43, 3-{[5-(2,3-dichlorophenyl)-1H-1,2,3,4-tetrazol-1-yl]methyl}pyridine; JNJ, N-[[4-(4-phenylpiperazin-1-yl)oxan-4-yl]methyl]-2-phenylsulfanylpyridine-3-carboxamide.

5 EFFECTS OF P2X RECEPTORS ANTAGONISTS ON GENE EXPRESSION

5.1 CHARACTERIZATION OF REAL-TIME RT-PCR AMPLIFICATION PRODUCTS

Possible effects of P2RX4 and P2RX7 antagonists on the mRNA gene expression of their respective receptors as well as on mRNA of the pro-inflammatory cytokines IL-1β, IL-6, TNF-α, and the anti-inflammatory cytokines IL-10 and IL-18 were investigated. First, real-time RT-PCR amplification products of LPS-primed monocytic THP-1 cells for the genes *PPIA, IL1B, P2RX4, P2RX7, IL6*, and *IL10* were analysed via separation by agarose gel electrophoresis to verify the product size. For *TNF* and *IL18*, amplification products of LPS-primed Monocytic THP-1 cells, LPS-primed THP-1 cell-derived macrophages and untreated hPBMCs were used. For every real-time RT-PCR experiment, a no template control (NTC) was included to check for possible contaminations.

For *PPIA*, every sample had the expected size of 179 bp (**Figure 23A**). The *IL1B* products had a size of 121 bp. The amplification products of *P2RX4* were 272 bp and *P2RX7* products 134 bp in size. For *IL6*, products had the size of 132 bp and for *IL10* 206 bp (**Figure 23B**). *TNF* products were 115 bp and *IL18* 171 bp in size (**Figure 23C**). All real-time RT-PCR products had the expected sizes that were previously determined using Primer-BLAST.

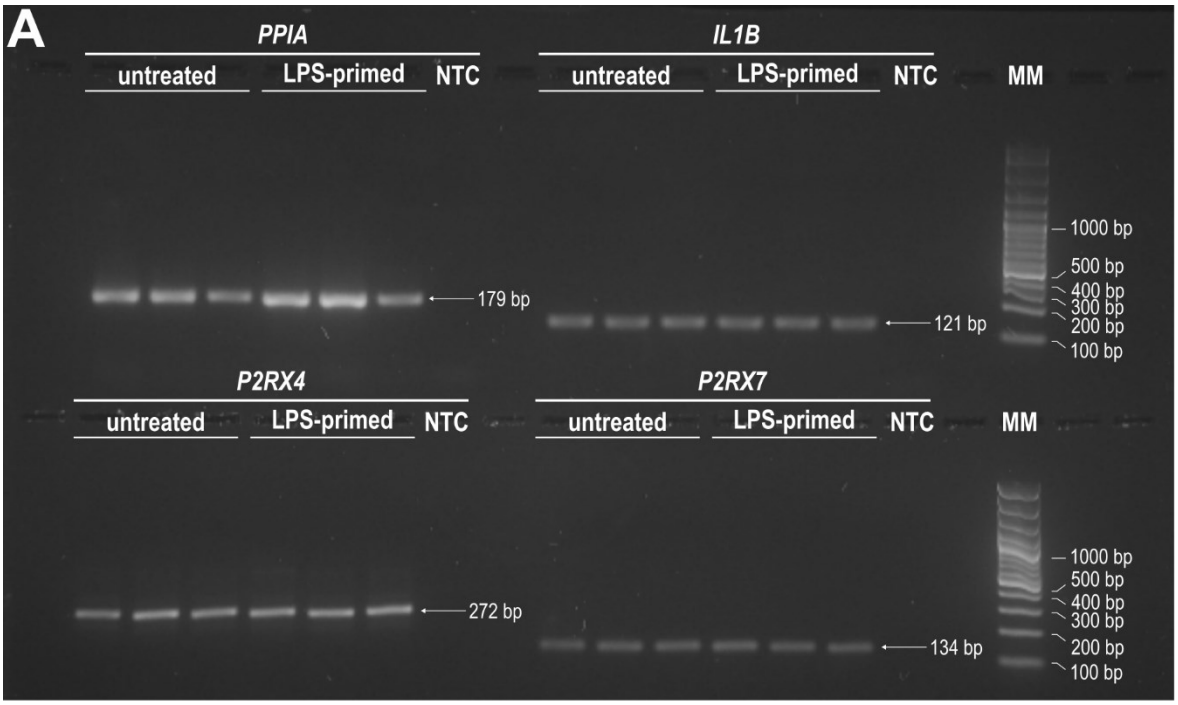
A
PPIA
untreated
LPS-primed
NTC
179 bp
IL1B
untreated
LPS-primed
NTC
121 bp
MM
1000 bp
500 bp
400 bp
300 bp
200 bp
100 bp
P2RX4
untreated
LPS-primed
NTC
272 bp
P2RX7
untreated
LPS-primed
NTC
134 bp
MM
1000 bp
500 bp
400 bp
300 bp
200 bp
100 bp

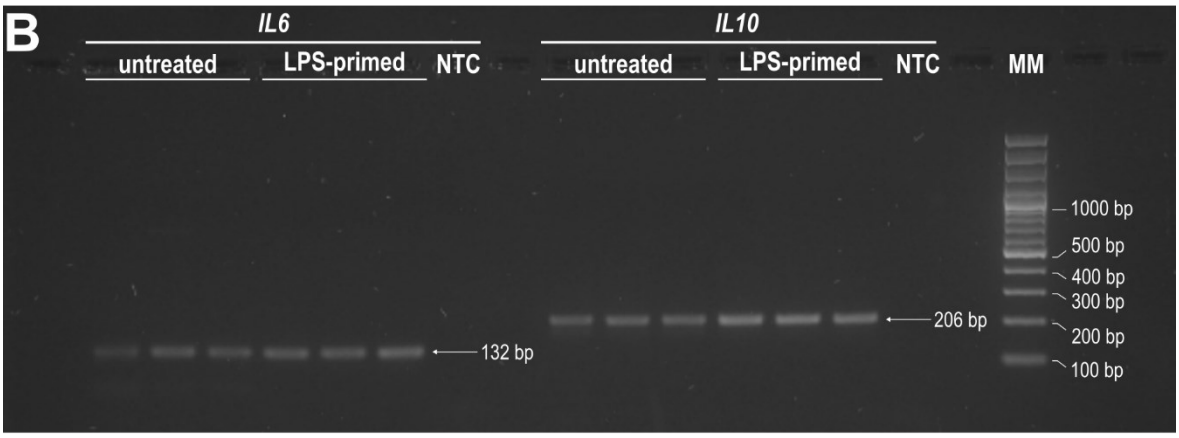
B
IL6
untreated
LPS-primed
NTC
132 bp
IL10
untreated
LPS-primed
NTC
206 bp
MM
1000 bp
500 bp
400 bp
300 bp
200 bp
100 bp

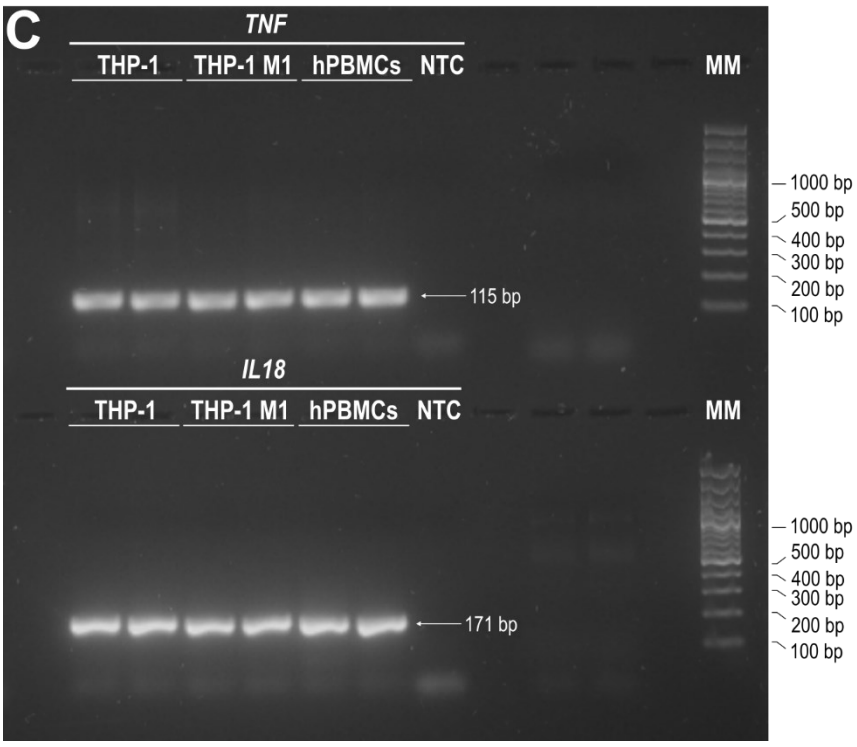
C
TNF
THP-1
THP-1 M1
hPBMCs
NTC
115 bp
MM
1000 bp
500 bp
400 bp
300 bp
200 bp
100 bp
IL18
THP-1
THP-1 M1
hPBMCs
NTC
171 bp
MM
1000 bp
500 bp
400 bp
300 bp
200 bp
100 bp

Figure 23: real-time RT-PCR amplification products of monocytic THP-1 cells, THP-1 cell-derived M1-like macrophages, and hPBMCs separated in an agarose gel. (A, B) real-time RT-PCR products from untreated and THP-1 M1-like macrophages, which were primed for 5 h with LPS (1 µg/ml), and the NTC were separated by agarose gel electrophoresis. Amplification products of the mRNA of **(A)** *PPIA, IL1B, P2RX4*, and *P2RX7* genes, **(B)** *IL6* and *IL10* genes. **(C)** real-time RT-PCR products from monocytic THP-1 cells (THP-1) and THP-1 cell-derived M1-like macrophages (THP-1 M1), which were primed for 5 h with LPS (1 µg/ml), untreated hPBMCs, and the NTC were separated by agarose gel electrophoresis. Amplification products of the *IL18* and *TNF* mRNA. 1.8 % agarose gel stained with GelRed nucleic acid stain. Bp, base pairs; LPS, lipopolysaccharide; NTC, no template control; MM, molecular mass marker; hPBMCs, human peripheral blood mononuclear cells.

5.2 mRNA EXPRESSION OF P2X RECEPTORS

5.2.1 mRNA EXPRESSION OF P2X RECEPTORS IN THP-1 CELLS

To test if the P2X receptors antagonists, when added before priming with LPS, alter the mRNA expression of their respective receptors, THP-1 cells were investigated. After 5 h incubation with LPS, the cells were frozen at -20°C for later RNA isolation, transcription into cDNA, and real-time PCR. The gene expression of target genes was calculated relative to the reference gene *PPIA*. The respective gene expression of control cells stimulated with LPS was set to 1 AU. In general, a fold change of 1.5 or of 0.5 was considered as threshold for biologically relevant upregulation or downregulation of the target gene, respectively. In a first set of experiments, the P2RX4 antagonists 5-B and PSB and of the P2RX7 antagonist A43 were investigated including two concentrations of 5-B and A43. Later, different sets of experiments were conducted, in which all antagonists were used at only one concentration. Respective controls were always included. These sets of experiments were combined in Figure 25 explaining the different n numbers.

In Monocytic THP-1 cells, stimulation with LPS did not upregulate *P2RX4* mRNA compared to untreated cells (**Figure 24A**). P2RX4 and P2RX7 antagonists did not alter P2RX4 mRNA compared to cells primed with LPS. *P2RX7* mRNA expression was not altered by LPS, 5-B, and the P2RX7 antagonists (**Figure 24B**). However, treatment with the P2RX4 antagonists PSB (~1.88-fold, $p = 0.028$) and PZB15 (~3.38-fold, $p = 0.028$) induced a minor upregulation of *P2RX7* mRNA compared to cells primed with LPS (**Figure 24B**). Some conditions induced statistically significant minor alterations, which, however, are not biologically relevant according to the definitions given above and are therefore not discussed.

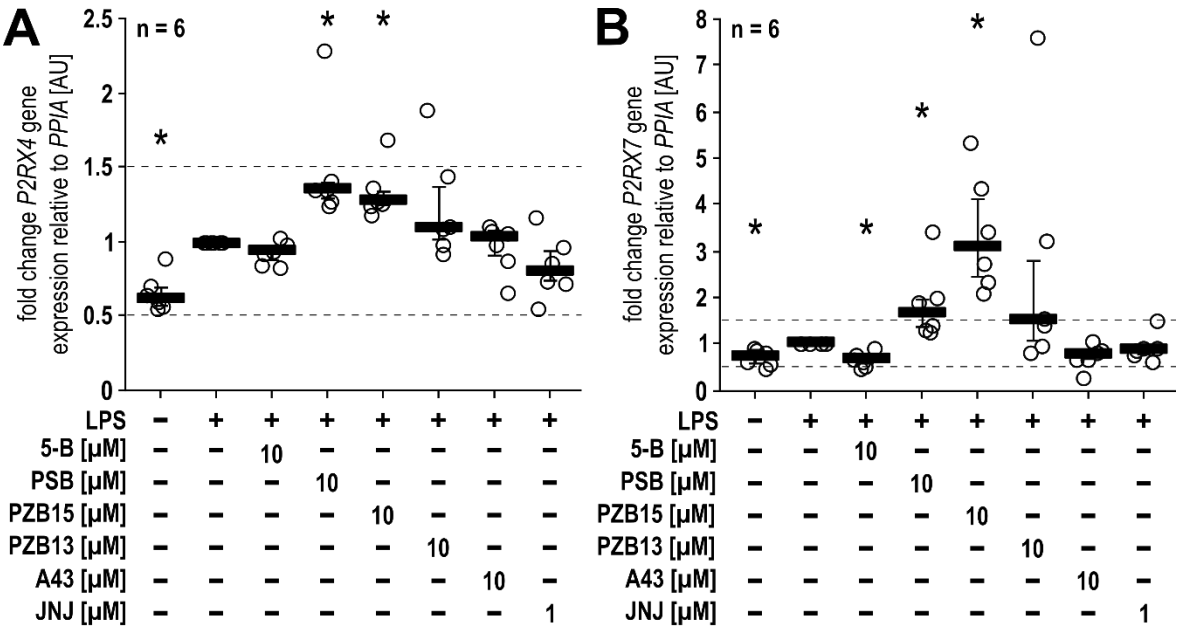

Figure 24: The impact of P2RX4 and P2RX7 antagonists on *P2RX4* and *P2RX7* mRNA expression by monocytic THP-1 cells. Cells were primed with LPS (1 µg/ml) for 5 h in the absence or presence of the P2RX4 antagonists 5-B (10 µM), PSB (10 µM), PZB15 (10 µM), or PZB13 (10 µM) or the P2RX7 antagonists A43 (10 µM) or JNJ (1 µM). After RNA isolation and transcription into cDNA, real-time PCR was performed to evaluate the mRNA expression of **(A)** *P2RX4* and **(B)** *P2RX7*. The human *PPIA* gene was selected as a reference gene. Changes in the mRNA expression levels of targeted genes were calculated by the $2^{\Delta CT}$ method, where ΔCT represents the difference between the CT value of the *PPIA* gene and the CT value of the gene of interest. The gene expression in experiments in which cells were primed in the presence of the vehicle was set to 1 AU and all other values were calculated accordingly. Data are presented as individual data points, bars represent median, whiskers percentiles 25 and 75, dashed lines indicate the threshold for biological relevant fold changes. Friedman-test followed by Wilcoxon signed-rank test. $*$ $p \leq 0.05$ significantly different from samples of LPS-primed monocytic THP-1 cells. AU, arbitrary units; LPS, lipopolysaccharide; 5-B, 5-(3-Bromophenyl)-1,3-dihydro-2H-benzofuro[3,2-e]-1,4-diazepin-2-one; PSB, PSB-15417; PZB15, PZB15517166A; PZB13, PZB13420052A; A43, 3-{[5-(2,3-dichlorophenyl)-1H-1,2,3,4-tetrazol-1-yl]methyl}pyridine; JNJ, N-[[4-(4-phenylpiperazin-1-yl)oxan-4-yl]methyl]-2-phenylsulfanylpyridine-3-carboxamide.

In THP-1 cell-derived M1-like macrophages, the results look similar to monocytic THP-1 cells. However, priming with LPS slightly upregulated *P2RX4* mRNA expression compared to untreated cells (~0.44-fold, p = 0.000) (**Figure 25A**). The P2RX4 and P2RX7 antagonists did not alter *P2RX4* mRNA levels over the set thresholds of biological relevance. The *P2RX7* mRNA expression in THP-1 cell-derived M1-like macrophages was not influenced in a relevant way by any treatment (**Figure 25B**).

When comparing the receptor mRNA expression levels in monocytic THP-1 cells, the cells seemed to express 164-fold more *P2RX4* than *P2RX7*, while THP-1 cell-derived macrophages showed no differences in gene expression levels of the receptors. Noteworthy, macrophages overall seemed to express 16-fold more *P2RX4* and even 4,470-fold more *P2RX7* than monocytic THP-1 cells.

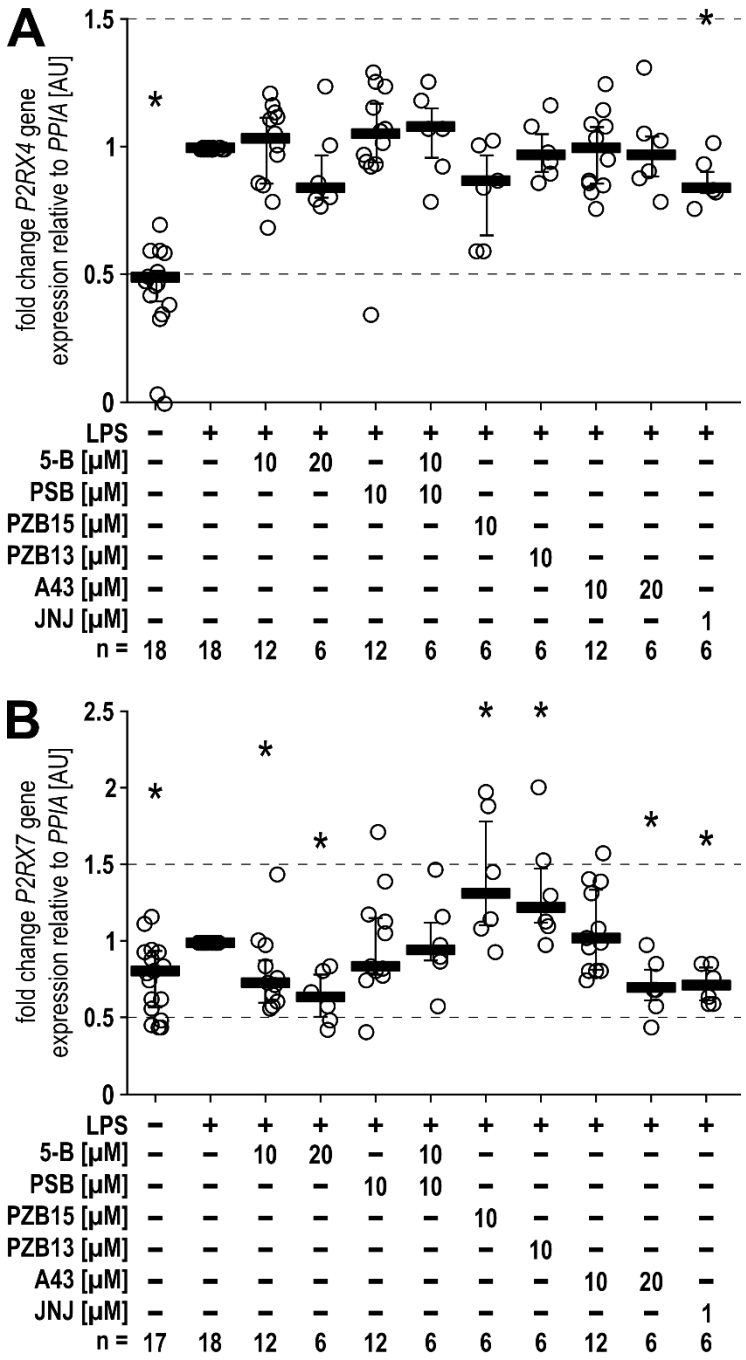

Figure 25: The impact of P2RX4 and P2RX7 antagonists on *P2RX4* and *P2RX7* mRNA expression by THP-1 cell-derived M1-like macrophages. THP-1 cells were differentiated into THP-1 M1-like macrophages. Cells were primed with LPS (1 µg/ml) for 5 h in the absence or presence of the P2RX4 antagonists 5-B (10, 20 µM), PSB (10 µM), PZB15 (10 µM), or PZB13 (10 µM) or the P2RX7 antagonists A43 (10, 20 µM) or JNJ (1 µM). After RNA isolation and transcription into cDNA, real-time PCR was performed to evaluate the mRNA expression of **(A)** *P2RX4* and **(B)** *P2RX7*. The human *PPIA* gene was selected as a reference gene. Changes in the mRNA expression levels of targeted genes were calculated by the $2^{\Delta CT}$ method, where ΔCT represents the difference between the CT value of the *PPIA* gene and the CT value of the gene of interest. The gene expression in experiments in which cells were primed in the presence of the vehicle was set to 1 AU and all other values were calculated accordingly. Data are presented as individual data points, bars represent median, whiskers percentiles 25 and 75, dashed lines indicate the threshold for biological relevant fold changes. Friedman-test followed by Wilcoxon signed-rank test. ∗ $p \leq 0.05$ significantly different from samples of LPS-primed THP-1 M1-like macrophages. AU, arbitrary units; LPS, lipopolysaccharide; 5-B, 5-(3-Bromophenyl)-1,3-dihydro-2H-benzofuro[3,2-e]-1,4-diazepin-2-one; PSB, PSB-15417; PZB15, PZB15517166A; PZB13, PZB13420052A; A43, 3-{[5-(2,3-dichlorophenyl)-1H-1,2,3,4-tetrazol-1-yl]methyl}pyridine; JNJ, N-[[4-(4-phenylpiperazin-1-yl)oxan-4-yl]methyl]-2-phenylsulfanylpyridine-3-carboxamide.

5.2.2 RNA EXPRESSION OF P2X RECEPTORS IN HPBMCS

Additionally, mRNA expression of *P2RX4* and *P2RX7* in hPBMCs treated with LPS was investigated to verify the data obtained for the THP-1 cells line in primary cells. After 3 h incubation with LPS and the P2RX4 or the P2RX7 antagonists, the cells were frozen at -20°C for later RNA isolation, transcription into cDNA, and real-time PCR. The mRNA expression of target genes was calculated relative to the reference gene *PPIA*. The respective gene expression of control samples of cells, which were primed with LPS, was set to 1 AU.

Figure 26A shows that *P2RX4* mRNA expression in hPBMCs was not influenced by stimulation with LPS compared to untreated cells. Also, the P2RX4 and P2RX7 antagonists did not induce any alterations (**Figure 26A**). However, *P2RX7* mRNA expression levels were slightly lower (~ 0.29-fold, p = 0.018) in untreated cells compare to cells primed with LPS (**Figure 26B**). Similar levels could be observed after treatment with 5-B (~ 0.37-fold, p = 0.018) or with PZB15 (~ 0.36-fold, p = 0.018). PSB did not induce any alterations. However, PZB13 induced an upregulation of *P2RX7* mRNA expression to about 2.32-fold (p = 0.018). The *P2RX7* mRNA expression was not influenced by the P2RX7 antagonist A43, while treatment with JNJ slightly reduced mRNA levels compared to treatment with LPS about 0.48-fold (p = 0.028) (**Figure 26B**). Some conditions induced statistically significant minor alterations, which are not biologically relevant according to the definitions given above.

Noteworthy, when comparing the mRNA expression levels of the receptors, hPBMCs seemed to express 57-fold more *P2RX4* than *P2RX7*.

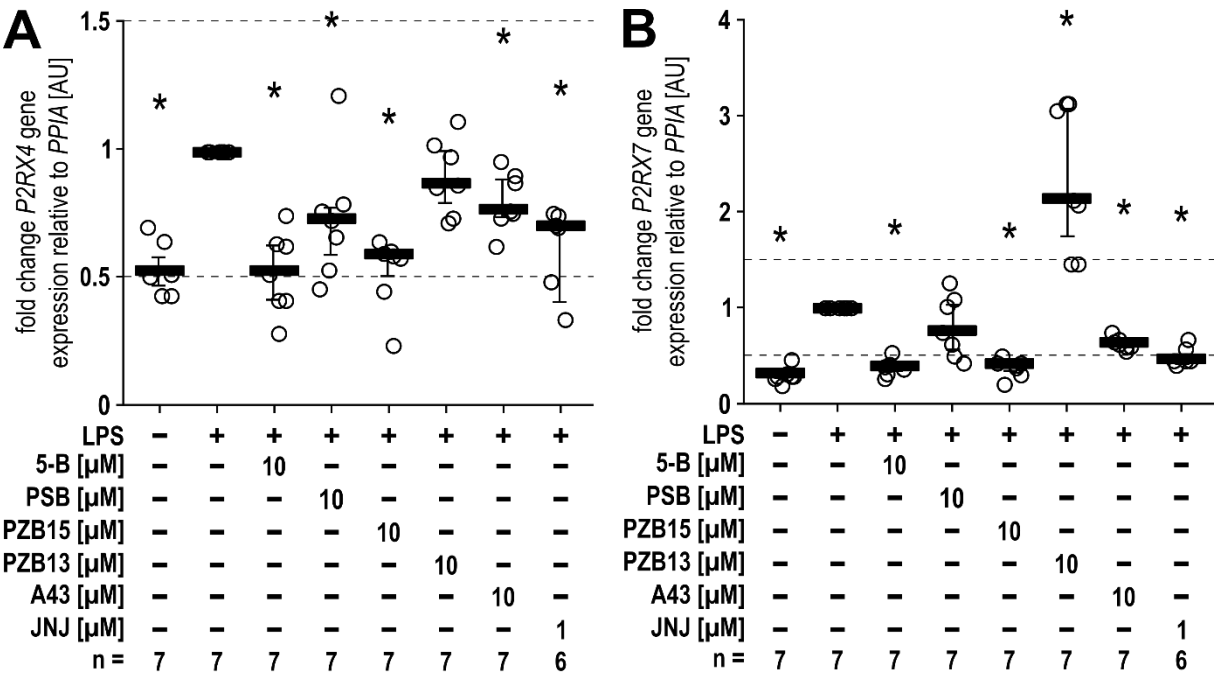

Figure 26: The impact of P2RX4 and P2RX7 antagonists on *P2RX4* and *P2RX7* mRNA expression by hPBMCs. Cells were primed with LPS (5 ng/ml) for 3 h in the absence or presence of the P2RX4 antagonists 5-B (10 µM), PSB (10 µM), PZB15 (10 µM), or PZB13 (10 µM) or the P2RX7 antagonists A43 (10 µM) or JNJ (1 µM). After RNA isolation and transcription into cDNA, real-time PCR was performed to evaluate the mRNA expression of **(A)** *P2RX4* and **(B)** *P2RX7*. The human *PPIA* gene was selected as a reference gene. Changes in the mRNA expression levels of targeted genes were calculated by the $2^{\Delta CT}$ method, where ΔCT represents the difference between the CT value of the *PPIA* gene and the CT value of the gene of interest. The gene expression in experiments in which cells were primed in the presence of the vehicle was set to 1 AU and all other values were calculated accordingly. Data are presented as individual data points, bars represent median, whiskers percentiles 25 and 75, dashed lines indicate the threshold for biological relevant fold changes. Friedman-test followed by Wilcoxon signed-rank test. ∗ $p \leq 0.05$ significantly different from samples of LPS-primed hPBMCs; AU, arbitrary units. LPS, lipopolysaccharide; 5-B, 5-(3-Bromophenyl)-1,3-dihydro-2H-benzofuro[3,2-e]-1,4-diazepin-2-one; PSB, PSB-15417; PZB15, PZB15517166A; PZB13, PZB13420052A; A43, 3-{[5-(2,3-dichlorophenyl)-1H-1,2,3,4-tetrazol-1-yl]methyl}pyridine; JNJ, N-[[4-(4-phenylpiperazin-1-yl)oxan-4-yl]methyl]-2-phenylsulfanylpyridine-3-carboxamide.

5.3 mRNA EXPRESSION OF CYTOKINES

5.3.1 mRNA EXPRESSION OF CYTOKINES IN THP-1 CELLS

To investigate possible effects of the P2RX4 and P2RX7 antagonists on mRNA expression levels of *IL1B*, *IL10*, *IL18*, *IL6*, and *TNF*, cells were primed with LPS in the absence or presence of the antagonists. After 5 h incubation, the cells were frozen at -20°C for later RNA isolation, transcription into cDNA, and real-time PCR. The mRNA expression of target genes was calculated relative to the reference gene *PPIA*. The respective gene expression of control cells stimulated with LPS was set to 1 AU. For THP-1 cell-derived macrophages, in a first set of experiments, the effects of P2RX4 antagonists 5-B and PSB and the P2RX7 antagonist A43 were investigated including two concentrations of 5-B and A43. Later, different sets of experiments were conducted, in which all antagonists were used at only one concentration. Respective controls were always included. These sets of experiments were combined in Figure 28 and 29 and explain the different n numbers.

First, treatment with LPS increased *IL1B* mRNA expression compared to 0.03-fold expression of untreated cells ($p = 0.028$) (**Figure 27A**). Stimulation with the P2RX4 antagonist 5-B resulted in an upregulation by about 4.48-fold compared to cells treated with LPS ($p = 0.028$). *IL1B* mRNA expression was not altered by the other P2RX4 antagonists and the P2RX7 antagonists (**Figure 27A**). Untreated monocytic THP-1 cells showed also very low *IL10* mRNA expression (~ 0.08-fold, $p = 0.028$ versus LPS) (**Figure 27B**). *IL10* expression was upregulated about 14.28-fold by stimulation with 5-B compared to stimulation with LPS ($p = 0.028$), while the other P2RX4 antagonists did not induce any alterations. Stimulation with P2RX7 antagonists did not induce changes (**Figure 27B**). Treatment with LPS did not alter *IL18* mRNA expression compared to untreated monocytic THP-1 cells (**Figure 27C**). The P2RX4 antagonists 5-B (~ 1.64-fold, $p = 0.028$) or PSB (~ 1.84-fold, $p = 0.028$) slightly increased *IL18* mRNA levels, while treatment with PZB15, PZB13, or the P2RX7 antagonists did not result in any changes compared to cells treated with LPS (**Figure 27C**). Treatment with LPS increased *IL6* mRNA expression compared to untreated cells ($p = 0.028$). P2RX4 and P2RX7 antagonists did not induce alterations compared to cells stimulated with LPS (**Figure 27D**). Treatment with LPS

increased *TNF* mRNA expression compared to untreated cells (p = 0.028) (**Figure 27E**). While stimulation with 5-B, PZB15, A43, and JNJ did not result in any changes, stimulation with PSB (~ 0.47-fold, p = 0.028) and PZB13 (~ 0.39-fold, p = 0.028) resulted in minor downregulation of *TNF* mRNA (**Figure 27E**).

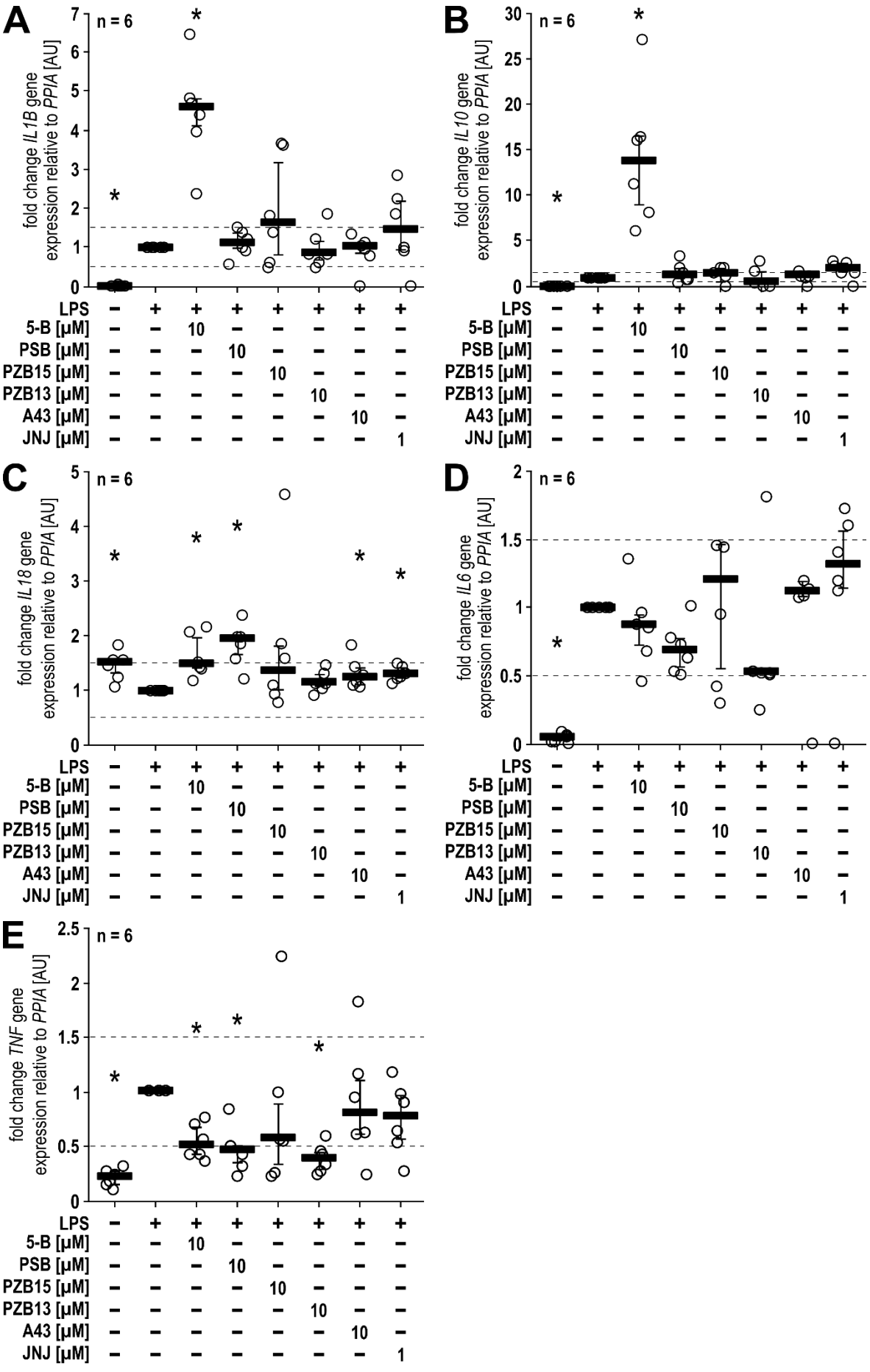
A
n = 6
fold change IL1B gene expression relative to PPIA [AU]
B
n = 6
fold change IL10 gene expression relative to PPIA [AU]
C
n = 6
fold change IL18 gene expression relative to PPIA [AU]
D
n = 6
fold change IL6 gene expression relative to PPIA [AU]
E
n = 6
fold change TNF gene expression relative to PPIA [AU]
LPS
5-B [µM]
PSB [µM]
PZB15 [µM]
PZB13 [µM]
A43 [µM]
JNJ [µM]

Figure 27: The impact of P2RX4 and P2RX7 antagonists on mRNA expression of cytokines by monocytic THP-1 cells. Cells were primed with LPS (1 µg/ml) for 5 h in the absence or presence of the P2RX4 antagonists 5-B (10 µM), PSB (10 µM), PZB15 (10 µM), or PZB13 (10 µM) or the P2RX7 antagonists A43 (10 µM) or JNJ (1 µM). After RNA isolation and transcription into cDNA, real-time PCR was performed to evaluate the mRNA expression of **(A)** *IL1B*, **(B)** *IL10*, **(C)** *IL18*, **(D)** *IL6*, and **(E)** *TNF*. The human *PPIA* gene was selected as a reference gene. Changes in the mRNA expression levels of targeted genes were calculated by the $2^{\Delta CT}$ method, where ΔCT represents the difference between the CT value of the *PPIA* gene and the CT value of the gene of interest. The gene expression in experiments in which cells were primed in the presence of the vehicle was set to 1 AU and all other values were calculated accordingly. Data are presented as individual data points, bars represent median, whiskers percentiles 25 and 75, dashed lines indicate the threshold for biological relevant fold changes. Friedman-test followed by Wilcoxon signed-rank test. $*$ $p \leq 0.05$ significantly different from samples of LPS-primed monocytic THP-1 cells. AU, arbitrary units; LPS, lipopolysaccharide; 5-B, 5-(3-Bromophenyl)-1,3-dihydro-2H-benzofuro[3,2-e]-1,4-diazepin-2-one; PSB, PSB-15417; PZB15, PZB15517166A; PZB13, PZB13420052A; A43, 3-{[5-(2,3-dichlorophenyl)-1H-1,2,3,4-tetrazol-1-yl]methyl}pyridine; JNJ, N-[[4-(4-phenylpiperazin-1-yl)oxan-4-yl]methyl]-2-phenylsulfanylpyridine-3-carboxamide.

Like monocytic THP-1 cells, *IL1B* mRNA expression increased upon stimulation with LPS compared to untreated THP-1 cell-derived M1-like macrophages ($p = 0.000$) (**Figure 28A**). No P2RX4 and P2RX7 antagonist altered *IL1B* mRNA expression levels (**Figure 28A**). *IL10* mRNA expression was also increased upon stimulation with LPS compared to 0.05-fold expression of untreated cells ($p = 0.000$), while the antagonists did not induce any changes compared to cells treated with LPS (**Figure 28B**). On the other hand, treatment with LPS downregulated *IL18* mRNA expression compared to untreated cells ($p = 0.028$) (**Figure 28C**). Again, stimulation with P2RX4 and P2RX7 antagonists did not result in alterations of *IL18* mRNA gene expression in THP-1 cell-derived macrophages (**Figure 28C**).

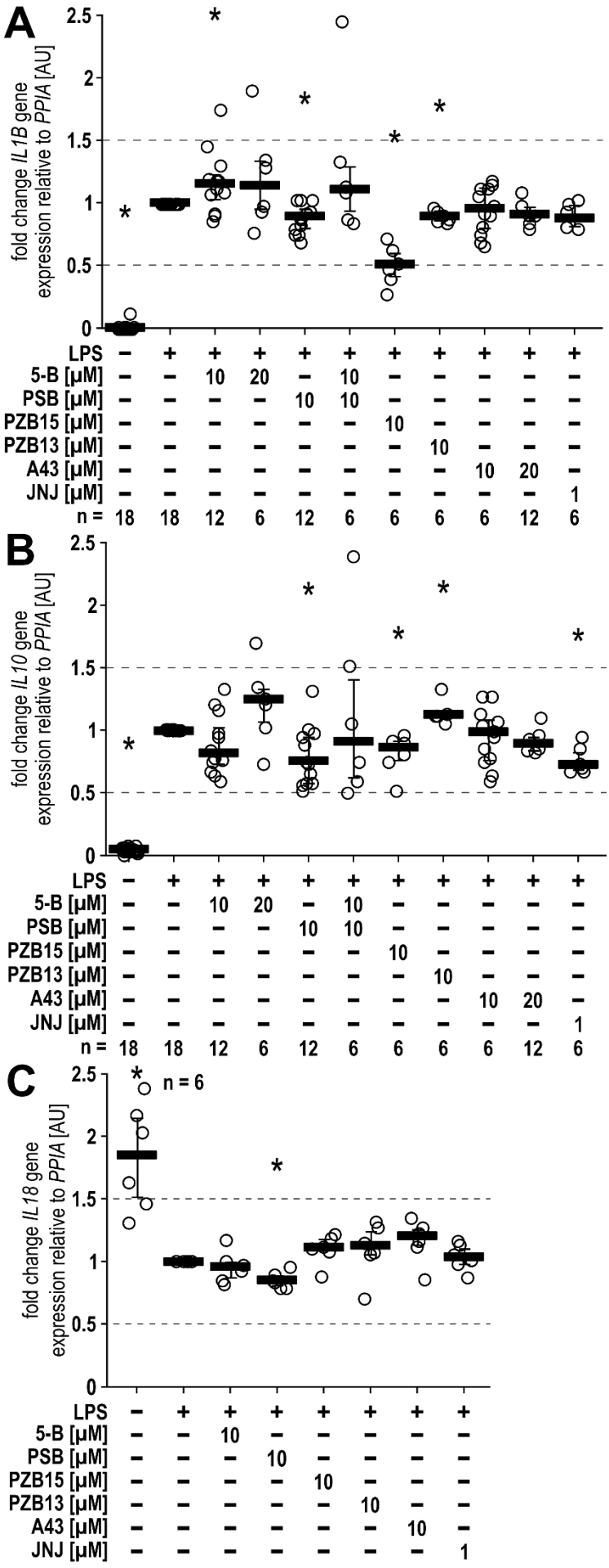
A
fold change IL1B gene expression relative to PPIA [AU]
2.5
2
1.5
1
0.5
0
LPS − + + + + + + + + + +
5-B [µM] − − 10 20 − 10 − − − − −
PSB [µM] − − − − 10 10 − − − − −
PZB15 [µM] − − − − − − 10 − − − −
PZB13 [µM] − − − − − − − 10 − − −
A43 [µM] − − − − − − − − 10 20 −
JNJ [µM] − − − − − − − − − − 1
n = 18 18 12 6 12 6 6 6 6 12 6
B
fold change IL10 gene expression relative to PPIA [AU]
2.5
2
1.5
1
0.5
0
LPS − + + + + + + + + + +
5-B [µM] − − 10 20 − 10 − − − − −
PSB [µM] − − − − 10 10 − − − − −
PZB15 [µM] − − − − − − 10 − − − −
PZB13 [µM] − − − − − − − 10 − − −
A43 [µM] − − − − − − − − 10 20 −
JNJ [µM] − − − − − − − − − − 1
n = 18 18 12 6 12 6 6 6 6 12 6
C
n = 6
fold change IL18 gene expression relative to PPIA [AU]
2.5
2
1.5
1
0.5
0
LPS − + + + + + + +
5-B [µM] − − 10 − − − − −
PSB [µM] − − − 10 − − − −
PZB15 [µM] − − − − 10 − − −
PZB13 [µM] − − − − − 10 − −
A43 [µM] − − − − − − 10 −
JNJ [µM] − − − − − − − 1

Figure 28: The impact of P2RX4 and P2RX7 antagonists on mRNA expression of cytokines by THP-1 cell-derived M1-like macrophages. THP-1 cells were differentiated into THP-1 M1-like macrophages. Cells were primed with LPS (1 µg/ml) for 5 h in the absence or presence of the P2RX4 antagonists 5-B (10, 20 µM), PSB (10 µM), PZB15 (10 µM), or PZB13 (10 µM) or the P2RX7 antagonists A43 (10, 20 µM) or JNJ (1 µM). After RNA isolation and transcription into cDNA, real-time PCR was performed to evaluate the mRNA expression of **(A)** *IL1B*, **(B)** *IL10*, and **(C)** *IL18*. The human *PPIA* gene was selected as a reference gene. Changes in the mRNA expression levels of targeted genes were calculated by the $2^{\Delta CT}$ method, where ΔCT represents the difference between the CT value of the *PPIA* gene and the CT value of the gene of interest. The gene expression in experiments in which cells were primed alone was set to 1 AU and all other values were calculated accordingly. Data are presented as individual data points, bars represent median, whiskers percentiles 25 and 75, dashed lines indicate the threshold for biological relevant fold changes. Friedman-test followed by Wilcoxon signed-rank test. $*$ $p \leq 0.05$ significantly different from samples of LPS-primed THP-1 M1-like macrophages. AU, arbitrary units; LPS, lipopolysaccharide; 5-B, 5-(3-Bromophenyl)-1,3-dihydro-2H-benzofuro[3,2-e]-1,4-diazepin-2-one; PSB, PSB-15417; PZB15, PZB15517166A; PZB13, PZB13420052A; A43, 3-{[5-(2,3-dichlorophenyl)-1H-1,2,3,4-tetrazol-1-yl]methyl}pyridine; JNJ, N-[[4-(4-phenylpiperazin-1-yl)oxan-4-yl]methyl]-2-phenylsulfanylpyridine-3-carboxamide.

IL6 mRNA expression increased upon stimulation with LPS compared to untreated THP-1 cell-derived M1-like macrophages ($p = 0.000$) (**Figure 29A**). From the P2RX4 antagonists, only PZB15 downregulated *IL6* about 0.37-fold compared to cells stimulated with LPS ($p = 0.028$). P2RX7 antagonists did not altered *IL6* mRNA expression (**Figure 29A**). *TNF* mRNA expression also increased upon stimulation with LPS compared to untreated cells ($p = 0.028$) (**Figure 29B**). Treatment with P2RX4 antagonists 5-B, PSB, or PZB13 did not induce any changes, while treatment with PZB15 resulted in a 0.45-fold downregulation of *TNF* mRNA compared to cells treated with LPS ($p = 0.028$). The P2RX7 antagonists A43 and JNJ did not change *TNF* mRNA expression levels in THP-1 cell-derived macrophages (**Figure 29B**).

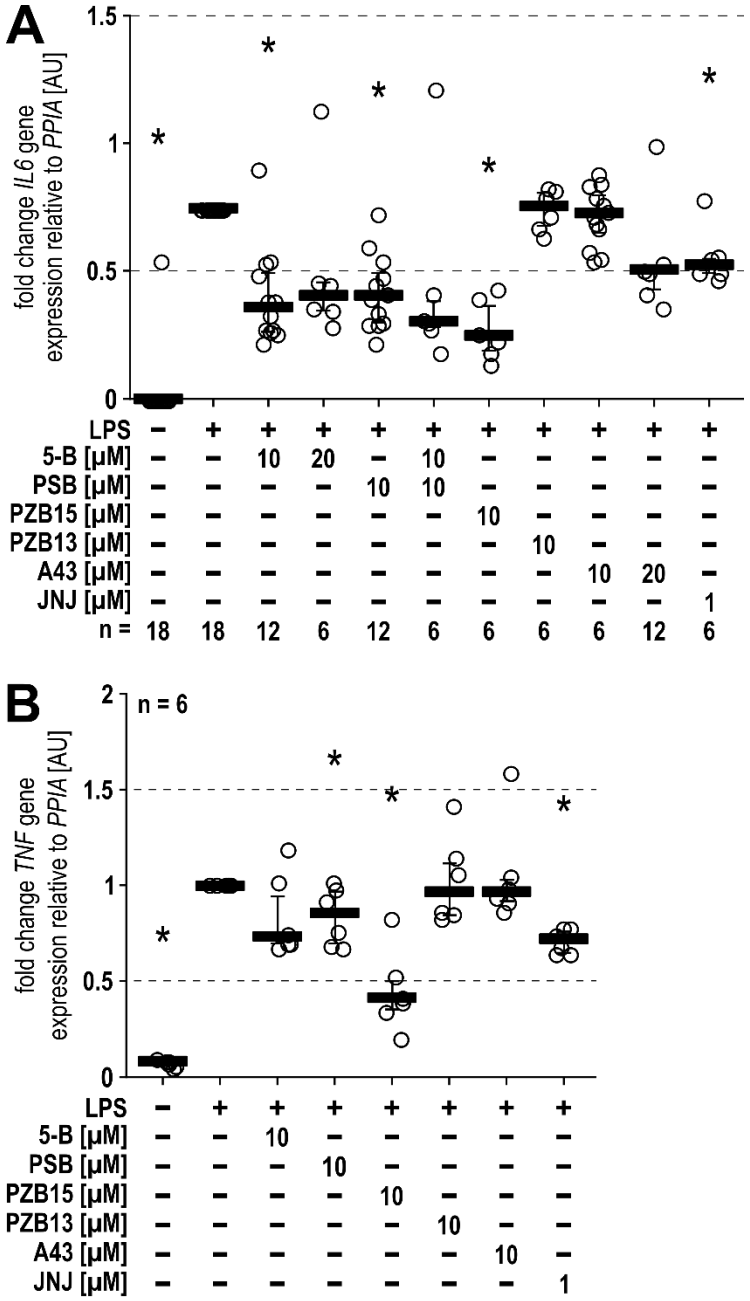

Figure 29: The impact of P2RX4 and P2RX7 antagonists on mRNA expression of cytokines by THP-1 cell-derived M1-like macrophages. THP-1 cells were differentiated into THP-1 M1-like macrophages. Cells were primed with LPS (1 µg/ml) for 5 h in the absence or presence of the P2RX4 antagonists 5-B (10, 20 µM), PSB (10 µM), PZB15 (10 µM), or PZB13 (10 µM) or the P2RX7 antagonists A43 (10, 20 µM) or JNJ (1 µM). After RNA isolation and transcription into cDNA, real-time PCR was performed to evaluate the mRNA expression of **(A)** *IL6* and **(B)** *TNF*. The human *PPIA* gene was selected as a reference gene. Changes in the mRNA expression levels of targeted genes were calculated by the $2^{\Delta CT}$ method, where ΔCT represents the difference between the CT value of the *PPIA* gene and the CT value of the gene of interest. The gene expression in experiments in which cells were primed in the presence of the vehicle was set to 1 AU and all other values were calculated accordingly. Data are presented as individual data points, bars represent median, whiskers percentiles 25 and 75, dashed lines indicate the threshold for biological relevant fold changes. Friedman-test followed by Wilcoxon signed-rank test. $*$ $p \leq 0.05$ significantly different from samples of LPS-primed THP-1 M1-like macrophages. AU, arbitrary units; LPS, lipopolysaccharide; 5-B, 5-(3-Bromophenyl)-1,3-dihydro-2H-benzofuro[3,2-e]-1,4-diazepin-2-one; PSB, PSB-15417; PZB15, PZB15517166A; PZB13, PZB13420052A; A43, 3-{[5-(2,3-dichlorophenyl)-1H-1,2,3,4-tetrazol-1-yl]methyl}pyridine; JNJ, N-[[4-(4-phenylpiperazin-1-yl)oxan-4-yl]methyl]-2-phenylsulfanylpyridine-3-carboxamide.

5.3.2 mRNA EXPRESSION OF CYTOKINES IN hPBMCs

The effects of P2X receptors antagonists during priming with LPS on the expression of *IL1B, IL10* and *IL6* mRNA in hPBMCs was also investigated for verification of the data obtained in the THP-1 cell line in primary cells. After 3 h incubation, the cells were frozen at -20°C for later RNA isolation, transcription into cDNA, and real-time PCR. The gene expression of target genes was calculated relative to the reference gene *PPIA*. The respective gene expression of LPS-stimulated cells was set to 1 AU.

Like THP-1 cells, *IL1B* mRNA expression increased upon stimulation with LPS compared to untreated hPBMCs ($p = 0.018$) (**Figure 30A**). Treatment with P2RX4 as well as P2RX7 antagonists did not induce changes in *IL1B* mRNA expression (**Figure 30A**). *IL10* mRNA expression increased upon stimulation with LPS compared to untreated cells ($p = 0.018$) (**Figure 30B**). While stimulation with PSB did not induce changes in *IL10* levels, 5-B (~ 4.88-fold, $p = 0.018$) and PZB13 (~ 3.44-fold, $p = 0.018$) clearly and PZB15 (~ 1.53-fold, $p = 0.004$) slightly upregulated *IL10* in cells compared to hPBMCs stimulated with LPS. The P2RX7 antagonists did not change expression levels (**Figure 30B**). Again, *IL6* mRNA expression increased upon stimulation with LPS compared to untreated hPBMCs ($p = 0.018$) (**Figure 30C**). Interestingly, all PRX4 antagonists upregulated or tended to upregulate *IL6* mRNA expression in hPBMCs: 5-B (~ 2.54-fold, $p = 0.018$), PSB (~ 1.98-fold, $p = 0.063$), PZB15 (~ 1.80-fold, $p = 0.043$), and PZB13(~ 2.24-fold, $p = 0.018$) compared to cells treated with LPS. Treatment with P2RX7 antagonists did not alter *IL6* mRNA expression (**Figure 30C**).

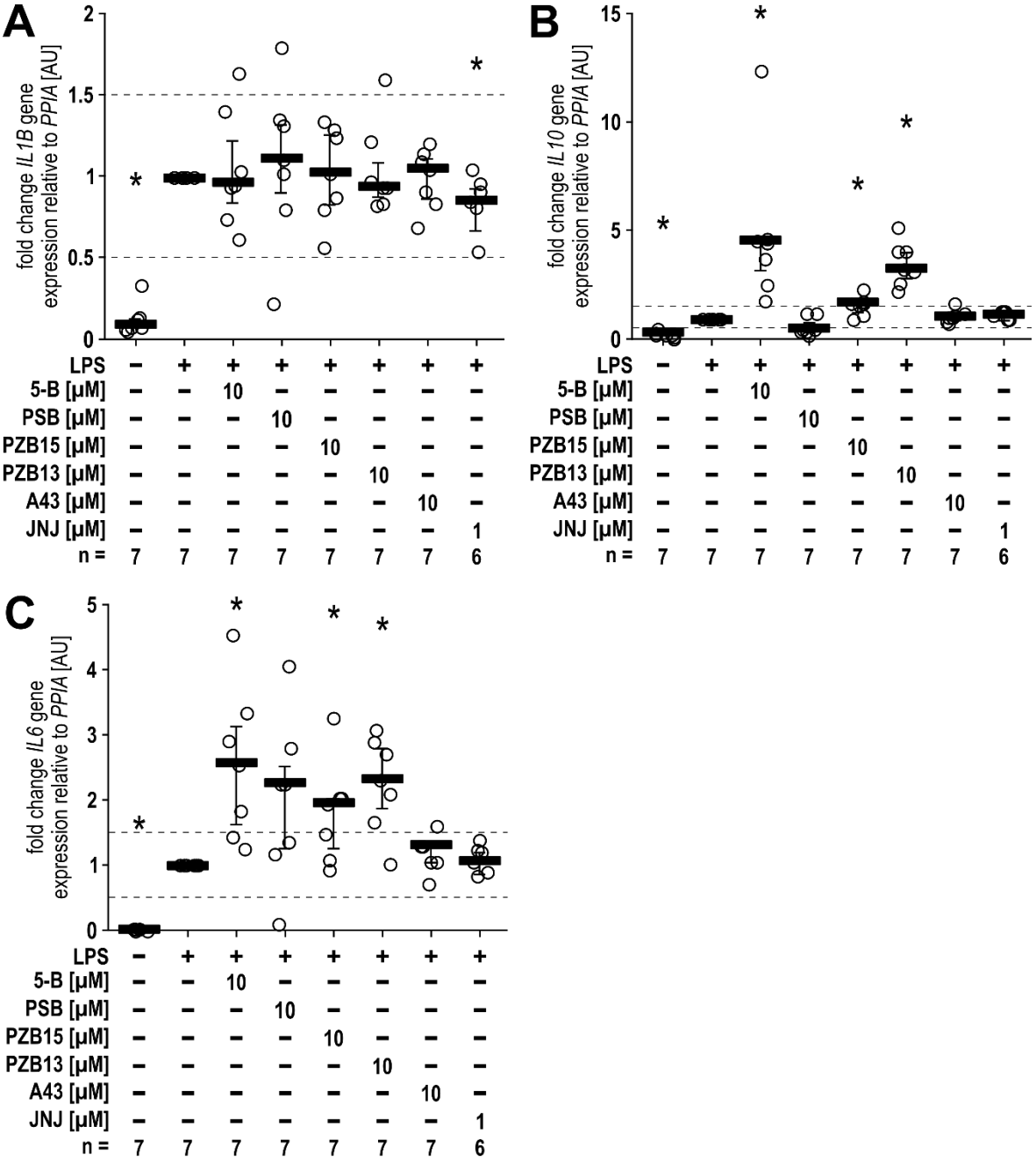

Figure 30: The impact of P2RX4 and P2RX7 antagonists on mRNA expression of cytokines by hPBMCs. Cells were primed with LPS (5 ng/ml) for 3 h in the absence or presence of the P2RX4 antagonists 5-B (10 µM), PSB (10 µM), PZB15 (10 µM), or PZB13 (10 µM) or the P2RX7 antagonists A43 (10 µM) or JNJ (1 µM). After RNA isolation and transcription into cDNA, real-time PCR was performed to evaluate the mRNA expression of **(A)** *IL1B*, **(B)** *IL10,* and **(C)** *IL6*. The human *PPIA* gene was selected as a reference gene. Changes in the mRNA expression levels of targeted genes were calculated by the $2^{\Delta CT}$ method, where ΔCT represents the difference between the CT value of the *PPIA* gene and the CT value of the gene of interest. The gene expression in experiments in which cells were primed in the presence of the vehicle was set to 1 AU and all other values were calculated accordingly. Data are presented as individual data points, bars represent median, whiskers percentiles 25 and 75, dashed lines indicate the threshold for biological relevant fold changes. Friedman-test followed by Wilcoxon signed-rank test. ∗ $p \leq 0.05$ significantly different from samples of LPS-primed hPBMCs. AU, arbitrary units; LPS, lipopolysaccharide; 5-B, 5-(3-Bromophenyl)-1,3-dihydro-2H-benzofuro[3,2-e]-1,4-diazepin-2-one; PSB, PSB-15417; PZB15, PZB15517166A; PZB13, PZB13420052A; A43, 3-{[5-(2,3-dichlorophenyl)-1H-1,2,3,4-tetrazol-1-yl]methyl}pyridine; JNJ, N-[[4-(4-phenylpiperazin-1-yl)oxan-4-yl]methyl]-2-phenylsulfanylpyridine-3-carboxamide.

6 EFFECTS OF P2RX4 ANTAGONISTS ON CASPASE-3/-7 ACTIVITY

6.1 CASPASE-3/-7 ACTIVITY IN MONOCYTIC THP-1 CELLS

At last, the activity of caspase-3 and caspase-7 was measured in monocytic THP-1 cells by caspase activity assays. To investigate a possible activation mediated by P2RX4 antagonists, THP-1 cells were primed with 1 µg/ml LPS for 5 h in the absence or presence of the antagonists 5-B, PSB, and PZB15, and the caspase inhibitor Z-VAD-FMK. The cytotoxic agent doxorubicin served as a positive control. The activity of caspase-3 and caspase-7 was measured after 30 and 60 min of incubation with the substrate. As the results did not differ strongly at the two time points, only the results obtained after 30 min are shown. Results from measurements after 60 min incubation are shown in Figure S-2.

Treatment with LPS did not induce any additional caspase activity compared to untreated cells (**Figure 31A**). The P2RX4 antagonist 5-B did not induce caspase activity when given alone, but it induced a significant increase, when given prior to priming with LPS ($p = 0.028$ versus LPS). Additional application of Z-VAD-FMK significantly reduced the caspase activity ($p = 0.028$ versus LPS). PSB given alone or prior to LPS did not induce any alterations in caspase-3/-7 activity, but addition of Z-VAD-FMK significantly reduced the activity ($p = 0.028$ versus LPS). The same results could be observed with PZB15 ($p = 0.028$ versus LPS) (**Figure 31A**). A significant increase of caspase activity by doxorubicin ($p = 0.028$ versus untreated) could be inhibited by Z-VAD-FMK ($p = 0.028$ versus untreated), while incubation with Z-VAD-FMK alone ($p = 0.028$ versus untreated) led to the lowest measured caspase-3/-7 activity compared to untreated cells (**Figure 31B**).

Additionally, the IL-1β concentration and LDH activity was measured in supernatants of monocytic THP-1 cells. Cells were treated with doxorubicin or the combination doxorubicin and Z-VAD-FMK in presence or absence of LPS. Additionally, cells were primed with LPS in presence of Z-VAD-FMK and later stimulated with BzATP or nigericin. After treatment with the reagents alone, IL-1β concentrations were below the limit of detection (**Table S-5**). Addition of Z-VAD-FMK decreased IL-1β concentrations of cells which were primed with LPS, additionally stimulated with BzATP or nigericin. LDH activity measurements showed that 5 h incubation with doxorubicin or Z-VAD-FMK induced only minor alterations of cell viability (**Table S-1**).

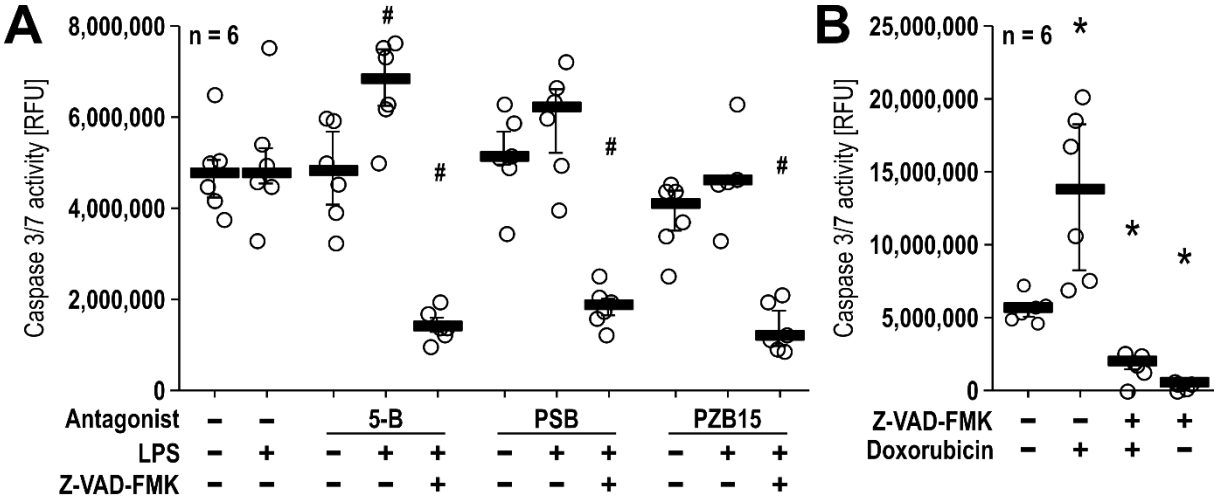

Figure 31: The impact of P2RX4 antagonists on caspase-3 and caspase-7 activity in monocytic THP-1 cells. **(A)** Cells were primed with LPS (1 µg/ml) for 5 h in absence or presence of the P2RX4 antagonists 5-B (10 µM), PSB (10 µM), or PZB15 (10 µM), or the caspase inhibitor Z-VAD-FMK (20 µM). **(B)** As positive control, cells were treated with doxorubicin (2.5 µM) for 5 h in the absence or presence of Z-VAD-FMK (20 µM). Thereafter, Apo-ONE® reagent was added for 30 min. Caspase-3 and -7 activity was measured by detecting fluorescence signals. Data are presented as individual data points, bars represent median, whiskers percentiles 25 and 75. Friedman-test followed by Wilcoxon signed-rank test. $*$ $p \leq 0.05$ significantly different from untreated samples. # $p \leq 0.05$ significantly different from samples in which LPS alone was given to monocytic THP-1 cells. RFU, relative fluorescence unit; LPS, lipopolysaccharide; 5-B, 5-(3-Bromophenyl)-1,3-dihydro-2H-benzofuro[3,2-e]-1,4-diazepin-2-one; PSB, PSB-15417; PZB15, PZB15517166A

DISCUSSION

1 OVERVIEW OF THE MAIN RESULTS

The objective of this exploratory study is to provide insight into the following questions: 1. which role plays the P2RX4 in the ATP-dependent IL-1β maturation; 2. which roles play P2RX4 and P2RX7 in the priming of human mononuclear phagocytes; 3. does the P2RX4 antagonist 5-B induce apoptosis?

In order to investigate the function of P2RX4 and P2RX7, a variety of antagonists are employed, including 5-B, PSB, PZB15, and PZB13 for P2RX4, as well as A43 and JNJ for P2RX7. In this study, these antagonists are administered to LPS-primed cells in order to determine the influence of P2RX4 and P2RX7 on NLRP3 assembly and IL-1β maturation. The results demonstrate that P2RX4 and P2RX7 antagonists effectively alleviate the ATP-dependent IL-1β release by monocytic THP-1 cells, hPBMCs, THP-1 cell-derived M1-like macrophages, and hPMs, while having no impact on the ATP-independent nigericin-induced IL-1β release. It is well-established that P2RX7 plays a pivotal role in mediating the effect of ATP on NLRP3 assembly and subsequent IL-1β release. Consequently, it was anticipated that P2RX7 antagonists would effectively block the receptor and inhibit the ATP-dependent IL-1β release. The analogous outcomes yielded by P2RX4 antagonists suggest that the P2RX4 may also be involved in NLRP3 assembly and IL-1β maturation.

Moreover, the antagonists are administered to the cells prior to priming with LPS. The assembly and activation of the NRLP3 inflammasome are investigated by measuring the IL-1β release, both in an ATP-dependent and ATP-independent manner. In monocytic THP-1 cells and hPBMCs, treatment with 5-B prior to priming increases the BzATP-induced and nigericin-induced IL-1β release. Furthermore, the 5-B-mediated increase in IL-1β is reversed by the addition of other P2RX4 antagonists but not P2RX7 antagonists. Nevertheless, while 5-B increases *IL1B* mRNA expression levels in monocytic THP-1 cells, no alterations in *IL1B* expression are detected in hPBMCs. In contrast to monocytic cells, the effect of 5-B is not observed in THP-1 cell-derived M1-like macrophages and hPMs. It is also noteworthy that there is a strong increase in the mRNA expression of the anti-inflammatory *IL10* in monocytic THP-1 cells and hPBMCs upon treatment with 5-B.

The activity of caspase-3 and caspase-7 is investigated in an attempt to elucidate the mode of action of 5-B. Treatment with 5-B before priming with LPS activates caspase-3 and caspase-7 in monocytic THP-1 cells suggesting that 5-B might induce apoptosis.

2 DISCUSSION OF THE METHODS

2.1 THP-1 CELLS AND PRIMARY CELLS

Mononuclear phagocytes are the main producers of IL-1β during inflammation. In this study, mononuclear phagocytes are represented by the THP-1 cell line and primary cells such as hPBMCs and hPMs. The THP-1 cell line was isolated from the peripheral blood of a one-year-old male patient with acute monocytic leukaemia in 1980. This cell line is widely used for studying the immune responses of monocytes and macrophages *in vitro* (Tsuchiya et al. 1980, Sharif et al. 2007, Chanput et al. 2010, Chanput et al. 2014, Kurynina et al. 2018). Upon exposure to PMA, monocytic THP-1 cells differentiate into macrophages with a phenotype similar to primary monocyte-derived macrophages in terms of phagocytic activity and production of IL-1β and TNF-α (Auwerx 1991, Schwende et al. 1996, Daigneault et al. 2010). THP-1 cells differentiated with PMA are adherent, have an increased cytoplasmic volume compared to undifferentiated THP-1 cells, resulting in a reduced nucleocytoplasmic ratio, and exhibit a flat and amoeboid morphology (Tsuchiya et al. 1982, Daigneault et al. 2010). For polarization to M1-like macrophages, differentiated THP-1 cells are further incubated with IFN-γ and/or LPS (Mantovani et al. 2004, Martinez et al. 2006, Genin et al. 2015). The morphology of THP-1 cell-derived macrophages, which is assessed in this study, conforms to these descriptions, displaying adherent and flat cells with an amoeboid morphology upon treatment with PMA, and a further decrease in the nucleocytoplasmic ratio and a more fibroblast-like morphology upon additional treatment with IFN-γ and LPS (**Figure 5**).

The main advantage of using cell lines is their simple culturing process, which is accompanied by a homogeneous genetic background that reduces the variability in cell phenotype (Chanput et al. 2014). However, it is important to note that cell lines are often derived from malignant cells, which may carry numerous mutations, and any reported effects may depend on the genotype of the cell line in question. On the other hand, primary human cells from healthy donors have an unaltered genotype and are more similar to the *in vivo* state, reflecting normal cell physiology. For this reason, hPBMCs, which contain a large proportion of primary monocytes, are also used in this study. The isolation of hPBMCs from blood samples is well established in our laboratory (Hecker et al. 2015, Richter et al. 2018b, Richter et al. 2020, Richter et al. 2023a). The process involves density gradient centrifugation to separate monocytes and lymphocytes from plasma, followed by culturing mononuclear cells with monocyte attachment medium and medium exchange after 3 h to enrich for adherent monocytes and reduce the number of lymphocytes. After adherence selection for 1 h, the monocyte yield is typically around 44 %, but the population is still mainly contaminated with lymphocytes (Nielsen et al. 2020). However, extending the time of adherence selection to 3 h may lead to higher purity. Another limitation is the high variability between individual donors

regarding cell number, purity, and responsiveness, which can impair the reproducibility of results.

The present study also involves hPMs, which are purified from peritoneal dialysate through centrifugation and incubation with RBC lysis buffer to eliminate erythrocytes. After overnight incubation and medium exchange, adherent cells are selected for cytokine release experiments. The purity of the adherent cell population is assessed by comparing it to the original composition of cell populations in the dialysate samples. Preliminary experiments reveal that dialysates contain monocytes, lymphocytes, and granulocytes (Keller H. unpublished). CD14 and CD68 are employed as macrophage markers (Eischen et al. 1994, Ruiz-Alcaraz et al. 2016, Ruiz-Alcaraz et al. 2018, Shapouri-Moghaddam et al. 2018). Immunocytochemical staining indicates that the percentages of macrophages represented by $CD14^+$ and $CD68^+$ cells significantly increase during isolation, resulting in 86.5 % (median) $CD14^+$ or 75.7 % $CD68^+$ cells in the adherent cell population (**Figure 7**). This suggests a successful enrichment of hPMs in the samples and a suitable source for primary macrophages. However, samples still contain 6.9 % (median) granulocytes and other unidentified cell types. Like hPBMCs, there is a considerable variation in IL-1β release among individual donors. hPMs from donors with pathological conditions may polarize macrophages towards a specific phenotype or activate them *in vivo*, hence the use of primary macrophages from healthy donors, which are difficult to obtain for ethical reasons, would be preferable.

2.2 IL-1β RELEASE BY THP-1 CELLS AND PRIMARY CELLS

This study is based on the ability of monocytes and macrophages to secrete IL-1β upon two danger signals. The process of cell activation involves the recognition of PAMPs or DAMPs, which triggers the priming step. This step includes the expression of various components, including NLRP3 and pro-IL-1β. A second signal, in the form of a DAMP or PAMP, induces changes in intracellular Ca^{2+} and K^+ levels, leading to the assembly of the NLRP3 inflammasome and to the processing and subsequent release of mature IL-1β. Secreted IL-1β can be measured using the ELISA technique, which is widely used for measuring protein levels in cell culture supernatants. However, the use of kits optimized for detecting mature IL-1β can also detect pro-IL-1β, which is typically present at low levels in supernatants but can be released from damaged cells. Therefore, it is not possible to distinguish between the precursor and mature forms of IL-1β. To induce the expression of pro-IL-1β and components of the NLRP3 inflammasome, monocytic THP-1 cells, THP-1 cell-derived macrophages, and hPBMCs and hPMs are primed with LPS. As expected, this priming leads to a small but significant increase in IL-1β release compared to untreated cells (**Figure 6**, **Figure 8**). While the two-signal model for NLRP3 assembly is commonly used, several studies have reported that priming with LPS can enhance NLRP3 inflammasome assembly in the absence of a

second signal (Juliana et al. 2012, Schroder et al. 2012). Monocytes secrete IL-1β upon stimulation with LPS, even in the absence of other stimuli, and the signalling molecule IRAK-1, which is downstream of TLR4 and MyD88, promotes inflammasome assembly and subsequent caspase-1 activation via NF-κB signalling in murine macrophages (Fernandes-Alnemri et al. 2013, Lin et al. 2014, Kim et al. 2016). In conclusion, activation with LPS alone can also lead to NLRP3 assembly and subsequent IL-1β release, although to a lesser extent compared to stimulation with two consecutive stimuli.

The results obtained from priming with LPS for 5 h indicate a low release of IL-1β in monocytic THP-1 cells (~9 pg/ml) and hPBMCs (~23 pg/ml). On the other hand, a higher release of IL-1β was observed in THP-1 cell-derived M1-like macrophages (~153 pg/ml) and hPMs (~47 pg/ml) (**Figure 6**, **Figure 8**). These findings align with other studies that report a difference in cytokine production levels upon LPS stimulation between monocytic THP-1 cells and hPBMCs, with the latter producing more IL-1β and *IL6* (Bruckmeier et al. 2012, Schildberger et al. 2013). This difference in cytokine production may be attributed to the higher baseline expression levels of these cytokines and the higher expression of CD14 by primary monocytes (Daigneault et al. 2010, Bruckmeier et al. 2012, Schildberger et al. 2013). Furthermore, monocytes and macrophages respond differently during inflammation *in vivo*, which correlates with elevated expression levels of TLR4 in monocyte-derived macrophages compared to monocytes (O'Mahony et al. 2008, Juarez et al. 2010, Smythies et al. 2010, Schneberger et al. 2011, Nahrendorf et al. 2013). The differences in LPS sensitivity between monocytic THP-1 cells and THP-1 cell-derived macrophages can be attributed to the elevated expression levels of CD14, TLR4, and MyD88 in the differentiated cells (Kim et al. 2022).

The application of a second signal, as expected, leads to a significant increase in IL-1β release compared to cells only primed with LPS (**Figure 6**, **Figure 8**). Initially, it was observed that extracellular ATP stimulates the secretion of IL-1β (Ferrari et al. 1996, Ferrari et al. 1997). Shortly thereafter, it was demonstrated that the synthetic ligand BzATP is approximately 30-fold more potent than ATP (Surprenant et al. 1996, Bianchi et al. 1999, Young et al. 2007). Previous studies from our laboratory have also shown that stimulation with 100 µM BzATP leads to successful IL-1β release from THP-1 cells and hPBMCs (Amati et al. 2017, Hiller et al. 2018, Richter et al. 2018b, Richter et al. 2018a, Richter et al. 2020, Richter et al. 2022, Richter et al. 2023a, Richter et al. 2023b). Furthermore, it was demonstrated previously that THP-1 cell-derived macrophages respond better to ATP than to BzATP (Richter et al. 2023a). Therefore, LPS-primed THP-1 cell-derived macrophages are stimulated with 1 mM ATP and 2 mM ATP, while stimulation with 2 mM ATP leads to a more robust IL-1β secretion (**Figure 10**). The concentrations used are sufficient to activate P2RX7 and are also of physiological relevance, as local ATP concentrations up to 100 mM can occur during inflammation (Di Virgilio et al. 2020).

Nigericin, derived from the Gram-positive bacterium *Streptomyces hygroscopicus*, functions as an antibiotic and is known to be a potent activator of the NLRP3 inflammasome and inducer of IL-1β release, independent of ATP (Watanabe et al. 1998, Warny et al. 1999, Mariathasan et al. 2006, Muñoz-Planillo et al. 2013). ATP or BzATP activate the ionotropic P2RX7, and nigericin, as an ionophore, allows for the efflux of K^+. This reduction in cytoplasmic K^+ concentration subsequently induces the assembly of the NLRP3 inflammasome. It can be inferred that stimulation of LPS-primed THP-1 cells, hPBMCs, and hPMs with BzATP, ATP, or nigericin results in NLRP3 assembly, caspase-1 activation, and subsequent IL-1β processing and release, which explains the significant increase in IL-1β concentrations in the cell supernatants (**Figure 6**, **Figure 8**). These findings align with previous studies from our laboratory and other researchers, as previously mentioned above. Like the results depicted here, previous studies from our laboratory also revealed a high variability in IL-1β concentrations of unknown origin, and therefore, these data and those of the present study were normalized (Richter et al. 2018b, Richter et al. 2020, Richter et al. 2022, Richter et al. 2023a, Richter et al. 2023b).

2.3 ESTIMATED CELL DEATH OF THP-1 CELLS AND PRIMARY CELLS

Although it is likely that cells release IL-1β upon appropriate stimulation, cells may release pro-inflammatory cytokines due to mechanical stress induced by handling. Moreover, the activation of the NLRP3 inflammasome not only leads to the maturation of IL-1β but also to the induction of pyroptosis, a lytic and pro-inflammatory form of cell death mediated by GSDMD, which is also cleaved by caspase-1 (Fink et al. 2006). Pyroptosis results in the release of intracellular material, including cytokines, from the ruptured immune cell, thereby promoting inflammatory processes in the surrounding environment (He et al. 2015). Therefore, the IL-1β levels measured in the supernatant of stimulated cells may be attributed to uncontrolled release during pyroptosis. To control for this, the LDH activity in the cell culture supernatants of every sample was measured. LDH is a stable cytosolic enzyme that is released from damaged cells, and the abundance of LDH in supernatants is a well-established parameter for cell damage. The overall low LDH activity (less than 20 %) in supernatants of monocytic THP-1 cells, THP-1 cell-derived macrophages, hPBMCs, and hPMs upon stimulation with LPS followed by BzATP or ATP indicates that the measured IL-1β release was not mediated by unspecific cell perforation (**Table S-1** – **Table S-4**).

Stimulation with nigericin can directly lead to elevated levels of LDH activity (above 20 %) in certain cases, particularly in M1-like macrophages derived from THP-1 cells and hPBMCs. In addition, LPS and nigericin can induce pyroptosis in various cell lines, including THP-1 cells (He et al. 2015, Hartigh et al. 2018, Zhou et al. 2020, Wu et al. 2023). Induction of pyroptosis and a LDH activity up to 100 % is described when LPS-primed THP-1 cells are incubated with

nigericin for 1 h (Zhou et al. 2020). In this study, the cells are incubated with nigericin for 30 – 40 min and the median LDH activity measured is 26 % with a maximal LDH activity of 57 % in supernatants of THP-1 cell-derived M1-like macrophages. This suggests that elevated LDH activity in samples may be due to cells undergoing pyroptosis or necrosis, leading to an uncontrolled release of pro-IL-1β, IL-1β, and LDH into the supernatant. Furthermore, hPBMCs treated with nigericin alone, without prior stimulation with LPS, can also exhibit increased LDH activity (**Table S-3**). It has been reported that nigericin can induce pyroptosis also in this cell type when applied alone, but only when the cells are incubated for 24 h (Wu et al. 2023). In general, measuring the optical density of lysed cells or supernatants containing nigericin shows lower extinction at 490 nm compared to samples without nigericin. This suggests that nigericin may interfere with the measurement of optical density of the LDH product, which could compromise the accuracy of cell death estimation.

Conclusively, these results indicate a successful induction of ATP-dependent and ATP-independent IL-1β release from monocytic THP-1 cells, THP-1 cell-derived M1-like macrophages, hPBMCs, and hPMs by priming the cells with LPS followed by stimulation with BzATP, ATP, or nigericin. The chosen cells appear to be suitable for the following investigations.

2.4 ESTIMATED PROTEIN LEVELS OF INTRACELLULAR IL-1β

Priming with LPS induces the expression of pro-IL-1β, which accumulates in the cytosol as processing relies on a second stimulus. The 31 kDa-sized precursor is cleaved by caspase-1 to the mature IL-1β form, 17 kDa in size. Although the ELISA is unable to distinguish between the two forms of IL-1β, Western blot analysis offers the advantage of discriminating proteins based on their size. However, the analysis is only semi-quantitative, as no statement can be made regarding the exact amount of the target protein; only how much there is in relation to another protein and sample can be determined. In this study, the amounts of IL-1β protein are estimated using β-actin as a reference protein. Actin microfilaments, comprising of the β- and γ-actin isoforms, constitute a fundamental component of the cytoskeleton (Dugina et al. 2019). They perform pivotal roles in essential cellular processes and in maintaining the structural integrity of the cell (Dugina et al. 2019). Therefore, β-actin is expressed at high levels in a wide range of tissues and is frequently employed as a reference protein in Western blotting. Some studies have questioned the validity of using β-actin as a reference protein, given that protein levels differ amongst tissues and that β-actin is largely overloaded at the protein concentrations most often used in Western blotting (Chen et al. 2015). However, the present results show that in THP-1 cell-derived M1-like macrophages, β-actin is not overloaded and exhibits stability under the experimental conditions (**Figure 19A**). Therefore, β-actin seems to be a suitable control for this study.

It should be noted that densitometrical data are not always directly proportional to protein abundance. Rather, they often fit non-proportional linear or hyperbolic mathematical models and can reach saturation (Butler et al. 2019). In the event that data are not directly proportional to protein abundance, it is inadvisable to employ normalisation techniques (Gassmann et al. 2009, Butler et al. 2019). It is therefore crucial to highlight that the results obtained through Western blotting represent only an estimation of protein levels. Furthermore, it is not possible to discount the potential for unknown errors to have influenced the outcome. Additionally, Western blot analysis of hPBMCs and monocytic THP-1 cells was not feasible due to technical constraints.

Western blot analysis of lysates of THP-1 cell-derived M1-like macrophages treated with LPS revealed the presence of pro-IL-1β, while mature IL-1β was not detectable. Untreated cells exhibited neither pro-IL-1β nor mature IL-1β protein expression (**Figure 19A**), which is consistent with previously reported findings (Radwan et al. 2010, Huang et al. 2012, Zhang et al. 2012, Zheng et al. 2015, Hadadi et al. 2016).

2.5 SEMI-QUANTIFICATION OF MRNA EXPRESSION LEVELS

Given that priming with LPS activates the TF NF-κB, which subsequently translocates to the nucleus and induces the translation of several genes for pro-inflammatory proteins, it is also of interest to quantify their mRNA. Real-time RT-PCR represents a well-established method for the semi-quantitative analysis of mRNA. The data obtained from real-time RT-PCR represent the relative mRNA expression of the gene of interest in comparison to a reference gene. The utilisation of standardised assay kits for the isolation and transcription of RNA into cDNA serves to minimise potential errors. The primer pairs used in this study were selected based on previous research, with the exception of *IL18*, which was generated using the Primer3.org tool (**Table 5**). The real-time RT-PCR efficiencies for the majority of primer pairs were found to be 100 %, indicating successful amplicon doubling per cycle. The NTCs demonstrate that there is no contamination with extraneous nucleic acid or primer dimer formation. The melting curves, which are specific for the amplified DNA fragments, demonstrated that the real-time RT-PCR resulted in the production of a single, homogeneous amplicon for each target sequence (data not shown). Moreover, the amplification products separated by agarose gel electrophoresis demonstrate the expected product size, which provides further evidence that the used primers are suitable for the amplification of the target genes (**Figure 23**).

PPIA is used as a reference gene for the calculation of the mRNA expression levels for the target genes *P2RX4*, *P2RX7*, *IL1B*, *IL10*, *IL18*, *IL6*, and *TNF*. The protein PPIA, also known as cyclophilin A, is an abundantly expressed enzyme that catalyses isomerisation of specific peptide bonds, thereby regulating a number of biological processes, including protein folding,

intracellular signalling and the regulation of immune function (Liao et al. 2021). *PPIA* is a suitable reference gene in LPS-stimulated THP-1 cells and hPBMCs (Cao et al. 2012, Radke et al. 2014, Bantulà et al. 2022, Diehl et al. 2022, Ren et al. 2022).

Following the calculation of mRNA levels, a threshold for biological relevance was established, defining a fold change of 1.5 as a relevant upregulation or a fold change of 0.5 as downregulation of the target genes, including also small fold changes. However, applying the same threshold for different genes implies that these genes are equally sensitive to changes in the dosage of their transcripts. Nonetheless, some genes may be generally transcribed at higher levels, and thus, upregulation must be much more severe to be biologically relevant than upregulation of a gene that has a low basal expression. This demonstrates that this application in question is context-specific, and that no overarching rule can be established that would facilitate a coherent interpretation of the data. Furthermore, the application of a threshold and a statistical analysis that are independent of one another results in the identification of fold changes below the threshold that have significant p-values. It is therefore inadvisable to attach undue significance to the statistical analyses.

In summary, real-time RT-PCR is an appropriate method for the examination of alterations in mRNA levels of *P2RX4*, *P2RX7*, *IL1B*, *IL10*, *IL18*, *IL6*, and *TNF* in THP-1 cells and hPBMCs. However, mRNA levels do not provide insight into the number of mRNA molecules that will be translated into protein. Additionally, intracellular protein levels of pro-IL-1β do not offer information about the NLRP3-mediated processing rate and release rate. It is possible that IL-1β may be influenced by a number of yet unknown factors. Nevertheless, the combination of real-time RT-PCR, Western blotting, and ELISA provides a comprehensive overview of the induction and processing of IL-1β upon priming with LPS and stimulation with BzATP, ATP, or nigericin.

2.6 THE P2RX4 AND P2RX7 ANTAGONISTS

The function of P2RX7 in the formation and activation of the NRLP3 inflammasome is well documented. However, some studies have also indicated a potential role for P2RX4 in this process (Kanellopoulos et al. 2021, Pelegrin 2021). P2RX4 and P2RX7 antagonists are employed in several experimental settings to elucidate the function of both receptors in the priming and the ATP-dependent IL-1β release by mononuclear phagocytes. The P2RX4 antagonist 5-B (Fischer R. et al. 12.03.2004) is a commercially available lipophilic benzodiazepine derivative that has been employed in numerous studies to target P2RX4. The half maximal inhibitory concentration (IC_{50}) has been observed to vary between 0.3 µM (Abdelrahman et al. 2017), 1.2 µM (Balázs et al. 2013), and 5.2 µM (Sophocleous et al. 2020), depending on the assays and cells used. Preliminary experiments of a dose-response curve indicate a modulatory effect on IL-1β release at 10 µM in monocytic THP-1 cells (Ettischer L.

unpublished). Furthermore, 5-B was also subjected to testing for bacterial endotoxins and pyrogens and was deemed to be free of any contamination (Ettischer L. unpublished). While 5-B is devoid of activity at other P2 receptors, the potential for off-target interactions remains unknown (Fischer R. et al. 12.03.2004, Abdelrahman et al. 2017, Coddou et al. 2019). The P2RX4 antagonist PSB is provided by Prof. Müller and has yet to undergo comprehensive characterisation. The addition of 10 µM PSB result in the complete inhibition of ATP-induced currents mediated by human P2RX4 stably expressed in *Xenopus laevis* oocytes (Schneider et al. 2017) or by endogenous P2RX4 in murine microglial cells (Trang et al. 2020). No published information is currently available regarding the other P2RX4 antagonists PZB15 and PZB13, which are also provided by Prof. Müller.

The commercially available A43 is a competitive P2RX7 antagonist (IC_{50} < 10 µM) with no known activity at other P2 receptors. Preliminary experiments conducted on monocytic THP-1 cells indicate that the compound exhibits a stable inhibitory effect on IL-1β release at a concentration of 10 µM (Ettischer L. unpublished). JNJ is another well-described competitive P2RX7 antagonist. The IC_{50} value has been determined to range from 2 to 3 µM in human blood and hPBMCs (Bhattacharya et al. 2013). Furthermore, a dose-response experiment conducted during this study reveals a potent inhibitory effect at 1 µM (**Figure S-1**). Selectivity tested with a panel of 50 other receptors, ion channels, and transporters demonstrates a high degree of selectivity for P2RX7 (Bhattacharya et al. 2013). The administration of JNJ successfully attenuates IL-1β release and BzATP-induced currents in human monocytes and microglial cells (Bhattacharya et al. 2013).

In conclusion, although the precise mode of action and specificity of each P2RX4 antagonist remains unclear, the utilisation of four distinct antagonists and a direct comparison with well-established P2RX7 antagonists provides a robust basis for investigating the role of P2RX4 in the expression and release of IL-1β by mononuclear phagocytes.

3 THE ROLES OF P2RX4 AND P2RX7 IN THE IL-1β RELEASE BY MONONUCLEAR PHAGOCYTES

The ionotropic P2RX7 was identified as the receptor mediating the effect of extracellular ATP on IL-1β release from macrophages almost three decades ago (Ferrari et al. 1996, Ferrari et al. 1997). Over the past decade, research has begun to demonstrate that IL-1β secretion is also affected by P2RX4 stimulation (Chen et al. 2013, Sakaki et al. 2013, Li et al. 2014, Han et al. 2020). The objective of this study is to clarify if both receptors also mediate IL-1β release by primed human mononuclear phagocytes, which have not been investigated so far. Consequently, monocytic THP-1 cells, hPBMCs, THP-1 cell-derived M1-like macrophages,

and hPMs are primed with LPS, followed by stimulation with BzATP or ATP in the presence of each P2X receptor antagonist.

As anticipated, the P2RX7 antagonists A43 and JNJ exert substantial inhibitory effects on the ATP- or BzATP-induced IL-1β release from monocytic THP-1 cells (**Figure 9**), hPBMCs (**Figure 11**), THP-1 cell-derived M1-like macrophages (**Figure 10**), and hPMs (**Figure 12**), respectively. As previously described, A43 inhibits IL-1β release by murine microglial cells (Clark et al. 2010) and most importantly by THP-1 cells (Nelson et al. 2006) and hPBMCs (Ward et al. 2010). The release of IL-1β from hPBMCs is effectively suppressed by the administration of JNJ (Bhattacharya et al. 2013). The two antagonists compete with BzATP or ATP for the binding site at the P2RX7. Upon binding of the antagonists to P2RX7, ATP is unable to induce the requisite conformational changes for pore opening. In the absence of K^+ efflux, NLRP3 does not assemble and the pro-IL-1β produced in response to priming with LPS is not processed. Consequently, the cells do not release IL-1β. The notion that A43 and JNJ exert their inhibiting function at an ATP receptor is corroborated by the observation that ATP-independent nigericin-induced IL-1β release from monocytic THP-1 cells (**Figure 13**) and THP-1 macrophages (**Figure 14**) is not considerably altered upon application of the P2RX7 antagonists. It is noteworthy that apyrase is added in these experiments to ensure that the nigericin-induced release of IL-1β is independent of ATP. The results presented here confirm that P2RX7 mediates ATP-induced IL-1β release from monocytic THP-1 cells, hPBMCs, THP-1 cell-derived M1-like macrophages, and hPMs.

Several P2RX4 antagonists are used to investigate if the P2RX4 participates in the ATP-/BzATP-mediated release of IL-1β. The BzATP-mediated IL-1β release from monocytic THP-1 cells is slightly attenuated by treatment with 5-B, strongly inhibited by PSB, and fully inhibited by treatment with PZB15 or PZB13 (**Figure 9**). In hPBMCs, 5-B has a more pronounced inhibitory effect on IL-1β release compared to monocytic THP-1 cells. In contrast, PSB and PZB15 effectively abrogate the IL-1β release, whereas PZB13 exhibits minimal efficacy (**Figure 11**). The release of IL-1β from monocytic THP-1 cells is not significantly affected by the application of P2RX4 antagonists immediately prior to the addition of nigericin as a stimulus for release (**Figure 13**). The clear reducing effect of P2RX4 antagonists on the ATP-mediated IL-1β release from monocytic cells is less pronounced in THP-1 cell-derived M1-like macrophages (**Figure 10**). The weak inhibitory effects observed following treatment with 5-B prior to stimulation with ATP are also evident in hPMs (**Figure 12**). While the effects of the individual P2RX4 antagonists differ from one another and are, in general, not particularly efficacious in macrophages, they do nonetheless inhibit IL-1β release. It is noteworthy that the addition of 5-B or PZB15 prior to stimulation with nigericin also inhibits the IL-1β release from THP-1 cell-derived M1-like macrophages (**Figure 14**). The current results remain inconclusive, but they suggest that these P2RX4 antagonists may exert off-target effects.

Nonetheless, the findings strongly suggest that the P2RX4 plays a role in the ATP-dependent IL-1β secretion by mononuclear phagocytes. This conclusion is supported by several studies. The P2RX4 antagonist TNP-ATP, an ATP derivative that binds to the ATP binding pocket of P2RX4, inhibits ATP-dependent IL-1β release from bone marrow-derived dendritic cells (Sakaki et al. 2013). The inhibitory effects of P2RX4 silencing on IL-1β release have been demonstrated in murine models for experimental rheumatoid arthritis and diabetic nephropathy (Chen et al. 2013, Li et al. 2014). P2RX4-deficient mice that have undergone renal ischemia and reperfusion injury also exhibit reduced IL-1β processing (Han et al. 2020). Moreover, treatment of wild-type mice with 5-B exerts a protective effect against ischemic acute kidney injury, which is presumably associated with the attenuation of NLRP3 assembly, caspase-1 induction and IL-1β release (Han et al. 2020). Treatment with 5-B attenuates high glucose-induced cleavage of IL-1β but also mitigates NLRP3 expression and cleavage of caspase-1 in a cell line derived from human kidney (Chen et al. 2013). However, alterations in NLRP3 expression and assembly and associated activity of caspase-1 indicate that treatment with 5-B influences the priming step rather than the ATP-dependent IL-1β secretion. These studies do not show whether P2RX4 plays a role in P2RX7-dependent signalling or whether it may independently activate IL-1β release. However, here, both P2RX4 antagonists and P2RX7 antagonists almost completely inhibit the IL-1β secretion indicating that both receptors are essential and presumably interact with each other via unknown mechanisms. Several studies have reported functional interactions between both receptors, yet the data situation remains ambiguous, and no conclusions can be drawn at the moment (Kawano et al. 2012, Sakaki et al. 2013, Zech et al. 2016).

Moreover, monocytic cells appear to be more responsive to P2RX4 modulation than macrophages, which may be attributed to discrepancies in the mRNA expression levels of P2RX4 and P2RX7. While THP-1 cell-derived M1-like macrophages show no differences in mRNA expression levels of both receptors, monocytic THP-1 cells and hPBMCs express substantially greater quantities of *P2RX4* than *P2RX7* mRNA. It is noteworthy that 5-B and PZB15 also inhibit nigericin-mediated IL-1β secretion by THP-1 macrophages, indicating that these substances influence IL-1β release from macrophages independently of ATP signalling via a yet unknown mechanism.

4 THE ROLE OF P2RX4 AND P2RX7 IN PRIMING MONOCYTIC CELLS

4.1 CHANGES IN THE IL-1β RELEASE

The preceding findings establish and confirm a correlation between P2RX4, P2RX7, and ATP-mediated IL-1β secretion by mononuclear phagocytes. Nevertheless, the function of both receptors in the priming phase of mononuclear phagocytes has yet to be elucidated. The objective of this study is also to investigate the role of P2RX4 and P2RX7 in the priming of human mononuclear phagocytes and the activation of NLRP3 assembly. Consequently, monocytic cells are stimulated with LPS in the presence of each P2X receptor antagonist, followed by stimulation with BzATP or nigericin.

When administered prior to the application of LPS, the P2RX4 antagonists PSB, PZB15, and PZB13 inhibit the BzATP-induced release of IL-1β from monocytic THP-1 cells, although not to the same extent as the P2RX7 antagonists A43 and JNJ, which completely abrogate the release (**Figure 9**). Conversely, the addition of 5-B significantly enhances the release of IL-1β. Previously mentioned findings by L. Ettischer confirm that the 5-B solution is free of bacterial endotoxins and pyrogens. It is of importance for the interpretation of these data that the antagonists are not washed out before the second stimulus is added. Therefore, the antagonists, depending on their stability in cell culture, may act on both, the cell priming and on the stimulation with ATP or BzATP.

Therefore, the nigericin-induced NLRP3 assembly and IL-1β processing may be a more suitable method for investigating the role of P2RX4 and P2RX7 in cell priming, because nigericin acts as an ionophore, mediating K^+ efflux independently of ATP. The cells are primed with LPS in the presence of each antagonist, followed by stimulation with nigericin. The increase in IL-1β release observed in response to 5-B is also evident in monocytic THP-1 cells (**Figure 13**). Furthermore, PZB13 increases the release, while PZB15 reduces the nigericin-induced IL-1β release and PSB has no effect. The release of IL-1β from monocytic THP-1 cells is modestly enhanced when the P2RX7 antagonist JNJ is applied prior to priming, whereas A43 does not induce any alterations (**Figure 13**).

Furthermore, the effects of priming can be distinguished from the ATP-mediated IL-1β release by removing the antagonists prior to the administration of the second stimulus. Monocytes are isolated from hPBMCs via adherence selection 20 min prior to the addition of BzATP or nigericin. At this step, the medium is replaced, which considerably dilutes the previously added substances. This allows for an isolated evaluation of the effect of 5-B on priming and stimulation with BzATP or nigericin in hPBMCs (**Figure 11**). When NLRP3 assembly and activation is triggered by nigericin, the addition of 5-B and PZB13 before priming with LPS enhances the IL-1β release from hPBMCs, thereby confirming the observations made in

monocytic THP-1 cells (**Figure 15**). The impact of PZB13 may only be apparent when nigericin prompts the secretion of IL-1β, as the inhibitory effect on BzATP-signalling may coincide with the PZB13-mediated increase during priming (**Figure 9**, **Figure 11**). If PZB13 is a potent inhibitor of the P2RX4, the residual concentration following medium exchange may still be sufficient to influence the BzATP-induced IL-1β secretion from hPBMCs (**Figure 11**). A concentration-effect curve needs to be established in future experiments to clarify this aspect.

The above described findings suggest that 5-B amplifies the priming effect in monocytic cells. As observed, the effects of PZB13 exhibit a comparable trend; nevertheless, when administered prior to priming, only the nigericin-induced release of IL-1β demonstrates an elevation in levels. This prompts the question of whether the gene expression of *P2RX4, P2RX7*, or *IL1B* is influenced by these P2RX4 antagonists.

Nonetheless, it is similarly conceivable that alterations in the ATP-independent IL-1β release may derive from the abundance and assembly of NLRP3 inflammasomes, which can be affected in ways that either augment caspase-1 activity and the turnover of pro-IL-1β or diminish processing and release of IL-1β. For instance, NLRP3 is subject to ubiquitination by a number of ubiquitin ligases, which impede the assembly of the inflammasome and induce proteasomal degradation (Kelley et al. 2019). Conversely, a number of deubiquitinases have been identified that positively regulate the assembly of the NLRP3 inflammasome. However, the most prominent regulatory mechanism is the abundance and activity of NLRP3-interacting proteins that are required for complex formation (reviewed in Kelley et al. 2019). For example, the NEK7 protein has been demonstrated to promote oligomerisation, ASC speck formation and caspase-1 activation downstream of the P2RX7-mediated K^+ efflux (He et al. 2016, Schmid-Burgk et al. 2016, Shi et al. 2016). Given the established link between P2RX7 and NEK7 activity, it is plausible that P2RX4 may also play a role in this process. The detection of ASC speck formation in response to stimulation with P2X receptor antagonists may offer insights into the rate of NLRP3 assembly and potentially elucidate the enhanced or diminished nigericin-induced IL-1β secretion by the P2RX4 antagonists, if *IL1B* mRNA levels do not provide sufficient explanation.

4.2 mRNA LEVELS OF *P2RX4* AND *P2RX7*

It is plausible that alterations in the mRNA levels of the *P2RX4* and *P2RX7* could elucidate the mechanisms underlying the effects of P2RX4 antagonists, such as 5-B and PZB13. Consequently, cells that have not undergone any treatment, cells that have been primed with LPS, and cells that have been stimulated with P2X receptor antagonists prior to priming are harvested for real-time RT-PCR after a period of 3 h or 5 h.

No alterations in *P2RX4* expression levels are observed in monocytic THP-1 cells (**Figure 24A**) or hPBMCs (**Figure 26A**) following any treatment. The P2RX4 antagonists PSB, PZB15, and PZB13 induce a slight upregulation of *P2RX7* in monocytic THP-1 cells (**Figure 24B**), while only PZB13 does so in hPBMCs (**Figure 26B**). The levels of *P2RX4* and *P2RX7* mRNA in untreated monocytic THP-1 cells and hPBMCs are similar. Although a study has suggested that P2RX4 or P2RX7 knockdown increases the expression of the other receptor due to compensatory mechanisms (Weinhold et al. 2010), other data are contrary to this hypothesis (Craigie et al. 2013, Zech et al. 2016, Sierra-Marquez et al. 2024). Therefore, and given the absence of significant alterations, it seems unlikely that a transient modulation of P2RX4 increases *P2RX7* expression as a result of compensatory mechanisms. It is noteworthy that untreated monocytic THP-1 cells and hPBMCs express 164-fold and 57-fold more *P2RX4* than *P2RX7* mRNA, respectively. These results, however, do not explain the impact of 5-B and PZB13 on the priming of monocytic cells.

4.3 mRNA LEVELS OF *IL1B*

It is possible that the differences in *IL1B* mRNA levels may be responsible for the altered IL-1β release by monocytic cells. Consequently, monocytic cells treated with P2RX4 or P2RX7 antagonists prior to priming with LPS are harvested for the measurement of *IL1B* mRNA levels via real-time RT-PCR after 3 or 5 h of incubation.

5-B increases *IL1B* mRNA in monocytic THP-1 cells, which aligns with the results of the cytokine release experiments. In contrast, PZB13 and the other antagonists do not induce alterations in this regard (**Figure 27A**). It is notable that the effect of 5-B cannot be confirmed in hPBMCs (**Figure 30A**). In LPS-primed monocytic THP-1 cells, *IL1B* mRNA reaches its peak levels at 1.5 h and then declines rapidly after 2.5 h (Ettischer L. unpublished). The additional application of 5-B prior to LPS results in a shift in the peak levels, which are now observed at 2.5–3 h. This indicates that stimulation with 5-B shifts the maximum *IL1B* mRNA amounts to a later time point (Ettischer L. unpublished). The stimulation of human blood monocytes with LPS has been demonstrated to induce *IL1B* expression within 15 min, with peak levels occurring at 4 h (Fenton et al. 1988, Dinarello 2018). It is possible that the time course for hPBMCs is similar to that of human blood monocytes. This would indicate that *IL1B* mRNA levels upon stimulation with 5-B for 3 h are still on the rise and are measured too early. The examination of a time response curve for hPBMCs may prove beneficial in clarifying this assumption. Nevertheless, the impact of 5-B on IL-1β secretion by monocytic THP-1 cells observed in cytokine release experiments may be attributed to its ability to modulate priming, thereby enhancing *IL1B* mRNA expression during 5 h of incubation. However, it remains unclear whether treatment with 5-B prior to priming affects *IL1B* transcription at the level of transcription initiation by directly modulating LPS signalling or by activating an additional, yet

unknown pathway that induces transcription, or whether 5-B enhances the stability of *IL1B* mRNA in monocytic THP-1 cells.

A limited number of studies has been conducted to investigate the enhancement of LPS signalling and subsequent elevated *IL1B* transcription. Notably, there is a complete absence of studies addressing the role of P2RX4 in this context. Consequently, it is challenging to align these findings with the existing literature. Nevertheless, previously mentioned investigations conducted by Han and colleagues or by Chen and colleagues show attenuated NLRP3 expression and assembly upon treatment with 5-B, which the authors, however, only linked to the role of P2RX4 in IL-1β secretion. In addition, there is again the problem with the unknown specificity of 5-B. Nevertheless, several unrelated mechanisms enhancing LPS-induced priming have been described. Stimulation with LPS also induces the expression of prostaglandin-E2, which binds to monocytes via its respective receptor, thereby promoting LPS-induced *IL1B* mRNA expression by activating a TF that drives *IL1B* transcription (Gray et al. 1993, Chandra et al. 1995, Zasłona et al. 2017). It is likely that this endogenous positive feedback loop serves to promote host defence during infection. Additionally, priming of the TLR3 through viral compounds enhances LPS-TLR4 signalling in endothelial cells, which is thought to occur via the upregulation of TLR4 (Koch et al. 2017). This finding is at odds with observations made in macrophages (Sato et al. 2002), which may be attributed to the differential expression of TLRs in leukocytes and endothelial cell subpopulations (Muzio et al. 2000). The cytokine IL-27 enhances LPS-induced IL-1β release from monocytes and macrophages (Petes et al. 2017). However, Petes and colleagues measured increased pro-IL-1β protein levels but did not assess alterations in mRNA levels. Further studies are required to elucidate the impact of simultaneous stimulation with 5-B and LPS on *IL1B* mRNA levels.

5 THE ROLE OF P2RX4 AND P2RX7 IN PRIMING MACROPHAGES

5.1 CHANGES IN THE IL-1β RELEASE

Furthermore, the role of the P2RX4 and the P2RX7 in priming is investigated in THP-1 cell-derived M1-like macrophages and hPMs, with the goal of comparing monocytic cells and macrophages. Macrophages are stimulated with LPS in the presence or absence of each P2X receptor antagonist, followed by stimulation with BzATP/ATP or nigericin.

The release of IL-1β from THP-1 cell-derived M1-like macrophages is reduced by treatment with P2RX4 antagonists and P2RX7 antagonists prior to priming with LPS (**Figure 10**). The inhibitory effects of 5-B and A43 are confirmed in hPMs (**Figure 12**). As the antagonists may be still present at the time of ATP application, ATP-independent IL-1β provides further insights into the effects on priming. In THP-1 macrophages, treatment with 5-B prior to priming has no

effect, while PSB, PZB15, and PZB13 unexpectedly reduce the nigericin-induced IL-1β release (**Figure 14**). Thus, the inhibitory effect of PZB15 on nigericin-induced IL-1β secretion by monocytic THP-1 cells is confirmed in THP-1 macrophages but is not observed in hPBMCs. Conversely, the P2RX4 antagonists PSB and PZB13 exert an attenuating effect on IL-1β secretion by THP-1 macrophages. Moreover, the pro-inflammatory effect of 5-B in monocytic cells is absent in macrophages, indicating that monocytic cells and macrophages respond differently to treatment with P2RX4 antagonists.

5.2 INTRACELLULAR PRO-IL-1β PROTEIN LEVELS

Another objective of this investigation is to ascertain whether the effects of the P2RX4 antagonists can be attributed to alterations in protein levels or to modulation of the releasing step that is independent of ATP. Consequently, THP-1 cell-derived M1-like macrophages are treated with P2RX4 antagonists, in addition to the P2RX7 antagonist A43, prior to being primed with LPS.

As observed in previous studies (reviewed in Dinarello 2018), priming with LPS induces the expression of pro-IL-1β (**Figure 19A**). Pro-IL-1β is a 31 kDa-sized protein that contains a conserved N-terminus, which prevents the final folding of the protein and thereby blocks its function (Hazuda et al. 1990, Hailey et al. 2009). This N-terminal region maintains the protein in a protease-sensitive state, which results in rapid processing upon activation of caspase-1. The remaining C-terminus is only 17 kDa in size and is capable of folding into the final active structure (Hailey et al. 2009). Given the accumulation of pro-IL-1β upon cell priming and its rapid release following maturation, commonly only the precursor form of IL-1β is detected intracellularly upon stimulation with LPS. The estimation of protein levels indicates that treatment with 5-B tends to increase pro-IL-1β, which is contrary to the cytokine release experiments (**Figure 19C**). Nevertheless, the observed increase is not statistically significant, does not exceed 1.5 AU and beyond that, the data exhibit a considerable variation. Moreover, treatment with 5-B prior to priming does not result in an increase in nigericin-induced IL-1β secretion, yet the data also exhibit considerable variation (**Figure 14**). Treatment with the other P2RX4 antagonists PSB, PZB15, and PZB13 result in a decrease in pro-IL-1β levels. Treatment with the P2RX7 antagonist A43 does not alter protein levels (**Figure 19C**), which coincide with protein levels of released IL-1β. These results lead to the assumption that the altered IL-1β release induced by nigericin upon stimulation with P2RX4 antagonists prior to priming is attributed to altered protein levels of pro-IL-1β. These alterations may be initiated at the level of gene expression for *IL1B*, or alternatively, by modulating the stability of *IL1B* mRNA or pro-IL-1β protein.

A number of mechanisms, some of which may be modulated by stimulation with P2RX4 antagonists during priming, can alter the stability of pro-IL-1β. One potential modification is the

ubiquitination of the precursor, which plays an important role in regulating IL-1β production. As a result of this modification, pro-IL-1β is no longer accessible to cleavage by caspase-1 and is instead rapidly degraded by proteasomes (Zhang et al. 2018, Vijayaraj et al. 2021, Mishra et al. 2023). The enhanced ubiquitylation and proteasomal targeting by administration of ATP or nigericin indicates that these NLRP3 activators can activate parallel pathways leading to pro-IL-1β degradation (Vijayaraj et al. 2021). Moreover, the NF-κB inhibitor and ubiquitin-modifying enzyme A20 regulates this process by suppressing pro-IL-1β ubiquitylation (Duong et al. 2015). If ATP activates pro-IL-1β degradation, potentially via P2X receptors, a similar mechanism may be initiated by the P2RX4 antagonists used in this investigation. Nevertheless, future studies should assess the ubiquitination rate of pro-IL-1β upon stimulation with PSB, PZB15, or PZB13 in combination with LPS before any conclusions can be drawn.

5.3 mRNA LEVELS OF *P2RX4* AND *P2RX7*

Prior to drawing conclusions regarding the mode of action of distinct P2RX4 antagonists, it is essential to investigate whether there have been any alterations in the levels of *P2RX4* and *P2RX7* mRNA. Therefore, untreated cells, cells that have been primed with LPS, and cells that have been stimulated with P2X receptor antagonists prior to priming are harvested after 5 h incubation for measuring *P2RX4* and *P2RX7* mRNA levels via real-time RT-PCR.

The expression levels of *P2RX4* and *P2RX7* are not altered to a relevant extend upon any treatment in THP-1 cell-derived M1-like macrophages (**Figure 25**). A comparison of the mRNA levels reveals that THP-1 macrophages express *P2RX4* and *P2RX7* at equal amounts, in contrast to monocytic cells, which exhibit a higher expression of *P2RX4* mRNA. This may provide an explanation for the observation that monocytic cells appear to be more susceptible to treatment with P2RX4 antagonists than macrophages in different experimental settings. It is important to note that mRNA levels do not necessarily correlate with protein amounts and therefore do not imply a corresponding difference in protein amounts.

5.4 mRNA LEVELS OF *IL1B*

To further investigate the inhibitory effects of PSB, PZB15, and PZB13 on the ATP-independent IL-1β secretion by THP-1 cell-derived M1-like macrophages, the expression of *IL1B* mRNA was also examined.

In THP-1 cell-derived M1-like macrophages, *IL1B* mRNA levels remain unaltered upon stimulation with LPS and P2X receptor antagonists (**Figure 28A**). The reduction in pro-IL-1β protein levels and subsequent decrease in ATP-independent IL-1β release observed following incubation with PSB, PZB15, or PZB13 does not seem to be a consequence of altered *IL1B* mRNA amounts. However, as discussed before, it cannot be excluded that relevant changes might be visible at other time points. It seems plausible to suggest that the presence of the

P2RX4 antagonists modulates the abundance of pro-IL-1β protein. The lack of alteration in *IL1B* mRNA levels following treatment with 5-B is consistent with the amounts of released IL-1β, indicating that the slight increase in pro-IL-1β levels is inconsequential. Moreover, the lack of the potentiating impact of 5-B in macrophages indicates that monocytic cells and macrophages respond differently to treatment with this P2RX4 antagonist. This could be attributed to the disparate mRNA ratios of P2RX4 and P2RX7. However, the selectivity of 5-B is a subject of debate and, thus far, has only been evaluated for other P2X receptors, rendering it unclear whether its effect is mediated by P2RX4 (Fischer R. et al. 12.03.2004, Abdelrahman et al. 2017, Coddou et al. 2019).

6 FIRST STEPS TO REVEAL THE MODE OF ACTION OF 5-B

6.1 IL-1β RELEASE AFTER COMBINING 5-B WITH OTHER ANTAGONISTS

5-B is described as a P2RX4 antagonist and has been used in a number of studies to investigate P2RX4 signalling (Casati et al. 2011, Balázs et al. 2013, Chen et al. 2013, Abdelrahman et al. 2017, Coddou et al. 2019, Han et al. 2020, Bidula et al. 2022). However, the degree of selectivity has not been comprehensively determined. The majority of studies focused on elucidating the physiological role of P2RX4, or on investigating the binding properties of 5-B at the P2RX4. It is therefore possible that 5-B may exert off-target effects. To investigate whether the 5-B-induced increase in IL-1β secretion by monocytic cells is mediated via the P2RX4, treatment with 5-B prior to priming is combined with a concomitant application of the other antagonists. As PZB13 also induced the release of elevated levels of IL-1β by monocytic cells, PZB13 is also combined with the other antagonists.

The elevated IL-1β levels resulting from the presence of 5-B during priming are mitigated by the concurrent administration of the P2RX4 antagonists PSB, PZB15, or PZB13 in hPBMCs, in which IL-1β release is triggered by stimulation with BzATP (**Figure 16A**). In this experimental setting, the residual P2RX4 antagonists may still exert an inhibitory effect on the second stimulus. Consequently, further experiments are performed in monocytic THP-1 cells using nigericin as a second stimulus, yielding similar results (**Figure 17A**). Similar experiments on hPBMCs give inconclusive results with a high degree of variability (**Figure 18**). The observed variability in the data may be attributed to inter-donor differences in cell numbers, purity, and responsiveness to the applied substances. It is also possible that the concentrations of the competing antagonists are not within the optimal range. Despite these limitations, these observations suggest that during priming, 5-B signals via P2RX4, as other selective P2RX4 antagonists can disrupt the effects of 5-B in the majority of the experiments.

Although the selectivity of 5-B is unclear, several studies have investigated the binding site of 5-B at the P2RX4. The observation that 5-B induces a rightward shift of the ATP concentration response curve without altering the maximal altitude in electrophysiological measurements suggests, that 5-B competitively inhibits P2RX4 and binds to the orthosteric binding site (Balázs et al. 2013, Coddou et al. 2019). It is noteworthy that the aforementioned studies utilise HEK293 cells that have been transfected with P2RX4. In contrast, studies that suggest allosteric binding of 5-B employ a cell line that endogenously expresses P2 receptors. This discrepancy may account for the disparate outcomes observed (Bidula et al. 2022). The ATP derivative TNP-ATP competes with radioactive ATP for its binding site at the P2RX4, demonstrating competitive binding properties. Conversely, 5-B does not replace the ligand, indicating that the antagonist binds at a different site (Abdelrahman et al. 2017). The hypothesis that 5-B acts as an allosteric modulator of P2RX4 is further supported by the fact that the predicted 5-B binding site is located between two subunits at an allosteric site of the human P2RX4, while orthosteric binding is less favourable (Bidula et al. 2022, Pasqualetto et al. 2023). Two residues of the predicted 5-B binding site are likely to be involved in the opening of the P2RX4 channel (Bidula et al. 2022). Interactions with 5-B and specific residues may therefore serve to stabilise the closed conformation, thereby inhibiting the channel opening upon ATP binding (Bidula et al. 2022). Two residues that are predicted to be necessary for 5-B binding also appear to be part of the binding site of BX430, another allosteric P2RX4 antagonist (Ase et al. 2015, Ase et al. 2019, Pasqualetto et al. 2023). Nevertheless, an analysis of diverse P2RX4 allosteric modulators indicates that distinct interactions within the binding pocket are specific to each antagonist, depending on their structure (Pasqualetto et al. 2023, Shen et al. 2023). It might be of interest to investigate the effects of BX340 in future studies. It is unfortunate that no information on the binding properties of the P2RX4 antagonists PSB, PZB15, and PZB13 is available.

Because PZB13 also enhances the effect of priming in monocytic THP-1 cells (**Figure 13**) and in hPBMCs (**Figure 15**), PZB13 is also combined with other P2RX4 antagonists. In this experiment, however, PZB13 does not consistently increase the priming effect (**Figure 17C, D**). Therefore, it remains unclear whether PZB13 exerts its effects via the P2RX4. It can only be stated that the effect of PZB13 on cell priming is not sufficiently robust to allow a conclusion to be drawn.

Furthermore, two additional control experiments are included. First, it is investigated whether the sensitivity to P2X receptor antagonists remains unchanged in cells primed in the presence of 5-B. Indeed, the addition of P2X receptor antagonists results in a reduction of IL-1β release from hPBMCs when they are added prior to BzATP. This result is most likely attributable to the blocking of BzATP-induced signalling, thereby allowing the conclusion that the presence of 5-B during priming has no relevant effect on the sensitivity of the cells towards BzATP (**Figure**

16B). The second question that arises is whether the P2X receptor antagonists affect the ATP-independent inflammasome assembly, IL-1β maturation or its release. Consequently, cells primed in the presence of 5-B are treated with P2X receptor antagonists shortly before stimulation with nigericin. As anticipated, the majority of antagonists do not impede the ATP-independent release of IL-1β (**Figure 17B**). PSB is the only antagonist to reduce the nigericin-induced IL-1β secretion by monocytic THP-1 cells, suggesting that PSB exerts some off-target effects that influence the machinery necessary for the maturation and release of IL-1β.

Taken together, the results of the experiments in which different P2X receptor antagonists are combined during priming demonstrate that the 5-B-induced increase in IL-1β release is mediated via the P2RX4. However, these results do not elucidate the mechanisms by which P2RX4 signalling modulates priming.

6.2 IS THE EFFECT OF 5-B CONFINED TO IL-1β?

6.2.1 CHANGES IN THE IL-6 RELEASE AND *IL6* MRNA LEVELS

The activation of mononuclear phagocytes with LPS also induces the expression of the pro-inflammatory cytokine IL-6, the release of which is independent of any inflammasomes. To ascertain the potential impact of P2RX4 antagonists on priming with LPS, the expression of *IL6* mRNA and the release of IL-6 are examined. Monocytic THP-1 cells, hPBMCs, and THP-1 cell-derived M1-like macrophages are treated with P2X receptor antagonists prior to priming with LPS. After 3 or 5 h incubation, supernatants are collected for ELISA, and cells are harvested for real-time RT-PCR experiments.

LPS induces an immediate and transient expression, which is directly followed by IL-6 release (Hirano 2021). Consequently, modulation of the process upstream of transcription, the stability of *IL6* mRNA, or secretion is a possibility. 5-B at 20 µM reduces and PZB15 tendentially reduces IL-6 release from monocytic THP-1 cells, while the other P2RX4 antagonists do not alter release (**Figure 20**). The P2RX7 antagonist A43 elicits a slight increase in IL-6 release, though this is only evident at the 20 µM concentration. The *IL6* mRNA levels are not affected by treatment with any P2X receptor antagonist in monocytic THP-1 cells (**Figure 27B**). The unaltered *IL6* mRNA and IL-6 protein amounts suggest that P2X receptors do not exert any notable influence on IL-6 expression and release in monocytic THP-1 cells. By contrast, in hPBMCs, 5-B and A43 increase IL-6 release, while A43 induces only slight alterations (**Figure 22**). It is noteworthy that all P2RX4 antagonists upregulate *IL6* mRNA in hPBMCs, whereas P2RX7 antagonists induce no such changes (**Figure 30C**).

LPS-primed THP-1 cell derived M1 like macrophages reduce IL 6 release after treatment with 5-B and when 5-B is simultaneously applied with PSB (**Figure 21**). The P2RX7 antagonist A43 slightly but significantly decreases IL 6 release. The altered release upon stimulation with 5-B

and PSB is consistent with the observed reduction in *IL6* mRNA levels following treatment with any P2RX4 antagonist (**Figure 29A**). However, A43 does not induce alterations in *IL6* mRNA levels, which is not inconsistent with the corresponding minor decrease in IL-6 secretion by macrophages.

A comparison of the total amount of IL-6 released upon priming with LPS reveals that THP-1 macrophages (median 2671 pg/ml) release significantly higher levels of IL-6 than monocytic THP-1 cells (34 pg/ml) or hPBMCs (121 pg/ml). A comparison of *IL6* mRNA levels also demonstrates that hPBMCs express 1775-fold more and THP-1 macrophages 1149-fold more *IL6* mRNA than monocytic THP-1 cells. It can thus be concluded that monocytic THP-1 cells are less appropriate for investigating the effects on IL-6 production. However, a comparison of hPBMCs and THP-1 cell-derived M1-like macrophages suggests that there may be a differential response of monocytes and macrophages to P2RX4 antagonists during priming. Specifically, monocytic cells appear to upregulate IL-6 mRNA, while macrophages downregulate IL-6 and subsequently secrete less IL-6 protein.

A number of studies have established a link between P2RX4, P2RX7, and IL-6 upregulation and release. P2RX4-deficient mice display a reduction in IL-6 levels in serum and liver tissue following the induction of experimental autoimmune hepatitis (Liu et al. 2024). Conversely, the overexpression of P2RX4 in the CNS of rats with experimental Parkinson's disease upregulates IL-6 expression (Ma et al. 2020). A reduction in serum IL-6 levels has been observed in rats with diarrhoea-predominant irritable bowel syndrome following treatment with 5-B (Tang et al. 2022). Moreover, treatment with 5-B mitigates surgical-induced hippocampal inflammation in murine models (Yuan et al. 2022). As previously described, during the inflammatory process, the concentration of extracellular ATP can increase significantly and stimulate various P2X receptors. In light of the aforementioned studies, it can be postulated that ATP-signalling via the P2RX4 has the potential to augment IL-6 levels. This is in accordance with the observation that in ATP-stimulated microglial cells, increased expression of *IL6* mRNA is attenuated by treatment with a different P2RX4 antagonist (Imraish et al. 2023). In the case of P2RX7, stimulation has been observed to result in the secretion of IL-6 from neurons, astrocytes, microglial cells, retinal cells, and pancreatic cancer cells, in a manner that is independent of NLRP3 (Solini et al. 1999, Shieh et al. 2014, Lu et al. 2017, Munoz et al. 2020, Shao et al. 2020, Magni et al. 2021). P2RX7 may induce IL-6 release by activating ROS production or by an increase in intracellular Ca^{2+} (Munoz et al. 2020, Shao et al. 2020). While these studies demonstrate that stimulation of the P2RX4 or P2RX7 with ATP induces secretion, no modulation of IL-6 production by other stimuli than ATP has been described. This is supported by the finding that 5-B exerts no influence on IL-6 release induced by high glucose in human cells derived from renal tissue (Chen et al. 2013).

It is conceivable that the observed inhibitory effects in macrophages are attributable to the blockade of endogenous extracellular ATP, which induces IL-6 expression, in addition to LPS. This may also account for the elevated levels of IL-6 released from THP-1 cell-derived M1-like macrophages. The additional application of apyrase would serve to abolish any ATP-mediated effects. This hypothesis is contradicted by the elevated IL-6 levels observed in hPBMCs and the 5-B-mediated increase in IL-6 secretion. The discrepancy in *P2RX4* and *P2RX7* mRNA levels previously observed in monocytic cells may contribute to an increased sensitivity to P2RX4 modulation. As only 5-B stably elevates *IL6* mRNA and IL-6 release, this further emphasises that 5-B promotes priming with LPS in monocytic cells and that this effect is not confined to IL-1β.

6.2.2 mRNA LEVELS OF OTHER CYTOKINES

Stimulation of the TLR4 also induces transcription of the pro-inflammatory *TNF* and the anti-inflammatory *IL10* (Dostert et al. 2019, Saraiva et al. 2020). The cytokine precursor of IL-18 is constitutively expressed in monocytes and macrophages and processed upon NLRP3 assembly in a manner analogous to pro-IL-1β (Yasuda et al. 2019). Modifications to the mRNA of *TNF* and *IL10* may offer further insight into the mechanisms by which 5-B influences priming. Consequently, mRNA levels are quantified through real-time RT-PCR assays in monocytic THP-1 cells, hPBMCs, and THP-1 cell-derived M1-like macrophages, which are treated with P2X receptor antagonists prior to priming with LPS for 3 or 5 h.

While treatment with P2X receptor antagonists does not induce considerable changes in *IL18* and *TNF* mRNA levels, *IL10* is markedly upregulated in monocytic THP-1 cells upon treatment with 5-B (**Figure 27B, C, E**). The upregulation of *IL10* is confirmed in hPBMCs and additionally observed following treatment with PZB13 (**Figure 30B**). In THP-1 cell-derived M1-like macrophages, there is no alteration in *IL10*, *IL18*, and *TNF* mRNA levels upon stimulation with LPS and P2X receptor antagonists (**Figure 28**, **Figure 29**). The absence of a 5-B-mediated effect in macrophages is consistent with previous findings of this study. The results demonstrate that stimulation with LPS induces the expression of *IL10*, which is in accordance with the existing literature(Saraiva et al. 2020). The anti-inflammatory cytokine IL-10 binds to its receptor and inhibits the production of several cytokines and chemokines via STAT3-signalling (Fiorentino et al. 1991, Waal Malefyt et al. 1991, Cassatella et al. 1993, Kasama et al. 1994, Balasingam et al. 1996). As demonstrated in macrophages, IL-10 functions as a counter-regulatory mechanism for inflammatory cytokines. Following the initial inflammatory burst, macrophages produce anti-inflammatory cytokines like IL-10, thereby dampening the inflammatory processes (Bogdan et al. 1991, Berlato et al. 2002). It can be hypothesised that the increased production of IL-1β upon stimulation with 5-B and LPS in monocytic cells may promotes IL-10 expression as a negative feedback. This finding is corroborated for stimulation with PZB13 in hPBMCs, but not for monocytic THP-1 cells. This may be because the PZB13-

induced increase in IL-1β secretion is more pronounced in hPBMCs than in monocytic THP-1 cells.

6.3 DOES THE INDUCTION OF APOPTOSIS PLAY A ROLE?

A study has shown that prolonged treatment with 5-B induces apoptosis in cancer cells (Rupert et al. 2023). It is therefore interesting to investigate the effect of 5-B on the activity of caspase-3 and 7, enzymes that play an important role in apoptosis. Monocytic THP-1 cells are stimulated with 5-B, PSB or PZB15 prior to priming with LPS and caspase-3 and -7 activity is measured. PSB and PZB15 are included to determine if the effect is limited to 5-B.

The results show that 5-B increases caspase-3/7 activity in the presence of LPS, whereas stimulation with 5-B alone or LPS alone does not induce activity (**Figure 31A**). Again, this appears to be a unique property of 5-B, as the other two P2RX4 antagonists do not induce caspase-3/7 activity (**Figure 31A**). These results suggest that 5-B induces apoptosis in LPS-primed monocytic THP-1 cells. This is consistent with a study showing 5-B-mediated induction of caspase-3/-7 activity and other apoptotic markers in renal cancer cells (Rupert et al. 2023). In cancer, lysosomes and mitochondria are essential energy providers in which lysosomal P2RX4 plays an important role by mediating Ca^{2+} influx upon luminal ATP binding (Huang et al. 2014, Rupert et al. 2023). The intracellular Ca^{2+} increase promotes mitochondrial metabolism, resistance to oxidative stress and necrosis, and drives motility and proliferation (Palinski et al. 2021, Rupert et al. 2023). Therefore, blockade of P2RX4 by 5-B leads to a reduction in mitochondrial activity and in cell death (Rupert et al. 2023). However, it is unclear whether this mechanism is applicable to mononuclear phagocytes. On the other hand, caspase-1 is also able to activate caspase-3 and-7 inducing apoptosis and blocking pyroptosis by cleaving GSDMD in monocytes and macrophages, linking apoptosis to the inflammatory pathway downstream of stimulation with LPS (Lamkanfi et al. 2008, Akhter et al. 2009, Taabazuing et al. 2017).

If apoptotic cells cannot be efficiently removed by efferocytosis, the cells undergo secondary necrosis and lose their membrane integrity (Sachet et al. 2017). The leakage of DAMPs drives inflammation and activates nearby immune cells. *In vivo*, secondary necrosis only occurs when the rapid removal of apoptotic cells, the efferocytosis, is impaired (Sachet et al. 2017). However, in cell culture of monocytic cells, this may be a more profound problem as monocytic cells have limited phagocytic properties compared to macrophages (Daigneault et al. 2010, Kurynina et al. 2018). Therefore, the induction of apoptosis by treatment with 5-B and LPS could lead to secondary necrosis of monocytic cells and promote pro-inflammatory responses such as the release of IL-1β. If 5-B also induces apoptosis in macrophages, a higher efferocytotic activity may prevent exacerbated pro-inflammatory responses. This might explain the different response to 5-B of monocytic cells compared to macrophages.

Comparison of LDH activity in the supernatants of cells treated with LPS and 5-B or the positive control doxorubicin does not reveal any prominent differences (**Table S-1**), although doxorubicin alone activates caspase-3 and -7 twice as much as LPS and 5-B (**Figure 31**). However, this is not so surprising as the process of apoptosis takes several h and LDH activity is only an indicator of late apoptosis and secondary necrosis (Sachet et al. 2017). This contradicts the hypothesis, that the 5-B-mediated increase in IL-1β release is an inflammatory response to secondary necrosis. However, the present results represent very preliminary experiments and no definitive conclusions can be drawn at this time regarding 5-B-mediated apoptosis in mononuclear phagocytes.

7 CLINICAL RELEVANCE OF THE RESULTS

The present study confirms the common notion that the release of IL-1β is triggered by the PAMP LPS in combination with the DAMP extracellular ATP. Nevertheless, it is possible that sterile inflammation occurs in the absence of pathogens and their PAMPs, when solely DAMPs are released due to tissue damage (Zindel et al. 2020). DAMPs are recognised by PRRs, including TLRs and NLRs, as well as non-PRRs, such as P2X receptors in the case of extracellular ATP (Li et al. 2021). In response, innate immune cells produce pro-inflammatory mediators, including nitric oxide, ROS, vasoactive histamine and serotonin, prostaglandins, TNF-α, and IL-1β (Zindel et al. 2020). For example, IL-1β mediates further immune responses in nearby cells and promotes the attraction of granulocytes to the tissue. On a systemic level, it induces vasodilatation and hypotension, a lowered pain threshold, and fever (Galozzi et al. 2021). Consequently, the initial damage and subsequent inflammation result in the disruption of barriers and the activation of endothelial cells, which then permit the extravasation of leukocytes, plasma proteins, and platelets with the objective of repairing the damaged tissue (Zindel et al. 2020). As a result, sterile inflammation is contingent upon the orchestrated migration of leukocytes and a precisely timed transition from an inflammatory to a reparative programme.

However, in certain pathologies, the failure of recruited leukocytes to remove DAMPs can be deleterious, leading to persistent inflammation (Zindel et al. 2020). Moreover, in response to major surgery or accidental trauma, the extensive release of ATP and other DAMPs induces the massive release of cytokines, which can be overwhelming and cause life-threatening systemic inflammation. The current therapeutic strategies preventing sterile hyperinflammation are mainly immunosuppressive, such as the neutralisation of antibodies or the use of TLR antagonists. Nevertheless, the use of TLR antagonists carries the risk of impeding host defence against infection, potentially exacerbating the vulnerability of the patient. It is therefore crucial to develop therapeutic strategies that can control inflammation without severely compromising host defence mechanisms. The current results reveal a novel property of the

P2RX4 antagonist 5-B, which may have potential for therapeutic use. While treatment with 5-B in the presence of ATP results in a reduction in the release of IL-1β, treatment in the presence of bacterial LPS leads to an increase in the production of the pro-inflammatory cytokine. This suggests that host defence against infection is enhanced, while inflammatory responses following extensive cellular damage are inhibited. However, if the inflammatory effect of 5-B is dependent on the induction of apoptosis, as indicated by some of the current results, it can be hypothesised that 5-B would not achieve the desired outcomes, because apoptotic cells are quickly and efficiently eliminated *in vivo*. Nevertheless, the data to date indicate that further investigation into the effects of 5-B in monocytic cells is warranted, as such a therapeutic could have significant medical value.

8 CONCLUSIONS

Human mononuclear phagocytes were represented by the monocytic THP-1 cell line, which is capable of easily differentiating into macrophages, as well as enriched primary monocytes and macrophages. The results obtained from the THP-1 cells and the corresponding primary cells demonstrate that they are appropriate for comparison and that the findings derived from the cell line can be reproduced in primary cells. This study employed well-established methodologies, including real-time RT-PCR, Western blotting, and ELISA, to assess alterations in mRNA expression levels, intracellular protein levels, and the amounts of released cytokines, respectively. Moreover, the impact of four distinct P2RX4 antagonists was directly compared with that of well-established P2RX7 antagonists. These circumstances provided a robust foundation for exploratory studies concerning the role of P2RX4 and P2RX7 in IL-1β expression and release by mononuclear phagocytes.

The objective of this exploratory study was to address the following questions:

1. Which role plays the P2RX4 in the ATP-dependent IL-1β maturation?

The results indicate that the P2RX4 may be involved in the ATP-dependent IL-1β release from human mononuclear phagocytes (**Figure 32**).

2. Which roles play the P2RX4 and P2RX7 in the priming of human mononuclear phagocytes?

The results do not indicate a role for P2RX7 in priming human mononuclear phagocytes. However, given the limitations of the present data, it is plausible to suggest cautiously that 5-B acts via P2RX4 and may facilitate priming of human monocytic cells (**Figure 32**). It is possible that PZB13 evokes similar effects, although the data were not entirely consistent.

It has been demonstrated that monocytic cells exhibit a markedly higher expression of *P2RX4* mRNA in comparison to *P2RX7* mRNA. Therefore, with all due caution, it can be postulated

that macrophages did not respond to 5-B treatment due to a more balanced ratio of P2RX4 and P2RX7 expression.

3. Does the P2RX4 antagonist 5-B induce apoptosis?

It is possible that treatment with 5-B and LPS induces apoptosis. However, the data are very preliminary and further validations are needed before a definitive conclusion can be made.

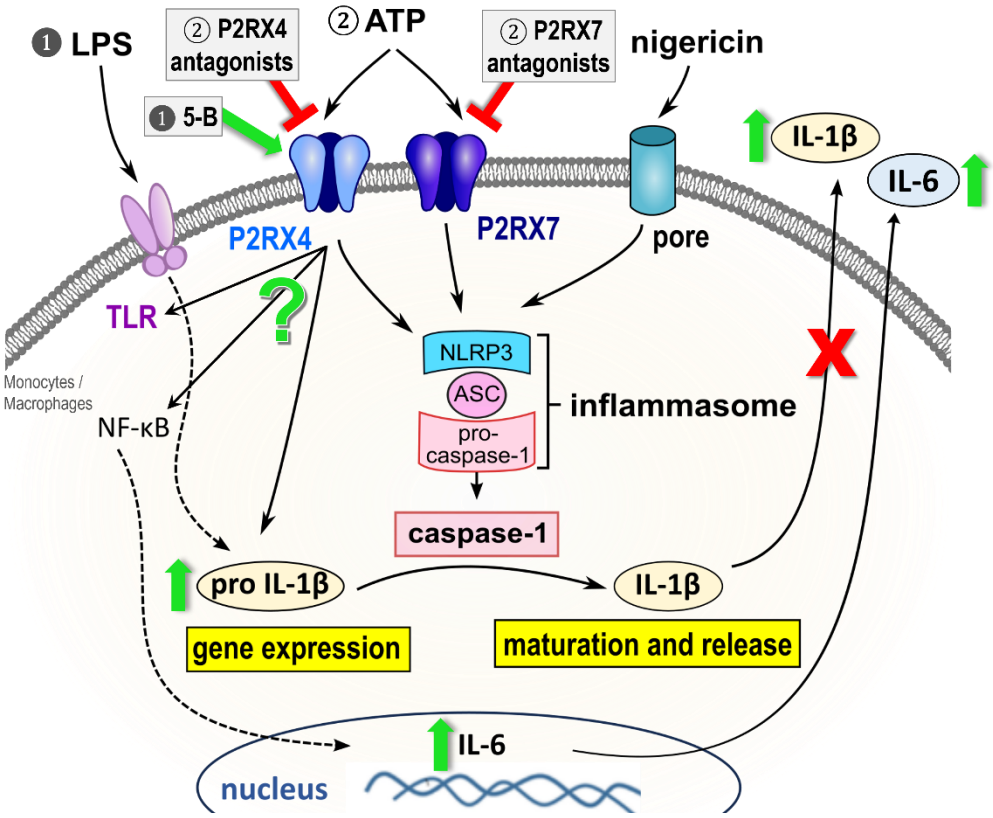

Figure 32: Overview of the findings obtained in the course of this study regarding IL-1β expression and maturation in mononuclear phagocytes. LPS serves as signal ❶, which primes monocytes or macrophages by binding to TLR4 and inducing the gene expression of pro-IL-1β inter alia via NF-κB signalling. Extracellular ATP binds to the P2RX4 and P2RX7 and the bacterial toxin nigericin induces pore formation in the plasma membrane of the activated cell. Stimulation with ATP or nigericin, representing signal ②, both induce the assembly of NLRP3, ASC, and pro-caspase-1 to the NLRP3 inflammasome. As a result, pro-caspase-1 is cleaved into its active form and cleaves pro-IL-1β into the mature IL-1β, which is then released from the cell. In the presence of ATP (②), P2RX4 and P2RX7 antagonists block the ATP-mediated activation of the respective receptors and downstream signalling resulting in inhibited IL-1β secretion from monocytes or macrophages. Binding of 5-B to P2RX4 during priming with LPS (❶) increases gene expression of pro-IL-1β and IL-6 and subsequent release of the cytokines, but only in monocytes. LPS, lipopolysaccharide; TLR, toll-like receptor; NF-κB, nuclear factor 'kappa-light-chain-enhancer' of activated B-cells; IL-1β, interleukin-1β; IL-6, interleukin-6; ATP, adenosine triphosphate; P2RX4/7, P2X purinoceptor 4/7; 5-B, 5-(3-Bromophenyl)-1,3-dihydro-2H-benzofuro[3,2-e]-1,4-diazepin-2-one; NLRP3, NLR family pyrin domain-containing protein 3; ASC, Apoptosis-associated speck-like protein containing a caspase-recruitment domain.

9 OUTLOOK

The findings of this exploratory study indicate that, in addition to P2RX7, P2RX4 plays a role in the ATP-dependent secretion of IL-1β from activated mononuclear phagocytes. Furthermore, the initial findings on the experimental use of 5-B provide insight into a novel role of P2RX4 in the priming step of monocytic cells. This paves the way for elucidating the mode of action of 5-B. However, some data are only very preliminary and do not allow any conclusions without further investigation.

P2RX4 is thought to be involved in the ATP-dependent release of IL-1β from human mononuclear phagocytes, although the assembly of NLRP3 and the activity of caspase-1 were not observed. It is unclear whether P2RX4 mediates these effects independently or if it interacts with or influences P2RX7 signalling. A comparison of ASC-speck formation in the absence or presence of P2RX4 antagonists can verify the assembly and activation of the NLRP3 inflammasome downstream of P2RX4. The formation of ASC-speck in THP-1 cells, in which P2RX4 or P2RX7 are silenced via siRNA, can elucidate the functional relevance of each receptor in the ATP-mediated activation of the NLRP3 inflammasome. The current objective is to establish the silencing of both receptors in monocytic THP-1 cells in our laboratory.

The results indicate that monocytic cells express a greater quantity of P2RX4 than P2RX7, whereas macrophages express both receptors in equal amounts. However, it should be noted that only mRNA levels were measured, and therefore further investigation is required to confirm these findings at the protein level. The detection of P2RX4 via fluorescence microscopy can estimate the protein amounts and cellular localization of the receptor within monocytic THP-1 cells and THP-1 cell-derived M1-like macrophages. This further defines the differences between monocytes and macrophages in terms of their responsiveness to P2X receptor stimulation.

5-B appears to promote priming of monocytic cells, presumably via the P2RX4. However, the specificity of 5-B is not yet confirmed, and the results must be verified by measuring *IL1B* mRNA, ATP-independent IL-1β release, as well as *IL6* mRNA and *IL6* release in monocytic THP-1 cells with silenced P2RX4, which will be treated with 5-B prior to priming with LPS. Additionally, experiments will be conducted to detect IL-10 release. Furthermore, studying other parameters of anti-inflammatory responses can help define the state of the cellular immune response induced by 5-B. Some results suggest that PZB13 evokes similar effects to 5-B. Conducting the same experiments with PZB13 will reveal possible similarities or discrepancies between the two P2RX4 antagonists.

Should 5-B (and presumably PZB13) promote priming via the P2RX4, further studies would be required to target signal transduction pathways. It may be possible to ascertain the mode of action of P2RX4 by investigating potential alterations in the protein levels of TLR4 or TFs

including NF-κB. Metabolic studies of THP-1 cells treated with 5-B before priming with LPS will elucidate potential metabolic alterations that may indicate cellular differentiation or define the immune response.

The elevated caspase-3/7 activity indicates the potential induction of apoptosis by the treatment with 5-B and LPS. Further apoptotic markers, such as annexin V staining and the detection of secondary necrosis, will assist in the interpretation of these preliminary findings. Furthermore, a comparison of these markers between monocytic cells and macrophages may elucidate whether this mechanism is associated with the 5-B-mediated upregulation of pro-inflammatory responses in monocytic cells or if these effects are independent of each other.

The capacity of 5-B treatment to stimulate host defences and mitigate DAMP-associated immune responses suggests that it may serve as a promising therapeutic agent for controlling inflammation while preserving host defence. The effect of systemic application of 5-B in mice during surgical trauma following a challenge with microbes or microbial structures will finally shed light on the practical applicability of 5-B.

REFERENCES

Abdelrahman, A.; Namasivayam, V.; Hinz, S.; Schiedel, A. C.; Köse, M. & Burton, M., et al. (2017): Characterization of P2X4 receptor agonists and antagonists by calcium influx and radioligand binding studies. *Biochemical pharmacology* 125. DOI 10.1016/j.bcp.2016.11.016.

Adinolfi, E.; Capece, M.; Franceschini, A.; Falzoni, S.; Giuliani, A. L. & Rotondo, A., et al. (2015): Accelerated tumor progression in mice lacking the ATP receptor P2X7. *Cancer research* 75(4). DOI 10.1158/0008-5472.CAN-14-1259.

Adinolfi, E.; Cirillo, M.; Woltersdorf, R.; Falzoni, S.; Chiozzi, P. & Pellegatti, P., et al. (2010): Trophic activity of a naturally occurring truncated isoform of the P2X7 receptor. *The FASEB Journal* 24(9). DOI 10.1096/fj.09-153601.

Akhter, A.; Gavrilin, M. A.; Frantz, L.; Washington, S.; Ditty, C. & Limoli, D., et al. (2009): Caspase-7 activation by the Nlrc4/Ipaf inflammasome restricts Legionella pneumophila infection. *PLOS Pathogens* 5(4). DOI 10.1371/journal.ppat.1000361.

Alberto, A. V. P.; Faria, R. X.; Couto, C. G. C.; Ferreira, L. G. B.; Souza, C. A. M. & Teixeira, P. C. N., et al. (2013): Is pannexin the pore associated with the P2X7 receptor? *Naunyn-Schmiedeberg's archives of pharmacology* 386(9). DOI 10.1007/s00210-013-0868-x.

Allsopp, R. C.; El Ajouz, S.; Schmid, R. & Evans, R. J. (2011a): Cysteine scanning mutagenesis (residues Glu52-Gly96) of the human P2X1 receptor for ATP: mapping agonist binding and channel gating. *Journal of Biological Chemistry* 286(33). DOI 10.1074/jbc.M111.260364.

Allsopp, R. C. & Evans, R. J. (2011b): The intracellular amino terminus plays a dominant role in desensitization of ATP-gated P2X receptor ion channels. *Journal of Biological Chemistry* 286(52). DOI 10.1074/jbc.M111.303917.

Amati, A.-L.; Zakrzewicz, A.; Siebers, R.; Wilker, S.; Heldmann, S. & Zakrzewicz, D., et al. (2017): Chemokines (CCL3, CCL4, and CCL5) Inhibit ATP-Induced Release of IL-1β by Monocytic Cells. *Mediators of inflammation* 2017. DOI 10.1155/2017/1434872.

Andrei, C.; Dazzi, C.; Lotti, L.; Torrisi, M. R.; Chimini, G. & Rubartelli, A. (1999): The secretory route of the leaderless protein interleukin 1beta involves exocytosis of endolysosome-related vesicles. *Molecular biology of the cell* 10(5). DOI 10.1091/mbc.10.5.1463.

Antonelli, L. R. V.; Gigliotti Rothfuchs, A.; Gonçalves, R.; Roffê, E.; Cheever, A. W. & Bafica, A., et al. (2010): Intranasal Poly-IC treatment exacerbates tuberculosis in mice through the pulmonary recruitment of a pathogen-permissive monocyte/macrophage population. *The Journal of clinical investigation* 120(5). DOI 10.1172/JCI40817.

Antonio, L. S.; Stewart, A. P.; Varanda, W. A. & Edwardson, J. M. (2014): Identification of P2X2/P2X4/P2X6 heterotrimeric receptors using atomic force microscopy (AFM) imaging. *FEBS letters* 588(12). DOI 10.1016/j.febslet.2014.04.048.

Antonio, L. S.; Stewart, A. P.; Xu, X. J.; Varanda, W. A.; Murrell-Lagnado, R. D. & Edwardson, J. M. (2011): P2X4 receptors interact with both P2X2 and P2X7 receptors in the form of

homotrimers. *British journal of pharmacology* 163(5). DOI 10.1111/j.1476-5381.2011.01303.x.

Ase, A. R.; Honson, N. S.; Zaghdane, H.; Pfeifer, T. A. & Séguéla, P. (2015): Identification and characterization of a selective allosteric antagonist of human P2X4 receptor channels. *Molecular pharmacology* 87(4). DOI 10.1124/mol.114.096222.

Ase, A. R.; Therrien, É. & Séguéla, P. (2019): An Allosteric Inhibitory Site Conserved in the Ectodomain of P2X Receptor Channels. *Frontiers in cellular neuroscience* 13. DOI 10.3389/fncel.2019.00121.

Auwerx, J. (1991): The human leukemia cell line, THP-1: a multifacetted model for the study of monocyte-macrophage differentiation. *Experientia* 47(1). DOI 10.1007/BF02041244.

Balasingam, V. & Yong, V. W. (1996): Attenuation of astroglial reactivity by interleukin-10. *The Journal of Neuroscience* 16(9). DOI 10.1523/JNEUROSCI.16-09-02945.1996.

Balázs, B.; Dankó, T.; Kovács, G.; Köles, L.; Hediger, M. A. & Zsembery, A. (2013): Investigation of the inhibitory effects of the benzodiazepine derivative, 5-BDBD on P2X4 purinergic receptors by two complementary methods. *Cellular physiology and biochemistry : international journal of experimental cellular physiology, biochemistry, and pharmacology* 32(1). DOI 10.1159/000350119.

Bantulà, M.; Arismendi, E.; Picado, C.; Mullol, J.; Roca-Ferrer, J. & Tubita, V. (2022): Reference Gene Validation for RT-qPCR in PBMCs from Asthmatic Patients with or without Obesity. *Methods and protocols* 5(3). DOI 10.3390/mps5030035.

Bauernfeind, F. G.; Horvath, G.; Stutz, A.; Alnemri, E. S.; MacDonald, K. & Speert, D., et al. (2009): Cutting edge: NF-kappaB activating pattern recognition and cytokine receptors license NLRP3 inflammasome activation by regulating NLRP3 expression. *Journal of immunology (Baltimore, Md. : 1950)* 183(2). DOI 10.4049/jimmunol.0901363.

Berlato, C.; Cassatella, M. A.; Kinjyo, I.; Gatto, L.; Yoshimura, A. & Bazzoni, F. (2002): Involvement of suppressor of cytokine signaling-3 as a mediator of the inhibitory effects of IL-10 on lipopolysaccharide-induced macrophage activation. *The Journal of Immunology* 168(12). DOI 10.4049/jimmunol.168.12.6404.

Beukers, M. W.; Pirovano, I. M.; van Weert, A.; Kerkhof, C. J.; IJzerman, A. P. & Soudijn, W. (1993): Characterization of ecto-ATPase on human blood cells. A physiological role in platelet aggregation? *Biochemical pharmacology* 46(11). DOI 10.1016/0006-2952(93)90637-c.

Bhattacharya, A.; Wang, Q.; Ao, H.; Shoblock, J. R.; Lord, B. & Aluisio, L., et al. (2013): Pharmacological characterization of a novel centrally permeable P2X7 receptor antagonist: JNJ-47965567. *British journal of pharmacology* 170(3). DOI 10.1111/bph.12314.

Bianchi, B. R.; Lynch, K. J.; Touma, E.; Niforatos, W.; Burgard, E. C. & Alexander, K. M., et al. (1999): Pharmacological characterization of recombinant human and rat P2X receptor subtypes. *European journal of pharmacology* 376(1-2). DOI 10.1016/s0014-2999(99)00350-7.

Bianco, F.; Pravettoni, E.; Colombo, A.; Schenk, U.; Möller, T. & Matteoli, M., et al. (2005): Astrocyte-derived ATP induces vesicle shedding and IL-1 beta release from microglia. *The Journal of Immunology* 174(11). DOI 10.4049/jimmunol.174.11.7268.

Bidula, S.; Nadzirin, I. B.; Cominetti, M.; Hickey, H.; Cullum, S. A. & Searcey, M., et al. (2022): Structural Basis of the Negative Allosteric Modulation of 5-BDBD at Human P2X4 Receptors. *Molecular pharmacology* 101(1). DOI 10.1124/molpharm.121.000402.

Bogdan, C.; Vodovotz, Y. & Nathan, C. (1991): Macrophage deactivation by interleukin 10. *Journal of Experimental Medicine* 174(6). DOI 10.1084/jem.174.6.1549.

Boué-Grabot, E.; Archambault, V. & Séguéla, P. (2000): A protein kinase C site highly conserved in P2X subunits controls the desensitization kinetics of P2X(2) ATP-gated channels. *Journal of Biological Chemistry* 275(14). DOI 10.1074/jbc.275.14.10190.

Boumechache, M.; Masin, M.; Edwardson, J. M.; Górecki, D. C. & Murrell-Lagnado, R. (2009): Analysis of assembly and trafficking of native P2X4 and P2X7 receptor complexes in rodent immune cells. *Journal of Biological Chemistry* 284(20). DOI 10.1074/jbc.M901255200.

Brough, D.; Le Feuvre, R. A.; Wheeler, R. D.; Solovyova, N.; Hilfiker, S. & Rothwell, N. J., et al. (2003): Ca2+ stores and Ca2+ entry differentially contribute to the release of IL-1 beta and IL-1 alpha from murine macrophages. *The Journal of Immunology* 170(6). DOI 10.4049/jimmunol.170.6.3029.

Bruckmeier, M.; Kuehnl, A.; Culmes, M.; Pelisek, J. & Eckstein, H.-H. (2012): Impact of oxLDL and LPS on C-type natriuretic peptide system is different between THP-1 cells and human peripheral blood monocytic cells. *Cellular physiology and biochemistry : international journal of experimental cellular physiology, biochemistry, and pharmacology* 30(1). DOI 10.1159/000339044.

Burm, S. M.; Zuiderwijk-Sick, E. A.; Weert, P. M. & Bajramovic, J. J. (2016): ATP-induced IL-1β secretion is selectively impaired in microglia as compared to hematopoietic macrophages. *Glia* 64(12). DOI 10.1002/glia.23059.

Burnstock, G. & Kennedy, C. (1985): Is there a basis for distinguishing two types of P2-purinoceptor? *General Pharmacology: The Vascular System* 16(5). DOI 10.1016/0306-3623(85)90001-1.

Butler, T. A. J.; Paul, J. W.; Chan, E.-C.; Smith, R. & Tolosa, J. M. (2019): Misleading Westerns: Common Quantification Mistakes in Western Blot Densitometry and Proposed Corrective Measures. *BioMed research international* 2019. DOI 10.1155/2019/5214821.

Cao, Q.; Zhong, X. Z.; Zou, Y.; Murrell-Lagnado, R.; Zhu, M. X. & Dong, X.-P. (2015): Calcium release through P2X4 activates calmodulin to promote endolysosomal membrane fusion. *The Journal of cell biology* 209(6). DOI 10.1083/jcb.201409071.

Cao, X.; Luo, X.; Liang, J.; Zhang, C.; Meng, X. & Guo, D. (2012): Critical selection of internal control genes for quantitative real-time RT-PCR studies in lipopolysaccharide-stimulated human THP-1 and K562 cells. *Biochemical and biophysical research communications* 427(2). DOI 10.1016/j.bbrc.2012.09.066.

Cao, Z.; Henzel, W. J. & Gao, X. (1996): IRAK: a kinase associated with the interleukin-1 receptor. *Science (New York, N.Y.)* 271(5252). DOI 10.1126/science.271.5252.1128.

Casas-Pruneda, G.; Reyes, J. P.; Pérez-Flores, G.; Pérez-Cornejo, P. & Arreola, J. (2009): Functional interactions between P2X4 and P2X7 receptors from mouse salivary epithelia. *The Journal of physiology* 587(Pt 12). DOI 10.1113/jphysiol.2008.167395.

Casati, A.; Frascoli, M.; Traggiai, E.; Proietti, M.; Schenk, U. & Grassi, F. (2011): Cell-autonomous regulation of hematopoietic stem cell cycling activity by ATP. *Cell death and differentiation* 18(3). DOI 10.1038/cdd.2010.107.

Cassatella, M. A.; Meda, L.; Bonora, S.; Ceska, M. & Constantin, G. (1993): Interleukin 10 (IL-10) inhibits the release of proinflammatory cytokines from human polymorphonuclear leukocytes. Evidence for an autocrine role of tumor necrosis factor and IL-1 beta in mediating the production of IL-8 triggered by lipopolysaccharide. *Journal of Experimental Medicine* 178(6). DOI 10.1084/jem.178.6.2207.

Chan, J. K.; Ng, C. S. & Hui, P. K. (1988): A simple guide to the terminology and application of leucocyte monoclonal antibodies. *Histopathology* 12(5). DOI 10.1111/j.1365-2559.1988.tb01967.x.

Chandra, G.; Cogswell, J. P.; Miller, L. R.; Godlevski, M. M.; Stinnett, S. W. & Noel, S. L., et al. (1995): Cyclic AMP signaling pathways are important in IL-1 beta transcriptional regulation. *The Journal of Immunology* 155(10). DOI 10.4049/jimmunol.155.10.4535.

Chanput, W.; Mes, J.; Vreeburg, R. A. M.; Savelkoul, H. F. J. & Wichers, H. J. (2010): Transcription profiles of LPS-stimulated THP-1 monocytes and macrophages: a tool to study inflammation modulating effects of food-derived compounds. *Food & Function* 1(3). DOI 10.1039/C0FO00113A.

Chanput, W.; Mes, J. J. & Wichers, H. J. (2014): THP-1 cell line: an in vitro cell model for immune modulation approach. *International immunopharmacology* 23(1). DOI 10.1016/j.intimp.2014.08.002.

Cheewatrakoolpong, B.; Gilchrest, H.; Anthes, J. C. & Greenfeder, S. (2005): Identification and characterization of splice variants of the human P2X7 ATP channel. *Biochemical and biophysical research communications* 332(1). DOI 10.1016/j.bbrc.2005.04.087.

Chen, K.; Zhang, J.; Zhang, W.; Zhang, J.; Yang, J. & Li, K., et al. (2013): ATP-P2X4 signaling mediates NLRP3 inflammasome activation: a novel pathway of diabetic nephropathy. *The international journal of biochemistry & cell biology* 45(5). DOI 10.1016/j.biocel.2013.02.009.

Chen, W. & Xu, W.-H. (2015): β-Actin as a loading control: Less than 2 μg of total protein should be loaded. *Electrophoresis* 36(17). DOI 10.1002/elps.201500138.

Chessell, I. P.; Hatcher, J. P.; Bountra, C.; Michel, A. D.; Hughes, J. P. & Green, P., et al. (2005): Disruption of the P2X7 purinoceptor gene abolishes chronic inflammatory and neuropathic pain. *PAIN* 114(3). DOI 10.1016/j.pain.2005.01.002.

Chessell, I. P.; Simon, J.; Hibell, A. D.; Michel, A. D.; Barnard, E. A. & Humphrey, P. P. (1998): Cloning and functional characterisation of the mouse P2X7 receptor. *FEBS Letters* 439(1-2). DOI 10.1016/S0014-5793(98)01332-5.

Chu, J.; Thomas, L. M.; Watkins, S. C.; Franchi, L.; Núñez, G. & Salter, R. D. (2009): Cholesterol-dependent cytolysins induce rapid release of mature IL-1beta from murine macrophages in a NLRP3 inflammasome and cathepsin B-dependent manner. *Journal of leukocyte biology* 86(5). DOI 10.1189/jlb.0309164.

Clark, A. K.; Staniland, A. A.; Marchand, F.; Kaan, T. K. Y.; McMahon, S. B. & Malcangio, M. (2010): P2X7-dependent release of interleukin-1beta and nociception in the spinal cord following lipopolysaccharide. *The Journal of Neuroscience* 30(2). DOI 10.1523/JNEUROSCI.3295-09.2010.

Clyne, J. D.; Wang, L.-F. & Hume, R. I. (2002): Mutational Analysis of the Conserved Cysteines of the Rat P2X 2 Purinoceptor. *The Journal of Neuroscience* 22(10). DOI 10.1523/JNEUROSCI.22-10-03873.2002.

Coddou, C.; Sandoval, R.; Hevia, M. J. & Stojilkovic, S. S. (2019): Characterization of the antagonist actions of 5-BDBD at the rat P2X4 receptor. *Neuroscience letters* 690. DOI 10.1016/j.neulet.2018.10.047.

Craigie, E.; Birch, R. E.; Unwin, R. J. & Wildman, S. S. (2013): The relationship between P2X4 and P2X7: a physiologically important interaction? *Frontiers in physiology* 4. DOI 10.3389/fphys.2013.00216.

Daigneault, M.; Preston, J. A.; Marriott, H. M.; Whyte, M. K. B. & Dockrell, D. H. (2010): The identification of markers of macrophage differentiation in PMA-stimulated THP-1 cells and monocyte-derived macrophages. *PLOS ONE* 5(1). DOI 10.1371/journal.pone.0008668.

Dal Ben, D.; Buccioni, M.; Lambertucci, C.; Marucci, G.; Thomas, A. & Volpini, R. (2015): Purinergic P2X receptors: structural models and analysis of ligand-target interaction. *European Journal of Medicinal Chemistry* 89. DOI 10.1016/j.ejmech.2014.10.071.

Denlinger, L. C.; Fisette, P. L.; Sommer, J. A.; Watters, J. J.; Prabhu, U. & Dubyak, G. R., et al. (2001): Cutting edge: the nucleotide receptor P2X7 contains multiple protein- and lipid-interaction motifs including a potential binding site for bacterial lipopolysaccharide. *The Journal of Immunology* 167(4). DOI 10.4049/jimmunol.167.4.1871.

Di Virgilio, F.; Dal Ben, D.; Sarti, A. C.; Giuliani, A. L. & Falzoni, S. (2017): The P2X7 Receptor in Infection and Inflammation. *Immunity* 47(1). DOI 10.1016/j.immuni.2017.06.020.

Di Virgilio, F.; Sarti, A. C. & Coutinho-Silva, R. (2020): Purinergic signaling, DAMPs, and inflammation. *American journal of physiology. Cell physiology* 318(5). DOI 10.1152/ajpcell.00053.2020.

Diehl, D.; Friedmann, A. & Bachmann, H. S. (2022): Evidence-based selection of reference genes for RT-qPCR assays in periodontal research. *Clinical and experimental dental research* 8(2). DOI 10.1002/cre2.525.

Dinarello, C. A. (2018): Overview of the IL-1 family in innate inflammation and acquired immunity. *Immunological reviews* 281(1). DOI 10.1111/imr.12621.

Donnelly-Roberts, D. L. & Jarvis, M. F. (2007): Discovery of P2X7 receptor-selective antagonists offers new insights into P2X7 receptor function and indicates a role in chronic pain states. *British journal of pharmacology* 151(5). DOI 10.1038/sj.bjp.0707265.

Dos-Santos-Pereira, M.; Acuña, L.; Hamadat, S.; Rocca, J.; González-Lizárraga, F. & Chehín, R., et al. (2018): Microglial glutamate release evoked by α-synuclein aggregates is prevented by dopamine. *Glia* 66(11). DOI 10.1002/glia.23472.

Dostert, C.; Grusdat, M.; Letellier, E. & Brenner, D. (2019): The TNF Family of Ligands and Receptors: Communication Modules in the Immune System and Beyond. *Physiological reviews* 99(1). DOI 10.1152/physrev.00045.2017.

Draganov, D.; Gopalakrishna-Pillai, S.; Chen, Y.-R.; Zuckerman, N.; Moeller, S. & Wang, C., et al. (2015): Modulation of P2X4/P2X7/Pannexin-1 sensitivity to extracellular ATP via Ivermectin induces a non-apoptotic and inflammatory form of cancer cell death. *Scientific Reports* 5. DOI 10.1038/srep16222.

Duffield, J. S.; Forbes, S. J.; Constandinou, C. M.; Clay, S.; Partolina, M. & Vuthoori, S., et al. (2005): Selective depletion of macrophages reveals distinct, opposing roles during liver injury and repair. *The Journal of clinical investigation* 115(1). DOI 10.1172/JCI22675.

Dugina, V. B.; Shagieva, G. S. & Kopnin, P. B. (2019): Biological role of actin isoforms in mammalian cells. *Biochemistry (Moscow)* 84(6). DOI 10.1134/S0006297919060014.

Duncan, J. A.; Bergstralh, D. T.; Wang, Y.; Willingham, S. B.; Ye, Z. & Zimmermann, A. G., et al. (2007): Cryopyrin/NALP3 binds ATP/dATP, is an ATPase, and requires ATP binding to mediate inflammatory signaling. *Proceedings of the National Academy of Sciences of the United States of America* 104(19). DOI 10.1073/pnas.0611496104.

Duong, B. H.; Onizawa, M.; Oses-Prieto, J. A.; Advincula, R.; Burlingame, A. & Malynn, B. A., et al. (2015): A20 restricts ubiquitination of pro-interleukin-1β protein complexes and suppresses NLRP3 inflammasome activity. *Immunity* 42(1). DOI 10.1016/j.immuni.2014.12.031.

Eischen, A.; Duclos, B.; Schmitt-Goguel, M.; Rouyer, N.; Bergerat, J. P. & Hummel, M., et al. (1994): Human resident peritoneal macrophages: phenotype and biology. *British journal of haematology* 88(4). DOI 10.1111/j.1365-2141.1994.tb05109.x.

Ennion, S. J. & Evans, R. J. (2002): Conserved Cysteine Residues in the Extracellular Loop of the Human P2X 1 Receptor Form Disulfide Bonds and Are Involved in Receptor Trafficking to the Cell Surface. *Molecular Pharmacology* 61(2). DOI 10.1124/mol.61.2.303.

Ensan, S.; Li, A.; Besla, R.; Degousee, N.; Cosme, J. & Roufaiel, M., et al. (2016): Self-renewing resident arterial macrophages arise from embryonic CX3CR1(+) precursors and circulating monocytes immediately after birth. *Nature Immunology* 17(2). DOI 10.1038/ni.3343.

Epelman, S.; Lavine, K. J.; Beaudin, A. E.; Sojka, D. K.; Carrero, J. A. & Calderon, B., et al. (2014): Embryonic and adult-derived resident cardiac macrophages are maintained through distinct mechanisms at steady state and during inflammation. *Immunity* 40(1). DOI 10.1016/j.immuni.2013.11.019.

Falzoni, S.; Munerati, M.; Ferrari, D.; Spisani, S.; Moretti, S. & Di Virgilio, F. (1995): The purinergic P2Z receptor of human macrophage cells. Characterization and possible physiological role. *The Journal of Clinical Investigation* 95(3). DOI 10.1172/JCI117770.

Feldmeyer, L.; Keller, M.; Niklaus, G.; Hohl, D.; Werner, S. & Beer, H.-D. (2007): The inflammasome mediates UVB-induced activation and secretion of interleukin-1beta by keratinocytes. *Current biology : CB* 17(13). DOI 10.1016/j.cub.2007.05.074.

Feng, Y.-H.; Li, X.; Wang, L.; Zhou, L. & Gorodeski, G. I. (2006): A truncated P2X7 receptor variant (P2X7-j) endogenously expressed in cervical cancer cells antagonizes the full-length P2X7 receptor through hetero-oligomerization. *The Journal of biological chemistry* 281(25). DOI 10.1074/jbc.M602999200.

Fenton, M. J.; Vermeulen, M. W.; Clark, B. D.; Webb, A. C. & Auron, P. E. (1988): Human pro-IL-1 beta gene expression in monocytic cells is regulated by two distinct pathways. *The Journal of Immunology* 140(7).

Fernandes-Alnemri, T.; Kang, S.; Anderson, C.; Sagara, J.; Fitzgerald, K. A. & Alnemri, E. S. (2013): Cutting edge: TLR signaling licenses IRAK1 for rapid activation of the NLRP3 inflammasome. *Journal of immunology (Baltimore, Md. : 1950)* 191(8). DOI 10.4049/jimmunol.1301681.

Ferrao, R.; Zhou, H.; Shan, Y.; Liu, Q.; Li, Q. & Shaw, D. E., et al. (2014): IRAK4 dimerization and trans-autophosphorylation are induced by Myddosome assembly. *Molecular Cell* 55(6). DOI 10.1016/j.molcel.2014.08.006.

Ferrari, D.; Chiozzi, P.; Falzoni, S.; Dal Susino, M.; Melchiorri, L. & Baricordi, O. R., et al. (1997): Extracellular ATP triggers IL-1 beta release by activating the purinergic P2Z receptor of human macrophages. *The Journal of Immunology* 159(3). DOI 10.4049/jimmunol.159.3.1451.

Ferrari, D.; Pizzirani, C.; Adinolfi, E.; Forchap, S.; Sitta, B. & Turchet, L., et al. (2004): The antibiotic polymyxin B modulates P2X7 receptor function. *The Journal of Immunology* 173(7). DOI 10.4049/jimmunol.173.7.4652.

Ferrari, D.; Villalba, M.; Chiozzi, P.; Falzoni, S.; Ricciardi-Castagnoli, P. & Di Virgilio, F. (1996): Mouse microglial cells express a plasma membrane pore gated by extracellular ATP. *The Journal of Immunology* 156(4). DOI 10.4049/jimmunol.156.4.1531.

Fink, S. L. & Cookson, B. T. (2006): Caspase-1-dependent pore formation during pyroptosis leads to osmotic lysis of infected host macrophages. *Cellular microbiology* 8(11). DOI 10.1111/j.1462-5822.2006.00751.x.

Fiorentino, D. F.; Zlotnik, A.; Mosmann, T. R.; Howard, M. & O'Garra, A. (1991): IL-10 inhibits cytokine production by activated macrophages. *The Journal of Immunology* 147(11). DOI 10.4049/jimmunol.147.11.3815.

Fischer, W.; Zadori, Z.; Kullnick, Y.; Gröger-Arndt, H.; Franke, H. & Wirkner, K., et al. (2007): Conserved lysin and arginin residues in the extracellular loop of P2X(3) receptors are involved in agonist binding. *European journal of pharmacology* 576(1-3). DOI 10.1016/j.ejphar.2007.07.068.

Fischer R.; Kalthof B.; Grützmann R.; Woltering E.; Stelte-Ludwig B.; Wuttke M.; Hernandez Blasco PJ. & Pina Gadea C. 12.03.2004: Benzofuro-1,4-diazepin-2-on-derivate.

Fitzgerald, K. A. & Kagan, J. C. (2020): Toll-like Receptors and the Control of Immunity. *Cell* 180(6). DOI 10.1016/j.cell.2020.02.041.

Fountain, S. J. & North, R. A. (2006): A C-terminal lysine that controls human P2X4 receptor desensitization. *Journal of Biological Chemistry* 281(22). DOI 10.1074/jbc.M600442200.

Franceschini, A.; Capece, M.; Chiozzi, P.; Falzoni, S.; Sanz, J. M. & Sarti, A. C., et al. (2015): The P2X7 receptor directly interacts with the NLRP3 inflammasome scaffold protein. *The FASEB Journal* 29(6). DOI 10.1096/fj.14-268714.

Franchi, L.; Eigenbrod, T. & Núñez, G. (2009): Cutting edge: TNF-alpha mediates sensitization to ATP and silica via the NLRP3 inflammasome in the absence of microbial stimulation. *Journal of immunology (Baltimore, Md. : 1950)* 183(2). DOI 10.4049/jimmunol.0900173.

Francistiová, L.; Vörös, K.; Lovász, Z.; Dinnyés, A. & Kobolák, J. (2021): Detection and Functional Evaluation of the P2X7 Receptor in hiPSC Derived Neurons and Microglia-Like Cells. *Frontiers in molecular neuroscience* 14. DOI 10.3389/fnmol.2021.793769.

Frey, E. A.; Miller, D. S.; Jahr, T. G.; Sundan, A.; Bazil, V. & Espevik, T., et al. (1992): Soluble CD14 participates in the response of cells to lipopolysaccharide. *Journal of Experimental Medicine* 176(6). DOI 10.1084/jem.176.6.1665.

Galozzi, P.; Bindoli, S.; Doria, A. & Sfriso, P. (2021): The revisited role of interleukin-1 alpha and beta in autoimmune and inflammatory disorders and in comorbidities. *Autoimmunity Reviews* 20(4). DOI 10.1016/j.autrev.2021.102785.

Gassmann, M.; Grenacher, B.; Rohde, B. & Vogel, J. (2009): Quantifying Western blots: pitfalls of densitometry. *Electrophoresis* 30(11). DOI 10.1002/elps.200800720.

Gay, N. J. & Keith, F. J. (1991): Drosophila Toll and IL-1 receptor. *Nature* 351(6325). DOI 10.1038/351355b0.

Geissmann, F.; Jung, S. & Littman, D. R. (2003): Blood monocytes consist of two principal subsets with distinct migratory properties. *Immunity* 19(1). DOI 10.1016/s1074-7613(03)00174-2.

Genin, M.; Clement, F.; Fattaccioli, A.; Raes, M. & Michiels, C. (2015): M1 and M2 macrophages derived from THP-1 cells differentially modulate the response of cancer cells to etoposide. *BMC cancer* 15. DOI 10.1186/s12885-015-1546-9.

Gioannini, T. L.; Teghanemt, A.; Zhang, D.; Coussens, N. P.; Dockstader, W. & Ramaswamy, S., et al. (2004): Isolation of an endotoxin-MD-2 complex that produces Toll-like receptor 4-dependent cell activation at picomolar concentrations. *Proceedings of the National Academy of Sciences of the United States of America* 101(12). DOI 10.1073/pnas.0306906101.

Giuliani, A. L.; Sarti, A. C. & Di Virgilio, F. (2019): Extracellular nucleotides and nucleosides as signalling molecules. *Immunology letters* 205. DOI 10.1016/j.imlet.2018.11.006.

Gordon, E. J.; Myers, K. J.; Dougherty, J. P.; Rosen, H. & Ron, Y. (1995): Both anti-CD11a (LFA-1) and anti-CD11b (MAC-1) therapy delay the onset and diminish the severity of experimental autoimmune encephalomyelitis. *Journal of Neuroimmunology* 62(2). DOI 10.1016/0165-5728(95)00120-2.

Gray, J. G.; Chandra, G.; Clay, W. C.; Stinnett, S. W.; Haneline, S. A. & Lorenz, J. J., et al. (1993): A CRE/ATF-like site in the upstream regulatory sequence of the human interleukin 1 beta gene is necessary for induction in U937 and THP-1 monocytic cell lines. *Molecular and cellular biology* 13(11). DOI 10.1128/mcb.13.11.6678-6689.1993.

Grech, A. P.; Gardam, S.; Chan, T.; Quinn, R.; Gonzales, R. & Basten, A., et al. (2005): Tumor necrosis factor receptor 2 (TNFR2) signaling is negatively regulated by a novel, carboxyl-

terminal TNFR-associated factor 2 (TRAF2)-binding site. *Journal of Biological Chemistry* 280(36). DOI 10.1074/jbc.M504849200.

Groß, C. J.; Mishra, R.; Schneider, K. S.; Médard, G.; Wettmarshausen, J. & Dittlein, D. C., et al. (2016): K+ Efflux-Independent NLRP3 Inflammasome Activation by Small Molecules Targeting Mitochondria. *Immunity* 45(4). DOI 10.1016/j.immuni.2016.08.010.

Gu, Y.; Kuida, K.; Tsutsui, H.; Ku, G.; Hsiao, K. & Fleming, M. A., et al. (1997): Activation of interferon-gamma inducing factor mediated by interleukin-1beta converting enzyme. *Science (New York, N.Y.)* 275(5297). DOI 10.1126/science.275.5297.206.

Guo, C.; Masin, M.; Qureshi, O. S. & Murrell-Lagnado, R. D. (2007): Evidence for functional P2X4/P2X7 heteromeric receptors. *Molecular Pharmacology* 72(6). DOI 10.1124/mol.107.035980.

Hadadi, E.; Zhang, B.; Baidžajevas, K.; Yusof, N.; Puan, K. J. & Ong, S. M., et al. (2016): Differential IL-1β secretion by monocyte subsets is regulated by Hsp27 through modulating mRNA stability. *Scientific Reports* 6. DOI 10.1038/srep39035.

Hailey, K. L.; Li, S.; Andersen, M. D.; Roy, M.; Woods, V. L. & Jennings, P. A. (2009): Pro-interleukin (IL)-1beta shares a core region of stability as compared with mature IL-1beta while maintaining a distinctly different configurational landscape: a comparative hydrogen/deuterium exchange mass spectrometry study. *Journal of Biological Chemistry* 284(38). DOI 10.1074/jbc.M109.027375.

Han, S. J.; Lovaszi, M.; Kim, M.; D'Agati, V.; Haskó, G. & Lee, H. T. (2020): P2X4 receptor exacerbates ischemic AKI and induces renal proximal tubular NLRP3 inflammasome signaling. *The FASEB Journal* 34(4). DOI 10.1096/fj.201903287R.

Hannum, C. H.; Wilcox, C. J.; Arend, W. P.; Joslin, F. G.; Dripps, D. J. & Heimdal, P. L., et al. (1990): Interleukin-1 receptor antagonist activity of a human interleukin-1 inhibitor. *Nature* 343(6256). DOI 10.1038/343336a0.

Harkat, M.; Peverini, L.; Cerdan, A. H.; Dunning, K.; Beudez, J. & Martz, A., et al. (2017): On the permeation of large organic cations through the pore of ATP-gated P2X receptors. *Proceedings of the National Academy of Sciences* 114(19). DOI 10.1073/pnas.1701379114.

Hartigh, A. B. den & Fink, S. L. (2018): Pyroptosis Induction and Detection. *Current protocols in immunology* 122(1). DOI 10.1002/cpim.52.

Hashimoto, D.; Chow, A.; Noizat, C.; Teo, P.; Beasley, M. B. & Leboeuf, M., et al. (2013): Tissue-resident macrophages self-maintain locally throughout adult life with minimal contribution from circulating monocytes. *Immunity* 38(4). DOI 10.1016/j.immuni.2013.04.004.

Hattori, M. & Gouaux, E. (2012): Molecular mechanism of ATP binding and ion channel activation in P2X receptors. *Nature* 485(7397). DOI 10.1038/nature11010.

Hausmann, R.; Kless, A. & Schmalzing, G. (2015): Key sites for P2X receptor function and multimerization: overview of mutagenesis studies on a structural basis. *Current medicinal chemistry* 22(7). DOI 10.2174/0929867322666141128163215.

Hazuda, D. J.; Strickler, J.; Kueppers, F.; Simon, P. L. & Young, P. R. (1990): Processing of precursor interleukin 1 beta and inflammatory disease. *Journal of Biological Chemistry* 265(11). DOI 10.1016/s0021-9258(19)39328-7.

Hazuda, D. J.; Strickler, J.; Simon, P. & Young, P. R. (1991): Structure-function mapping of interleukin 1 precursors. Cleavage leads to a conformational change in the mature protein. *Journal of Biological Chemistry* 266(11).

He, M.-L.; Koshimizu, T.; Tomić, M. & Stojilkovic, S. S. (2002): Purinergic P2X(2) receptor desensitization depends on coupling between ectodomain and C-terminal domain. *Molecular pharmacology* 62(5). DOI 10.1124/mol.62.5.1187.

He, W.; Wan, H.; Hu, L.; Chen, P.; Wang, X. & Huang, Z., et al. (2015): Gasdermin D is an executor of pyroptosis and required for interleukin-1β secretion. *Cell research* 25(12). DOI 10.1038/cr.2015.139.

He, Y.; Zeng, M. Y.; Yang, D.; Motro, B. & Núñez, G. (2016): NEK7 is an essential mediator of NLRP3 activation downstream of potassium efflux. *Nature* 530(7590). DOI 10.1038/nature16959.

Hecker, A.; Küllmar, M.; Wilker, S.; Richter, K.; Zakrzewicz, A. & Atanasova, S., et al. (2015): Phosphocholine-Modified Macromolecules and Canonical Nicotinic Agonists Inhibit ATP-Induced IL-1β Release. *Journal of immunology (Baltimore, Md. : 1950)* 195(5). DOI 10.4049/jimmunol.1400974.

Heink, S.; Yogev, N.; Garbers, C.; Herwerth, M.; Aly, L. & Gasperi, C., et al. (2017): Trans-presentation of IL-6 by dendritic cells is required for the priming of pathogenic TH17 cells. *Nature Immunology* 18(1). DOI 10.1038/ni.3632.

Heppner, F. L.; Greter, M.; Marino, D.; Falsig, J.; Raivich, G. & Hövelmeyer, N., et al. (2005): Experimental autoimmune encephalomyelitis repressed by microglial paralysis. *Nature medicine* 11(2). DOI 10.1038/nm1177.

Hiller, S. D.; Heldmann, S.; Richter, K.; Jurastow, I.; Küllmar, M. & Hecker, A., et al. (2018): β-Nicotinamide Adenine Dinucleotide (β-NAD) Inhibits ATP-Dependent IL-1β Release from Human Monocytic Cells. *International journal of molecular sciences* 19(4). DOI 10.3390/ijms19041126.

Hirano, T. (2021): IL-6 in inflammation, autoimmunity and cancer. *International immunology* 33(3). DOI 10.1093/intimm/dxaa078.

Hohl, T. M.; Rivera, A.; Lipuma, L.; Gallegos, A.; Shi, C. & Mack, M., et al. (2009): Inflammatory monocytes facilitate adaptive CD4 T cell responses during respiratory fungal infection. *Cell host & microbe* 6(5). DOI 10.1016/j.chom.2009.10.007.

Hoshino, K.; Takeuchi, O.; Kawai, T.; Sanjo, H.; Ogawa, T. & Takeda, Y., et al. (1999): Cutting edge: Toll-like receptor 4 (TLR4)-deficient mice are hyporesponsive to lipopolysaccharide: evidence for TLR4 as the Lps gene product. *Journal of immunology (Baltimore, Md. : 1950)* 162(7).

Howard, A. D.; Chartrain, N.; Ding, G. F.; Kostura, M. J.; Limjuco, G. & Schmidt, J. A., et al. (1991): Probing the role of interleukin-1 beta convertase in interleukin-1 beta secretion. *Agents and actions. Supplements* 35.

Hsieh, C. S.; Macatonia, S. E.; Tripp, C. S.; Wolf, S. F.; O'Garra, A. & Murphy, K. M. (1993): Development of TH1 CD4+ T cells through IL-12 produced by Listeria-induced macrophages. *Science (New York, N.Y.)* 260(5107). DOI 10.1126/science.8097338.

Hsu, H.; Xiong, J. & Goeddel, D. V. (1995): The TNF receptor 1-associated protein TRADD signals cell death and NF-kappa B activation. *Cell* 81(4). DOI 10.1016/0092-8674(95)90070-5.

Hu, L.; Yu, Y.; Huang, H.; Fan, H.; Hu, L. & Yin, C., et al. (2016): Epigenetic Regulation of Interleukin 6 by Histone Acetylation in Macrophages and Its Role in Paraquat-Induced Pulmonary Fibrosis. *Frontiers in Immunology* 7. DOI 10.3389/fimmu.2016.00696.

Huang, P.; Zou, Y.; Zhong, X. Z.; Cao, Q.; Zhao, K. & Zhu, M. X., et al. (2014): P2X4 forms functional ATP-activated cation channels on lysosomal membranes regulated by luminal pH. *Journal of Biological Chemistry* 289(25). DOI 10.1074/jbc.M114.552158.

Huang, T.-T.; Ojcius, D. M.; Young, J. D.; Wu, Y.-H.; Ko, Y.-F. & Wong, T.-Y., et al. (2012): The anti-tumorigenic mushroom Agaricus blazei Murill enhances IL-1β production and activates the NLRP3 inflammasome in human macrophages. *PLOS ONE* 7(7). DOI 10.1371/journal.pone.0041383.

Igawa, T.; Abe, Y.; Tsuda, M.; Inoue, K. & Ueda, T. (2015): Solution structure of the rat P2X4 receptor head domain involved in inhibitory metal binding. *FEBS Letters* 589(6). DOI 10.1016/j.febslet.2015.01.034.

Iliopoulos, D.; Hirsch, H. A. & Struhl, K. (2009): An epigenetic switch involving NF-kappaB, Lin28, Let-7 MicroRNA, and IL6 links inflammation to cell transformation. *Cell* 139(4). DOI 10.1016/j.cell.2009.10.014.

Iliopoulos, D.; Jaeger, S. A.; Hirsch, H. A.; Bulyk, M. L. & Struhl, K. (2010): STAT3 activation of miR-21 and miR-181b-1 via PTEN and CYLD are part of the epigenetic switch linking inflammation to cancer. *Molecular Cell* 39(4). DOI 10.1016/j.molcel.2010.07.023.

Imraish, A.; Abu-Thiab, T. & Hammad, H. (2023): P2X and P2Y receptor antagonists reduce inflammation in ATP-induced microglia. *Pharmacy practice* 21(1). DOI 10.18549/PharmPract.2023.1.2788.

Iwasaki, A. & Medzhitov, R. (2015): Control of adaptive immunity by the innate immune system. *Nature immunology* 16(4). DOI 10.1038/ni.3123.

Jakubzick, C.; Gautier, E. L.; Gibbings, S. L.; Sojka, D. K.; Schlitzer, A. & Johnson, T. E., et al. (2013): Minimal differentiation of classical monocytes as they survey steady-state tissues and transport antigen to lymph nodes. *Immunity* 39(3). DOI 10.1016/j.immuni.2013.08.007.

Jakubzick, C. V.; Randolph, G. J. & Henson, P. M. (2017): Monocyte differentiation and antigen-presenting functions. *Nature reviews. Immunology* 17(6). DOI 10.1038/nri.2017.28.

Janeway, C. A. (1989): Approaching the asymptote? Evolution and revolution in immunology. *Cold Spring Harbor symposia on quantitative biology* 54 Pt 1. DOI 10.1101/sqb.1989.054.01.003.

Jetten, N.; Verbruggen, S.; Gijbels, M. J.; Post, M. J.; Winther, M. P. J. de & Donners, M. M. P. C. (2014): Anti-inflammatory M2, but not pro-inflammatory M1 macrophages promote angiogenesis in vivo. *Angiogenesis* 17(1). DOI 10.1007/s10456-013-9381-6.

Jiang, L. H.; Rassendren, F.; Surprenant, A. & North, R. A. (2000): Identification of amino acid residues contributing to the ATP-binding site of a purinergic P2X receptor. *Journal of Biological Chemistry* 275(44). DOI 10.1074/jbc.M005481200.

Juarez, E.; Nuñez, C.; Sada, E.; Ellner, J. J.; Schwander, S. K. & Torres, M. (2010): Differential expression of Toll-like receptors on human alveolar macrophages and autologous peripheral monocytes. *Respiratory Research* 11(1). DOI 10.1186/1465-9921-11-2.

Julia, V.; Hessel, E. M.; Malherbe, L.; Glaichenhaus, N.; O'Garra, A. & Coffman, R. L. (2002): A restricted subset of dendritic cells captures airborne antigens and remains able to activate specific T cells long after antigen exposure. *Immunity* 16(2). DOI 10.1016/s1074-7613(02)00276-5.

Juliana, C.; Fernandes-Alnemri, T.; Kang, S.; Farias, A.; Qin, F. & Alnemri, E. S. (2012): Non-transcriptional priming and deubiquitination regulate NLRP3 inflammasome activation. *Journal of Biological Chemistry* 287(43). DOI 10.1074/jbc.M112.407130.

Kagan, J. C. & Medzhitov, R. (2006): Phosphoinositide-mediated adaptor recruitment controls Toll-like receptor signaling. *Cell* 125(5). DOI 10.1016/j.cell.2006.03.047.

Kagan, J. C.; Su, T.; Horng, T.; Chow, A.; Akira, S. & Medzhitov, R. (2008): TRAM couples endocytosis of Toll-like receptor 4 to the induction of interferon-beta. *Nature immunology* 9(4). DOI 10.1038/ni1569.

Kamada, N.; Hisamatsu, T.; Okamoto, S.; Chinen, H.; Kobayashi, T. & Sato, T., et al. (2008): Unique CD14 intestinal macrophages contribute to the pathogenesis of Crohn disease via IL-23/IFN-gamma axis. *The Journal of clinical investigation* 118(6). DOI 10.1172/JCI34610.

Kanellopoulos, J. M.; Almeida-da-Silva, C. L. C.; Rüütel Boudinot, S. & Ojcius, D. M. (2021): Structural and Functional Features of the P2X4 Receptor: An Immunological Perspective. *Frontiers in Immunology* 12. DOI 10.3389/fimmu.2021.645834.

Kasama, T.; Strieter, R. M.; Lukacs, N. W.; Burdick, M. D. & Kunkel, S. L. (1994): Regulation of neutrophil-derived chemokine expression by IL-10. *The Journal of Immunology* 152(7). DOI 10.4049/jimmunol.152.7.3559.

Kawano, A.; Tsukimoto, M.; Noguchi, T.; Hotta, N.; Harada, H. & Takenouchi, T., et al. (2012): Involvement of P2X4 receptor in P2X7 receptor-dependent cell death of mouse macrophages. *Biochemical and biophysical research communications* 419(2). DOI 10.1016/j.bbrc.2012.01.156.

Kawate, T.; Michel, J. C.; Birdsong, W. T. & Gouaux, E. (2009): Crystal structure of the ATP-gated P2X(4) ion channel in the closed state. *Nature* 460(7255). DOI 10.1038/nature08198.

Kelley, N.; Jeltema, D.; Duan, Y. & He, Y. (2019): The NLRP3 Inflammasome: An Overview of Mechanisms of Activation and Regulation. *International journal of molecular sciences* 20(13). DOI 10.3390/ijms20133328.

Kim, H. M.; Park, B. S.; Kim, J.-I.; Kim, S. E.; Lee, J. & Oh, S. C., et al. (2007): Crystal structure of the TLR4-MD-2 complex with bound endotoxin antagonist Eritoran. *Cell* 130(5). DOI 10.1016/j.cell.2007.08.002.

Kim, J.-E. & Kang, T.-C. (2011): The P2X7 receptor-pannexin-1 complex decreases muscarinic acetylcholine receptor-mediated seizure susceptibility in mice. *The Journal of Clinical Investigation* 121(5). DOI 10.1172/JCI44818.

Kim, M.; Jiang, L. H.; Wilson, H. L.; North, R. A. & Surprenant, A. (2001): Proteomic and functional evidence for a P2X7 receptor signalling complex. *The EMBO journal* 20(22). DOI 10.1093/emboj/20.22.6347.

Kim, S.-J.; Cha, J.-Y.; Kang, H. S.; Lee, J.-H.; Lee, J. Y. & Park, J.-H., et al. (2016): Corosolic acid ameliorates acute inflammation through inhibition of IRAK-1 phosphorylation in macrophages. *BMB reports* 49(5). DOI 10.5483/bmbrep.2016.49.5.241.

Kim, T. S. & Braciale, T. J. (2009): Respiratory dendritic cell subsets differ in their capacity to support the induction of virus-specific cytotoxic CD8+ T cell responses. *PloS one* 4(1). DOI 10.1371/journal.pone.0004204.

Kim, Y. K.; Hwang, J. H. & Lee, H. T. (2022): Differential susceptibility to lipopolysaccharide affects the activation of toll-like-receptor 4 signaling in THP-1 cells and PMA-differentiated THP-1 cells. *Innate immunity* 28(3-4). DOI 10.1177/17534259221100170.

Koch, S. R.; Lamb, F. S.; Hellman, J.; Sherwood, E. R. & Stark, R. J. (2017): Potentiation and tolerance of toll-like receptor priming in human endothelial cells. *Translational research : the journal of laboratory and clinical medicine* 180. DOI 10.1016/j.trsl.2016.08.001.

Kopp, R.; Krautloher, A.; Ramírez-Fernández, A. & Nicke, A. (2019): P2X7 interactions and signaling - making head or tail of it. *Frontiers in molecular neuroscience* 12. DOI 10.3389/fnmol.2019.00183.

Koshimizu, T.; Koshimizu, M. & Stojilkovic, S. S. (1999): Contributions of the C-terminal domain to the control of P2X receptor desensitization. *Journal of Biological Chemistry* 274(53). DOI 10.1074/jbc.274.53.37651.

Kurowska-Stolarska, M.; Stolarski, B.; Kewin, P.; Murphy, G.; Corrigan, C. J. & Ying, S., et al. (2009): IL-33 amplifies the polarization of alternatively activated macrophages that contribute to airway inflammation. *Journal of immunology (Baltimore, Md. : 1950)* 183(10). DOI 10.4049/jimmunol.0901575.

Kurynina, A. V.; Erokhina, M. V.; Makarevich, O. A.; Sysoeva, V. Y.; Lepekha, L. N. & Kuznetsov, S. A., et al. (2018): Plasticity of Human THP-1 Cell Phagocytic Activity during Macrophagic Differentiation. *Biochemistry. Biokhimiia* 83(3). DOI 10.1134/S0006297918030021.

Lamkanfi, M.; Kanneganti, T.-D.; van Damme, P.; Vanden Berghe, T.; Vanoverberghe, I. & Vandekerckhove, J., et al. (2008): Targeted peptidecentric proteomics reveals caspase-7 as a substrate of the caspase-1 inflammasomes. *Molecular & Cellular Proteomics* 7(12). DOI 10.1074/mcp.M800132-MCP200.

Lang, R.; Patel, D.; Morris, J. J.; Rutschman, R. L. & Murray, P. J. (2002): Shaping gene expression in activated and resting primary macrophages by IL-10. *The Journal of Immunology* 169(5). DOI 10.4049/jimmunol.169.5.2253.

Li, D. & Wu, M. (2021): Pattern recognition receptors in health and diseases. *Signal transduction and targeted therapy* 6(1). DOI 10.1038/s41392-021-00687-0.

Li, F.; Guo, N.; Ma, Y.; Ning, B.; Wang, Y. & Kou, L. (2014): Inhibition of P2X4 suppresses joint inflammation and damage in collagen-induced arthritis. *Inflammation* 37(1). DOI 10.1007/s10753-013-9723-y.

Liao, Y.; Luo, D.; Peng, K. & Zeng, Y. (2021): Cyclophilin A: a key player for etiological agent infection. *Applied microbiology and biotechnology* 105(4). DOI 10.1007/s00253-021-11115-2.

Lin, K.-M.; Hu, W.; Troutman, T. D.; Jennings, M.; Brewer, T. & Li, X., et al. (2014): IRAK-1 bypasses priming and directly links TLRs to rapid NLRP3 inflammasome activation. *Proceedings of the National Academy of Sciences of the United States of America* 111(2). DOI 10.1073/pnas.1320294111.

Lin, S.-C.; Lo, Y.-C. & Wu, H. (2010): Helical assembly in the MyD88-IRAK4-IRAK2 complex in TLR/IL-1R signalling. *Nature* 465(7300). DOI 10.1038/nature09121.

Liu, Z.; Sun, M.; Liu, W.; Feng, F.; Li, X. & Jin, C., et al. (2024): Deficiency of purinergic P2X4 receptor alleviates experimental autoimmune hepatitis in mice. *Biochemical pharmacology* 221. DOI 10.1016/j.bcp.2024.116033.

Lopez-Castejon, G.; Luheshi, N. M.; Compan, V.; High, S.; Whitehead, R. C. & Flitsch, S., et al. (2013): Deubiquitinases regulate the activity of caspase-1 and interleukin-1β secretion via assembly of the inflammasome. *Journal of Biological Chemistry* 288(4). DOI 10.1074/jbc.M112.422238.

Lu, W.; Albalawi, F.; Beckel, J. M.; Lim, J. C.; Laties, A. M. & Mitchell, C. H. (2017): The P2X7 receptor links mechanical strain to cytokine IL-6 up-regulation and release in neurons and astrocytes. *Journal of neurochemistry* 141(3). DOI 10.1111/jnc.13998.

Lust, J. A.; Donovan, K. A.; Kline, M. P.; Greipp, P. R.; Kyle, R. A. & Maihle, N. J. (1992): Isolation of an mRNA encoding a soluble form of the human interleukin-6 receptor. *Cytokine* 4(2). DOI 10.1016/1043-4666(92)90043-q.

Ma, J.; Gao, J.; Niu, M.; Zhang, X.; Wang, J. & Xie, A. (2020): P2X4R Overexpression Upregulates Interleukin-6 and Exacerbates 6-OHDA-Induced Dopaminergic Degeneration in a Rat Model of PD. *Frontiers in aging neuroscience* 12. DOI 10.3389/fnagi.2020.580068.

MacKenzie, A.; Wilson, H. L.; Kiss-Toth, E.; Dower, S. K.; North, R. A. & Surprenant, A. (2001): Rapid secretion of interleukin-1beta by microvesicle shedding. *Immunity* 15(5). DOI 10.1016/s1074-7613(01)00229-1.

Magni, L.; Bouazzi, R.; Heredero Olmedilla, H.; Petersen, P. S. S.; Tozzi, M. & Novak, I. (2021): The P2X7 Receptor Stimulates IL-6 Release from Pancreatic Stellate Cells and Tocilizumab Prevents Activation of STAT3 in Pancreatic Cancer Cells. *Cells* 10(8). DOI 10.3390/cells10081928.

Manji, G. A.; Wang, L.; Geddes, B. J.; Brown, M.; Merriam, S. & Al-Garawi, A., et al. (2002): PYPAF1, a PYRIN-containing Apaf1-like protein that assembles with ASC and regulates activation of NF-kappa B. *The Journal of biological chemistry* 277(13). DOI 10.1074/jbc.M112208200.

Mansoor, S. E.; Lü, W.; Oosterheert, W.; Shekhar, M.; Tajkhorshid, E. & Gouaux, E. (2016): X-ray structures define human P2X(3) receptor gating cycle and antagonist action. *Nature* 538(7623). DOI 10.1038/nature19367.

Mantovani, A.; Dinarello, C. A.; Molgora, M. & Garlanda, C. (2019): Interleukin-1 and related cytokines in the regulation of inflammation and immunity. *Immunity* 50(4). DOI 10.1016/j.immuni.2019.03.012.

Mantovani, A. & Garlanda, C. (2023): Humoral Innate Immunity and Acute-Phase Proteins. *The New England journal of medicine* 388(5). DOI 10.1056/NEJMra2206346.

Mantovani, A.; Sica, A.; Sozzani, S.; Allavena, P.; Vecchi, A. & Locati, M. (2004): The chemokine system in diverse forms of macrophage activation and polarization. *Trends in immunology* 25(12). DOI 10.1016/j.it.2004.09.015.

Mantovani, A.; Sozzani, S.; Locati, M.; Allavena, P. & Sica, A. (2002): Macrophage polarization: tumor-associated macrophages as a paradigm for polarized M2 mononuclear phagocytes. *Trends in immunology* 23(11). DOI 10.1016/S1471-4906(02)02302-5.

Mariathasan, S.; Weiss, D. S.; Newton, K.; McBride, J.; O'Rourke, K. & Roose-Girma, M., et al. (2006): Cryopyrin activates the inflammasome in response to toxins and ATP. *Nature* 440(7081). DOI 10.1038/nature04515.

Martinez, F. O.; Gordon, S.; Locati, M. & Mantovani, A. (2006): Transcriptional profiling of the human monocyte-to-macrophage differentiation and polarization: new molecules and patterns of gene expression. *The Journal of Immunology* 177(10). DOI 10.4049/jimmunol.177.10.7303.

Martinon, F.; Burns, K. & Tschopp, J. (2002): The Inflammasome. *Molecular Cell* 10(2). DOI 10.1016/S1097-2765(02)00599-3.

Masuda, K.; Ripley, B.; Nishimura, R.; Mino, T.; Takeuchi, O. & Shioi, G., et al. (2013): Arid5a controls IL-6 mRNA stability, which contributes to elevation of IL-6 level in vivo. *Proceedings of the National Academy of Sciences* 110(23). DOI 10.1073/pnas.1307419110.

Masuda, T.; Iwamoto, S.; Yoshinaga, R.; Tozaki-Saitoh, H.; Nishiyama, A. & Mak, T. W., et al. (2014): Transcription factor IRF5 drives P2X4R+-reactive microglia gating neuropathic pain. *Nature communications* 5. DOI 10.1038/ncomms4771.

Masuda, T.; Tsuda, M.; Yoshinaga, R.; Tozaki-Saitoh, H.; Ozato, K. & Tamura, T., et al. (2012): IRF8 is a critical transcription factor for transforming microglia into a reactive phenotype. *Cell reports* 1(4). DOI 10.1016/j.celrep.2012.02.014.

McEwan, T. B.-D.; Sophocleous, R. A.; Cuthbertson, P.; Mansfield, K. J.; Sanderson-Smith, M. L. & Sluyter, R. (2021): Autocrine regulation of wound healing by ATP release and P2Y2 receptor activation. *Life sciences* 283. DOI 10.1016/j.lfs.2021.119850.

Medzhitov, R.; Preston-Hurlburt, P. & Janeway, C. A. (1997): A human homologue of the Drosophila Toll protein signals activation of adaptive immunity. *Nature* 388(6640). DOI 10.1038/41131.

Meng, G.; Zhang, F.; Fuss, I.; Kitani, A. & Strober, W. (2009): A mutation in the Nlrp3 gene causing inflammasome hyperactivation potentiates Th17 cell-dominant immune responses. *Immunity* 30(6). DOI 10.1016/j.immuni.2009.04.012.

Mishra, V.; Crespo-Puig, A.; McCarthy, C.; Masonou, T.; Glegola-Madejska, I. & Dejoux, A., et al. (2023): IL-1β turnover by the UBE2L3 ubiquitin conjugating enzyme and HECT E3 ligases limits inflammation. *Nature communications* 14(1). DOI 10.1038/s41467-023-40054-x.

Montilla, A.; Mata, G. P.; Matute, C. & Domercq, M. (2020): Contribution of P2X4 Receptors to CNS Function and Pathophysiology. *International journal of molecular sciences* 21(15). DOI 10.3390/ijms21155562.

Mosley, B.; Urdal, D. L.; Prickett, K. S.; Larsen, A.; Cosman, D. & Conlon, P. J., et al. (1987): The interleukin-1 receptor binds the human interleukin-1 alpha precursor but not the interleukin-1 beta precursor. *Journal of Biological Chemistry* 262(7).

Munerati, M.; Cortesi, R.; Ferrari, D.; Di Virgilio, F. & Nastruzzi, C. (1994): Macrophages loaded with doxorubicin by ATP-mediated permeabilization: potential carriers for antitumor therapy. *Biochimica et biophysica acta* 1224(2). DOI 10.1016/0167-4889(94)90200-3.

Munoz, F. M.; Patel, P. A.; Gao, X.; Mei, Y.; Xia, J. & Gilels, S., et al. (2020): Reactive oxygen species play a role in P2X7 receptor-mediated IL-6 production in spinal astrocytes. *Purinergic signalling* 16(1). DOI 10.1007/s11302-020-09691-5.

Muñoz-Planillo, R.; Kuffa, P.; Martínez-Colón, G.; Smith, B. L.; Rajendiran, T. M. & Núñez, G. (2013): K^+ efflux is the common trigger of NLRP3 inflammasome activation by bacterial toxins and particulate matter. *Immunity* 38(6). DOI 10.1016/j.immuni.2013.05.016.

Muzio, M.; Bosisio, D.; Polentarutti, N.; D'amico, G.; Stoppacciaro, A. & Mancinelli, R., et al. (2000): Differential expression and regulation of toll-like receptors (TLR) in human leukocytes: selective expression of TLR3 in dendritic cells. *The Journal of Immunology* 164(11). DOI 10.4049/jimmunol.164.11.5998.

Nahrendorf, M. & Swirski, F. K. (2013): Monocyte and macrophage heterogeneity in the heart. *Circulation Research* 112(12). DOI 10.1161/CIRCRESAHA.113.300890.

Nahrendorf, M.; Swirski, F. K.; Aikawa, E.; Stangenberg, L.; Wurdinger, T. & Figueiredo, J.-L., et al. (2007): The healing myocardium sequentially mobilizes two monocyte subsets with divergent and complementary functions. *The Journal of experimental medicine* 204(12). DOI 10.1084/jem.20070885.

Nelms, K.; Keegan, A. D.; Zamorano, J.; Ryan, J. J. & Paul, W. E. (1999): The IL-4 receptor: signaling mechanisms and biologic functions. *Annual review of immunology* 17. DOI 10.1146/annurev.immunol.17.1.701.

Nelson, D. W.; Gregg, R. J.; Kort, M. E.; Perez-Medrano, A.; Voight, E. A. & Wang, Y., et al. (2006): Structure-activity relationship studies on a series of novel, substituted 1-benzyl-5-phenyltetrazole P2X7 antagonists. *Journal of medicinal chemistry* 49(12). DOI 10.1021/jm051202e.

Nicke, A. (2008): Homotrimeric complexes are the dominant assembly state of native P2X7 subunits. *Biochemical and biophysical research communications* 377(3). DOI 10.1016/j.bbrc.2008.10.042.

Nielsen, M. C.; Andersen, M. N. & Møller, H. J. (2020): Monocyte isolation techniques significantly impact the phenotype of both isolated monocytes and derived macrophages in vitro. *Immunology* 159(1). DOI 10.1111/imm.13125.

O'Farrell, A. M.; Liu, Y.; Moore, K. W. & Mui, A. L. (1998): IL-10 inhibits macrophage activation and proliferation by distinct signaling mechanisms: evidence for Stat3-dependent and -independent pathways. *The EMBO journal* 17(4). DOI 10.1093/emboj/17.4.1006.

O'Mahony, D. S.; Pham, U.; Iyer, R.; Hawn, T. R. & Liles, W. C. (2008): Differential constitutive and cytokine-modulated expression of human Toll-like receptors in primary neutrophils, monocytes, and macrophages. *International journal of medical sciences* 5(1). DOI 10.7150/ijms.5.1.

Palframan, R. T.; Jung, S.; Cheng, G.; Weninger, W.; Luo, Y. & Dorf, M., et al. (2001): Inflammatory chemokine transport and presentation in HEV: a remote control mechanism for monocyte recruitment to lymph nodes in inflamed tissues. *The Journal of experimental medicine* 194(9). DOI 10.1084/jem.194.9.1361.

Palinski, W.; Monti, M.; Camerlingo, R.; Iacobucci, I.; Bocella, S. & Pinto, F., et al. (2021): Lysosome purinergic receptor P2X4 regulates neoangiogenesis induced by microvesicles from sarcoma patients. *Cell Death & Disease* 12(9). DOI 10.1038/s41419-021-04069-w.

Park, B. S.; Song, D. H.; Kim, H. M.; Choi, B.-S.; Lee, H. & Lee, J.-O. (2009): The structural basis of lipopolysaccharide recognition by the TLR4-MD-2 complex. *Nature* 458(7242). DOI 10.1038/nature07830.

Pasqualetto, G.; Zuanon, M.; Brancale, A. & Young, M. T. (2023): Identification of the molecular determinants of antagonist potency in the allosteric binding pocket of human P2X4. *Frontiers in pharmacology* 14. DOI 10.3389/fphar.2023.1101023.

Passlick, B.; Flieger, D. & Ziegler-Heitbrock, H. W. (1989): Identification and characterization of a novel monocyte subpopulation in human peripheral blood. *Blood* 74(7).

Pelegrin, P. (2021): P2X7 receptor and the NLRP3 inflammasome: Partners in crime. *Biochemical pharmacology* 187. DOI 10.1016/j.bcp.2020.114385.

Pellegatti, P.; Falzoni, S.; Pinton, P.; Rizzuto, R. & Di Virgilio, F. (2005): A novel recombinant plasma membrane-targeted luciferase reveals a new pathway for ATP secretion. *Molecular biology of the cell* 16(8). DOI 10.1091/mbc.e05-03-0222.

Pellegatti, P.; Raffaghello, L.; Bianchi, G.; Piccardi, F.; Pistoia, V. & Di Virgilio, F. (2008): Increased level of extracellular ATP at tumor sites: in vivo imaging with plasma membrane luciferase. *PLOS ONE* 3(7). DOI 10.1371/journal.pone.0002599.

Perregaux, D. & Gabel, C. A. (1994): Interleukin-1 beta maturation and release in response to ATP and nigericin. Evidence that potassium depletion mediated by these agents is a necessary and common feature of their activity. *Journal of Biological Chemistry* 269(21). DOI 10.1016/S0021-9258(17)36591-2.

Perregaux, D. G.; McNiff, P.; Laliberte, R.; Conklyn, M. & Gabel, C. A. (2000): ATP acts as an agonist to promote stimulus-induced secretion of IL-1 beta and IL-18 in human blood. *The Journal of Immunology* 165(8). DOI 10.4049/jimmunol.165.8.4615.

Petes, C.; Wynick, C.; Guzzo, C.; Mehta, D.; Logan, S. & Banfield, B. W., et al. (2017): IL-27 enhances LPS-induced IL-1β in human monocytes and murine macrophages. *Journal of leukocyte biology* 102(1). DOI 10.1189/jlb.3A0316-098R.

Pippel, A.; Stolz, M.; Woltersdorf, R.; Kless, A.; Schmalzing, G. & Markwardt, F. (2017): Localization of the gate and selectivity filter of the full-length P2X7 receptor. *Proceedings of the National Academy of Sciences* 114(11). DOI 10.1073/pnas.1610414114.

Pizzirani, C.; Ferrari, D.; Chiozzi, P.; Adinolfi, E.; Sandonà, D. & Savaglio, E., et al. (2007): Stimulation of P2 receptors causes release of IL-1beta-loaded microvesicles from human dendritic cells. *Blood* 109(9). DOI 10.1182/blood-2005-06-031377.

Poltorak, A.; He, X.; Smirnova, I.; Liu, M. Y.; van Huffel, C. & Du, X., et al. (1998): Defective LPS signaling in C3H/HeJ and C57BL/10ScCr mice: mutations in Tlr4 gene. *Science (New York, N.Y.)* 282(5396). DOI 10.1126/science.282.5396.2085.

Py, B. F.; Kim, M.-S.; Vakifahmetoglu-Norberg, H. & Yuan, J. (2013): Deubiquitination of NLRP3 by BRCC3 critically regulates inflammasome activity. *Molecular Cell* 49(2). DOI 10.1016/j.molcel.2012.11.009.

Qu, Y.; Franchi, L.; Nunez, G. & Dubyak, G. R. (2007): Nonclassical IL-1 beta secretion stimulated by P2X7 receptors is dependent on inflammasome activation and correlated with exosome release in murine macrophages. *The Journal of Immunology* 179(3). DOI 10.4049/jimmunol.179.3.1913.

Qureshi, O. S.; Paramasivam, A.; Yu, J. C. H. & Murrell-Lagnado, R. D. (2007): Regulation of P2X4 receptors by lysosomal targeting, glycan protection and exocytosis. *Journal of Cell Science* 120(Pt 21). DOI 10.1242/jcs.010348.

Qureshi, S. T.; Larivière, L.; Leveque, G.; Clermont, S.; Moore, K. J. & Gros, P., et al. (1999): Endotoxin-tolerant mice have mutations in Toll-like receptor 4 (Tlr4). *The Journal of experimental medicine* 189(4). DOI 10.1084/jem.189.4.615.

Radke, L.; Giese, C.; Lubitz, A.; Hinderlich, S.; Sandig, G. & Hummel, M., et al. (2014): Reference gene stability in peripheral blood mononuclear cells determined by qPCR and NanoString. *Microchimica Acta* 181(13-14). DOI 10.1007/s00604-014-1221-x.

Radwan, M.; Stiefvater, R.; Grunert, T.; Sharif, O.; Miller, I. & Marchetti-Deschmann, M., et al. (2010): Tyrosine kinase 2 controls IL-1ß production at the translational level. *Journal of immunology (Baltimore, Md. : 1950)* 185(6). DOI 10.4049/jimmunol.0904000.

Ren, G.; Juhl, M.; Peng, Q.; Fink, T. & Porsborg, S. R. (2022): Selection and validation of reference genes for qPCR analysis of differentiation and maturation of THP-1 cells into M1 macrophage-like cells. *Immunology and cell biology* 100(10). DOI 10.1111/imcb.12590.

Richter, K.; Asci, N.; Singh, V. K.; Yakoob, S. H.; Meixner, M. & Zakrzewicz, A., et al. (2023a): Activation of endothelial NO synthase and P2X7 receptor modification mediates the cholinergic control of ATP-induced interleukin-1β release by mononuclear phagocytes. *Frontiers in immunology* 14. DOI 10.3389/fimmu.2023.1140592.

Richter, K.; Herz, S. M.; Stokes, C.; Damaj, M. I.; Grau, V. & Papke, R. L. (2023b): Pharmacological profiles and anti-inflammatory activity of pCN-diEPP and mCN-diEPP,

new alpha9alpha10 nicotinic receptor ligands. *Neuropharmacology* 240. DOI 10.1016/j.neuropharm.2023.109717.

Richter, K.; Koch, C.; Perniss, A.; Wolf, P. M.; Schweda, E. K. H. & Wichmann, S., et al. (2018a): Phosphocholine-Modified Lipooligosaccharides of Haemophilus influenzae Inhibit ATP-Induced IL-1β Release by Pulmonary Epithelial Cells. *Molecules (Basel, Switzerland)* 23(8). DOI 10.3390/molecules23081979.

Richter, K.; Ogiemwonyi-Schaefer, R.; Wilker, S.; Chaveiro, A. I.; Agné, A. & Hecker, M., et al. (2020): Amyloid Beta Peptide (Aβ1-42) Reverses the Cholinergic Control of Monocytic IL-1β Release. *Journal of clinical medicine* 9(9). DOI 10.3390/jcm9092887.

Richter, K.; Papke, R. L.; Stokes, C.; Roy, D. C.; Espinosa, E. S. & Wolf, P. M. K., et al. (2022): Comparison of the Anti-inflammatory Properties of Two Nicotinic Acetylcholine Receptor Ligands, Phosphocholine and pCF3-diEPP. *Frontiers in cellular neuroscience* 16. DOI 10.3389/fncel.2022.779081.

Richter, K.; Sagawe, S.; Hecker, A.; Küllmar, M.; Askevold, I. & Damm, J., et al. (2018b): C-Reactive Protein Stimulates Nicotinic Acetylcholine Receptors to Control ATP-Mediated Monocytic Inflammasome Activation. *Frontiers in immunology* 9. DOI 10.3389/fimmu.2018.01604.

Rietschel, E. T.; Kirikae, T.; Schade, F. U.; Mamat, U.; Schmidt, G. & Loppnow, H., et al. (1994): Bacterial endotoxin: molecular relationships of structure to activity and function. *FASEB journal : official publication of the Federation of American Societies for Experimental Biology* 8(2). DOI 10.1096/fasebj.8.2.8119492.

Rivero Vaccari, J. P. de; Bastien, D.; Yurcisin, G.; Pineau, I.; Dietrich, W. D. & Koninck, Y. de, et al. (2012): P2X4 receptors influence inflammasome activation after spinal cord injury. *The Journal of neuroscience : the official journal of the Society for Neuroscience* 32(9). DOI 10.1523/JNEUROSCI.4930-11.2012.

Roberts, J. A.; Digby, H. R.; Kara, M.; El Ajouz, S.; Sutcliffe, M. J. & Evans, R. J. (2008): Cysteine substitution mutagenesis and the effects of methanethiosulfonate reagents at P2X2 and P2X4 receptors support a core common mode of ATP action at P2X receptors. *Journal of Biological Chemistry* 283(29). DOI 10.1074/jbc.M800294200.

Roberts, J. A.; Valente, M.; Allsopp, R. C.; Watt, D. & Evans, R. J. (2009): Contribution of the region Glu181 to Val200 of the extracellular loop of the human P2X1 receptor to agonist binding and gating revealed using cysteine scanning mutagenesis. *Journal of neurochemistry* 109(4). DOI 10.1111/j.1471-4159.2009.06035.x.

Rokic, M. B.; Tvrdoňová, V.; Vávra, V.; Jindřichová, M.; Obšil, T. & Stojilkovic, S. S., et al. (2010): Roles of conserved ectodomain cysteines of the rat P2X4 purinoreceptor in agonist binding and channel gating. *Physiological Research*. DOI 10.33549/physiolres.931979.

Royle, S. J.; Bobanović, L. K. & Murrell-Lagnado, R. D. (2002): Identification of a non-canonical tyrosine-based endocytic motif in an ionotropic receptor. *Journal of Biological Chemistry* 277(38). DOI 10.1074/jbc.M204844200.

Ruiz-Alcaraz, A. J.; Carmona-Martínez, V.; Tristán-Manzano, M.; Machado-Linde, F.; Sánchez-Ferrer, M. L. & García-Peñarrubia, P., et al. (2018): Characterization of human peritoneal

monocyte/macrophage subsets in homeostasis: Phenotype, GATA6, phagocytic/oxidative activities and cytokines expression. *Scientific Reports* 8(1). DOI 10.1038/s41598-018-30787-x.

Ruiz-Alcaraz, A. J.; Tapia-Abellán, A.; Fernández-Fernández, M. D.; Tristán-Manzano, M.; Hernández-Caselles, T. & Sánchez-Velasco, E., et al. (2016): A novel CD14(high) CD16(high) subset of peritoneal macrophages from cirrhotic patients is associated to an increased response to LPS. *Molecular immunology* 72. DOI 10.1016/j.molimm.2016.02.012.

Rupert, C.; Dell' Aversana, C.; Mosca, L.; Montanaro, V.; Arcaniolo, D. & Sio, M. de, et al. (2023): Therapeutic targeting of P2X4 receptor and mitochondrial metabolism in clear cell renal carcinoma models. *Journal of experimental & clinical cancer research : CR* 42(1). DOI 10.1186/s13046-023-02713-1.

Sachet, M.; Liang, Y. Y. & Oehler, R. (2017): The immune response to secondary necrotic cells. *Apoptosis : an international journal on programmed cell death* 22(10). DOI 10.1007/s10495-017-1413-z.

Sakaki, H.; Fujiwaki, T.; Tsukimoto, M.; Kawano, A.; Harada, H. & Kojima, S. (2013): P2X4 receptor regulates P2X7 receptor-dependent IL-1β and IL-18 release in mouse bone marrow-derived dendritic cells. *Biochemical and biophysical research communications* 432(3). DOI 10.1016/j.bbrc.2013.01.135.

Sanman, L. E.; Qian, Y.; Eisele, N. A.; Ng, T. M.; van der Linden, W. A. & Monack, D. M., et al. (2016): Disruption of glycolytic flux is a signal for inflammasome signaling and pyroptotic cell death. *eLife* 5. DOI 10.7554/eLife.13663.

Saraiva, M.; Vieira, P. & O'Garra, A. (2020): Biology and therapeutic potential of interleukin-10. *The Journal of experimental medicine* 217(1). DOI 10.1084/jem.20190418.

Sathanoori, R.; Swärd, K.; Olde, B. & Erlinge, D. (2015): The ATP Receptors P2X7 and P2X4 Modulate High Glucose and Palmitate-Induced Inflammatory Responses in Endothelial Cells. *PLOS ONE* 10(5). DOI 10.1371/journal.pone.0125111.

Sato, S.; Takeuchi, O.; Fujita, T.; Tomizawa, H.; Takeda, K. & Akira, S. (2002): A variety of microbial components induce tolerance to lipopolysaccharide by differentially affecting MyD88-dependent and -independent pathways. *International immunology* 14(7). DOI 10.1093/intimm/dxf046.

Schildberger, A.; Rossmanith, E.; Eichhorn, T.; Strassl, K. & Weber, V. (2013): Monocytes, peripheral blood mononuclear cells, and THP-1 cells exhibit different cytokine expression patterns following stimulation with lipopolysaccharide. *Mediators of inflammation* 2013. DOI 10.1155/2013/697972.

Schindler, R.; Ghezzi, P. & Dinarello, C. A. (1990): IL-1 induces IL-1. IV. IFN-gamma suppresses IL-1 but not lipopolysaccharide-induced transcription of IL-1. *Journal of immunology (Baltimore, Md. : 1950)* 144(6).

Schmid-Burgk, J. L.; Chauhan, D.; Schmidt, T.; Ebert, T. S.; Reinhardt, J. & Endl, E., et al. (2016): A Genome-wide CRISPR (Clustered Regularly Interspaced Short Palindromic Repeats)

Screen Identifies NEK7 as an Essential Component of NLRP3 Inflammasome Activation. *Journal of Biological Chemistry* 291(1). DOI 10.1074/jbc.C115.700492.

Schneberger, D.; Aharonson-Raz, K. & Singh, B. (2011): Monocyte and macrophage heterogeneity and Toll-like receptors in the lung. *Cell and Tissue Research* 343(1). DOI 10.1007/s00441-010-1032-2.

Schneider, M.; Prudic, K.; Pippel, A.; Klapperstück, M.; Braam, U. & Müller, C. E., et al. (2017): Interaction of Purinergic P2X4 and P2X7 Receptor Subunits. *Frontiers in pharmacology* 8. DOI 10.3389/fphar.2017.00860.

Schroder, K.; Sagulenko, V.; Zamoshnikova, A.; Richards, A. A.; Cridland, J. A. & Irvine, K. M., et al. (2012): Acute lipopolysaccharide priming boosts inflammasome activation independently of inflammasome sensor induction. *Immunobiology* 217(12). DOI 10.1016/j.imbio.2012.07.020.

Schwende, H.; Fitzke, E.; Ambs, P. & Dieter, P. (1996): Differences in the state of differentiation of THP-1 cells induced by phorbol ester and 1,25-dihydroxyvitamin D3. *Journal of leukocyte biology* 59(4). DOI 10.1002/jlb.59.4.555.

Seong, S.-Y. & Matzinger, P. (2004): Hydrophobicity: an ancient damage-associated molecular pattern that initiates innate immune responses. *Nature reviews. Immunology* 4(6). DOI 10.1038/nri1372.

Serbina, N. V.; Salazar-Mather, T. P.; Biron, C. A.; Kuziel, W. A. & Pamer, E. G. (2003): TNF/iNOS-producing dendritic cells mediate innate immune defense against bacterial infection. *Immunity* 19(1). DOI 10.1016/s1074-7613(03)00171-7.

Shao, X.; Guha, S.; Lu, W.; Campagno, K. E.; Beckel, J. M. & Mills, J. A., et al. (2020): Polarized Cytokine Release Triggered by P2X7 Receptor from Retinal Pigmented Epithelial Cells Dependent on Calcium Influx. *Cells* 9(12). DOI 10.3390/cells9122537.

Shapouri-Moghaddam, A.; Mohammadian, S.; Vazini, H.; Taghadosi, M.; Esmaeili, S.-A. & Mardani, F., et al. (2018): Macrophage plasticity, polarization, and function in health and disease. *Journal of cellular physiology* 233(9). DOI 10.1002/jcp.26429.

Sharif, O.; Bolshakov, V. N.; Raines, S.; Newham, P. & Perkins, N. D. (2007): Transcriptional profiling of the LPS induced NF-kappaB response in macrophages. *BMC Immunology* 8(1). DOI 10.1186/1471-2172-8-1.

Shen, C.; Zhang, Y.; Cui, W.; Zhao, Y.; Sheng, D. & Teng, X., et al. (2023): Structural insights into the allosteric inhibition of P2X4 receptors. *Nature communications* 14(1). DOI 10.1038/s41467-023-42164-y.

Sheng, J.; Ruedl, C. & Karjalainen, K. (2015): Most Tissue-Resident Macrophages Except Microglia Are Derived from Fetal Hematopoietic Stem Cells. *Immunity* 43(2). DOI 10.1016/j.immuni.2015.07.016.

Shi, H.; Wang, Y.; Li, X.; Zhan, X.; Tang, M. & Fina, M., et al. (2016): NLRP3 activation and mitosis are mutually exclusive events coordinated by NEK7, a new inflammasome component. *Nature Immunology* 17(3). DOI 10.1038/ni.3333.

Shieh, C.-H.; Heinrich, A.; Serchov, T.; van Calker, D. & Biber, K. (2014): P2X7-dependent, but differentially regulated release of IL-6, CCL2, and TNF-α in cultured mouse microglia. *Glia* 62(4). DOI 10.1002/glia.22628.

Shimazu, R.; Akashi, S.; Ogata, H.; Nagai, Y.; Fukudome, K. & Miyake, K., et al. (1999): MD-2, a molecule that confers lipopolysaccharide responsiveness on Toll-like receptor 4. *The Journal of experimental medicine* 189(11). DOI 10.1084/jem.189.11.1777.

Shinozaki, Y.; Sumitomo, K.; Tsuda, M.; Koizumi, S.; Inoue, K. & Torimitsu, K. (2009): Direct observation of ATP-induced conformational changes in single P2X(4) receptors. *PLOS Biology* 7(5). DOI 10.1371/journal.pbio.1000103.

Sierra-Marquez, J.; Schaller, L.; Sassenbach, L.; Ramírez-Fernández, A.; Alt, P. & Rissiek, B., et al. (2024): Different localization of P2X4 and P2X7 receptors in native mouse lung - lack of evidence for a direct P2X4-P2X7 receptor interaction. *Frontiers in Immunology* 15. DOI 10.3389/fimmu.2024.1425938.

Sinadinos, A.; Young, C. N. J.; Al-Khalidi, R.; Teti, A.; Kalinski, P. & Mohamad, S., et al. (2015): P2RX7 purinoceptor: a therapeutic target for ameliorating the symptoms of duchenne muscular dystrophy. *PLoS medicine* 12(10). DOI 10.1371/journal.pmed.1001888.

Smythies, L. E.; Shen, R.; Bimczok, D.; Novak, L.; Clements, R. H. & Eckhoff, D. E., et al. (2010): Inflammation anergy in human intestinal macrophages is due to Smad-induced IkappaBalpha expression and NF-kappaB inactivation. *Journal of Biological Chemistry* 285(25). DOI 10.1074/jbc.M109.069955.

Solini, A.; Chiozzi, P.; Morelli, A.; Fellin, R. & Di Virgilio, F. (1999): Human primary fibroblasts in vitro express a purinergic P2X7 receptor coupled to ion fluxes, microvesicle formation and IL-6 release. *Journal of Cell Science* 112 (Pt 3)(3). DOI 10.1242/jcs.112.3.297.

Solle, M.; Labasi, J.; Perregaux, D. G.; Stam, E.; Petrushova, N. & Koller, B. H., et al. (2001): Altered cytokine production in mice lacking P2X(7) receptors. *Journal of Biological Chemistry* 276(1). DOI 10.1074/jbc.M006781200.

Song, N.; Liu, Z.-S.; Xue, W.; Bai, Z.-F.; Wang, Q.-Y. & Dai, J., et al. (2017): NLRP3 Phosphorylation Is an Essential Priming Event for Inflammasome Activation. *Molecular Cell* 68(1). DOI 10.1016/j.molcel.2017.08.017.

Sophocleous, R. A.; Berg, T.; Finol-Urdaneta, R. K.; Sluyter, V.; Keshiya, S. & Bell, L., et al. (2020): Pharmacological and genetic characterisation of the canine P2X4 receptor. *British journal of pharmacology* 177(12). DOI 10.1111/bph.15009.

Srinivasula, S. M.; Poyet, J.-L.; Razmara, M.; Datta, P.; Zhang, Z. & Alnemri, E. S. (2002): The PYRIN-CARD protein ASC is an activating adaptor for caspase-1. *Journal of Biological Chemistry* 277(24). DOI 10.1074/jbc.C200179200.

Stein, M.; Keshav, S.; Harris, N. & Gordon, S. (1992): Interleukin 4 potently enhances murine macrophage mannose receptor activity: a marker of alternative immunologic macrophage activation. *Journal of Experimental Medicine* 176(1). DOI 10.1084/jem.176.1.287.

Surprenant, A.; Rassendren, F.; Kawashima, E.; North, R. A. & Buell, G. (1996): The cytolytic P2Z receptor for extracellular ATP identified as a P2X receptor (P2X7). *Science (New York, N.Y.)* 272(5262). DOI 10.1126/science.272.5262.735.

Swirski, F. K.; Libby, P.; Aikawa, E.; Alcaide, P.; Luscinskas, F. W. & Weissleder, R., et al. (2007): Ly-6Chi monocytes dominate hypercholesterolemia-associated monocytosis and give rise to macrophages in atheromata. *The Journal of clinical investigation* 117(1). DOI 10.1172/JCI29950.

Swirski, F. K.; Pittet, M. J.; Kircher, M. F.; Aikawa, E.; Jaffer, F. A. & Libby, P., et al. (2006): Monocyte accumulation in mouse atherogenesis is progressive and proportional to extent of disease. *Proceedings of the National Academy of Sciences of the United States of America* 103(27). DOI 10.1073/pnas.0604260103.

Taabazuing, C. Y.; Okondo, M. C. & Bachovchin, D. A. (2017): Pyroptosis and Apoptosis Pathways Engage in Bidirectional Crosstalk in Monocytes and Macrophages. *Cell chemical biology* 24(4). DOI 10.1016/j.chembiol.2017.03.009.

Tacke, F.; Alvarez, D.; Kaplan, T. J.; Jakubzick, C.; Spanbroek, R. & Llodra, J., et al. (2007): Monocyte subsets differentially employ CCR2, CCR5, and CX3CR1 to accumulate within atherosclerotic plaques. *The Journal of clinical investigation* 117(1). DOI 10.1172/JCI28549.

Tan, Y.; Zanoni, I.; Cullen, T. W.; Goodman, A. L. & Kagan, J. C. (2015): Mechanisms of Toll-like Receptor 4 Endocytosis Reveal a Common Immune-Evasion Strategy Used by Pathogenic and Commensal Bacteria. *Immunity* 43(5). DOI 10.1016/j.immuni.2015.10.008.

Tang, H.-Y.; Chen, X.-Q.; Wang, H.; Chu, H.-R.; Zhu, C.-F. & Huang, S., et al. (2022): Acupuncture relieves the visceral pain of diarrhea-predominant irritable bowel syndrome rats by regulating P2X4 expression. *American Journal of Translational Research* 14(8).

Ting, J. P.-Y.; Lovering, R. C.; Alnemri, E. S.; Bertin, J.; Boss, J. M. & Davis, B. K., et al. (2008): The NLR gene family: a standard nomenclature. *Immunity* 28(3). DOI 10.1016/j.immuni.2008.02.005.

Torre-Minguela, C. de; Barberà-Cremades, M.; Gómez, A. I.; Martín-Sánchez, F. & Pelegrín, P. (2016): Macrophage activation and polarization modify P2X7 receptor secretome influencing the inflammatory process. *Scientific Reports* 6. DOI 10.1038/srep22586.

Torres, G. E.; Egan, T. M. & Voigt, M. M. (1999): Hetero-oligomeric assembly of P2X receptor subunits. Specificities exist with regard to possible partners. *Journal of Biological Chemistry* 274(10). DOI 10.1074/jbc.274.10.6653.

Trang, M.; Schmalzing, G.; Müller, C. E. & Markwardt, F. (2020): Dissection of P2X4 and P2X7 Receptor Current Components in BV-2 Microglia. *International journal of molecular sciences* 21(22). DOI 10.3390/ijms21228489.

Triantafilou, M.; Miyake, K.; Golenbock, D. T. & Triantafilou, K. (2002): Mediators of innate immune recognition of bacteria concentrate in lipid rafts and facilitate lipopolysaccharide-induced cell activation. *Journal of Cell Science* 115(Pt 12). DOI 10.1242/jcs.115.12.2603.

Tsuchiya, S.; Kobayashi, Y.; Goto, Y.; Okumura, H.; Nakae, S. & Konno, T., et al. (1982): Induction of Maturation in Cultured Human Monocytic Leukemia Cells by a Phorbol Diester. *Cancer Research* 42(4).

Tsuchiya, S.; Yamabe, M.; Yamaguchi, Y.; Kobayashi, Y.; Konno, T. & Tada, K. (1980): Establishment and characterization of a human acute monocytic leukemia cell line (THP-1). *International journal of cancer* 26(2). DOI 10.1002/ijc.2910260208.

Tsujioka, H.; Imanishi, T.; Ikejima, H.; Kuroi, A.; Takarada, S. & Tanimoto, T., et al. (2009): Impact of heterogeneity of human peripheral blood monocyte subsets on myocardial salvage in patients with primary acute myocardial infarction. *Journal of the American College of Cardiology* 54(2). DOI 10.1016/j.jacc.2009.04.021.

Uderhardt, S.; Martins, A. J.; Tsang, J. S.; Lämmermann, T. & Germain, R. N. (2019): Resident Macrophages Cloak Tissue Microlesions to Prevent Neutrophil-Driven Inflammatory Damage. *Cell* 177(3). DOI 10.1016/j.cell.2019.02.028.

Vajjhala, P. R.; Mirams, R. E. & Hill, J. M. (2012): Multiple binding sites on the pyrin domain of ASC protein allow self-association and interaction with NLRP3 protein. *Journal of Biological Chemistry* 287(50). DOI 10.1074/jbc.M112.381228.

Valera, S.; Hussy, N.; Evans, R. J.; Adami, N.; North, R. A. & Surprenant, A., et al. (1994): A new class of ligand-gated ion channel defined by P2x receptor for extracellular ATP. *Nature* 371(6497). DOI 10.1038/371516a0.

van Furth, R.; Cohn, Z. A.; Hirsch, J. G.; Humphrey, J. H.; Spector, W. G. & Langevoort, H. L. (1972): The mononuclear phagocyte system: a new classification of macrophages, monocytes, and their precursor cells. *Bulletin of the World Health Organization* 46(6).

Vázquez-Villoldo, N.; Domercq, M.; Martín, A.; Llop, J.; Gómez-Vallejo, V. & Matute, C. (2014): P2X4 receptors control the fate and survival of activated microglia. *Glia* 62(2). DOI 10.1002/glia.22596.

Verreck, F. A. W.; Boer, T. de; Langenberg, D. M. L.; Hoeve, M. A.; Kramer, M. & Vaisberg, E., et al. (2004): Human IL-23-producing type 1 macrophages promote but IL-10-producing type 2 macrophages subvert immunity to (myco)bacteria. *Proceedings of the National Academy of Sciences* 101(13). DOI 10.1073/pnas.0400983101.

Vijay, K. (2018): Toll-like receptors in immunity and inflammatory diseases: Past, present, and future. *International immunopharmacology* 59. DOI 10.1016/j.intimp.2018.03.002.

Vijayaraj, S. L.; Feltham, R.; Rashidi, M.; Frank, D.; Liu, Z. & Simpson, D. S., et al. (2021): The ubiquitylation of IL-1β limits its cleavage by caspase-1 and targets it for proteasomal degradation. *Nature communications* 12(1). DOI 10.1038/s41467-021-22979-3.

Visintin, A.; Mazzoni, A.; Spitzer, J. A. & Segal, D. M. (2001): Secreted MD-2 is a large polymeric protein that efficiently confers lipopolysaccharide sensitivity to Toll-like receptor 4. *Proceedings of the National Academy of Sciences of the United States of America* 98(21). DOI 10.1073/pnas.211445098.

Waal Malefyt, R. de; Abrams, J.; Bennett, B.; Figdor, C. G. & Vries, J. E. de (1991): Interleukin 10(IL-10) inhibits cytokine synthesis by human monocytes: an autoregulatory role of IL-10 produced by monocytes. *Journal of Experimental Medicine* 174(5). DOI 10.1084/jem.174.5.1209.

Wang, C.; Deng, L.; Hong, M.; Akkaraju, G. R.; Inoue, J. & Chen, Z. J. (2001): TAK1 is a ubiquitin-dependent kinase of MKK and IKK. *Nature* 412(6844). DOI 10.1038/35085597.

Ward, J. R.; West, P. W.; Ariaans, M. P.; Parker, L. C.; Francis, S. E. & Crossman, D. C., et al. (2010): Temporal interleukin-1beta secretion from primary human peripheral blood monocytes by P2X7-independent and P2X7-dependent mechanisms. *Journal of Biological Chemistry* 285(30). DOI 10.1074/jbc.M109.072793.

Warny, M. & Kelly, C. P. (1999): Monocytic cell necrosis is mediated by potassium depletion and caspase-like proteases. *The American journal of physiology* 276(3). DOI 10.1152/ajpcell.1999.276.3.C717.

Watanabe, N.; Kawaguchi, M. & Kobayashi, Y. (1998): Activation of interleukin-1beta-converting enzyme by nigericin is independent of apoptosis. *Cytokine* 10(9). DOI 10.1006/cyto.1998.0341.

Weinhold, K.; Krause-Buchholz, U.; Rödel, G.; Kasper, M. & Barth, K. (2010): Interaction and interrelation of P2X7 and P2X4 receptor complexes in mouse lung epithelial cells. *Cellular and molecular life sciences : CMLS* 67(15). DOI 10.1007/s00018-010-0355-1.

Werner, P.; Seward, E. P.; Buell, G. N. & North, R. A. (1996): Domains of P2X receptors involved in desensitization. *Proceedings of the National Academy of Sciences* 93(26). DOI 10.1073/pnas.93.26.15485.

Wilhelm, K.; Ganesan, J.; Müller, T.; Dürr, C.; Grimm, M. & Beilhack, A., et al. (2010): Graft-versus-host disease is enhanced by extracellular ATP activating P2X7R. *Nature Medicine* 16(12). DOI 10.1038/nm.2242.

Wright, S. D.; Ramos, R. A.; Tobias, P. S.; Ulevitch, R. J. & Mathison, J. C. (1990): CD14, a receptor for complexes of lipopolysaccharide (LPS) and LPS binding protein. *Science (New York, N.Y.)* 249(4975). DOI 10.1126/science.1698311.

Wu, L.; Bai, S.; Huang, J.; Cui, G.; Li, Q. & Wang, J., et al. (2023): Nigericin Boosts Anti-Tumor Immune Response via Inducing Pyroptosis in Triple-Negative Breast Cancer. *Cancers* 15(12). DOI 10.3390/cancers15123221.

Xiao, J.; Huang, Y.; Li, X.; Li, L.; Yang, T. & Huang, L., et al. (2016): TNP-ATP is Beneficial for Treatment of Neonatal Hypoxia-Induced Hypomyelination and Cognitive Decline. *Neuroscience Bulletin* 32(1). DOI 10.1007/s12264-015-0003-8.

Xu, J.; Chai, H.; Ehinger, K.; Egan, T. M.; Srinivasan, R. & Frick, M., et al. (2014): Imaging P2X4 receptor subcellular distribution, trafficking, and regulation using P2X4-pHluorin. *Journal of General Physiology* 144(1). DOI 10.1085/jgp.201411169.

Yang, D.; He, Y.; Muñoz-Planillo, R.; Liu, Q. & Núñez, G. (2015): Caspase-11 Requires the Pannexin-1 Channel and the Purinergic P2X7 Pore to Mediate Pyroptosis and Endotoxic Shock. *Immunity* 43(5). DOI 10.1016/j.immuni.2015.10.009.

Yasuda, K.; Nakanishi, K. & Tsutsui, H. (2019): Interleukin-18 in Health and Disease. *International journal of molecular sciences* 20(3). DOI 10.3390/ijms20030649.

Yona, S.; Kim, K.-W.; Wolf, Y.; Mildner, A.; Varol, D. & Breker, M., et al. (2013): Fate mapping reveals origins and dynamics of monocytes and tissue macrophages under homeostasis. *Immunity* 38(1). DOI 10.1016/j.immuni.2012.12.001.

Yoshida, K.; Ito, M. & Matsuoka, I. (2017): Divergent regulatory roles of extracellular ATP in the degranulation response of mouse bone marrow-derived mast cells. *International immunopharmacology* 43. DOI 10.1016/j.intimp.2016.12.014.

Yoshida, K.; Ito, M.-A.; Sato, N.; Obayashi, K.; Yamamoto, K. & Koizumi, S., et al. (2020): Extracellular ATP Augments Antigen-Induced Murine Mast Cell Degranulation and Allergic Responses via P2X4 Receptor Activation. *Journal of immunology (Baltimore, Md. : 1950)* 204(12). DOI 10.4049/jimmunol.1900954.

Young, M. T.; Pelegrin, P. & Surprenant, A. (2006): Identification of Thr283 as a key determinant of P2X7 receptor function. *British journal of pharmacology* 149(3). DOI 10.1038/sj.bjp.0706880.

Young, M. T.; Pelegrin, P. & Surprenant, A. (2007): Amino acid residues in the P2X7 receptor that mediate differential sensitivity to ATP and BzATP. *Molecular pharmacology* 71(1). DOI 10.1124/mol.106.030163.

Yuan, H.; Lu, B.; Ji, Y.; Meng, B.; Wang, R. & Sun, D., et al. (2022): Role of P2X4/NLRP3 Pathway-Mediated Neuroinflammation in Perioperative Neurocognitive Disorders. *Mediators of inflammation* 2022. DOI 10.1155/2022/6355805.

Zabala, A.; Vazquez-Villoldo, N.; Rissiek, B.; Gejo, J.; Martin, A. & Palomino, A., et al. (2018): P2X4 receptor controls microglia activation and favors remyelination in autoimmune encephalitis. *EMBO molecular medicine* 10(8). DOI 10.15252/emmm.201708743.

Zasłona, Z.; Pålsson-McDermott, E. M.; Menon, D.; Haneklaus, M.; Flis, E. & Prendeville, H., et al. (2017): The Induction of Pro-IL-1β by Lipopolysaccharide Requires Endogenous Prostaglandin E2 Production. *Journal of immunology (Baltimore, Md. : 1950)* 198(9). DOI 10.4049/jimmunol.1602072.

Zech, A.; Wiesler, B.; Ayata, C. K.; Schlaich, T.; Dürk, T. & Hoßfeld, M., et al. (2016): P2rx4 deficiency in mice alleviates allergen-induced airway inflammation. *Oncotarget* 7(49). DOI 10.18632/oncotarget.13375.

Zhang, L.; Liu, Y.; Wang, B.; Xu, G.; Yang, Z. & Tang, M., et al. (2018): POH1 deubiquitinates pro-interleukin-1β and restricts inflammasome activity. *Nature communications* 9(1). DOI 10.1038/s41467-018-06455-z.

Zhang, X.; Cheng, Y.; Xiong, Y.; Ye, C.; Zheng, H. & Sun, H., et al. (2012): Enterohemorrhagic Escherichia coli specific enterohemolysin induced IL-1β in human macrophages and EHEC-induced IL-1β required activation of NLRP3 inflammasome. *PLOS ONE* 7(11). DOI 10.1371/journal.pone.0050288.

Zheng, S.-C.; Zhu, X.-X.; Xue, Y.; Zhang, L.-H.; Zou, H.-J. & Qiu, J.-H., et al. (2015): Role of the NLRP3 inflammasome in the transient release of IL-1β induced by monosodium urate crystals in human fibroblast-like synoviocytes. *Journal of inflammation (London, England)* 12. DOI 10.1186/s12950-015-0070-7.

Zhou, Z.; Li, X.; Qian, Y.; Liu, C.; Huang, X. & Fu, M. (2020): Heat shock protein 90 inhibitors suppress pyroptosis in THP-1 cells. *The Biochemical journal* 477(20). DOI 10.1042/BCJ20200351.

Ziegler-Heitbrock, L.; Ancuta, P.; Crowe, S.; Dalod, M.; Grau, V. & Hart, D. N., et al. (2010): Nomenclature of monocytes and dendritic cells in blood. *Blood* 116(16). DOI 10.1182/blood-2010-02-258558.

Zindel, J. & Kubes, P. (2020): DAMPs, PAMPs, and LAMPs in Immunity and Sterile Inflammation. *Annual review of pathology* 15. DOI 10.1146/annurev-pathmechdis-012419-032847.

SUPPLEMENTS

Table S-1: LDH activity [%] in supernatants of monocytic THP-1 cells. Incubation with LPS [1 µg/ml] for 5 h, with BzATP / nigericin for 40 min. ①, incubation prior to LPS-priming. ②, incubation prior to BzATP / nigericin. LPS, lipopolysaccharide; BzATP, 2'(3')-O-(4-Benzoylbenzoyl)adenosine-5'-triphosphate; 5-B, 5-(3-Bromophenyl)-1,3-dihydro-2H-benzofuro[3,2-e]-1,4-diazepin-2-one; PSB, PSB-15417; PZB15, PZB15517166A; PZB13, PZB13420052A; A43, 3-{[5-(2,3-dichlorophenyl)-1H-1,2,3,4-tetrazol-1-yl]methyl}pyridine; JNJ, N-[[4-(4-phenylpiperazin-1-yl)oxan-4-yl]methyl]-2-phenylsulfanylpyridine-3-carboxamide; LDH, lactate dehydrogenase; min, minimum; max, maximum; n, number of individual experiments.

Figures	Treatment	LDH activity [%] median (min, max)	n
6, 9, 14, 15, 20, 24, 27, 31	Untreated	4.6 (1.1, 12.3)	78
31	Doxorubicin [2.5 µM]	6.5 (4.0, 10.0)	6
31	Doxorubicin [2.5 µM], Z-VAD-FMK [10 µM]	12.5 (4.0, 20.0)	6
6, 9, 14, 15, 20, 24, 27, 31	LPS	5.0 (1.3, 22.0)	77
9, 14, 15, 20, 24, 27	LPS, 5-B [10 µM] ①	10.1 (4.2, 18.4)	18
9, 14, 15, 20, 24, 27	LPS, PSB [10 µM] ①	8.6 (2.4, 11.6)	6
9, 14, 15, 20, 24, 27	LPS, PZB15 [10 µM] ①	7.5 (5.1, 11.7)	6
9, 14, 15, 20, 24, 27	LPS, PZB13 [10 µM] ①	6.7 (4.0, 14.0)	6
9, 14, 15, 20, 24, 27	LPS, A43 [10 µM] ①	3.6 (2.6, 5.6)	6
9, 14, 15, 20, 24, 27	LPS, JNJ [1 µM] ①	5.4 (4.6, 11.3)	6
31	LPS, Doxorubicin [2.5 µM]	11.0 (5.0, 21.0)	6
31	LPS, Doxorubicin [2.5 µM,] Z-VAD-FMK [10 µM]	17.5 (6.0, 27.0)	6
6, 9, 31	LPS, BzATP [100 µM]	6.3 (3.0, 18.0)	30
6, 9	LPS, DMSO [0.1 %] ①, BzATP [100 µM]	6.7 (3.0, 15.3)	21
9	LPS, 5-B [10 µM] ①, BzATP [100 µM]	7.9 (4.7, 19.2)	6
9	LPS, 5-B [20 µM] ①, BzATP [100 µM]	10.1 (6.0, 21.2)	6
9	LPS, PSB [10 µM] ①, BzATP [100 µM]	6.0 (3.0, 10.8)	6
9	LPS, PZB15 [10 µM] ①, BzATP [100 µM]	8.2 (4.0, 16.5)	6
9	LPS, PZB13 [10 µM] ①, BzATP [100 µM]	9.6 (3.0, 19.2)	6
9	LPS, A43 [10 µM] ①, BzATP [100 µM]	7.2 (2.7, 14.5)	15
S-1	LPS, JNJ [0.01 µM] ①, BzATP [100 µM]	7.3 (4.9, 15.1)	6
S-1	LPS, JNJ [0.1 µM] ①, BzATP [100 µM]	11.8 (7.0, 22.8)	6
9, S-1	LPS, JNJ [1 µM] ①, BzATP [100 µM]	7.3 (3.0, 15.0)	12
S-1	LPS, JNJ [5 µM] ①, BzATP [100 µM]	10.9 (7.8, 19.4)	6
S-1	LPS, JNJ [10 µM] ①, BzATP [100 µM]	9.7 (5.4, 21.4)	6
9	LPS, 5-B [10 µM] ②, BzATP [100 µM]	12.1 (5.3, 17.9)	6
9	LPS, 5-B [20 µM] ②, BzATP [100 µM]	9.7 (6.0, 19.8)	6
9	LPS, PSB [10 µM] ②, BzATP [100 µM]	8.5 (5.0, 17.9)	6
9	LPS, PZB15 [10 µM] ②, BzATP [100 µM]	8.8 (5.0, 20.1)	6
9	LPS, PZB13 [10 µM] ②, BzATP [100 µM]	9.0 (5.0, 14.1)	6
9	LPS, A43 [10 µM] ②, BzATP [100 µM]	8.9 (2.9, 14.4)	15
S-1	LPS, JNJ [0.01 µM] ②, BzATP [100 µM]	10.3 (7.3, 13.0)	6
S-1	LPS, JNJ [0.1 µM] ②, BzATP [100 µM]	17.1 (9.5, 24.4)	6
9, S-1	LPS, JNJ [1 µM] ②, BzATP [100 µM]	7.6 (4.5, 15.9)	12

S-1	LPS, JNJ [5 μM] ②, BzATP [100 μM]	10.3 (7.9, 20.8)	6
S-1	LPS, JNJ [10 μM] ②, BzATP [100 μM]	11.1 (8.0, 23.6)	6
31	LPS, Z-VAD-FMK [10 μM], BzATP [100 μM]	12.5 (4.0, 24.0)	6
9, 14, 15, 31	LPS, nigericin [50 μM]	13.1 (4.5, 33.0)	57
6, 14, 15	LPS, DMSO [0.1 %] ①, nigericin [50 μM]	13.1 (3.6, 28.8)	51
14, 15	LPS, 5-B [10 μM] ①, nigericin [50 μM]	19.4 (5.4, 59.2)	36
15	LPS, 5-B [10 μM] ①, PSB [10 μM] ①, nigericin [50 μM]	16.9 (9.6, 30.7)	6
15	LPS, 5-B [10 μM] ①, PZB15 [10 μM] ①, nigericin [50 μM]	15.6 (13.0, 18.8)	6
15	LPS, 5-B [10 μM] ①, PZB13 [10 μM] ①, nigericin [50 μM]	26.8 (21.2, 31.9)	6
15	LPS, 5-B [10 μM] ①, A43 [10 μM] ①, nigericin [50 μM]	23.9 (19.8, 36.9)	6
15	LPS, 5-B [10 μM] ①, JNJ [1 μM] ①, nigericin [50 μM]	27.8 (22.8, 41.1)	6
15	LPS, 5-B [10 μM] ①, 5-B [10 μM] ②, nigericin [50 μM]	20.7 (15.2, 33.3)	6
15	LPS, 5-B [10 μM] ①, PSB [10 μM] ②, nigericin [50 μM]	16.4 (11.2, 22.0)	6
15	LPS, 5-B [10 μM] ①, PZB15 [10 μM] ②, nigericin [50 μM]	15.4 (10.7, 25.5)	6
15	LPS, 5-B [10 μM] ①, PZB13 [10 μM] ②, nigericin [50 μM]	14.8 (9.5, 26.7)	6
15	LPS, 5-B [10 μM] ①, A43 [10 μM] ②, nigericin [50 μM]	15.9 (12.7, 27.1)	6
15	LPS, 5-B [10 μM] ①, JNJ [1 μM] ②, nigericin [50 μM]	18.0 (12.6, 32.0)	6
14	LPS, PSB [10 μM] ①, nigericin [50 μM]]	12.4 (3.8, 28.2)	12
14	LPS, PZB15 [10 μM] ①, nigericin [50 μM]	11.5 (4.3, 28.8)	12
14	LPS, PZB13 [10 μM] ①, nigericin [50 μM]	14.7 (3.4, 29.1)	27
15	LPS, PZB13 [10 μM] ①, 5-B [10 μM] ①, nigericin [50 μM]	26.7 (13.9, 36.4)	6
15	LPS, PZB13 [10 μM] ①, PSB [10 μM] ①, nigericin [50 μM]	19.6 (12.1, 32.2)	6
15	LPS, PZB13 [10 μM] ①, PZB15 [10 μM] ①, nigericin [50 μM]	23.6 (13.1, 44.0)	6
15	LPS, PZB13 [10 μM] ①, A43 [10 μM] ①, nigericin [50 μM]	24.5 (10.8, 44.1)	6
15	LPS, PZB13 [10 μM] ①, JNJ [1 μM] ①, nigericin [50 μM]	29.7 (13.9, 49.7)	6
15	LPS, PZB13 [10 μM] ①, 5-B [10 μM] ②, nigericin [50 μM]	20.4 (8.4, 27.9)	9
15	LPS, PZB13 [10 μM] ①, PSB [10 μM] ②, nigericin [50 μM]	17.0 (5.4, 30.9)	9
15	LPS, PZB13 [10 μM] ①, PZB15 [10 μM] ②, nigericin [50 μM]	20.6 (6.7, 40.3)	9
15	LPS, PZB13 [10 μM] ①, PZB13 [10 μM] ②, nigericin [50 μM]	15.9 (5.1, 38.1)	9
15	LPS, PZB13 [10 μM] ①, A43 [10 μM] ②, nigericin [50 μM]	19.4 (8.1, 38.4)	9
15	LPS, PZB13 [10 μM] ①, JNJ [1 μM] ②, nigericin [50 μM]	18.5 (7.5, 38.1)	9
14	LPS, A43 [10 μM] ①, nigericin [50 μM]	14.8 (4.4, 32.8)	12
14	LPS, JNJ [1 μM] ①, nigericin [50 μM]]	20.5 (7.3, 35.7)	6
14	LPS, 5-B [10 μM] ②, nigericin [50 μM]	15.1 (7.5, 20.0)	6
14	LPS, PSB [10 μM] ②, nigericin [50 μM]]	12.3 (6.7, 18.5)	6
14	LPS, PZB15 [10 μM] ②, nigericin [50 μM]	13.2 (5.7, 17.0)	6
14	LPS, PZB13 [10 μM] ②, nigericin [50 μM]	14.7 (6.7, 20.2)	6
14	LPS, A43 [10 μM] ②, nigericin [50 μM]	9.9 (5.4, 18.2)	6
14	LPS, JNJ [1 μM] ②, nigericin [50 μM]]	20.7 (5.9, 37.8)	6
31	LPS, Z-VAD-FMK [10 μM], nigericin [50 μM]	37.0 (24.0, 43.0)	6

Table S-2: LDH activity [%] in supernatants of THP-1 cell-derived M1-like macrophages. Incubation with LPS [1 µg/ml] for 5 h, with ATP / nigericin for 40 min. Fig, figure. ①, incubation prior to LPS-priming. ②, incubation prior to ATP / nigericin. LPS, lipopolysaccharide; ATP, adenosine triphosphate; 5-B, 5-(3-Bromophenyl)-1,3-dihydro-2H-benzofuro[3,2-e]-1,4-diazepin-2-one; PSB, PSB-15417; PZB15, PZB15517166A; PZB13, PZB13420052A; A43, 3-{[5-(2,3-dichlorophenyl)-1H-1,2,3,4-tetrazol-1-yl]methyl}pyridine; JNJ, N-[[4-(4-phenylpiperazin-1-yl)oxan-4-yl]methyl]-2-phenylsulfanylpyridine-3-carboxamide; LDH, lactate dehydrogenase; min, minimum; max, maximum; n, number of individual experiments.

Figures	Treatment	LDH activity [%] median (min, max)	n
6, 10, 16, 21, 25, 28, 29	Untreated	5.0 (0.0, 18.3)	60
8	ATP [1 mM]	11.6 (6.0, 26.6)	9
8	ATP [2 mM]	12.1 (8.0, 31.0)	9
8	5-B [20 µM]	5.4 (1.7, 8.0)	6
8	A43 [10 µM]	4.8 (0.3, 7.5)	6
13	JNJ [1 µM]	4.8 (0.5, 8.3)	6
6, 10, 16, 21, 25, 28, 29	LPS	8.7 (0.0, 43.2)	72
10, 16, 21, 19, 25, 28, 29	LPS, 5-B [10 µM] ①	13.4 (4.8, 25.2)	15
10, 21, 25, 28, 29	LPS, 5-B [20 µM] ①	14.5 (8.5, 26.7)	6
10, 16, 21, 19, 25, 28, 29	LPS, PSB [10 µM] ①	9.4 (1.7, 29.4)	9
21, 25, 28, 29	LPS, 5-B [10 µM] ①, PSB [10 µM] ①	12.5 (6.0, 15.0)	6
10, 16, 21, 19, 25, 28, 29	LPS, PZB15 [10 µM] ①	21.2 (14.0, 25.0)	3
10, 16, 21, 19, 25, 28, 29	LPS, PZB13 [10 µM] ①	15.6 (10.1, 21.1)	3
10, 16, 21, 19, 25, 28, 29	LPS, A43 [10 µM] ①	8.4 (0.0, 18.3)	15
10, 16, 21, 25, 28, 29	LPS, JNJ [1 µM] ①	8.0 (6.4, 15.7)	6
10, 16	LPS, 5-B [10 µM] ②	19.7 (18.2, 19.8)	3
10, 16	LPS, PSB [10 µM] ②	19.3 (18.3, 21.5)	3
10, 16	LPS, PZB15 [10 µM] ②	24.3 (21.8, 25.4)	3
10, 16	LPS, PZB13 [10 µM] ②	27.1 (23.2, 31.6)	3
10	LPS, ATP [1 mM]	19.0 (7.4, 38.9)	16
10	LPS, DMSO [0.1 %] ①, ATP [1 mM]	19.5 (10.7, 39.2)	16
10	LPS, 5-B [10 µM] ①, ATP [1 mM]	16.0 (7.6, 35.5)	13
10	LPS, 5-B [20 µM] ①, ATP [1 mM]	25.0 (17.0, 35.6)	9
10	LPS, PSB [10 µM] ①, ATP [1 mM]	13.1 (6.9, 33.3)	13
10	LPS, PZB15 [10 µM] ①, ATP [1 mM]	10.0 (6.9, 39.4)	7
10	LPS, PZB13 [10 µM] ①, ATP [1 mM]	9.7 (5.7, 34.2)	7
10	LPS, A43 [20 µM] ①, ATP [1 mM]	9.7 (6.8, 25.5)	9
10	LPS, 5-B [10 µM] ②, ATP [1 mM]	15.8 (6.7, 37.2)	13
10	LPS, 5-B [20 µM] ②, ATP [1 mM]	19.2 (13.0, 29.7)	9
10	LPS, PSB [10 µM] ②, ATP [1 mM]	13.0 (8.5, 39.7)	7
10	LPS, PZB15 [10 µM] ②, ATP [1 mM]	9.9 (7.0, 32.1)	7
10	LPS, PZB13 [10 µM] ②, ATP [1 mM]	10.9 (6.6, 37.7)	7

10	LPS, A43 [20 µM] ②, ATP [1 mM]	9.5 (5.6, 24.2)	9
10, S-1	LPS, ATP [2 mM]	18.8 (6.7, 43.2)	38
10, S-1	LPS, DMSO [0.1 %] ①, ATP [2 mM]	18.6 (7.1, 42.8)	38
10	LPS, 5-B [10 µM] ①, ATP [2 mM]	18.6 (5.8, 44.0)	19
10	LPS, 5-B [20 µM] ①, ATP [2 mM]	23.1 (17.0, 31.0)	9
10	LPS, PSB [10 µM] ①, ATP [2 mM]	12.8 (7.5, 27.0)	13
10	LPS, PZB15 [10 µM] ①, ATP [2 mM]	13.3 (8.0, 24.7)	7
10	LPS, PZB13 [10 µM] ①, ATP [2 mM]	11.9 (5.8, 22.7)	7
10, S-1	LPS, A43 [20 µM] ①, ATP [2 mM]	11.2 (4.2, 21.8)	17
S-1	LPS, JNJ [0.01 µM] ①, ATP [2 mM]	10.1 (4.1, 14.8)	8
S-1	LPS, JNJ [0.1 µM] ①, ATP [2 mM]	10.1 (4.4, 21.1)	8
10, S-1	LPS, JNJ [1 µM] ①, ATP [2 mM]	15.3 (9.0, 23.8)	8
S-1	LPS, JNJ [5 µM] ①, ATP [2 mM]	14.7 (6.7, 25.2)	8
S-1	LPS, JNJ [10 µM] ①, ATP [2 mM]	13.4 (6.3, 19.8)	8
10	LPS, 5-B [10 µM] ②, ATP [2 mM]	12.1 (8.7, 25.0)	13
10	LPS, 5-B [20 µM] ②, ATP [2 mM]	18.5 (13.7, 30.3)	8
10	LPS, PSB [10 µM] ②, ATP [2 mM]	18.7 (9.2, 26.6)	7
10	LPS, PZB15 [10 µM] ②, ATP [2 mM]	14.3 (8.6, 23.8)	7
10	LPS, PZB13 [10 µM] ②, ATP [2 mM]	14.0 (8.1, 24.1)	7
10, S-1	LPS, A43 [20 µM] ②, ATP [2 mM]	10.1 (4.4, 22.2)	17
S-1	LPS, JNJ [0.01 µM] ①, ATP [2 mM]	14.4 (2.9, 27.4)	8
S-1	LPS, JNJ [0.1 µM] ①, ATP [2 mM]	11.2 (4.0, 28.7)	8
10, S-1	LPS, JNJ [1 µM] ①, ATP [2 mM]	11.6 (6.5, 30.2)	8
S-1	LPS, JNJ [5 µM] ①, ATP [2 mM]	13.4 (4.1, 26.8)	8
S-1	LPS, JNJ [10 µM] ②, ATP [2 mM]	11.6 (5.2, 15.6)	8
16	LPS, nigericin [50 µM]	23.6 (0.0, 50.0)	21
16	LPS, DMSO [0.1 %] ①, nigericin [50 µM]	23.6 (0.0, 57.0)	21
16	LPS, 5-B [10 µM] ①, nigericin [50 µM]	28.8 (10.8, 48.6)	12
16	LPS, PSB [10 µM] ①, nigericin [50 µM]	24.8 (9.1, 36.4)	6
16	LPS, PZB15 [10 µM] ①, nigericin [50 µM]	24.0 (6.4, 33.0)	6
16	LPS, PZB13 [10 µM] ①, nigericin [50 µM]	36.0 (13.5, 47.0)	6
16	LPS, A43 [10 µM] ①, nigericin [50 µM]	27.0 (1.4, 50.4)	12
16	LPS, JNJ [1 µM] ①, nigericin [50 µM]	31.8 (0.0, 47.0)	6
16	LPS, 5-B [10 µM] ②, nigericin [50 µM]	33.0 (10.3, 37.1)	3
16	LPS, PSB [10 µM] ②, nigericin [50 µM]	31.3 (8.2, 52.1)	3
16	LPS, PZB15 [10 µM] ②, nigericin [50 µM]	27.8 (10.1, 30.7)	3
16	LPS, PZB13 [10 µM] ②, nigericin [50 µM]	36.4 (12.4, 38.3)	3
16	LPS, A43 [10 µM] ②, nigericin [50 µM]	41.7 (9.8, 60.0)	9
16	LPS, JNJ [1 µM] ②, nigericin [50 µM]	28.5 (1.4, 54.0)	6

Table S-3: LDH activity [%] in supernatants of hPBMCs. LPS [5 ng/ml] for 3 h, BzATP / nigericin incubation for 30 min. ①, incubation prior to LPS-priming. ②, incubation prior to BzATP / nigericin. LPS, lipopolysaccharide; BzATP, 2'(3')-O-(4-Benzoylbenzoyl)adenosine-5'-triphosphate; 5-B, 5-(3-Bromophenyl)-1,3-dihydro-2H-benzofuro[3,2-e]-1,4-diazepin-2-one; PSB, PSB-15417; PZB15, PZB15517166A; PZB13, PZB13420052A; A43, 3-{[5-(2,3-dichlorophenyl)-1H-1,2,3,4-tetrazol-1-yl]methyl}pyridine; JNJ, N-[[4-(4-phenylpiperazin-1-yl)oxan-4-yl]methyl]-2-phenylsulfanylpyridine-3-carboxamide; LDH, lactate dehydrogenase; min, minimum; max, maximum; n, number of individual experiments.

Figures	Treatment	LDH activity [%] median (min, max)	n
8, 11, 12, 17, 18, 22, 26, 30	Untreated	1.0 (0.0, 9.0)	16
11, 12	BzATP [100 µM]	2.0 (1.1, 4.4)	6
17, 18	Nigericin [50 µM]	1.7 (2 3.0, 39.7)	7
8, 11, 12, 17, 18, 22, 26, 30	LPS	0.7 (0.0, 2.8)	15

11, 12	LPS, BzATP [100 µM]	2.5 (1.7, 3.0)	7
11, 12	LPS, DMSO [0.1 %] ①, BzATP [100 µM]	2.1 (1.3, 5.0)	7
11, 12	LPS, 5-B [10 µM] ①, BzATP [100 µM]	2.0 (0.5, 4.3)	7
12	LPS, 5-B [10 µM] ①, PSB [10 µM] ①, BzATP [100 µM]	3.0 1.3, 5.0)	7
12	LPS, 5-B [10 µM] ①, PZB15 [10 µM] ①, BzATP [100 µM]	2.5 (1.7, 6.3)	7
12	LPS, 5-B [10 µM] ①, PZB13 [10 µM] ①, BzATP [100 µM]	2.6 (0.6, 4.8)	7
12	LPS, 5-B [10 µM] ①, JNJ [1 µM] ①, BzATP [100 µM]	2.7 (2.0, 4.1)	7
12	LPS, 5-B [10 µM] ①, 5-B [10 µM] ②, BzATP [100 µM]	5.4 (2.6, 8.0)	7
12	LPS, 5-B [10 µM] ①, PSB [10 µM] ②, BzATP [100 µM]	3.4 (1.9, 6.7)	7
12	LPS, 5-B [10 µM] ①, PZB15 [10 µM] ②, BzATP [100 µM]	3.5 (2.4, 7.0)	7
12	LPS, 5-B [10 µM] ①, PZB13 [10 µM] ②, BzATP [100 µM]	4.8 (2.7, 8.9)	7
12	LPS, 5-B [10 µM] ①, JNJ [1 µM] ②, BzATP [100 µM]	4.3 (2.0, 5.7)	7
11	LPS, PSB [10 µM] ①, BzATP [100 µM]	2.1 (1.6, 3.5)	7
11	LPS, PZB15 [10 µM] ①, BzATP [100 µM]	2.0 (0.4, 5.4)	7
11	LPS, PZB13 [10 µM] ①, BzATP [100 µM]	2.7 (1.6, 3.9)	7
11	LPS, JNJ [1 µM] ①, BzATP [100 µM]	2.7 (2.1, 5.2)	7
11	LPS, 5-B [10 µM] ②, BzATP [100 µM]	5.0 (2.2, 8.0)	6
11	LPS, PSB [10 µM] ②, BzATP [100 µM]	2.9 (1.7, 4.1)	6
11	LPS, PZB15 [10 µM] ②, BzATP [100 µM]	2.9 (1.6, 8.5)	6
11	LPS, PZB13 [10 µM] ②, BzATP [100 µM]	3.3 (2.6, 7.6)	6
11	LPS, JNJ [1 µM] ②, BzATP [100 µM]	3.7 (2.7, 12.0)	6
17, 18	LPS, nigericin [50 µM]	23.5 (8.8, 35.0)	9
17, 18	LPS, DMSO [0.1 %] ①, nigericin [50 µM]	24.0 (8.1, 39.4)	9
17, 18	LPS, 5-B [10 µM] ①, nigericin [50 µM]	29.0 (8.1, 39.7)	9
18	LPS, 5-B [10 µM] ①, PSB [10 µM] ①, nigericin [50 µM]	25.2 (8.1, 75.0)	8
18	LPS, 5-B [10 µM] ①, PZB15 [10 µM] ①, nigericin [50 µM]	29.5 (9.4, 36.7)	8
18	LPS, 5-B [10 µM] ①, PZB13 [10 µM] ①, nigericin [50 µM]	32.0 (14.4, 51.3)	8
18	LPS, 5-B [10 µM] ①, A43 [10 µM] ①, nigericin [50 µM]	29.5 (9.4, 41.4)	8
18	LPS, 5-B [10 µM] ①, JNJ [1 µM] ①, nigericin [50 µM]	33.0 (14.4, 67.1)	8
17	LPS, PSB [10 µM] ①, nigericin [50 µM]	36.3 (9.4, 55.2)	8
17	LPS, PZB15 [10 µM] ①, nigericin [50 µM]	30.1 (12.5, 47.0)	8
17	LPS, PZB13 [10 µM] ①, nigericin [50 µM]	16.9 (8.1, 53.5)	8
17	LPS, A43 [10 µM] ①, nigericin [50 µM]	19.1 (2.0, 54.0)	8
17	LPS, JNJ [1 µM] ①, nigericin [50 µM]	18.4 (2.0, 31.4)	7

Table S-4: LDH activity [%] in supernatants of hPMs. LPS [0.1 µg/ml] for 5 h, BzATP incubation for 40 min. ①, incubation prior to LPS-priming. ②, incubation prior to BzATP. LPS, lipopolysaccharide; BzATP, 2'(3')-O-(4-Benzoylbenzoyl)adenosine-5'-triphosphate; 5-B, 5-(3-Bromophenyl)-1,3-dihydro-2H-benzofuro[3,2-e]-1,4-diazepin-2-one; PSB, PSB-15417; PZB15, PZB15517166A; PZB13, PZB13420052A; A43, 3-{[5-(2,3-dichlorophenyl)-1H-1,2,3,4-tetrazol-1-yl]methyl}pyridine; JNJ, N-[[4-(4-phenylpiperazin-1-yl)oxan-4-yl]methyl]-2-phenylsulfanylpyridine-3-carboxamide; LDH, lactate dehydrogenase; min, minimum; max, maximum; n, number of individual experiments.

Figures	Treatment	LDH activity [%] median (min, max)	n
8, 13	Untreated	2.0 (0.0, 13.7)	5
8, 13	LPS	3.0 (0.0, 11.0)	5
13	LPS, 5-B [20 µM] ①	6.0 (0.0, 29.1)	5
13	LPS, PSB [10 µM] ①	13.7	1
13	LPS, A43 [20 µM] ①	2.0 (0.0, 14.3)	5
13	LPS, 5-B [20 µM] ②	3.0 (0.0, 15.2)	5
13	LPS, PSB [10 µM] ②	12.0	1

13	LPS, A43 [20 µM] ②	6.7 (0.0, 12.6)	5
8, 13	LPS, BzATP [100 µM]	15.2 (0.0, 24.0)	5
8, 13	LPS, DMSO [0.1 %] ①, BzATP [100 µM]	19.1 (0.0, 28.0)	5
13	LPS, 5-B [1 µM] ①, BzATP [100 µM]	10.8 (4.0, 17.6)	2
13	LPS, 5-B [10 µM] ①, BzATP [100 µM]	10.5 (4.0, 16.9)	2
13	LPS, 5-B [20 µM] ①, BzATP [100 µM]	20.3 (6.0, 31.0)	5
13	LPS, PSB [1 µM] ①, BzATP [100 µM]	17.0	1
13	LPS, PSB [10 µM] ①, BzATP [100 µM]	14.3	1
13	LPS, A43 [20 µM] ①, BzATP [100 µM]	4.0 (0.0, 14.3)	5
13	LPS, 5-B [20 µM] ②, BzATP [100 µM]	17.0 (0.0, 22.0)	5
13	LPS, PSB [10 µM] ②, BzATP [100 µM]	18.7	1
13	LPS, A43 [20 µM] ②, BzATP [100 µM]	3.0 (0.0, 9.5)	5

Table S-5: Absolute values of IL-1β in supernatants of control samples by monocytic THP-1 cells. LPS [1 µg/ml] for 5 h, BzATP / nigericin incubation for 40 min. ①, incubation prior to LPS-priming. MAD, mean absolute deviation. LPS, lipopolysaccharide; BzATP, 2'(3')-O-(4-Benzoylbenzoyl)adenosine-5'-triphosphate; 5-B, 5-(3-Bromophenyl)-1,3-dihydro-2H-benzofuro[3,2-e]-1,4-diazepin-2-one; PSB, PSB-15417; PZB15, PZB15517166A; PZB13, PZB13420052A; A43, 3-{[5-(2,3-dichlorophenyl)-1H-1,2,3,4-tetrazol-1-yl]methyl}pyridine; JNJ, N-[[4-(4-phenylpiperazin-1-yl)oxan-4-yl]methyl]-2-phenylsulfanylpyridine-3-carboxamide; min, minimum; max, maximum; n, number of individual experiments.

Figures	Treatment	IL-1β secretion [pg /ml] median (min, max)	n
9, 14, 31	Untreated	0.4 (0.0, 14.0)	12
31	Doxorubicin [2.5 µM]	1.0 (0.0, 14.0)	6
31	Doxorubicin [2.5 µM], Z-VAD-FMK [10 µM]	1.0 (0.0, 2.0)	6
9, 14	LPS	9.0 (5.3, 13.2)	6
9, 14	LPS, 5-B [10 µM] ①	15.9 (9.3, 35.4)	6
9, 14	LPS, PSB [10 µM] ①	12.4 (9.3, 28.2)	6
9, 14	LPS, PZB15 [10 µM] ①	8.7 (2.1, 50.3)	6
9, 14	LPS, PZB13 [10 µM] ①	14.7 (2.9, 47.0)	6
9, 14	LPS, A43 [10 µM] ①	7.3 (0.0, 10.4)	6
9, 14	LPS, JNJ [1 µM] ①	11.8 (0.1, 17.6)	6
31	LPS, Doxorubicin [2.5 µM]	10.0 (3.0, 14.0)	6
31	LPS, Doxorubicin [2.5 µM,] Z-VAD-FMK [10 µM]	2.0 (1.0, 3.0)	6
31	LPS, BzATP [100 µM]	104.5 (18.0, 179.0)	9
31	LPS, Z-VAD-FMK [10 µM], BzATP [100 µM]	14.5 (5.0, 36.0)	6
31	LPS, nigericin [50 µM]	240.0 (40.0, 435.0)	6
31	LPS, Z-VAD-FMK [10 µM], nigericin [50 µM]	47.0 (11.0, 102.0)	6

Table S-6: Absolute values of IL-1β in supernatants of control samples by THP-1 cell-derived M1-like macrophages. LPS [1 µg/ml] for 5 h, BzATP / nigericin incubation for 40 min. ①, incubation prior to LPS-priming. ②, incubation after 5 h incubation with LPS. MAD, mean absolute deviation. LPS, lipopolysaccharide; ATP, adenosine triphosphate; 5-B, 5-(3-Bromophenyl)-1,3-dihydro-2H-benzofuro[3,2-e]-1,4-diazepin-2-one; PSB, PSB-15417; PZB15, PZB15517166A; PZB13, PZB13420052A; A43, 3-{[5-(2,3-dichlorophenyl)-1H-1,2,3,4-tetrazol-1-yl]methyl}pyridine; JNJ, N-[[4-(4-phenylpiperazin-1-yl)oxan-4-yl]methyl]-2-phenylsulfanylpyridine-3-carboxamide; min, minimum; max, maximum; n, number of individual experiments.

Figures	Treatment	IL-1β secretion [pg /ml] median (min, max)	n
10, 16	Untreated	38.5 (21.0, 64.0)	18
10, 16	5-B [10 µM] ①	37.0 (34.0, 43.0)	3
10, 16	5-B [20 µM] ①	55.0 (21.0, 110.0)	6
10, 16	PSB [10 µM] ①	32.0 (31.0, 35.0)	3
10, 16	PZB15 [10 µM] ①	29.0 (26.0, 31.0)	3
10, 16	PZB13 [10 µM] ①	34.0 (33.0, 35.0)	3
10, 16	A43 [10 µM] ①	41.0 (33.0, 62.0)	9
10, 16	JNJ [1 µM] ①	44.5 (36.0, 65.0)	6

10, 16	LPS	137.0 (93.0, 247.0)	18
10, 16	LPS, 5-B [10 µM] ①	153.0 (118.0, 184.0)	12
10, 16	LPS, 5-B [20 µM] ①	553.0 (212.0, 663.0)	6
10, 16	LPS, PSB [10 µM] ①	103.0 (75.0, 157.0)	12
10, 16	LPS, PSB [10 µM] ①, 5-B [10 µM] ①	181.5 (127.0, 426.0)	6
10, 16	LPS, PZB15 [10 µM] ①	89.0 (64.0, 111.0)	6
10, 16	LPS, PZB13 [10 µM] ①	106.0 (90.0, 117.0)	6
10, 16	LPS, A43 [10 µM] ①	128.5 (91.0, 185.0)	12
10, 16	LPS, A43 [20 µM] ①	156.0 (133.0, 184.0)	6
10, 16	LPS, JNJ [1 µM] ①	125.5 (92.0, 143.0)	6
10, 16	LPS, 5-B [10 µM] ②	208.0 (146.0, 220.0)	3
10, 16	LPS, PSB [10 µM] ②	101.0 (98.0, 104.4)	3
10, 16	LPS, PZB15 [10 µM] ②	100.0 (74.0, 106.0)	3
10, 16	LPS, PZB13 [10 µM] ②	136.0 (119.0, 136.0)	3

Table S-7: Absolute values of IL-1β in supernatants of control samples by hPMs. LPS [0.1 µg/ml] for 5 h, BzATP incubation for 40 min. ①, incubation prior to LPS-priming. ②, incubation prior to BzATP. LPS, lipopolysaccharide; BzATP, 2'(3')-O-(4-Benzoylbenzoyl)adenosine-5'-triphosphate; 5-B, 5-(3-Bromophenyl)-1,3-dihydro-2H-benzofuro[3,2-e]-1,4-diazepin-2-one; PSB, PSB-15417; PZB15, PZB15517166A; PZB13, PZB13420052A; A43, 3-{[5-(2,3-dichlorophenyl)-1H-1,2,3,4-tetrazol-1-yl]methyl}pyridine; JNJ, N-[[4-(4-phenylpiperazin-1-yl)oxan-4-yl]methyl]-2-phenylsulfanylpyridine-3-carboxamide; min, minimum; max, maximum; n, number of individual experiments.

Figure	Treatment	IL-1β secretion [pg /ml] median (min, max)	n
13	Untreated	0.7 (0.0, 29.0)	5
13	LPS	47.0 (22.0, 111.0)	5
13	LPS, 5-B [20 µM] ①	428.0 (302.0, 1836.0)	5
13	LPS, PSB [10 µM] ①	84.0	1
13	LPS, A43 [20 µM] ①	78.0 (44.0, 130.0)	5
13	LPS, 5-B [20 µM] ②	222.0 (99.0, 278.0)	5
13	LPS, PSB [10 µM] ②	118.0	1
13	LPS, A43 [20 µM] ②	88.0 (48.0, 113.0)	5

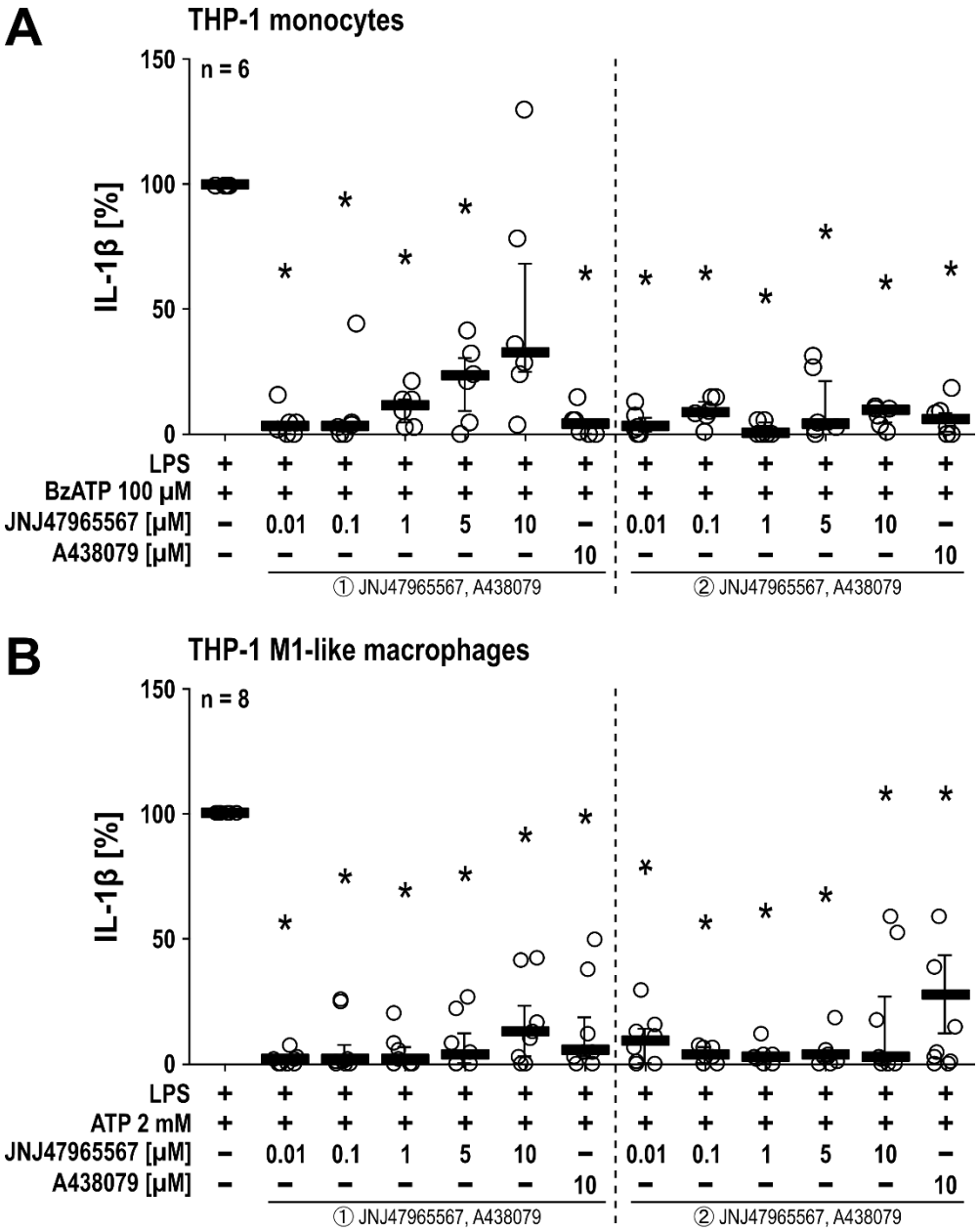

Figure S-1: Dose response curve of the P2RX7 inhibitor JNJ in (A) Monocytic THP-1 cells and (B) THP-1 cell-derived M1-like macrophages. Cells were primed with LPS (1 µg/ml) for 5 h in the absence of presence (①) of the P2RX7 inhibitors JNJ (0.01, 0.1, 1, 5, 10 µM) or A43 (10 µM). Thereafter, **(A)** BzATP (100 µM) or **(B)** ATP (2 mM) was added for 40 min in the absence or presence (②) of the antagonists and IL-1β was measured in cell culture supernatants by ELISA. The IL-1β concentration in experiments in which primed cells were stimulated with BzATP alone was set to 100 % and all other values were calculated accordingly. Data are presented as individual data points, bars represent median, whiskers percentiles 25 and 75. Friedman-test followed by Wilcoxon signed-rank test. ∗ $p \leq 0.05$ significantly different from samples in which only BzATP or ATP was given to LPS-primed cells. LPS, lipopolysaccharide; BzATP, 2'(3')-O-(4-Benzoylbenzoyl)adenosine-5'-triphosphate; ATP, adenosine triphosphate; 5-B, 5-(3-Bromophenyl)-1,3-dihydro-2H-benzofuro[3,2-e]-1,4-diazepin-2-one; PSB, PSB-15417; PZB15, PZB15517166A; PZB13, PZB13420052A; A43, 3-{[5-(2,3-dichlorophenyl)-1H-1,2,3,4-tetrazol-1-yl]methyl}pyridine; JNJ, N-[[4-(4-phenylpiperazin-1-yl)oxan-4-yl]methyl]-2-phenylsulfanylpyridine-3-carboxamide.

Table S-8: mRNA expression controls in THP-1 cell-derived M1-like macrophages. Corresponding to figures 25, 28, 29. ①, incubation prior to LPS-priming. MAD, mean absolute deviation. LPS, lipopolysaccharide; 5-B, 5-(3-Bromophenyl)-1,3-dihydro-2H-benzofuro[3,2-e]-1,4-diazepin-2-one; PSB, PSB-15417; PZB15, PZB15517166A; PZB13, PZB13420052A; A43, 3-{[5-(2,3-dichlorophenyl)-1H-1,2,3,4-tetrazol-1-yl]methyl}pyridine; JNJ, N-[[4-(4-phenylpiperazin-1-yl)oxan-4-yl]methyl]-2-phenylsulfanylpyridine-3-carboxamide; AU, arbitrary units; min, minimum; max, maximum; n, number of individual experiments.

Treatment	Target gene	Fold change gene expression relative to *PPIA* [AU] median (min, max)	n
Untreated	*IL1B*	0.1251 (0.0060, 1.9312)	15
	IL6	0.0005 (0.0000, 0.0100)	
	IL10	0.0006 (0.0000, 0.0017)	
	P2RX4	0.0386 (0.0006, 1.3430)	
	P2RX7	0.0041 (0.0004, 0.0556)	
5-B [10 µM] ①	*IL1B*	0.2559 (0.0792, 1.7210)	9
	IL6	0.0005 (0.0000, 0.4485)	
	IL10	0.0013 (0.0000, 0.0063)	
	P2RX4	0.0552 (0.0153, 1.1315)	
	P2RX7	0.0030 (0.0008, 0.0364)	
PSB [10 µM] ①	*IL1B*	0.0575 (0.0412, 0.0767)	3
	IL6	0.0000 (0.0000, 0.0002)	
	IL10	0.0009 (0.0000, 0.0015)	
	P2RX4	0.0217 (0.0197, 1.1450)	
	P2RX7	0.0032 (0.0021, 0.0547)	
PZB15 [10 µM] ①	*IL1B*	0.0293 (0.0202, 0.0527)	3
	IL6	0.0001 (0.0000, 0.0003)	
	IL10	0.0003 (0.0000, 0.0009)	
	P2RX4	0.0200 (0.0120, 1.0926)	
	P2RX7	0.0044 (0.0017, 0.0441)	
PZB13 [10 µM] ①	*IL1B*	0.0567 (0.0477, 0.1200)	3
	IL6	0.0001 (0.0000, 0.0005)	
	IL10	0.0010 (0.0000, 0.0012)	
	P2RX4	0.0250 (0.0134, 1.2870)	
	P2RX7	0.0050 (0.0017, 0.0495)	
A43 [10 µM] ①	*IL1B*	0.0793 (0.0035, 0.1901)	6
	IL6	0.0003 (0.0000, 0.0024)	
	IL10	0.0004 (0.0000, 0.0012)	
	P2RX4	0.0508 (0.0067, 0.1628)	
	P2RX7	0.0020 (0.0004, 0.0106)	
JNJ [1 µM] ①	*IL1B*	0.0821 (0.0038, 0.1527)	6
	IL6	0.0002 (0.0000, 0.0024)	
	IL10	0.0003 (0.0000, 0.0009)	
	P2RX4	0.0428 (0.0058, 0.1282)	
	P2RX7	0.0015 (0.0003, 0.0060)	

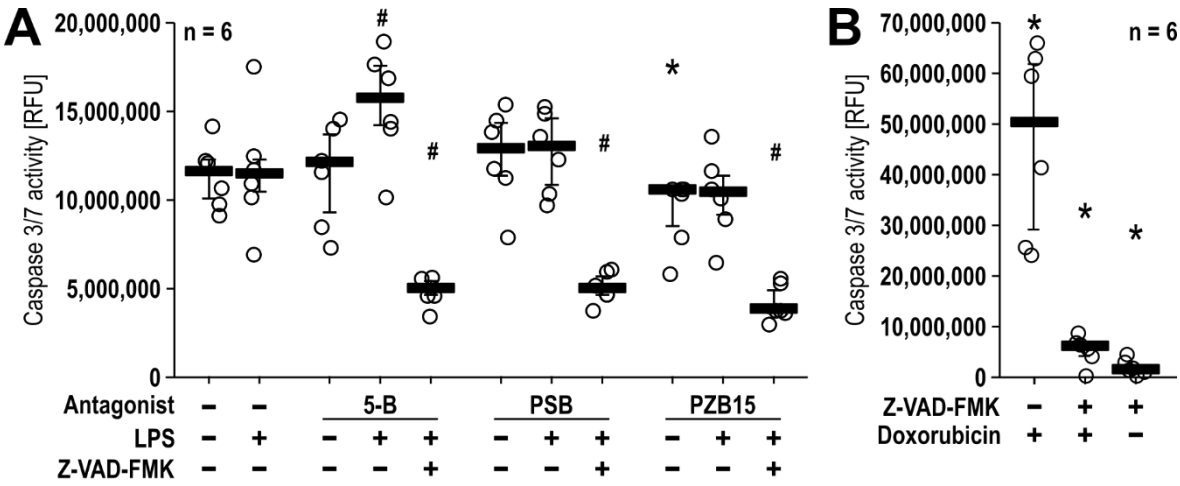

Figure S-2: **The impact of P2RX4 antagonists on caspase-3 and caspase-7 activity in monocytic THP-1 cells**. **(A)** Cells were primed with LPS (1 µg/ml) for 5 h in absence or presence of the P2RX4 antagonists 5-B (10 µM), PSB (10 µM), or PZB15 (10 µM), or the caspase inhibitor Z-VAD-FMK (20 µM). **(B)** As a positive control, cells were treated with doxorubicin (2.5 µM) for 5 h in the absence or presence of Z-VAD-FMK (20 µM). Thereafter, Apo-ONE® reagent was added for 60 min. Caspase-3 and -7 activity was measured by detecting fluorescence signals. Data are presented as individual data points, bars represent median, whiskers percentiles 25 and 75. Friedman-test followed by Wilcoxon signed-rank test. ∗ $p \leq 0.05$ significantly different from untreated samples. # $p \leq 0.05$ significantly different from samples in which LPS alone was given to monocytic THP-1 cells. RFU, relative fluorescence unit; LPS, lipopolysaccharide; 5-B, 5-(3-Bromophenyl)-1,3-dihydro-2H-benzofuro[3,2-e]-1,4-diazepin-2-one; PSB, PSB-15417; PZB15, PZB15517166A

DANKSAGUNG

*Vielen, vielen Dank an **Veronika Grau** für die unermüdliche Unterstützung, Fürsorge, für guten Rat und gemeinsame Ratlosigkeit. Danke, dass du nicht aufgegeben hast, als wir nicht weiterwussten.*

*Ich danke **Katrin Richter** von ganzem Herzen, dass du mich mit diesem Projekt aufgefangen hast, für die fachliche Unterstützung, deine Ehrlichkeit, deinen unerschütterlichen Optimismus und gute Gespräche.*

*Danke an **Ivan Manzini** für die Betreuung im Fachbereich 08 und auch an **Oliver Rossbach** und **Kai Thormann** für die Bewertung der Disputation.*

*Ich bedanke mich bei **Prof. Dr. Christa Müller** für die Bereitstellung der Antagonisten und fachliche Unterstützung.*

*Danke an **Gabi Fuchs-Moll, Kathrin Petri** und **Sabine Stumpf** für die großartige Unterstützung im Labor und die unermüdliche Hilfsbereitschaft. Vielen Dank an **Christina Buschhaus** für die Freundschaft über die PC-Bildschirme hinweg und darüber hinaus. Ich danke auch alle anderen der **AG Grau**, die während meiner Zeit für schöne Stunden gesorgt haben.*

Ich danke meinem Partner für die Geduld und meinen guten „Frens“ für ihre stets offenen Ohren.

Vor allem danke ich meinen Eltern. Nur durch eure bedingungslose und stetige Unterstützung und eurem unbeirrbaren Glauben an mich konnte ich immer meine Interessen verfolgen und letztendlich diesen wunderbaren, wenn auch beschwerlichen, Werdegang wählen.

Zuletzt danke ich mir selbst. Das darf auch mal sein.